ENVIRONMENTAL RESEARCH

Ontario

STUDIES OF OXIDANT FORMATION IN SOUTHERN ONTARIO FINAL REPORT

RAC Project No. 716G

MINISTRY OF ENVIRONMENT AND ENERGY

ISBN 0-7778-5245-4

STUDIES OF OXIDANT FORMATION

IN SOUTHERN ONTARIO

FINAL REPORT

RAC Project No. 716G

FEBRUARY 1996

PIBS 3427E

STUDIES OF OXIDANT FORMATION

IN SOUTHERN ONTARIO

FINAL REPORT

RAC Project No. 716G

Report prepared by:

D.R. Hastie[1,2], J.C. McConnell[2,3],
M. Mozurkewich[1,2], and P.B. Shepson[1,2,4]

[1]Department of Chemistry
[2]Centre for Atmospheric Chemistry
[3]Department of Earth and Atmospheric Science
York University
4700 Keele Street
North York, Ontario M3J 1P3

[4]Current affiliation, Departments of Chemistry and
Earth and Atmospheric Science, Purdue University,
West Lafayette, Indiana

ACKNOWLEDGEMENT AND DISCLAIMER

This report was prepared for the Ontario Ministry of Environment and Energy as part of a Ministry funded project. The views expressed in this report are those of the author and do not necessarily reflect the views and policies of the Ministry of Environment and Energy, nor does mention of trade names or commercial products constitute endorsement or recommendation for use. The Ministry, however, encourages the distribution of information and strongly supports technology transfer and diffusion.

TABLE OF CONTENTS

SUMMARY

This project continued the data analysis and the modelling efforts in support of SONTOS. The main focus was on the interpretation of the 1993 Hastings data. This was achieved through tests on the data, and by use of a 1-D photochemical model. A second activity was a small experimental effort to improve our knowledge of urban concentrations for initialization of this 1-D model.

Conclusions from this work are:

- Ozone events in this area are an intermittent occurrence
- The number of ozone molecules produced by each NO_x molecule emitted is 11-12 consistent with observations at other North American sites.
- High ozone concentrations result from high NO_x levels rather than more highly oxidized air masses
- The hypothesis that air entrained over Lake Ontario can produce elevated ozone concentrations that subsequently move over the land, remains viable. These air masses have less NO_x oxidation than most air masses
- The elevated ozone measured at Hastings is produced upwind of the site and advected into the area.
- Measurements of carbonyl and nitrate concentrations point to additional sources of carbonyl compounds not currently in our models.
- Measurements show organic nitrates contribute little to the nitrogen oxide balance at the site, although the inability to measure the nitrates of isoprene leaves this question open.
- The organic nitrate measurements also show that the small radicals (HO_2 and CH_3O_2) are responsible for most of the NO to NO_2 oxidation and subsequent ozone production
- Measurements are not sufficiently precise and of sufficient time resolution to investigate the nitrogen balance at the site
- Hydrogen peroxide measured at Hastings is produced upwind of the site and advected into the area.
- There is evidence of the production of new particles from the intrusion of SO_2 into the air masses at Hastings

- There is also evidence for new particle production in the morning and following a thunderstorm
- Indicators of NO_x-hydrocarbon sensitivity point strongly to ozone production at Hastings as being under NO_x control.
- Measurements of ozone, NO, NO_x, NO_y, CO, SO_2, radiation and meteorological parameters at York University have improved the data base for air masses leaving the city

I INTRODUCTION

This is the final report on the project "Studies of Oxidant Formation in Southern Ontario" which commenced in June 1994, and for which a no cost extension until December 30 1995 was authorized.

The project proposed to continue the data analysis and the modelling efforts in support of SONTOS. The main focus was to be on interpretation of the 1993 Hastings data, with a small experimental effort to improve our knowledge of urban concentrations for initialization of our 1-D model.

This report does not give the background climatology of the site. This was done in a previous grant and the results are to be found in the collection of SONTOS papers listed in Section IX. Only the new data and the results from additional analysis are reported here.

The first task proposed was to integrate the data sets obtained by the various groups at the Hastings site. Once the data were fully integrated into a single data set, the project was to use the data and the modelling efforts to examine the chemistry at the site and in particular to look at the following questions.

Q1 How is the ozone concentration related to the age of the air mass?

Q2 To what extent is the ozone locally produced?

Q3 Can we use the measurements of the carbonyl compounds to investigate the role of specific precursor hydrocarbons that may be responsible for ozone production in the area?

Q4 Can we use the measurements of the organic nitrates to identify the organic radicals present at the site and assess their importance in local ozone production?

Q5 Can we gain new insights on the "nitrogen shortfall" observed at other sites?

Q6 Does the PAN contribution to NO_y depend on the extent of isoprene chemistry?

Q7 Can we explain the H_2O_2 production and/or concentration from the radical measurements?

Q8 Is the presence of atmospheric aerosol impacting the radical chemistry at the site?

The second task was to use data, obtained from the roof of the Petrie building at York University, to establish representative concentrations and concentration ratios within a Canadian city. Such data are required to initialise models of the impact of cities, such as Toronto, on the surrounding rural areas.

II INTEGRATION AND INTERPRETATION OF THE HASTINGS DATA

II.i. Integration of the Hastings data sets

This activity dealt with the data collected in the second SONTOS field study from July 15 to August 27 1993. There are 7 data sets from York alone, specifically the basic data set (NO, NO_2, O_3, solar radiation, wind speed, wind direction, temperature and humidity), the data from the tunable diode laser (CH_2O and H_2O_2), the PAN data, the concentrations of the carbonyl compounds, the radical data, the organic nitrate data set, and the aerosol concentration and size distributions. In addition we needed to incorporate the Ontario Hydro data for CO, NO_y, SO_2, and meteorology parameters, and the Ministry filterpack data (HNO_3, NO_3^-, and NH_4^+). We have produced a data set with 5 minute averages for NO, NO_2, NO_x, O_3, CO, NO_y, SO_2, radicals, solar radiation, wind speed, wind direction, temperature and humidity. These data have also been averaged and included with the radical, CH_2O and H_2O_2 data to give 30 minute data set. A one hour data set has been produced, primarily to accommodate the PAN data, by averaging all the above data, adding the PAN data and interpolating the filterpack data. The carbonyl and organic nitrate data are in a separate data set, as are all the aerosol data. This has been done for convenience and has not proven to be a problem in analysis, as yet.

The data described here represent one of the best data sets for oxidant research in North America. They are in QuattroPro worksheets and are available on request to the funding agencies or to any scientific group involved in oxidant research. We encourage such groups to undertake joint projects with us as we are best able to assess the validity of using the data in particular applications. Examples of groups who are using the data, in addition to ourselves, are Prof. P. Taylor and David Sills of York University for an MOEE study, and Prof. N. Bunce and A. Barrett of the University of Guelph as part of an ozone impact study for the Ministry of Agriculture.

Figure 1 shows the averaged diurnal concentrations of the major species measured over the six weeks of the 1993 measurement campaign.

There were several differences noted between these data and those obtained in 1992.

Most of these could be attributed to the significantly warmer summer in 1993 and a consequent increase in the extent of atmospheric chemistry. However, the gross features in the data were the same as reported in the published SONTOS papers.

II.ii Modelling

We are continuing the use of the 1-D model to assist in the interpretation of the data. The model has been run for the clean air case, and found to give satisfactory agreement with all the measurements, with the exception of the radicals. It has also been run in a Lagrangian mode to simulate the Toronto plume impacting the site at Hastings. We have used it to examine the effect of decreased vertical mixing over Lake Ontario on the concentration of precursors and ozone, as part of our study of the importance of the lake in producing elevated ozone levels. The most recent work has been in the interpretation of some of the aerosol data. There are cases in the data when the influx of high concentrations of SO_2 into the area appears to result in the production of nucleation mode particles. We have added primitive sulphur chemistry and nucleation to the model to test our understanding of the production of sulphuric acid against the data. The results of these calculations will be presented at the CMOS meeting in May.

Overall the 1-D model has been very valuable in helping interpret the data obtained at Hastings. However, as we said in the proposal, this type of model is most useful in examining the fast chemistry occurring at the site. To fully model the inputs of the ozone precursors, it is necessary to move to a 3-D model, which can realistically transport material into the study domain. David Plummer is now working on a new 3-D model. It is based on the MC2 mesoscale meteorological model developed by RPN and AES. He is including the chemistry package developed for the 1-D model into this model. This work is continuing to be a key contribution to the multi-institutional efforts to model oxidant chemistry in Southern Ontario..

II.iii Interpretation of the Hastings data sets

The aim of the 1992 field study was to determine the chemical climatology of the site. In other words, much of the work was exploratory in nature. For the 1993 study we aimed to address some particular issues. In the proposal we posed eight questions that, if answered, would contribute to the understanding of the oxidant chemistry issues. We made significant progress in answering these and the results follow below. In addition, in the course of the work other issues have arisen. They are included with the relevant sections below and in the additional section.

II.iii.1 (Q1) How is the ozone concentration related to the age of the air mass?

This question was aimed at assessing the extent to which the nitrogen oxides were consumed in transit to Hastings and to study the associated ozone production.

The nitrogen oxide emission is in the form of NO, which quickly reaches a steady state concentration with NO_2, therefore the ratio of NO_x ($NO + NO_2$) to the total nitrogen oxides (NO_y), is an inverse measure of the extent of the nitrogen oxide oxidation. Figure 2 shows the fraction of the NO_y present as NO_x. At night the NO_x source under the nocturnal inversion increases the NO_x/NO_y ratio to a maximum. During the day this value drops to be approximately constant at ~ 25%. This is a higher fraction than reported for the 1992 field study and for Egbert, but similar to that at the flatland sites of Scotia and Bondville, (Parrish et al. 1993). This shows that in 1993 there has been more nitrogen oxidation in these air masses than in the EMEFS Egbert data and in the Hastings 1992 data. This is likely due to the warmer and sunnier conditions present in 1993 resulting in more hydrocarbon and NO_x oxidation. Figure 3 shows that there was an increase in solar radiation data from 1992 to 1993.

Trainer et al. (1993) have shown that the number of ozone molecules that are produced for every NO_x that is oxidized, i.e. the chain length for the production of ozone in the atmosphere, can be obtained from a plot of the ozone concentration against NO_z (NO_y - NO_x), and that the intercept gives the regional background ozone level, before the air masses are

impacted with additional NO_x. They found that such a plot is linear, and report a chain length of 8.5 for a site in rural Pennsylvania. Other groups have reported values of 12.3 in Tennessee (Olszyna et al. 1994), and 11.4 in Georgia (Kleinman et al. 1994). Figure 4 shows that in the daytime there is also a linear relationship at Hastings for both years with an average chain length of 12 in 1992 and 11 in 1993. This shows that ozone production at all rural North American sites is driven by the same chemistry, and that the lower ozone concentrations observed at the Hastings site is due to the lower availability and conversion of NO_x. Since there is less nitrogen oxidation observed in the Hastings data, there is still ample NO_x to make ozone in the air masses being sampled at Hastings. The background ozone, as determined from the intercept of these plots, is 21 and 25 ppbv, similar to that observed in Georgia, but less than the 35 and 42 observed in Scotia and Tennessee respectively (Trainer 1993, Kleinman et al. 1994, Olszyna et al. 1994). Thus, not only is there less impact due to the recent NO_x inputs, but the background regional ozone concentration in this part of North America is lower.

Since a number of field studies do not have accurate NO_2 measurements, the literature shows a number of plots of ozone against NO_y. Figures 4c and d give these plots for our data, for comparison purposes.

It is clear, from the two sets of data we have obtained, that ozone events, or the impact of polluted air masses on the rural areas, is an intermittent occurrence. Therefore to better understand the factors that drive these events we have examined the nitrogen data for conditions of different ozone concentration. Daytime data for ozone concentrations greater or less than a threshhold ozone concentration (set at 50 or 80 ppbv) are presented in Table 1. The NO_y and NO_z data clearly show there are higher nitrogen oxide levels associated with the higher ozone concentrations. However there is no significant difference in the NO_x/NO_y ratio indicating the same extent of NO_x oxidation. The O_3/NO_z ratios show no significant differences even when corrected for background ozone levels. The corresponding plots of the segregated O_3 against NO_z (Figure 5) show lower slopes and higher intercepts but much lower r^2 values than the the entire data set. This is likely due to the narrower range of data being plotted. While the data are not overly clear they appear to preclude a marked increase in the

amount of ozone produced from each NO_x oxidized. Therefore, it appears that the same amount of oxidation has occurred and that the different ozone level encountered is due entirely to the presence of elevated NO_y levels, rather than sampling of more oxidized air.

One of the major findings of SONTOS has been the observation of incursions of air containing high concentrations of ozone and its precursors which appear to come from over Lake Ontario. It is hypothesized that polluted air from the Golden Horseshoe is entrained over the Lake where the limited vertical mixing maintains higher concentrations of precursors and consequently faster chemistry than is observed over the land. This air can then move over the land, under the influence of a lake breeze, to produce rapid increases in all pollutants at Hastings late in the afternoon. This effect was observed 5 times in 1993 and the ozone and NO_x data for these days are shown in Figure 6A. We have examined the NO_x/NO_y ratio and the O_3/NO_z relationship within these events, again to examine the nitrogen chemistry that is operative. These events occur late in the afternoon when a number of parameters are varying even in the absence of events. Therefore we have selected 2 days when there was no event, and the average for the study, to use as a base case against which to compare the event data. The ozone and NO_x data for these three cases is shown in Figure 6B. Identical time periods were used in both data sets to minimize the impact of solar radiation and temperature. We examined the difference between the parameters in the event time period and before. The results of the comparison are shown in Table 2. For comparison the plots of these parameters for the 5 days where the effect was noted and the three reference days are presented in Figure 7A and 7B respectively. The tabulated data show that the NO_x/NO_y ratio is significantly *higher* in the event case. For 4 events the difference is significant at the 99% level and for the other it is significant at the 90% level. This is also visible in the diurnal plots. This means that the air mass that is postulated as having been over the Lake has a smaller fraction of the NO_x processed than air coming over the land. The differences in the O_3/NO_z relationship are inconclusive. This suggests the number of ozone molecules produced per NO_x oxidized is the same in the different air masses. Therefore the high ozone observed in these events is a result of much higher NO_x levels but a smaller fraction of NO_y conversion.

II.iii.2 (Q2) To what extent is the ozone locally produced?

The local ozone production rate can be determined from measurements of the total peroxy radical (RO_2) and NO concentrations by the equation:

$$\frac{d[O_3]}{dt} = k[RO_2][NO]$$

where k is the rate coefficient for the reaction of peroxy radicals (RO_2) with NO to produce NO_2. This can be contrasted with the actual accumulation of ozone during the day which can be obtained from the variation in ozone concentration. A comparison of these two production rates allows us to estimate the relative contributions of local ozone production versus transport from upwind sources. Figure 8 shows results from three typical days on which this analysis can be performed. On each ozone plot , the actual rate of ozone increase is given by the straight line and the slope of this line section is converted to an ozone increase in ppbv/hr and included on the plot. The local production rate is also plotted for the whole day and the average rate over the same time period as in the ozone plot is indicated. In all cases the local ozone production is less than the observed increase at the site. Table 3 summarises the data from the 19 periods where an ozone increase was clearly demonstrated. There are no cases where the calculated ozone production rate could explain the rate of ozone increase. Furthermore, this calculation of the local ozone production rate would overestimate the real increase, since no deposition or reactive losses are included. Therefore, it appears as if 21-91% of the ozone increase at the site after 1030 hrs is due to horizontal advection. This does not preclude photochemical production of this ozone prior to advection. In fact the continual increase in the ozone concentration suggests photochemical production upwind of the site, earlier in the day, where the precursor concentrations and solar radiation could be higher. This is consistent with the maximum in the ozone concentration occurring at ~1800 hrs, over 3 hours after the maximum local production rate. Furthermore at the time of the concentration maximum the ozone production rate is only 25% of its maximum value.

II.iii.3 (Q3) Can we use the measurements of the carbonyl compounds to investigate the role of specific precursor hydrocarbons that may be responsible for ozone production in the area?

The first step in the oxidation of hydrocarbons produces carbonyl compounds. The aim of this work was to measure the concentrations these compounds and, from these measurements, infer the hydrocarbons that were undergoing reaction. In particular we aimed to measure the concentrations of methylvinyl ketone (MVK) and methacrolein, the two major carbonyl products of the hydroxyl radical initiated oxidation of isoprene. However the measurement of carbonyl compounds larger than CH_2O, CH_3CHO, and $CH_3C(O)CH_3$ remains a problem. The tunable diode laser system remains the most reliable method for formaldehyde measurements but we have subsequently moved from the DNPH method, developed in the first stage of the previous RAC grant, to a GC/MSD based system. Measurements were only made with the DNPH system in the 1992 and 1993 field campaigns. Since we were not able to obtain reliable MVK and methacrolein data we have concentrated on the use of the measurements of the smaller carbonyls and the organic nitrates to yield further information on the radicals involved in the chemistry at the site. Such analysis has provided evidence for additional sources of these reactive carbonyl compounds, not presently in our model. For example, if we assume acetone and 2 propyl nitrate come only from the 2-propyl peroxy radical, then the concentrations of the stable products should have a constant ratio of 22.8, given by the branching ratio of the reaction with NO. A plot of acetone against 2 propyl nitrate is shown in Figure 9. It has a slope of 46 and an intercept of 2.4 ppbv. The large slope and the non-zero intercept suggest that there is an additional source of acetone. This may be either a direct emission source or an indirect production. In either case it does not involve the 2-propyl peroxy radical. We are continuing to look at such relationships, and with the development of the improved carbonyl measurement methodology more information will be available in future field programs.

II.iii.4 (Q4) Can we use the measurements of the organic nitrates to identify the organic radicals present at the site and assess their importance in local ozone production?

Since the nitrates are produced from the reaction of organic peroxy radicals with NO, the identification of the organic nitrate identifies the parent radical. This can give information on the dominant radicals undergoing reaction and point towards the most reactively important hydrocarbons. The purpose of this activity was to extend the capability to measure organic nitrates and use the measurements to improve our knowledge of factors controlling oxidant production.

Several groups are measuring alkyl nitrates but we are the only group that is able to identify and quantify hydroxynitrates. These are products of the reaction of hydroxyl radicals with alkenes, and since this reaction is faster than the corresponding alkane reaction these nitrates were thought to be potentially very important. We undertook measurements in both the 1992 and 1993 Hastings field studies.

We found very similar distributions among the alkyl nitrates in both of the 1992 and 1993 measurement campaigns. In 1993 we attempted to improve our time resolution, however this resulted in a number of the hydroxy nitrate measurements being below the detection limit. Figure 10 shows the concentrations of the alkyl and hydroxy nitrates measured in 1992 and the alkyl nitrates measured in 1993. Clearly the smaller nitrates are more abundant than the larger nitrates in all sets. The alkyl nitrates represent over 80% of the identified organic nitrates although, as only 4 hydroxy nitrates were quantified, it is reasonable to assume that more hydroxy nitrates may be present.

Our technique allows us to quantify alkyl nitrates concentrations for species that are passed by the chromatographic column. This is because the luminol detector ensures we are only measuring organic nitrates and has the same response to all such nitrates. Inclusion of these additional nitrates increases the total organic nitrate concentration over that from the identified nitrates by up to 8%. There is one major remaining concern, in that we may not be measuring the most important nitrates. Preliminary laboratory studies have shown that the

nitrates resulting from isoprene oxidation are not stable to the analytical procedure used here. This prevents us from assessing the importance of the radicals from ispoprene and may cause us to severely underestimate the total organic nitrate loading. The 1-D model calculations suggest the isoprene nitrates could contribute as much as all other organic nitrates combined. We are continuing to improve our analytical method to measure the concentrations of these nitrates.

We can infer the presence of a range of organic peroxy radicals from their production of organic nitrates, but in addition we can determine the relative amounts of the peroxy radicals that have been active in the airmass, from these measurements and the known branching ratio for the reaction

$$RO_2 + NO \rightarrow RONO_2$$

$$RO_2 + NO \rightarrow RO + NO_2$$

Figure 11 shows the relative concentrations of these radicals and the radical concentration, as with the nitrates themselves, decreases as the size of the R group increases. It appears that the 4 identified hydroxy peroxy radicals contribute about 37% to the total peroxy radical concentration.

We can also assess the importance of the various radicals in ozone production. A plot of the total organic nitrate concentration against that of ozone will be a straight line with the slope being the average branching ratio for the reaction above, in the air mass being sampled. Since the branching ratio increases monotonically with the sizze of the R group, comparison with the known branching ratios for specific peroxy radicals, this will yield information on the average size of the peroxy radical responsible for ozone production. Figure 12 shows this plot for the 1993 data. The slope is 2.1×10^{-3}, which shows that the bulk of NO oxidation is performed by the CH_3O_2 or HO_2 radicals, consistent with the chain length of 11 determined in section II.iii.1 above.

II.iii.5 (Q5) Can we gain new insights on the "nitrogen shortfall" observed at other sites?

In many studies, (eg. Ridley et al 1991, Parrish 1993) the sum of all the measured nitrogen species (usually NO, NO_2, HNO_3, PAN) is significantly less than the total NO_y measured independently. This shortfall can be as high as 20% of the total odd nitrogen present. Given the importance of nitogen oxides in the chemistry of ozone, the possible presence of an additional reservoir of nitrogen is cause for investigation.

Figure 13 shows the average ratios of NO_x, PAN, HNO_3 and their sum, to NO_y for the 1993 Hastings data. These data show that within our ability to measure these concentrations, there is no shortfall at this site. It should be pointed out that we lack sufficiently high time resolution in the HNO_3 data to be able to comment further.

Organic nitrates have been postulated as a possible reservoir species in previous studies, although the contribution has only been found to be 1-2% of the total NO_y. With our ability to measure a wider range of nitrates than other groups we specifically investigated their contribution. Figure 14 shows the measured fractional contribution of the organic nitrates to NO_y. Including all the nitrates measured, whether identified or not, yields a nitrate contribution 0.5-4.9%, with the maxima in the daytime. This reaches as high as double that previously reported, but still represents a small contribution to the total NO_y. Excluding the possible impact of the nitrates resulting from isoprene oxidation, organic nitrates are not a significant reservoir of NO_x in this environment.

II.iii.6 (Q6) Does the PAN contribution to NO_y depend on the extent of isoprene chemistry?

Comparison of the EMEFS data for the ratio PAN/NO_y with regional oxidant model output indicates that the models significantly (eg. ~2x) overestimate this ratio in rural areas. One possible explanation is that the models overestimate the production of PAN precursors from the oxidation of isoprene. We proposed to compare our 1-D model output with the observed PAN/NO_y ratio to help us gain insight into this problem. No improvement in our

understanding has resulted from looking into this question.

II.iii.7 (Q7) Can we explain the H_2O_2 production and/or concentration from the radical measurements?

Hydrogen peroxide is an important oxidant in the atmosphere, eg. in the aqueous phase oxidation of SO_2. In addition it is an extremely good indicator of the presence of hydroperoxy radicals as their self reaction is the only atmospheric gas phase source via.

$$HO_2 + HO_2 \rightarrow H_2O_2$$

The radical detector measures the concentration of all peroxy radicals, but the results from II.ii.1 and II.iii.4 above show that most of these are HO_2 radicals. Therefore, similarly to section II.iii.2, we can determine an upper limit on the local rate of hydrogen peroxide production from this concentration and the known rate coefficient for the reaction:

$$\frac{d[H_2O_2]}{dt} = k[HO_2]^2$$

The ambient H_2O_2 measurements from the tunable diode laser system can be used to determine the real increase in concentration.

This analysis is similar to that for ozone production above. The hydrogen peroxide data are more limited so there are only 6 days on which it can be undertaken. Figure 15 shows the data used in the analysis and Table 4 provides a summary. As with the ozone production rate analysis, this shows that there is insufficient chemistry at the site to explain the production of H_2O_2. The local production rate averages 15% and ranges from 5 to 26%of the measured increase. Hence we conclude that over 75% of the hydrogen peroxide observed is being produced in an environment of higher radical concentrations and advected to the site.

II.iii.8 (Q8) Is the presence of atmospheric aerosol impacting the radical chemistry at the site?

Two activities were undertaken related to this question. In the first we undertook the development of an instrument to measure the rate of photolysis of ozone to give $O(^1D)$. In the second we made detailed particulate measurements at the Hastings site during the 1993 intensive.

We were concerned about the radical balance at the site. Initial model calculations predicted much higher concentrations than we had measured with the radical detector. This suggested that either the model was producing radicals at a faster rate than was achieved in the atmosphere, or that there was an addiational radical removal process in the atmosphere that was not included in the model. We examined two aspects of this problem. In the first we wanted to be able to measure the rate of radical production, in the second we wanted to examine possible loss of radicals through interaction with atmospheric aerosol.

In the Hastings area the major radical source is ozone photolysis at wavelengths below 320 nm.

$$O_3 + h\nu \rightarrow O_2 + O(^1D)$$
$$O(^1D) + H_2O \rightarrow 2HO$$

To better define the rate of radical production, it is necessary to measure the ozone photolysis rate, J_{O3}, and the water concentration. The water concentration is easily measured but that is not the case for J_{O3}.

An instrument that measures J_{O3} by exposing known concentrations of ozone to sunlight was built. In this instrument the $O(^1D)$ produced is reacted with N_2O to produce NO, which reacts with the excess ozone to produce NO_2. The NO_2 concentration is measured and so the value of J_{O3} is determined. The values obtained by the instrument, on the roof of the Petrie building at York, were consistently higher than model predictions. This may be due to the neglect of a long tail at the long wavelength end of the ozone absorption in the calculations. We were not able to reconcile these differences in time for the field study and still have insufficient model determinations of J_{O3} to fully reject instrumental artifacts as the cause of this

discrepancy.

In the second thrust of this work we made extensive measurements of the aerosol concentration distribution as part of the 1993 study. In many cases the total particulate concentration follows the indicators of urban pollution. Of more interest to us has been the possible photochemical production of new aerosol. Of particular interest are the intensive days of August 25-27 1993. Figure 16 gives the particle and related gas phase concentrations for these days. August 25 is a typical day with a small amount of ozone production, but by no means an ozone event day. It does, however, show a very interesting aerosol behaviour. While the oxidant related species (O_3, NO_x, CO and radicals) are not changing, there is a large increase in the nucleation mode particles associated with an increase in SO_2 near mid day (see Figure 16a). These data appear to imply a nearby emission of SO_2 and local particle formation when high concentrations of SO_2 are introduced into a photochemically active air mass. This is the system that is being examined using the 1-D model. For the more photochemically active days, August 26-27 where the ozone reached 100 ppbv, there are no incursions of SO_2 and no rapid increases in new particle formation. However, in the mornings there is a constant number of particles in the accumulation mode but a variable number in the nucleation mode. This indicates a local source of the smaller particles. This appears to be due to gas to particle conversion, especially on the 27th where the median diameter of the short lived nucleation mode particles steadily increases with time. The thunderstorm of August 27 provided an interesting experiment as it rapidly depleted the total particle number. Following the storm the total volume grew back gradually, consistent with local nucleation after washout of the existing particles.

It is clear that our understanding of the factors governing the aerosol concentrations and size distributions is well behind that for the gas phase species. The observations made here implicate the aerosols in the photochemical processes and point to the need for more detailed study.

II.iii.9 Indicators of ozone-NO_x-hydrocarbon sensitivity

From even the most naive modelling it is clear that the control of ozone can be achieved by control of NO_x, hydrocarbons or both. Depending on the relative concentrations of these classes of compounds, it may be sufficient to control only one of these. In fact there is evidence that controlling the wrong class can have no impact on ozone concentrations, in spite of the huge financial investment. Recently Sillman (1995) has used a model to examine the ability of a number of indicator species to predict whether an air mass is in a NO_x or a hydrocarbon sensitive regime, i.e will a decrease in the concentration of one of these classes of compounds reduce the ozone concentration. He found that hydrocarbon-sensitive chemistry is linked to afternoon $NO_y > 20$ ppbv, $O_3/(NO_y\text{-}NO_x) < 7$, $HCHO/NO_y < 0.28$ and $H_2O_2/HNO_3 < 0.4$. Lower NO_y concentrations and higher ratios correspond with NO_x sensitive ozone. We have tested our data sets against these indicators and the results are in Figure 17. For each of these parameters we have plotted the mean diurnal profile for the study period along with the threshold from Sillman (1995). The nitric acid data is averaged over a six hour period so the use of these data may lead to misleading conclusions. Recognizing that HNO_3 is a product of NO_x oxidation, the substitution of the overall oxidation products NO_z ($NO_y\text{-}NO_x$) into the last ratio we see that H_2O_2/NO_z can be a useful surrogate. We have included this plot with a threshold value from Sillman's calculations of 0.25 indicated. All parameters indicate NO_x sensitivity throughout the day. This implies to control ozone in rural areas of Ontario, it is necessary to control NO_x.

While this supports the growing concensus in favor of NO_x control, one must be careful in the application of these results. It must be recognized that the measurements used in this analysis are made well away from the emission centres and that in the early stages of ozone production the controlling factors may be different. One needs to undertake this analysis at a number of different sites, of different chemical climatology, before a full picture of the best control strategy for the whole province can be determined.

III MEASUREMENT PROGRAM AT YORK UNIVERSITY

In modelling the impact of an urban plume at the Hastings site it was found that we needed a better understanding of the actual composition of the air mass leaving a Canadian urban centre. This arose from our use of the 1-D model in the Lagrangian mode where we need inputs that are different than those measured at Hastings. We undertook a measurement program at York to measure trace gas concentrations typical of suburban Toronto. From June to December 1994, we measured ozone, NO, NO_2, NO_y, CO, SO_2, UV radiation, and meteorological parameters from the roof of our laboratory building on the York campus. Professor Niki's group also measured hydrocarbons and CO over this period.

Figure 18 shows the average ozone concentration for each month from July to December 1994. Ozone exhibits a concentration minimum in the early morning, consistent with the presence of a nocturnal inversion under which ozone is lost to the surface or by reaction with freshly emitted nitric oxide (NO). The ozone concentration increases after the mid-morning break up of the nocturnal inversion, as air from above, which has not been depleted overnight, is mixed down. The ozone concentration reaches a maximum in the mid-afternoon, consistent with photochemical ozone production. The monthly averages show the highest concentrations in August and decreasing steadily until December, following the changes in mean daily temperature.

The nitric oxide concentrations are shown in Figure 19, whereas Figure 20 shows the ratio of NO_x (NO + NO_2) to NO_y (all nitrogen oxide compounds). Nitric oxide is a directly emitted pollutant which undergoes rapid reaction with ozone and so shows very low levels at night. In the morning it establishes a steady state concentration with NO_2 and there is a marked morning peak due to fresh emissions from rush hour traffic. The concentration then drops as the NO is dispersed upwards and remains low during the day. There is no evidence of an evening rush hour in the data. This is likely due to the stronger vertical mixing in the afternoon compared to the morning. NO_x shows a nighttime maximum, due to oxidation of the emitted NO by ozone and the trapping of emissions under the nocturnal inversion, and a daytime minimum. There is little difference in NO_x concentrations from August to September

despite the huge increase in local traffic due to the opening of the University. This is also seen in the hydrocarbon data of Prof. Niki's group. Thus we believe we are sampling air that is representative of a much larger region than just that of the local York University vicinity. The increase in NO_x through the fall into the winter therefore reflects the less efficient mixing as the solar radiation decreases. The NO_x to NO_y ratios remain close to unity showing that the atmospheric composition is still dominated by fresh emissions and there has been insufficient time for the NO_x emissions to be oxidized to nitrates.

The monthly average carbon monoxide concentrations for July through October are shown in Figure 21. They show a similar profile to NO. This is expected as they are both directly emitted from automobile exhaust. The CO concentration is higher at night than in the daytime but the most notable feature is the morning rush hour peak. This coincides with the NO maximum and the ozone minimum. The peak is more noticeable than in the NO data as there is no reactive loss of CO as there is with NO. The daytime values show a small variation from month to month but there is no obvious trend.

Figure 22 shows the correlations between CO and NO_x for each of the months studied. These are two of the major contributors to ozone production so their ratio is important in determining which is dominant in controlling ozone production. Since they are primarily produced from automobile exhaust, most models have a constant ratio of these two species in the emission inventories for mobile sources. Since the measurements of CO and NO_x concentration are so strongly correlated and appear to be dominated by fresh emissions, the slopes of these plots should represent the raw ratio of the emissions. The values range from 5 to 16 ppbv(CO)/ppbv(NO_x). The value assumed in the emission inventories and found in measurements in Colorado (Parrish et al. 1991) suggest a CO/NO_x ratio of 10 is indicative of fresh combustion emissions, consistent with our observations. However, Fujita et al. (1992) measured morning values in the Los Angeles area of around 20 and ascribed this value to fresh emissions. At Hastings we have consistently found a ratio of around 20, which would be consistent with the aging of the air mass from the Golden Horseshoe.

It is particularly notable that, although the slopes are consistent, the intercepts of the

plots in Figure 22 are different for each month, and there appears to be more than one line in any one month. This we interpret to be due to air from different source regions bringing different background concentrations into the region as the mean wind direction changes. Air from the northern quadrants has spent less time over urban sources so would have lower CO concentrations compared to that from the south, where it would receive emissions from the Golden Horseshoe area.

Figures 23 and 24 show the plots of ozone against NO_y and NO_y-NO_x as plotted in Figure 4. In the rural area there was a positive correlation with a slope of 10-12, indicating the production of ozone. In the city the plots have a zero or negative slope indicating that there is insufficient time for ozone production. The only nitrogen oxide chemistry observed is the loss of ozone by titration with the freshly emitted NO.

$$NO + O_3 \rightarrow NO_2 + O_2$$

It is not until the air mass has had time to age that the NO_2 photolysis and radical chemistry can produce ozone.

We now have a much better measure of the ozone precursor concentrations and we also know that there is essentially no ozone production in the Toronto area itself. These data have been used in some of the 1-D model runs.

References

Fujita E.M., Croes B.E., Bennett C.L., Lawson D.R., Lurmann F.W., and Main H.H. (1992) Comparison of emission inventory and ambient concentration ratios of CO. NMOG, and NO_x in California's south coast air basin. *J. Air Waste Manage. Assoc.* **42,** 264-276.

Kleinman L., Lee Y-N., Springston S.R., Nunnermacker L., Zhou X., Brown R., Hallock K., Klotz P., Leahy D., Lee J.H., and Newman L. (1994). Ozone Formation in a Rural Site in the Southeastern United States. *J. Geophys. Res.* **99**, 3469-3482.

Olszyna, K. J., Bailey, E. M., Simonaitis, R., and Meagher, J. F. (1994) O_3 and NO_y relationships at a rural site. *J. Geophys. Res.* **99**, 14,557-14,563.

Parrish D.D., Trainer M., Buhr M.P., Watkins B.A., and Fehsenfeld F.C. (1991) Carbon monoxide concentrations and their relation to concentrations of total reactive oxidized nitrogen at two rural U.S. sites. *J. Geophys. Res.* **96**, 9309-9320.

Parrish D.D., Buhr M.P., Trainer M., Norton R.B., Shimshock J.P., Fehsenfeld F.C., Anlauf K.G., Bottenheim J.W., Tang Y.Z., Wiebe H.A., Roberts J.M., TannerR.L. , Newman L., Bowersox V.C., Olszyna K.J., Bailey E.M., Rodgers M. O., Wang T., Berrensheim H., Roychowdhury U. K., and Demerjian K.L. (1993) The total reactive oxidized nitrogen levels and the partitioning between the individual species at six rural sites in eastern North America. *J. Geophys. Res.* **98**, 2927-2939.

Ridley B. A. Recent Measurements of Oxidized Nitrogen Compounds in the Troposphere. *Atmos. Environ.* **25A**, 1905-1926 (1991).

Sillman S., The use of NO_y, H_2O_2, and HNO_3 as indicators for ozone-NO_x-hydrocarbon sensitivity in urban locations *J. Geophys. Res.* **100** 14,175-14,188 (1995)

Trainer M., Parrish D.D., Buhr M.P., Norton R.B., Fehsenfeld F.C., Anlauf K.G., Bottenheim J.W., Tang Y.Z., Wiebe H.A., Roberts J.M., Tanner R.L., Newman L., Bowersox V.C., Meagher J.F., Olszyna K.J., Rodgers M.O., Wang T., Berrensheim H., Demerjian K.L., and Roychowdhury U.K. (1993) Correlation of ozone with NO_y in photochemically aged air. *J. Geophys. Res.* **98**, 2917-2925.

Figure Captions

Figure 1. Average diurnal variation of the measured species for the full 1993 field study. a. ozone, b. NO, c. NO_2, d. NO_x ($NO+NO_2$), e. NO_y (all odd nitrogen) f. PAN, g. HNO_3, h. CO, i. radicals, j. CH_2O, k. H_2O_2, l. SO_2, m. Temperature, n. Relative humidity, o. Solar radiation.

Figure 2. Average diurnal variation of the fraction of NO_y present as NO_x.

Figure 3. Comparison of the radiometer data for the 1992 and 1993 field studies.

Figure 4. Plots of ozone against nitrogen parameters for the daytime data from both field studies.
a. Ozone versus NO_z (NO_y-NO_x) for 1992, b. Ozone versus NO_z (NO_y-NO_x) for 1993, c Ozone versus NO_y for 1992 d. Ozone versus NO_y for 1993.

Figure 5. Plots of ozone against NO_z (NO_y-NO_x) for the daytime data from the 1993 field study broken into high and low ozone cases.

Figure 6A. Ozone and NO_x data for the 5 days in which there is an incursion of polluted air in the late afternoon.

Figure 6B. Ozone and NO_x data for the 3 days in which there is no incursion of polluted air in the late afternoon. These data are used for comparison with the data in Figure 6A.

Figure 7A. NO_x/NO_y and O_3/NO_z plots for the 5 days in Figure 6A.

Figure 7B. NO_x/NO_y and O_3/NO_z plots for the 3 days in Figure 6B.

Figure 8. Diurnal plots of ozone, for three days in which the ozone production can be compared with that for the radical data, and the corresponding ozone production rate from the radical data. Nineteen such periods were examined.

Figure 9. Plot of acetone against 2 propyl nitrate.

Figure 10. Concentrations of the organic nitrates.

Figure 11. Relative abundances of the peroxy radicals, obtained from the organic nitrate measurements.

Figure 12. Plot of the organic nitrate concentration against that of ozone. The slope is the average branching ratio for the reaction of the peroxy radical with NO.

IV PERSONNEL

This project builds on the previous SONTOS projects supported by the Ministry. While the number of people actually working on the data in the last year is small, a large group of people have been involved in the project. All such people, in addition to the investigators, are included here. Those involved in this activity in the last year are asterisked.

Post-Doctoral Fellows
K. Muthuramu (organic nitrate synthesis)
C. Hao (organic nitrate instrumentation)

Technicians
Sangeeta Sharma (instrument maintenance and database management)
Walter Polesel (instrument maintenance)
Karen So (PAN instrument testing and calibration)
Kumar Jaipersaud (data analysis, instrument maintenance and calibration)
*Julie Narayan (data analysis)
Anna-Pearl Sirju (Carbonyl Measurements and data analysis)

Graduate students
*Corina Arias (RO_x Measurements)
Anna-Pearl Sirju (Carbonyl Measurements)
*Jason O'Brien (Nitrate technique development)
Sydney Peel (1-D modelling)
*David Plummer (1-D modelling)
*Bart Verheggen, Wageningen Agricultural University, the Netherlands (1-D modelling)

Undergraduate Project Students
E. Frankford (Physical properties of organic nitrates)
Eileen Dahl (RO_x measurements)
Ulrike Gambert (LMA-3 interferences)
Jason O'Brien (Nitrate technique development)
Catherine Sutherland (Box Modelling)
Sonia Campagnolo (York Data)

Summer Students
Craig Stroud
Rob Nikifork
Zahra Hassanloo
Sonia Campagnolo
Emma Kerjekian
*Jennifer Wilson

V CONFERENCE PRESENTATIONS RESULTING FROM THIS PROJECT

Atmospheric Radical Measurements (C. Arias and D.R. Hastie), AGU Meeting, San Francisco, December 1992.

SONTOS Case Study: 6 August 1992 (N.W. Reid, H. Niki, D.R. Hastie, P.B. Shepson, P. Roussel, O. Melo, G. Mackay, I. Drummond, H. Schiff and L. Poissant), Presented at Regional Photochemical Measurement & Modeling Studies - International Conference, San Diego, 1993.

SONTOS Case Study: 22 and 23 August 1992 (N.W. Reid, H. Niki, D.R. Hastie, P.B. Shepson, P. Roussel, O. Melo, G. Mackay, J. Drummond, H. Schiff and L. Poissant), Presented at Regional Photochemical Measurement & Modeling Studies - International Conference, San Diego, 1993.

Observation of O_3 and Precursor Levels at Two Sites Around Toronto, Ontario, During SONTOS (P.B. Roussel, X. Lin, F. Camacho, S. Laszlo, R. Taylor, O.T. Melo, P.B. Shepson, D.R. Hastie and H. Niki), Presented at Regional Photochemical Measurement & Modeling Studies - International Conference, San Diego, 1993.

Summertime NO_x, NO_y and Ozone in Rural Ontario, Results from SONTOS (D.R. Hastie, P.B. Shepson, P. Roussel, S. Laszlo and O. Melo), Presented at Regional Photochemical Measurement & Model Studies - International Conference, San Diego, 1993.

Radical Chemistry at the SONTOS Site in Rural Ontario (M.C. Arias, M. Mozurkewich, D.R. Hastie, R. Taylor and O. Melo), Presented at Regional Photochemical Measurement & Model Studies - International Conference, San Diego, 1993.

Impacts of Toronto Urban Emissions on Ozone Levels Downwind During a Case Study from SONTOS 92 (X. Lin, P.B. Roussel, S. Lazslo, R. Taylor, O.T. Melo, P.B. Shepson, D.R. Hastie and H. Niki), Presented at Regional Photochemical Measurement & Model Studies - International Conference, San Diego, 1993.

SONTOS Overview Analysis: Principal Component Analysis (L. Poissant, J.W. Bottenheim, N.W. Reid, H. Niki, D.R. Hastie, P.B. Shepson, P. Roussel, O. Melo, G. Mackay and H. Schiff), Presented at Regional Photochemical Measurement & Model Studies - International Conference, San Diego, 1993.

Modeling of Ozone Formation at a Rural Site in Southern Ontario (D. Plummer, J. McConnell, P. B. Shepson, D.R. Hastie and H. Niki), Presented at Regional Photochemical Measurement & Model Studies - International Conference, San Diego, 1993.

VI PAPERS RESULTING FROM THIS PROJECT

1. Preparation, Analysis, and Atmospheric Production of Multifunctional Organic Nitrates. Muthuramu K., Shepson P. B., and O'Brien J. M. *Environ. Sci. Technol.*,27 1117-1124 (1993)

2. Alkyl Nitrates and Their Contribution to Reactive Nitrogen at a Rural Site in Ontario. P. B. Shepson, K. G. Anlauf, J. W. Bottenheim, A. Wiebe, N. Gao, K. Muthuramu, and G. I. Mackay *Atmos. Environ.*, 27A 749-757 (1993).

3. A Laboratory and Field Investigation of the DNPH Cartridge Technique for the Measurement of Atmospheric Carbonyl Compounds. A-P Sirju and P. B. Shepson Accepted by *Environ. Sci. Technol.*, August 1994.

4. Summertime NO_x NO_y and Ozone at a Site in Rural Ontario: Results from SONTOS. D.R. Hastie, P.B. Shepson, N.W. Reid, P.B. Roussel and O.T. Melo. Submitted to *Atmospheric Environment*, Jan., 1994.

5. Impact of Toronto Urban Emissions on Ozone Levels Downwind - A Case Study. X. Lin, P.B. Roussel, S. Laszlo, R. Taylor, O.T. Melo, P.B. Shepson, D.R. Hastie and H. Niki. Submitted to *Atmospheric Environment*, Jan., 1994.

6. Observation of O_3 and Precursors Levels at Two Sites Around Toronto-Ontario, During SONTOS 92. P.B. Roussel, X. Lin, F. Camacho, S. Laszlo, R. Taylor, O.T. Melo, P.B. Shepson, D.R. Hastie and H. Niki. Submitted to *Atmospheric Environment*, Jan., 1994.

7. Measurements of Alkyl and Multifunctional Organic Nitrates at a Rural Site in Ontario. J.M. O'Brien, P.B. Shepson, K. Muthuramu, C. Hao, H. Niki, D.R. Hastie, R. Taylor and P.B. Roussel, *J. Geophys. Res.*, Jan., 1994.

8. The Southern Ontario Oxidant Study (SONTOS): Overview and Case Studies for 1992. N.W. Reid, H. Niki, D.R. Hastie, P.B. Shepson, P.B. Roussel, O.T. Melo, G.I. Mackay, J. Drummond, H.I. Schiff, L. Poissant and W. Moroz. Submitted to *Atmospheric Environment*, , Jan., 1994.

9. Radical Chemistry at the SONTOS Site in Rural Ontario. M.C. Arias and D.R. Hastie. Submitted to *Atmospheric Environment*, March 1994.

10. Modelling of Ozone Formation at a Rural Site in Southern Ontario. D. Plummer, J. C. McConnell, P.B. Shepson, D. R. Hastie, and H. Niki. Submitted to *Atmospheric Environment*, June 1994.

Table 1 Nitrogen Oxide and Oxidant parameters for cases of High and Low Ozone.

10:00 to 18:00	O3>80	O3<80	O3>50	O3<50
NOy	6.978	2.834	4.668	2.328
	std dev=0.775	std dev=1.593	std dev=1.571	std dev=1.380
NOx/NOy	0.218	0.273	0.255	0.285
	std dev=0.057	std dev=0.097	std dev=0.086	std dev=0.101
O3/NOz	16.045	22.512	19.479	23.762
	std dev=1.975	std dev=6.370	std dev=4.638	std dev=7.068
O3-20ppb/NOz	12.303	10.954	13.013	10.113
	std dev=1.489	std dev=3.870	std dev=2.934	std dev=4.004
CH2O/NOy	0.600	1.025	0.743	1.208
	std dev=0.130	std dev=0.486	std dev=0.289	std dev=0.492
NOz	5.456	2.108	3.439	1.656
	std dev=0.758	std dev=1.059	std dev=1.153	std dev=0.690
DATA POINTS	119	2613	810	2070

Table 2. Comparison of O_3/NO_z and NO_x/NO_y ratios for incursions of polluted air with no incursions of polluted air

		NOx/NOy		95%	O3/NOz		95%	(O3-20)/NOz		95%		TIME O
DATE	TIME	OBSERVED	Difference	C.L. (1.15)	OBSERVED	Difference	C.L. (1.15)	OBSERVED	Difference	C.L. (1.15)	MAX O3	MAX O3
AUG01	10:00-16:30	0.317			33.262			17.250			74.3	19:00
		std dev=0.086			std dev=7.431			std dev=3.392				
			-0.098	1.727		3.370	1.771		-3.974	0.495		
	16:35-20:00	0.415			29.892			21.224				
		Std dev=0.054			std dev=2.319			std dev=1.317				
AUG08	10:00-17:55	0.237			29.944			14.609			58.8	18:50
		std dev=0.073			std dev=5.538			std dev=3.355				
			-0.273	4.890		-2.628	0.743		-5.958	1.413		
	18:05-20:00	0.510			32.572			20.567				
		std dev=0.114			std dev=13.759			std dev=7.779				
AUG15	10:00-14:50	0.369			35.976			11.922			40	16:35
		std dev=0.061			std dev=8.414			std dev=3.255				
			-0.206	3.675		-17.296	6.892		-10.683	3.597		
	14:55-18:50	0.575			53.272			22.605				
		std dev=0.121			std dev=23.944			std dev=9.829				
AUG18	10:00-17:55	0.255			24.892			5.049			36.1	19:35
		std dev=0.061			std dev=5.391			std dev=2.374				
			-0.234	4.191		0.977	0.768		-4.436	0.709		
	18:00-20:00	0.489			23.914			9.485				
		std dev=0.218			std dev=11.283			std dev=5.470				
AUG26	10:00-13:45	0.404			37.795			17.207				
	&15:15-16:40	std dev=0.076			std dev=9.266			std dev=5.977				
			-0.208	3.707		-76.848	31.856		-58.149	25.546		
	13:50-15:10	0.612			114.643			75.356			56.7	14:30
	&16:45-20:20	std dev=0.201			std dev=208.998			std dev=137.04				

Table 2. (Cont.)

AUG05	10:00-16:00	0.369			37.223			9.786				
		std dev=0.153			std dev=10.137			std dev=4.468				
			-0.079			-2.769			-4.661			
	16:05-20:00	0.448			39.992			14.447				
		std dev=0.104			std dev=5.995			std dev=2.239				
AUG22	10:00-16:00	0.473			26.898			12.615				
		std dev=0.168			std dev=24.622			std dev=12.322				
			0.050			-2.304			-4.192			
	16:05-20:00	0.423			29.202			16.807				
		std dev=0.137			std dev=7.320			std dev=2.590				
AVGS	10:00-16:00	0.478			27.963			13.029				
		std dev=0.051			std dev=4.618			std dev=3.397				
			0.021			2.508			0.143			
	16:05-20:00	0.457			25.455			12.886				
		std dev=0.074			std dev=1.790			std dev=0.567				

END	START	END
16:30	16:35	20:00
17:55	18:05	20:00
14:50	14:55	18:50
17:55	18:00	20:00
13:45	13:50	20:20
15:10	15:15	
16:40	16:45	
16:06	16:12	19:50

	x	s	50% (0.67s)	90% (1.64s)	95% (1.96s	99% (2.58s)
	-0.002	0.055	0.037	0.091	0.108	0.143
	-0.855	2.385	1.598	3.912	4.676	6.155
	-2.903	2.163	1.449	3.547	4.239	5.579

	NOx/NOy	x+zs	x-zs	O3/NOz	x+zs	x-zs	(O3-20)/N	x+zs	x-zs
x=mean	-0.002			-0.855			-2.903		
s=std dev	0.055			2.385			2.163		
50% (0.67s)	0.037	0.035	-0.039	1.598	0.743	-2.453	1.449	-1.454	-4.352
90% (1.64s)	0.091	0.088	-0.093	3.912	3.057	-4.767	3.547	0.643	-6.450
95% (1.96s)	0.108	0.106	-0.111	4.676	3.820	-5.531	4.239	1.335	-7.142
99% (2.58s)	0.143	0.140	-0.145	6.155	5.299	-7.010	5.579	2.676	-8.483

Table 3. Observed and Calculated Ozone production rates.

DATE	TIME INTERVAL	OBSERVED OZONE INCREASE ppb/hr	CALCULATED OZONE INCREASE ppb/hr	PERCENTAGE CONTIBUTION OF THE CALCULATED OZONE INCREASE
Jul 15	14:15-19:35	0.92	0.71	78
Jul 21	13:00-17:15	0.99	0.41	41
Jul 22	09:30-16:55	0.46	0.37	79
Jul 23	09:35-14:55	1.44	0.27	19
Jul 24	11:20-13:40	2.33	0.52	22
Jul 25	11:05-14:35	2.27	0.58	25
Jul 31	12:20-18:10	0.47	0.30	64
Aug 05	10:00-12:10	1.44	0.13	9.3
Aug 05	12:20-15:00	1.18	0.19	16
Aug 06	08:45-13:45	3.23	0.23	7.3
Aug 08	10:40-13:20	2.86	0.48	17
Aug 11	08:30-12:25	0.85	0.27	32
Aug 11	12:40-16:30	1.45	0.45	31
Aug 12	12:30-16:45	1.48	0.21	14
Aug 19	10:30-13:10	1.76	0.53	30
Aug 22	11:00-18:05	3.09	0.78	25
Aug 26	12:05-13:55	2.32	0.52	23
Aug 26	15:10-16:40	2.32	0.64	28
Aug 27	10:00-14:30	7.46	0.58	7.8

Table 4. Observed and Calculated Hydrogen Peroxide production rates.

Date	TIME INTERVAL	OBSERVED $[H_2O_2]$ INCREASE ppb/hr	CALCULATED $[H_2O_2]$ INCREASE ppb/hr	PERCENTAGE CONTRIBUTION OF THE CALCULATED $[H_2O_2]$ INCREASE
Aug 10	12:30-16:30	0.219	0.056	26
Aug 11	12:30-16:30	0.178	0.036	20
Aug 12	10:00-14:30	0.129	0.007	5
Aug 13	10:30-14:30	0.190	0.010	5
Aug 25	11:30-15:30	0.047	0.012	24
Aug 27	08:30-13:00	0.182	0.015	8
Average		0.157	0.023	15

Table 5. Kinetic Data used for Calculation of Relative Abundance of the Peroxy Radicals, obtained from the Organic Nitrate Measurements.

Compound number	Organic nitrate	k_{OH} [a]	RO_2 yield, γ [b]	Branching ratio, α (k_{2a}/k_2) [f]
1	2-propyl nitrate	1.15×10^{-12}	0.693	0.042
2	1-propyl nitrate	1.15×10^{-12}	0.307	0.02
3	2-butyl nitrate	2.54×10^{-12}	0.853	0.09
3	isobutyl nitrate	2.34×10^{-12}	0.233	0.036
4	1-butyl nitrate	2.54×10^{-12}	0.147	0.036
5	3-pentyl nitrate	3.94×10^{-12}	0.354	0.131
6	2-pentyl nitrate	3.94×10^{-12}	0.551	0.129
7	1-pentyl nitrate	3.94×10^{-12}	0.095	0.052
8	3-methyl-2-butyl nitrate	3.90×10^{-12}	0.270	0.141
9	2-methyl-1-butyl nitrate	3.90×10^{-12}	0.094	0.056
10	3-methyl-1-butyl nitrate	3.90×10^{-12}	0.047	0.056
11	3-hexyl nitrate	5.61×10^{-12}	0.524	0.230
12	2-hexyl nitrate	5.61×10^{-12}	0.406	0.209
13	2-nitrooxyethanol	8.52×10^{-12}	1.00	0.01 [g]
14	1-nitrooxy-2-propanol	2.63×10^{-11}	0.333 [c,d]	0.019 [h]
15	2-nitrooxy-1-propanol	2.63×10^{-11}	0.618 [c,d]	0.022 [h]
16	3-nitrooxy-2-butanol	5.64×10^{-11} (*cis*) 6.40×10^{-11} (*trans*)	0.90 [e] 0.90 [e]	0.037 [i] 0.037 [i]
17	1-nitrooxy-2-butanol	3.14×10^{-11}	0.315 [d,e]	0.037 [g]
18	2-nitrooxy-1-butanol	3.14×10^{-11}	0.585 [d,e]	0.037 [g]
19	isoprene nitrates	1.01×10^{-10}	1.00	0.12 [j]

a. These are room temperature rate constants, in units of cm^3 $molecule^{-1}$ s^{-1}, for the reaction of OH radicals with parent hydrocarbons (from Atkinson (1989)).

b. For C_3-C_6 alkyl nitrate production, the RO_2 yield from respective alkanes was calculated as described by Atkinson (1987).

c. Assuming 5% of OH reaction by H-atom abstraction (see Atkinson (1989)).

d. Assuming 65% of OH addition to the terminal carbon (see Atkinson (1989)).

e. Assuming 10% of OH reaction by H-atom abstraction (see Atkinson (1989)).

f. The branching ratios for formation of C_3-C_6 alkyl nitrates are either experimentally obtained values or estimated values from Carter and Atkinson (1989).

g. Estimated value.

h. Shepson et al. (1985).

i. Muthuramu et al. (1993).

j. Tuazon and Atkinson (1990)

Figure 1a. Average diurnal variation of O_3 at Hastings 1993 field study.

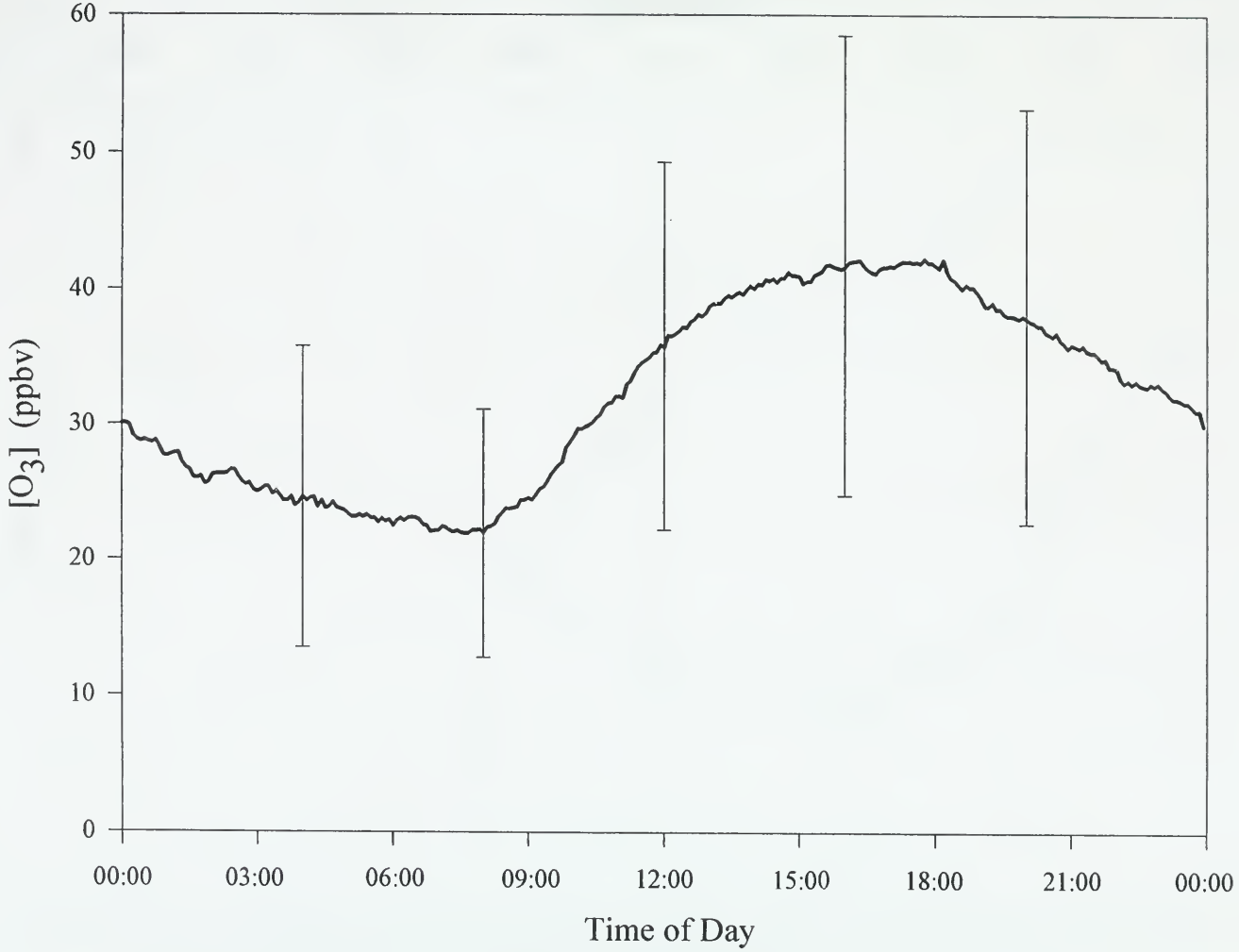

Figure 1b. Average diurnal variation of NO at Hastings 1993 field study.

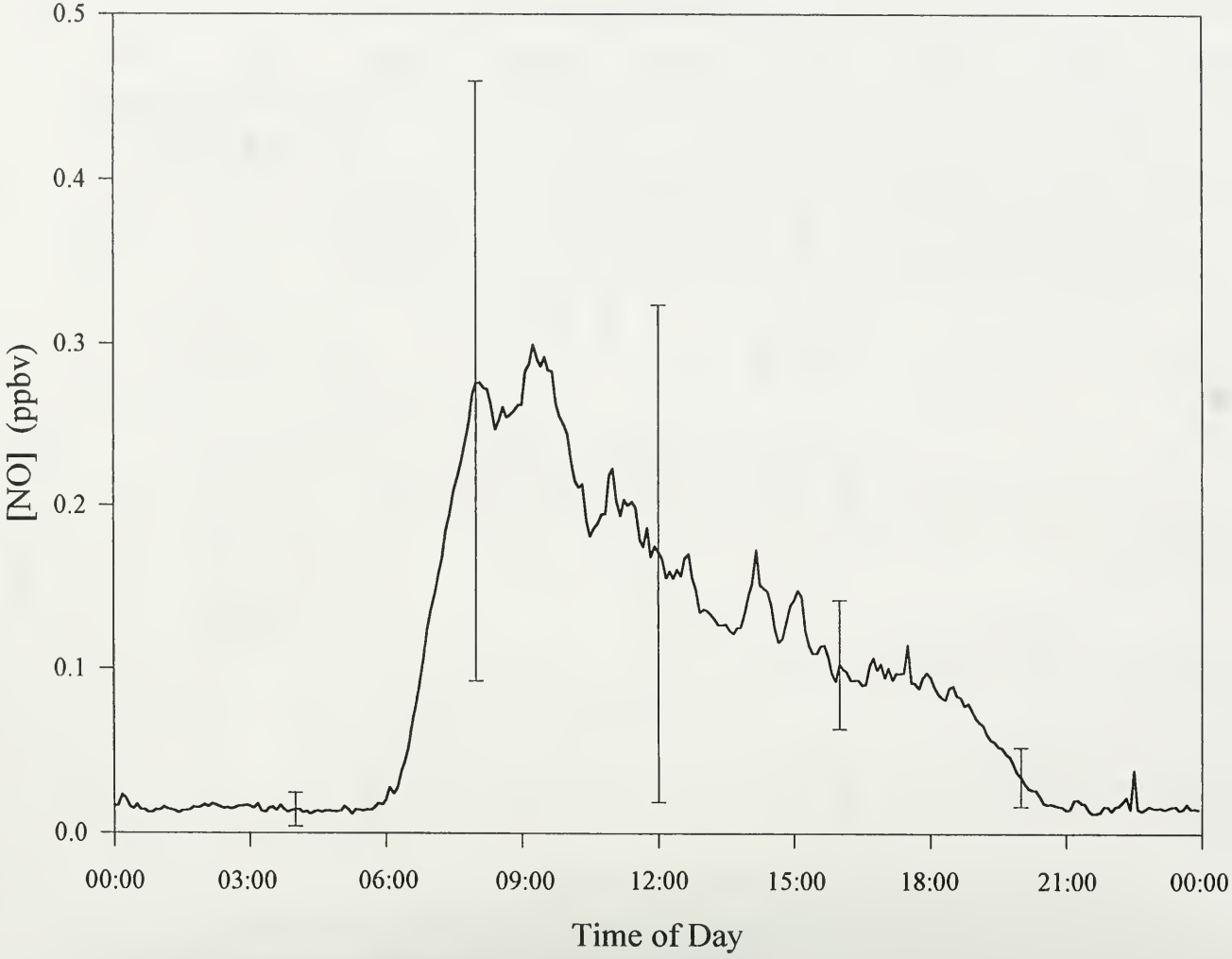

Figure 1c. Average diurnal variation of NO_2 at Hastings 1993 field study.

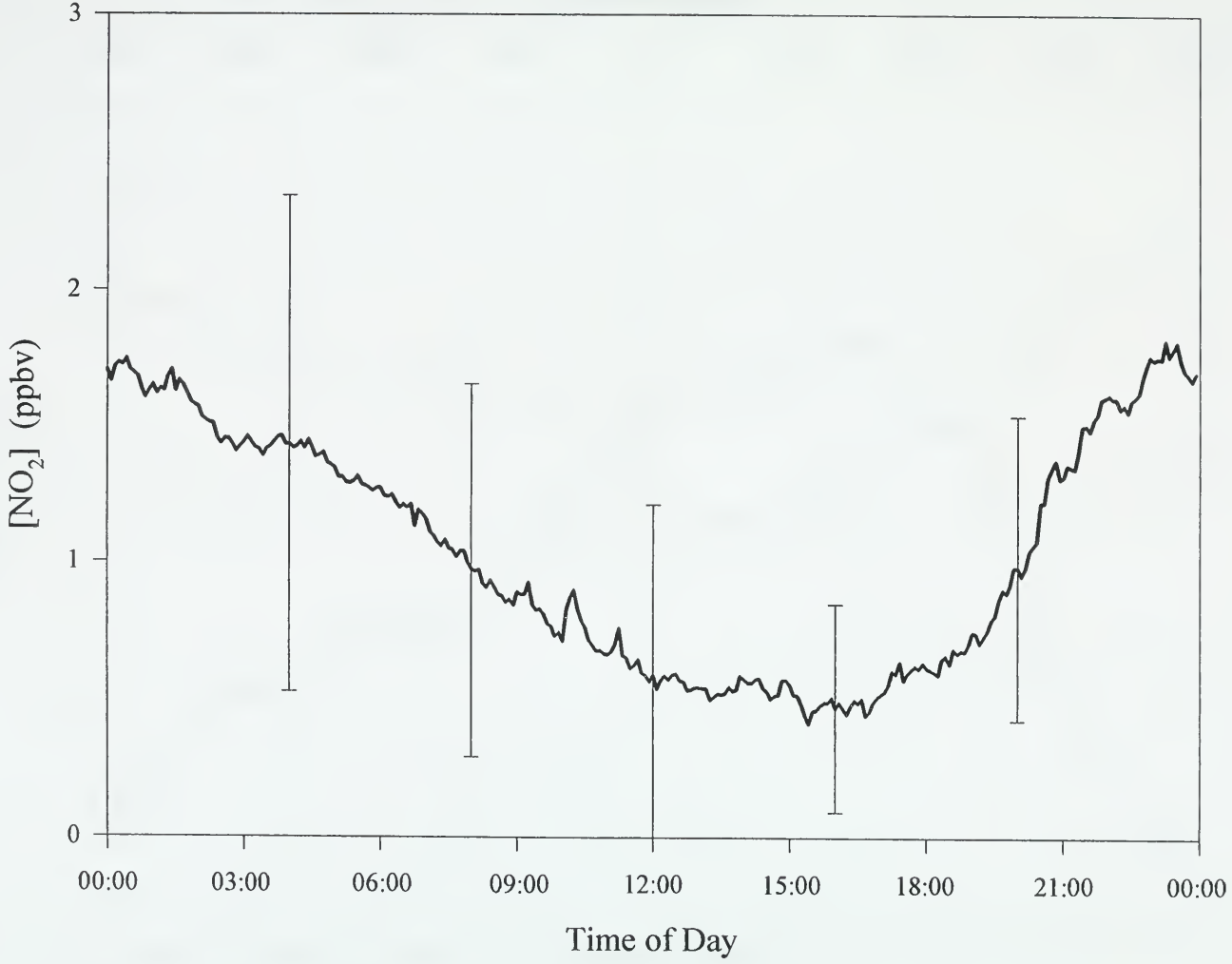

Figure 1d. Average diurnal variation of NO_x at Hastings 1993 field study.

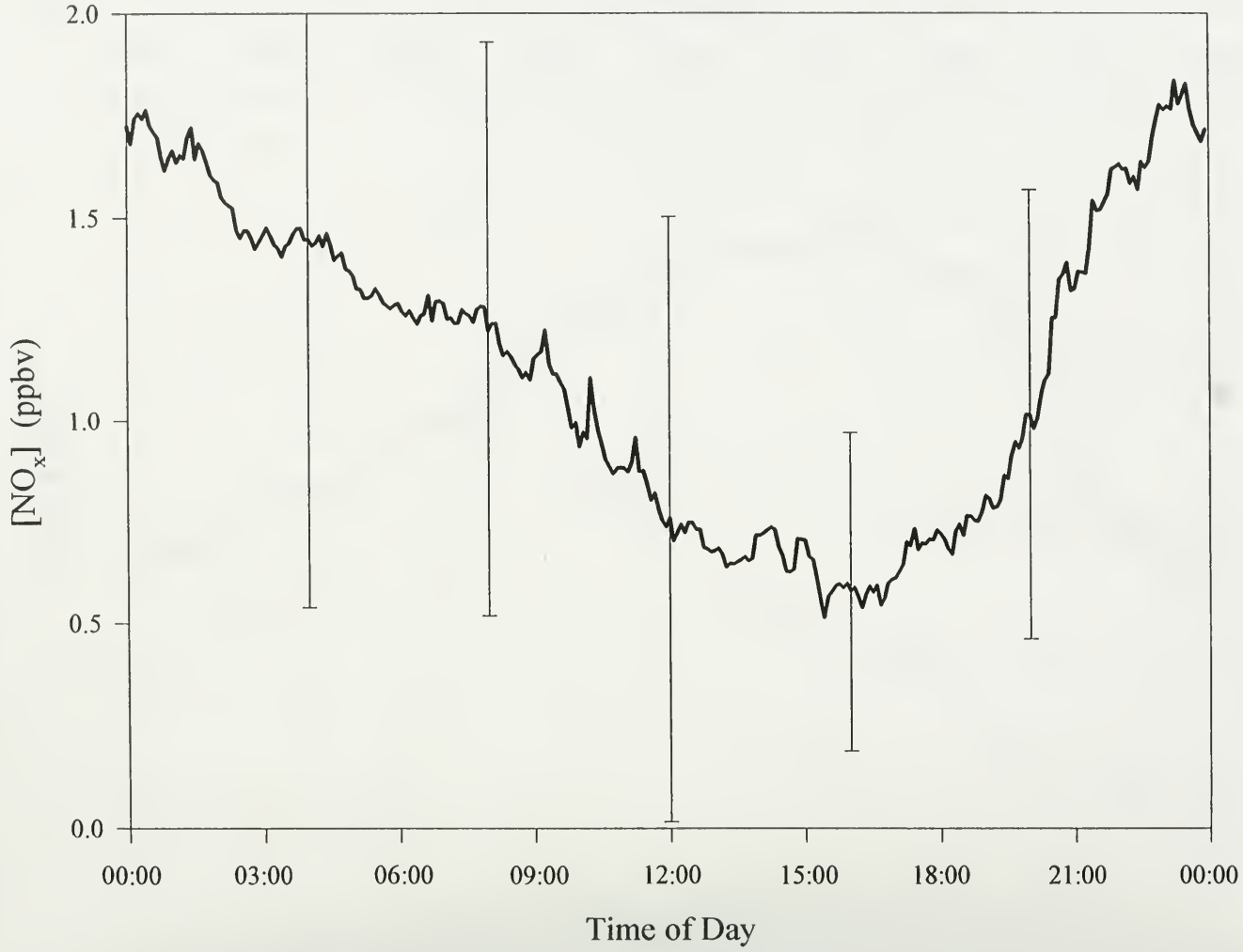

Figure 1e. Average diurnal variation of NO_y at Hastings 1993 field study

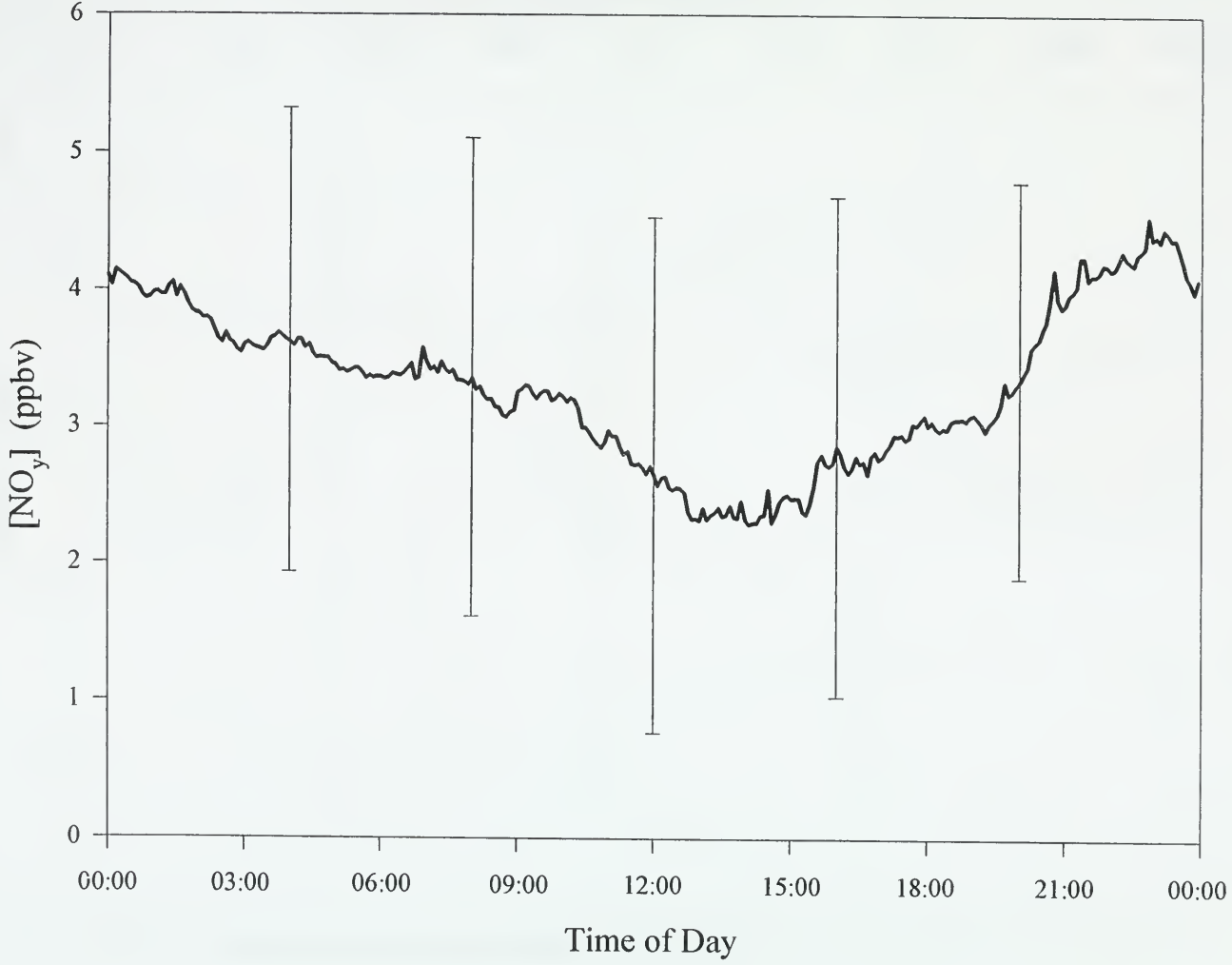

Figure 1f. Average diurnal variation of PAN at Hastings 1993 field study.

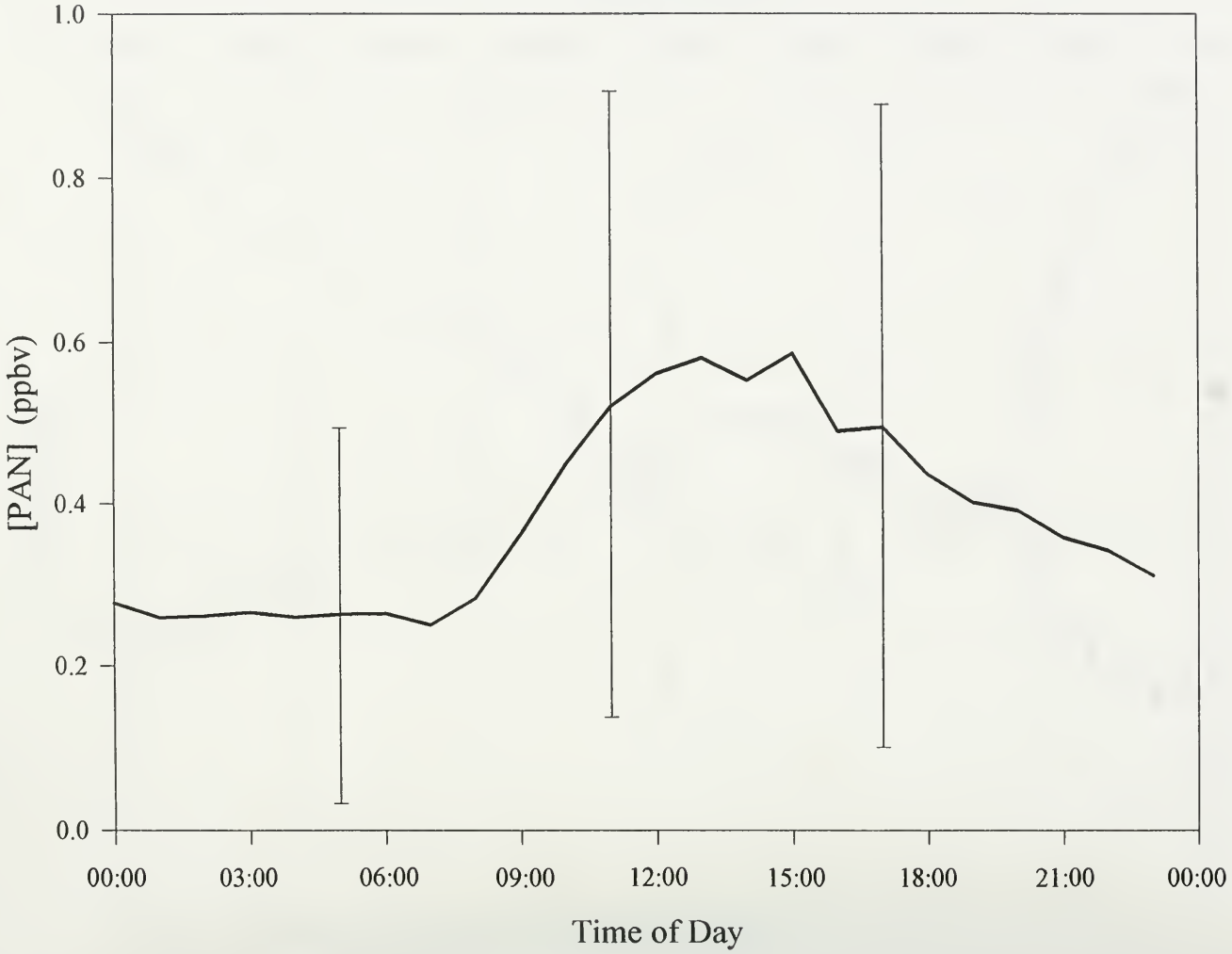

Figure 1g. Average diurnal variation of HNO_3 at Hastings 1993 field study.

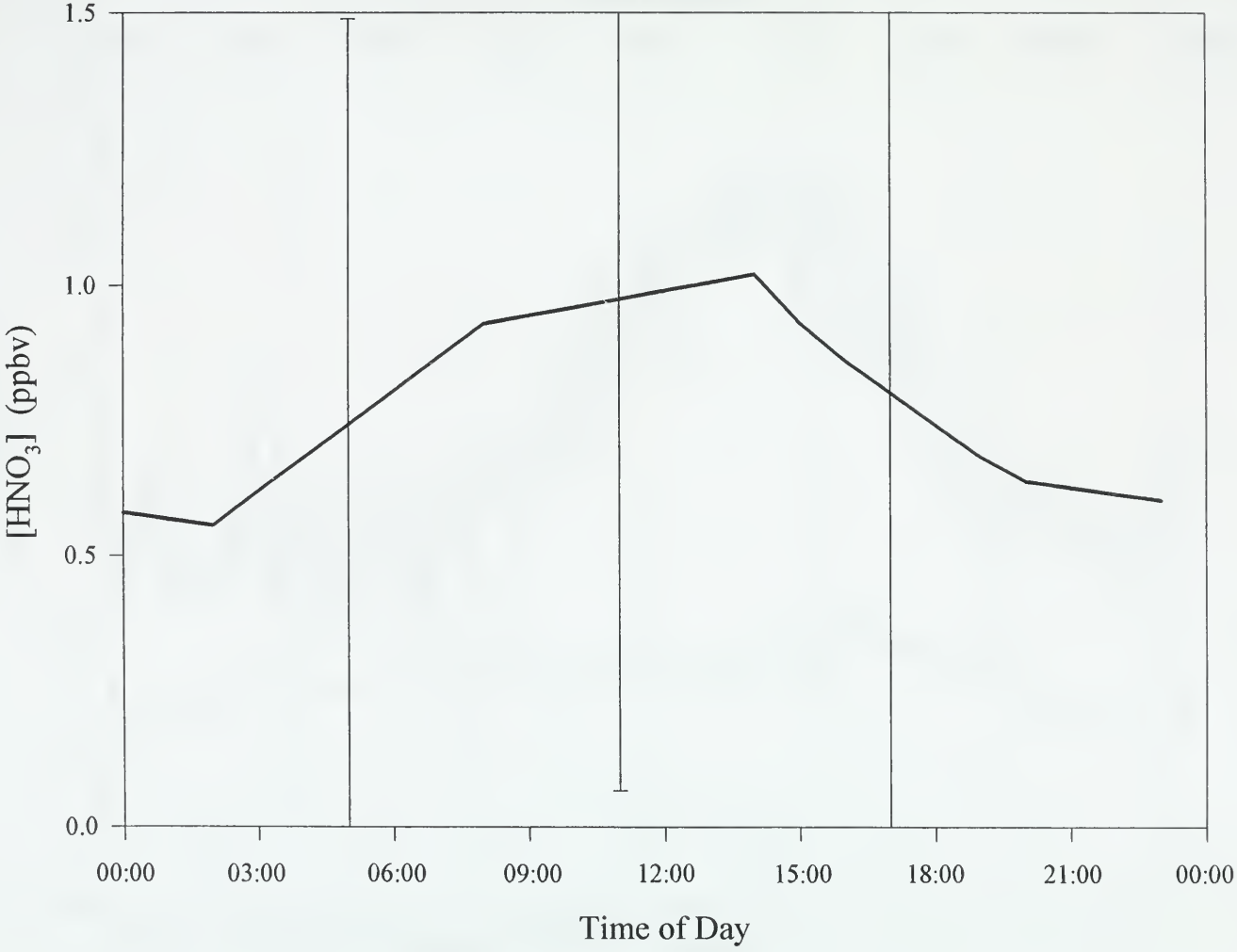

Figure 1h. Average diurnal variation of CO at Hastings 1993 field study.

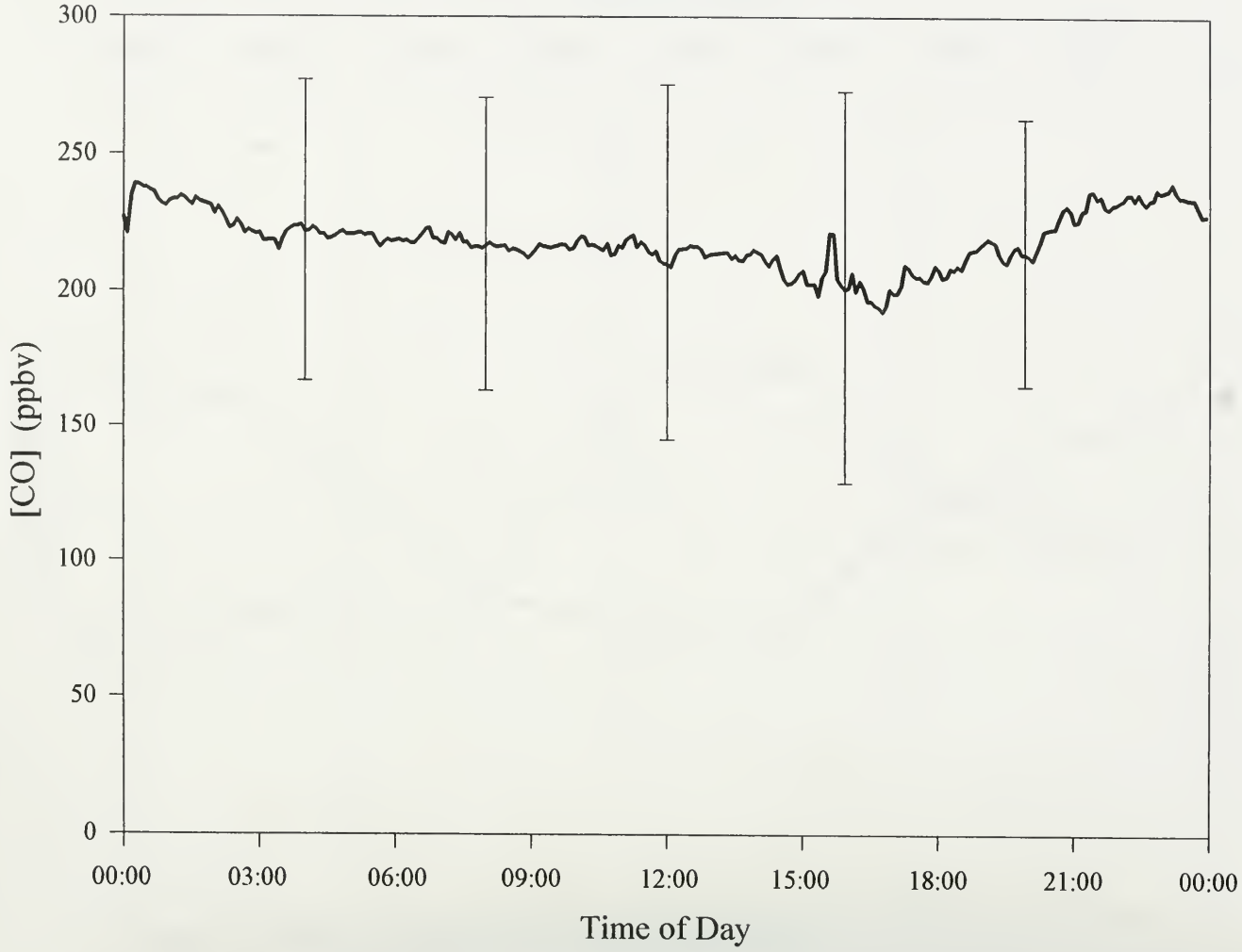

Figure 1i. Average diurnal variation of Radicals at Hastings 1993 field study.

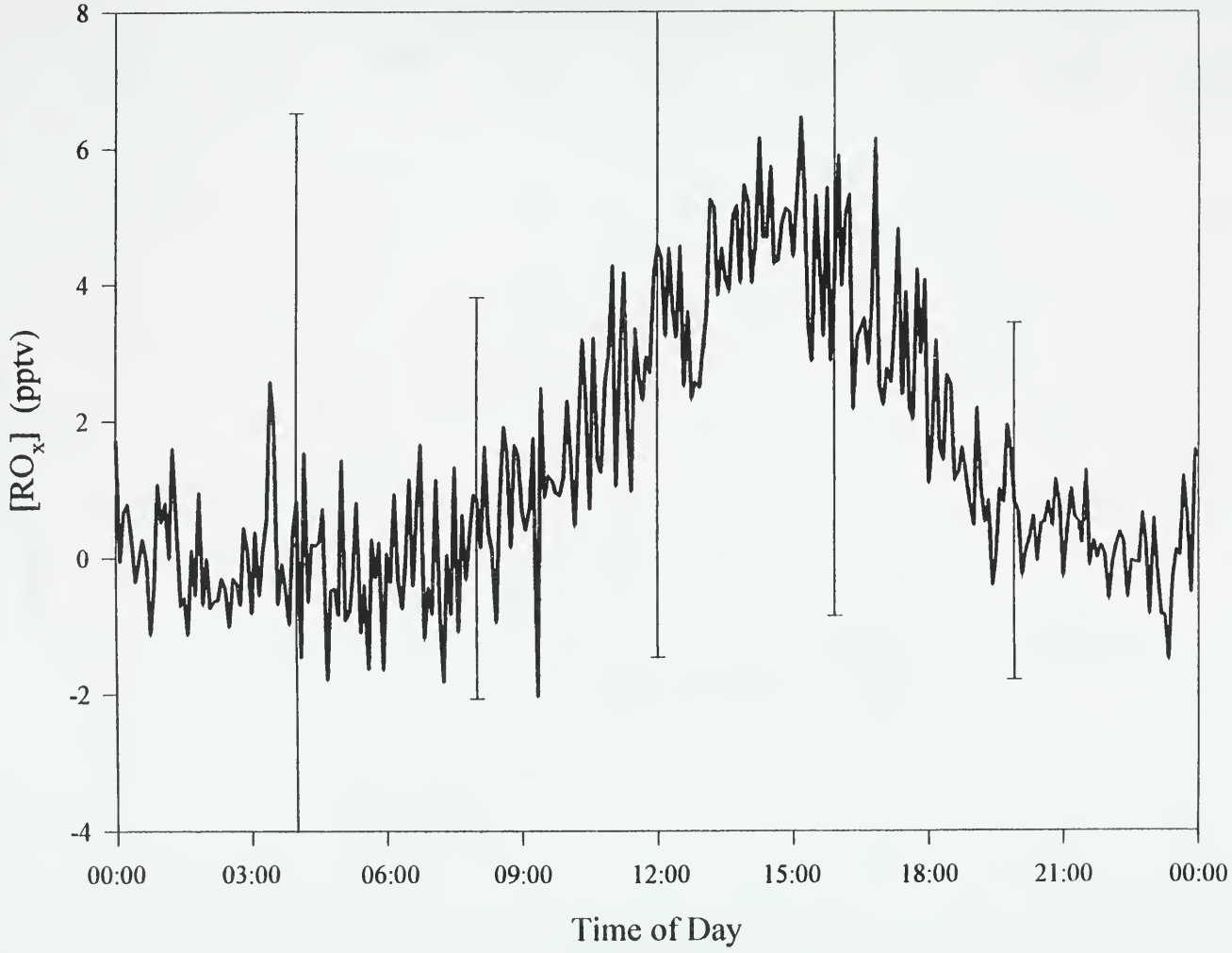

Figure 1j. Average diurnal variation of CH_2O at Hastings 1993 field study.

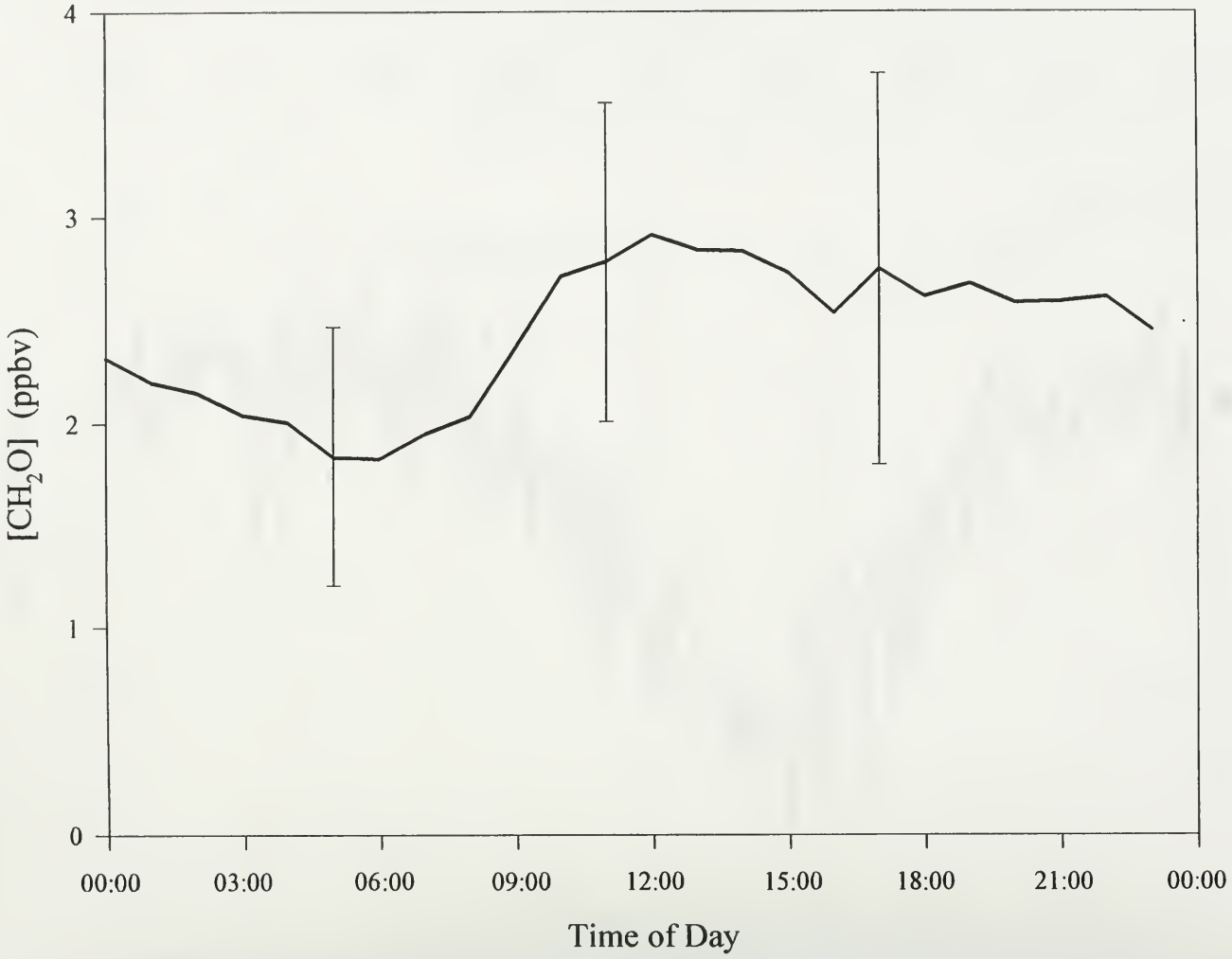

Figure 1k. Average diurnal variation of H_2O_2 at Hastings 1993 field study.

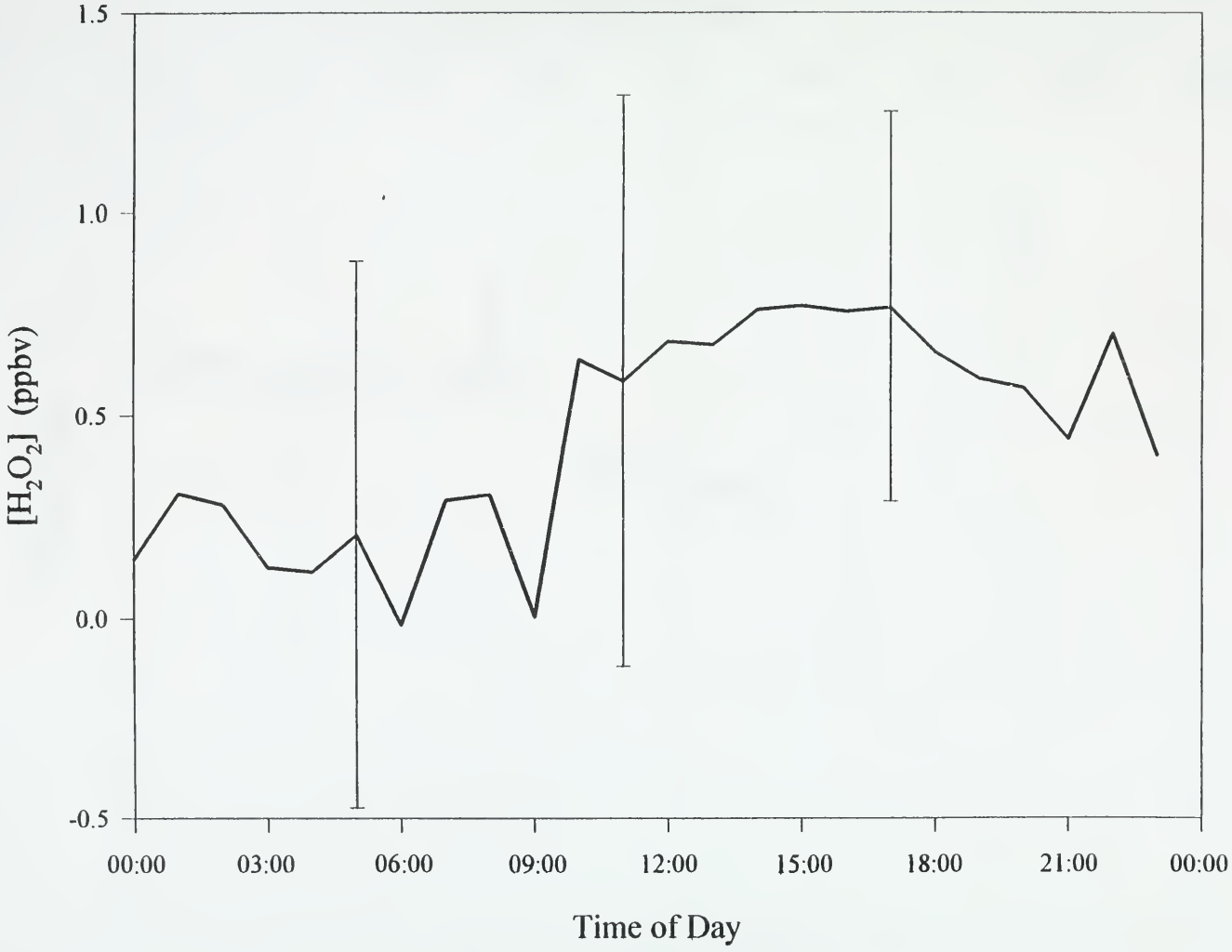

Figure 11. Average diurnal variation of SO_2 at Hastings 1993 field study.

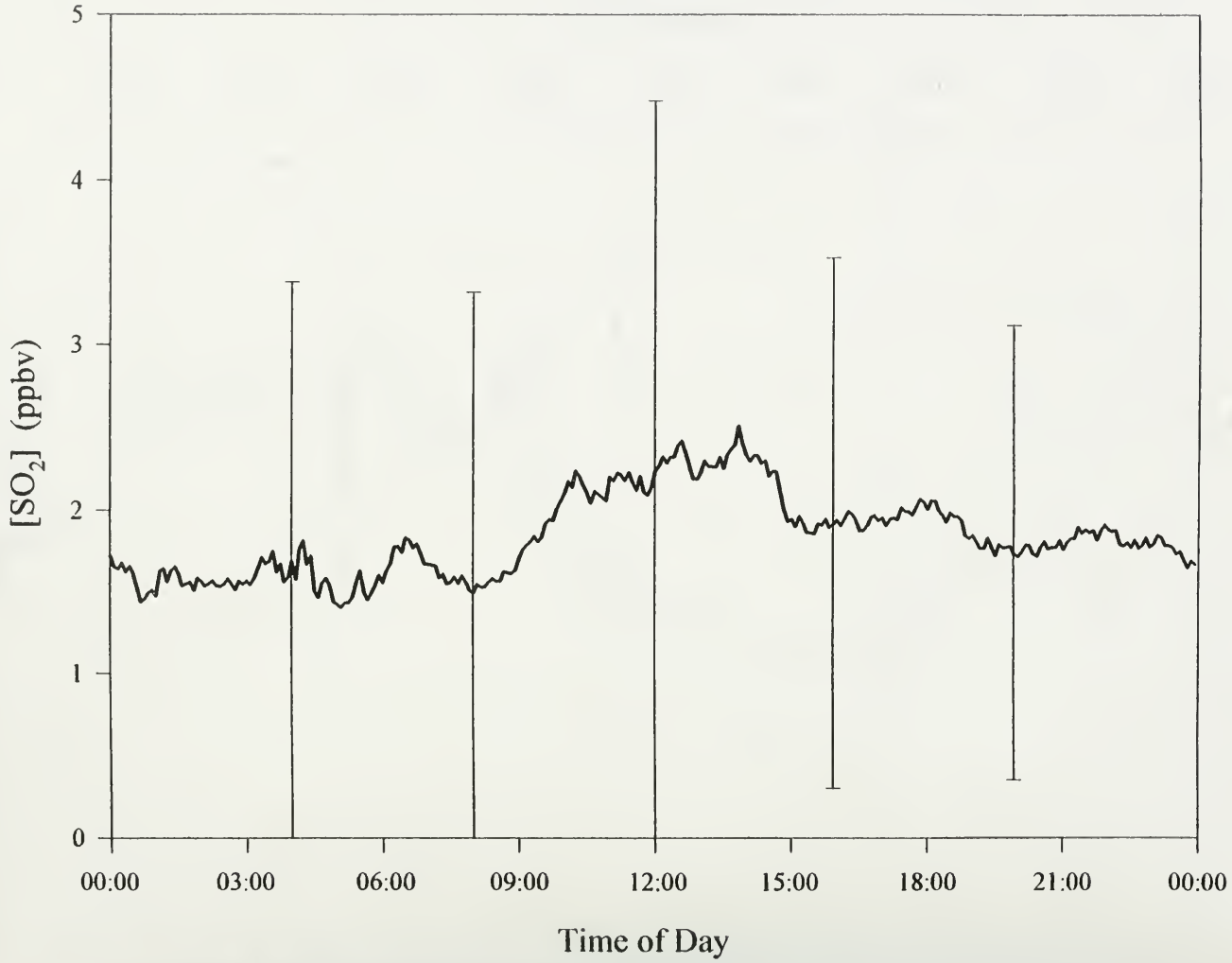

Figure 1m. Average diurnal variation of Temperature at Hastings 1993 field study.

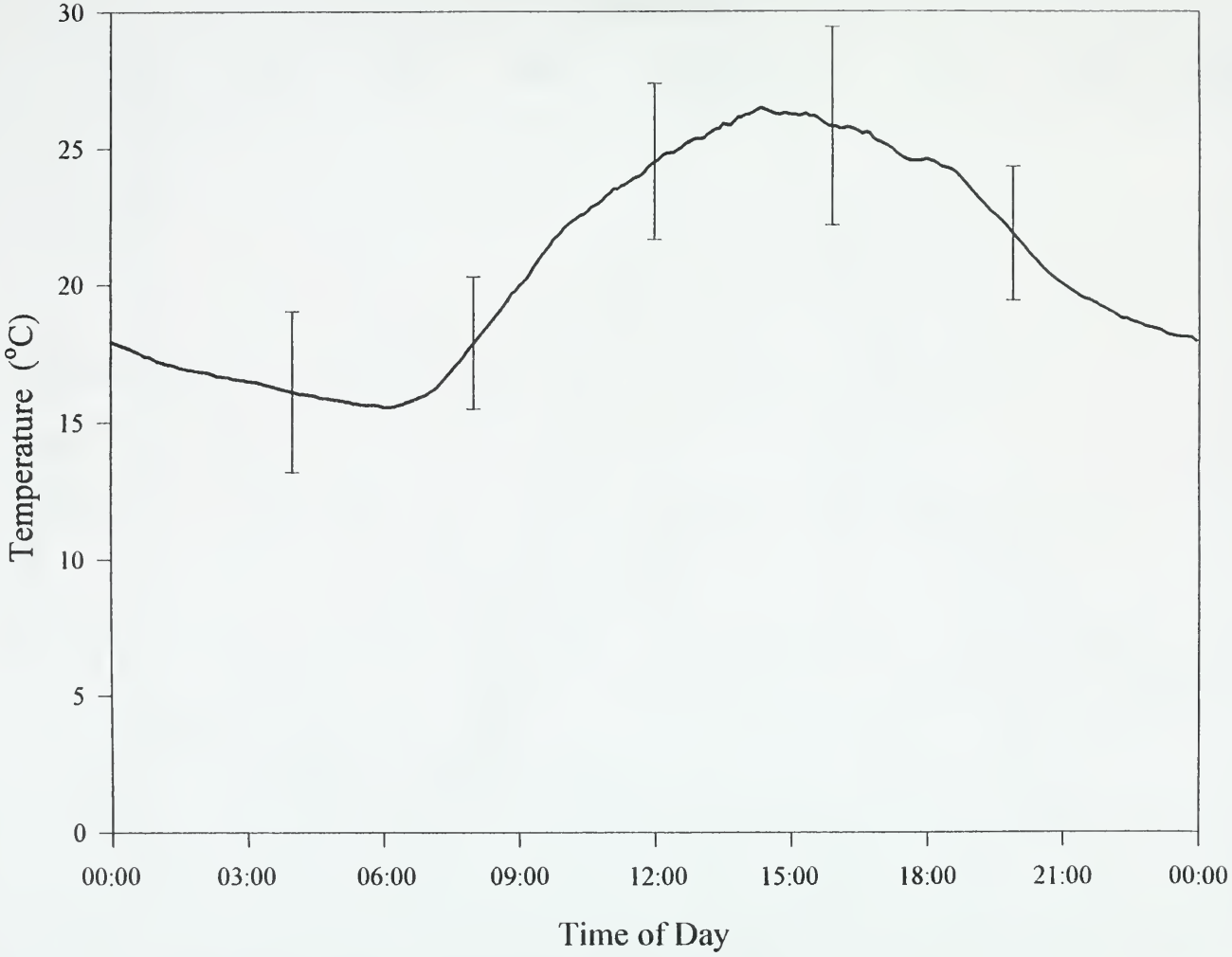

Figure 1n. Average diurnal variation of Relative Humidity at Hastings 1993 field study.

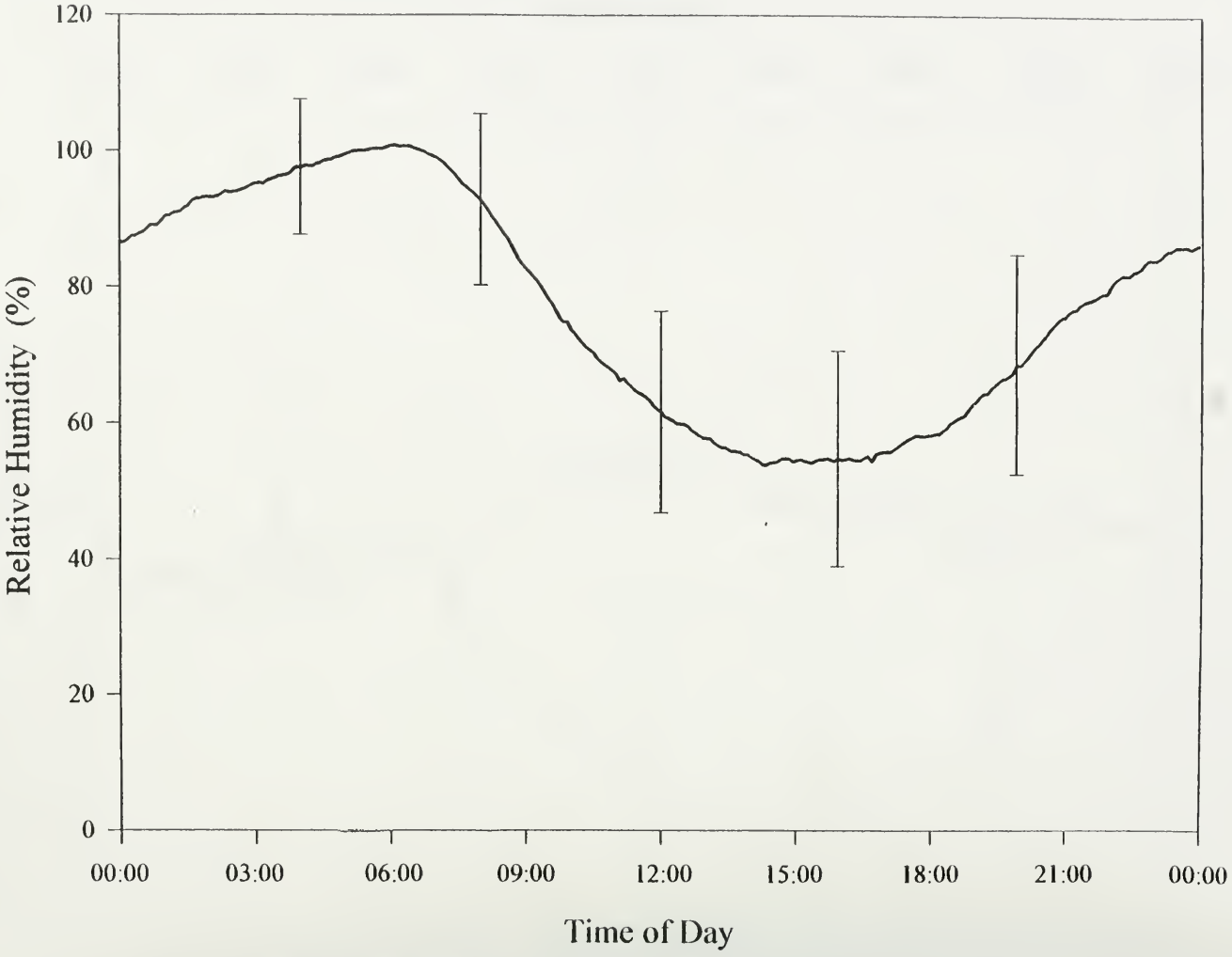

Figure 1o. Average diurnal variation of Solar Radiation at Hastings 1993 field study.

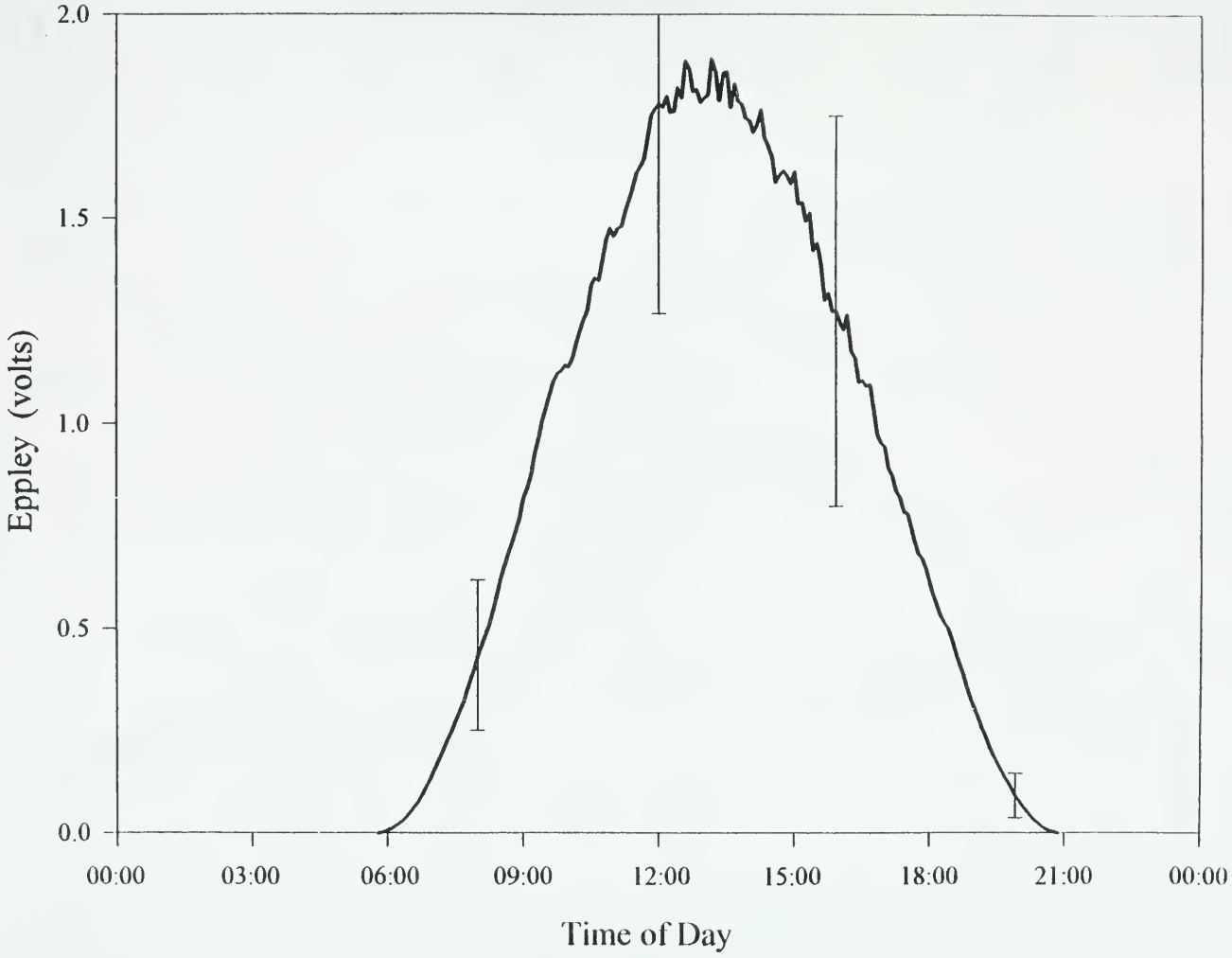

Figure 2. Average diurnal variation of the fraction of NO_x present as NO_y at Hastings 1993 field study.

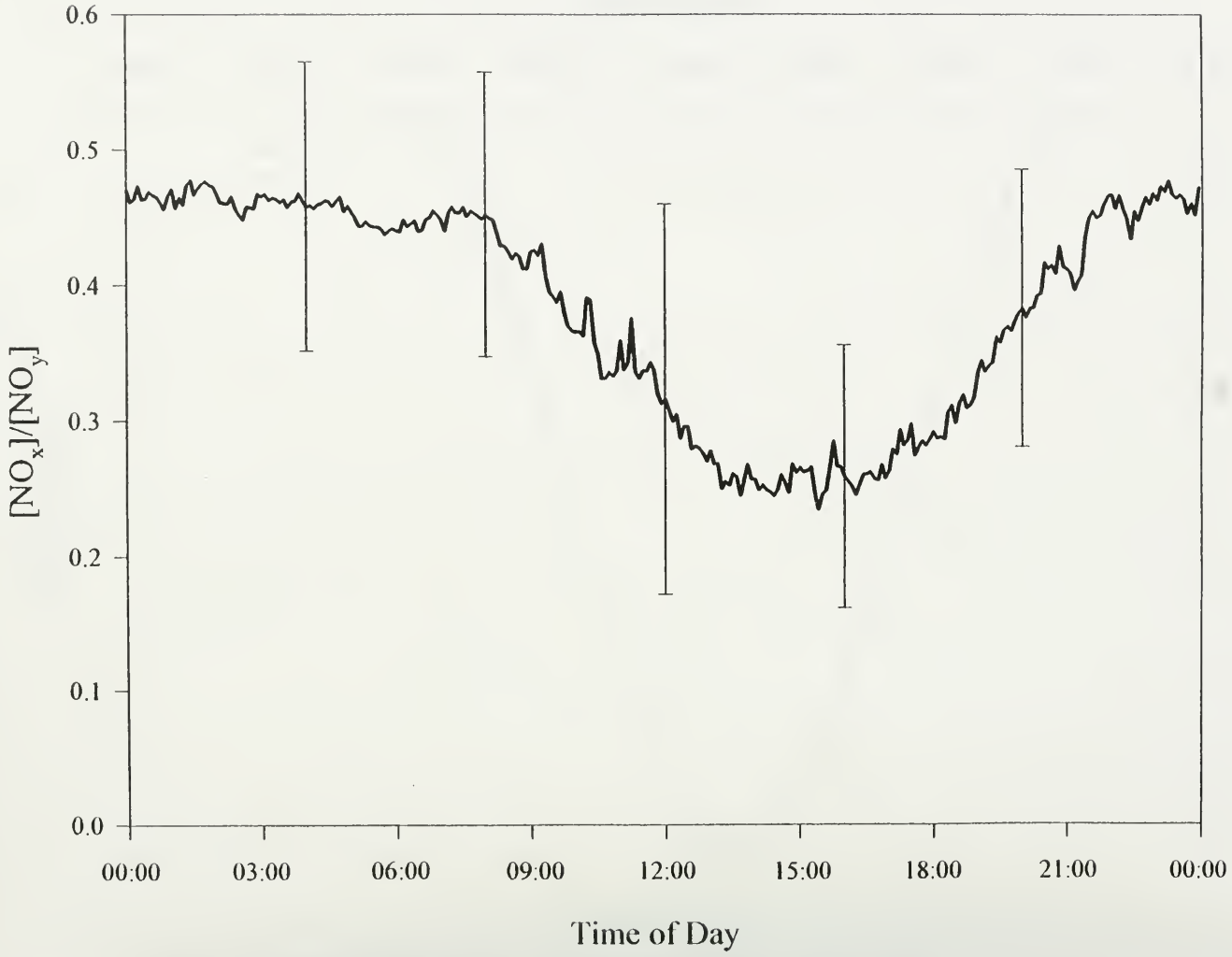

Figure 3. Comparison of the radiometer data for the 1992 and 1993 field studies.

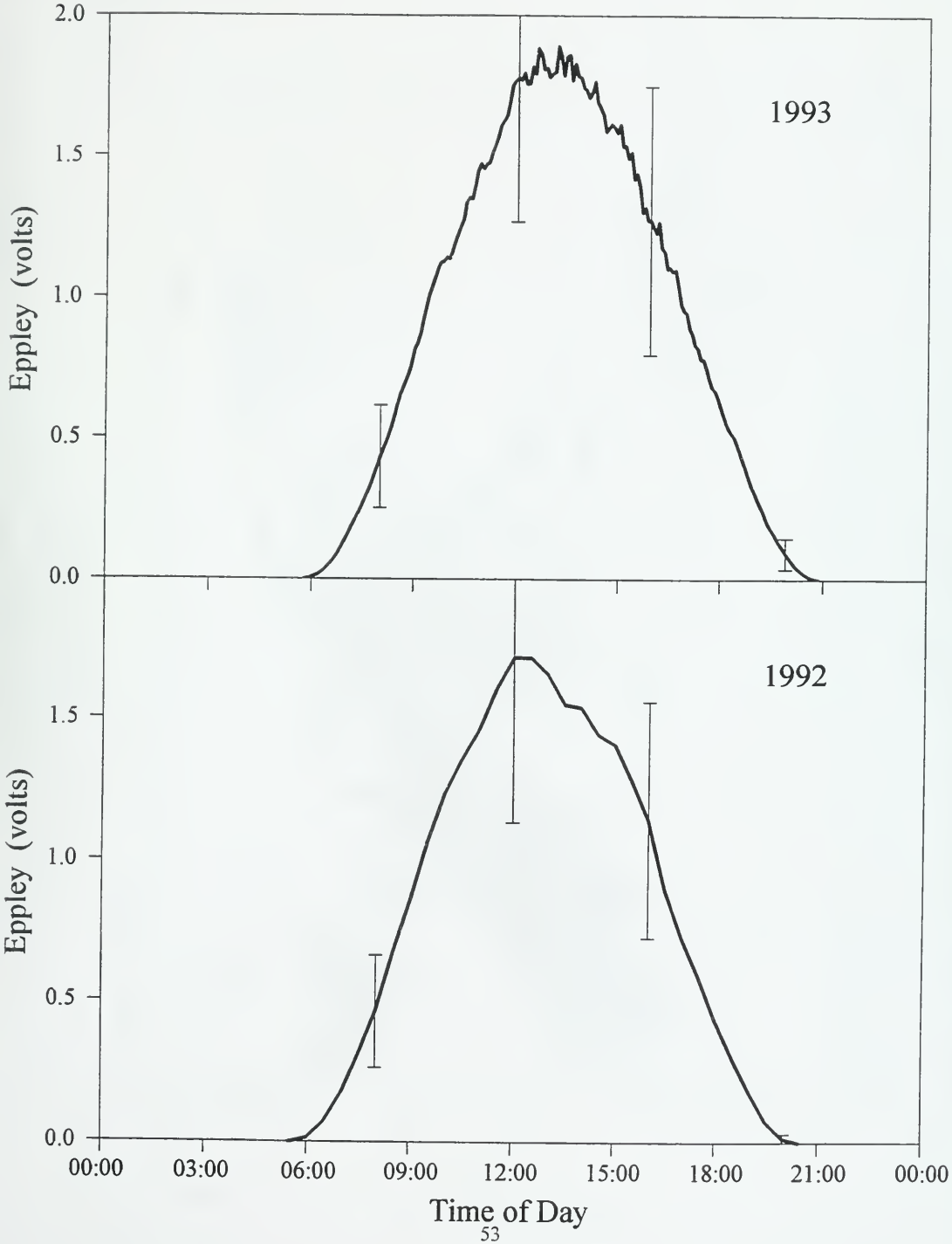

Figure 4a. Plot of Ozone against NO_z (NO_y-NO_x) for the daytime (10am-6pm) for 1992.

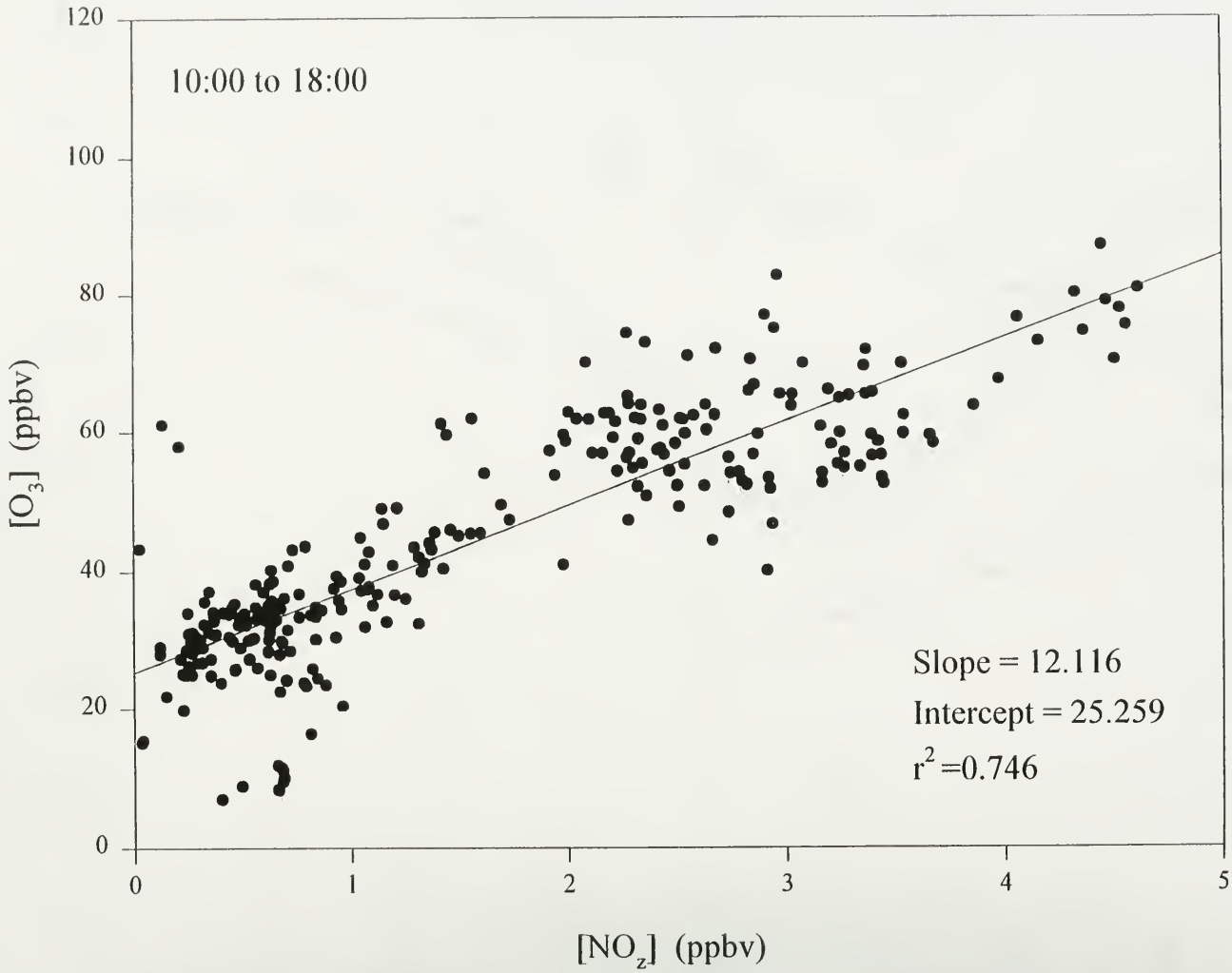

Figure 4b. Plot of Ozone against NO_z (NO_y-NO_x) for the daytime (10am-6pm) for 1993.

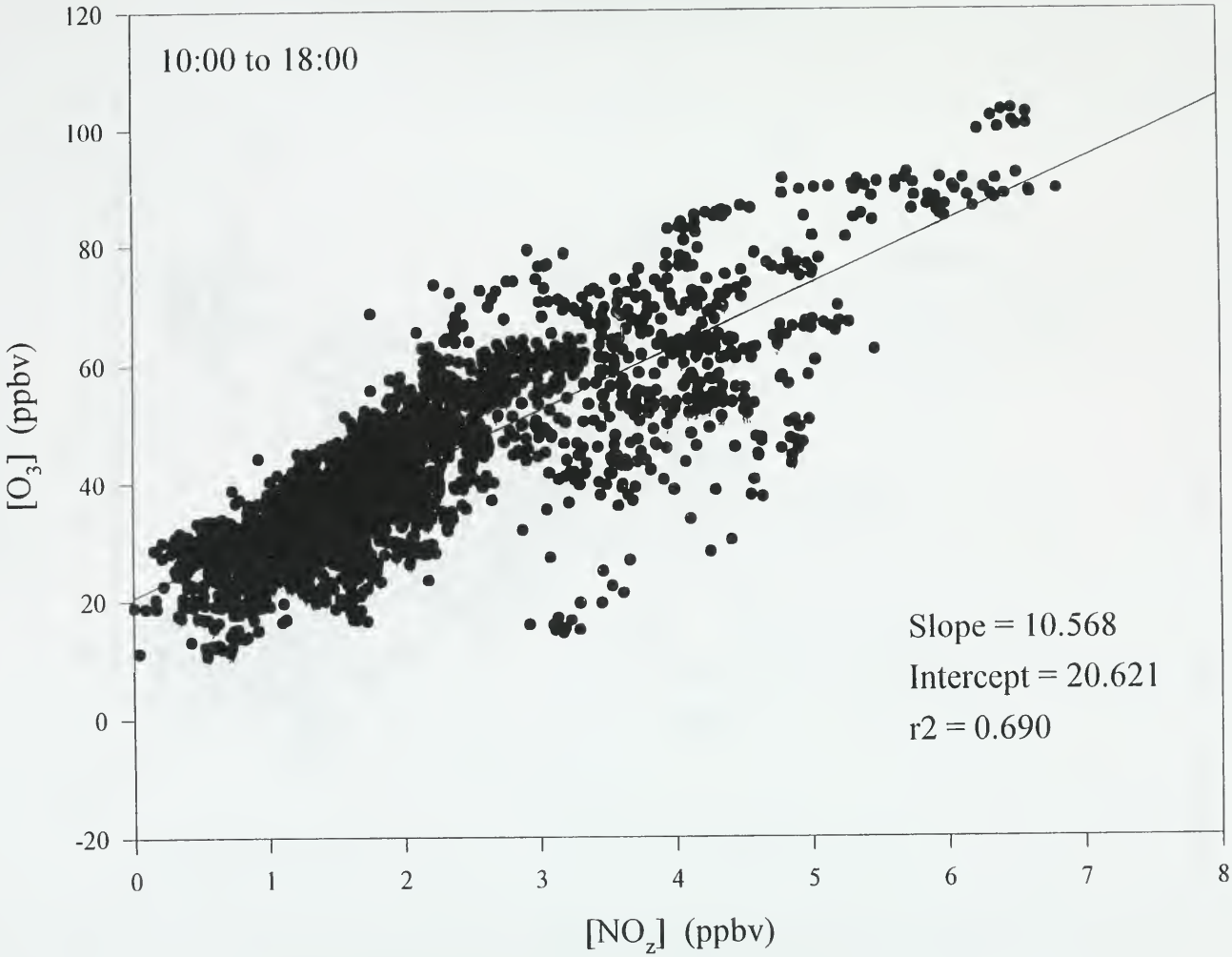

Figure 4c. Plot of Ozone against NO_y for the daytime (10am-6pm) for 1992.

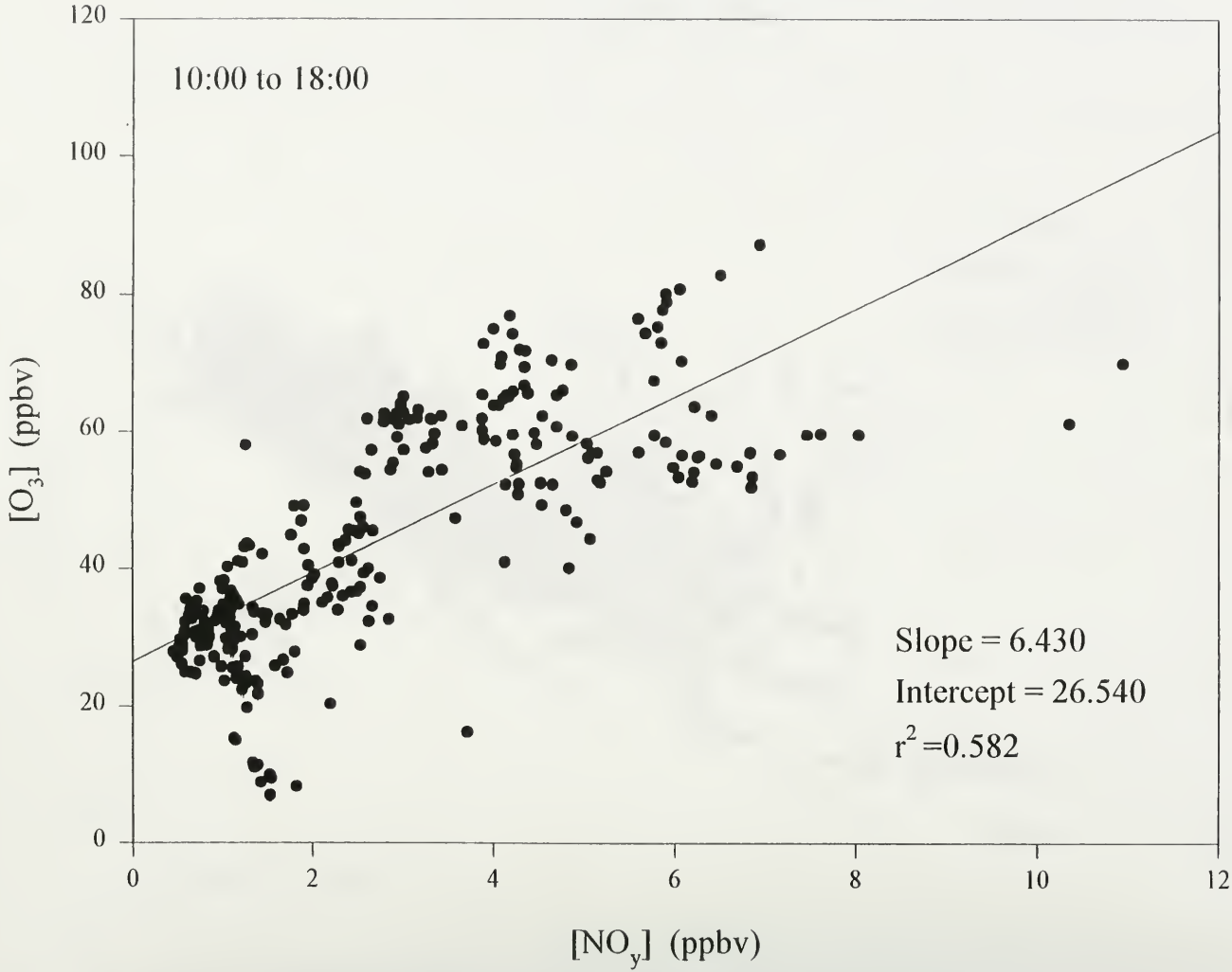

Figure 4d. Plot of Ozone against NO_y for the daytime (10am-6pm) for 1993.

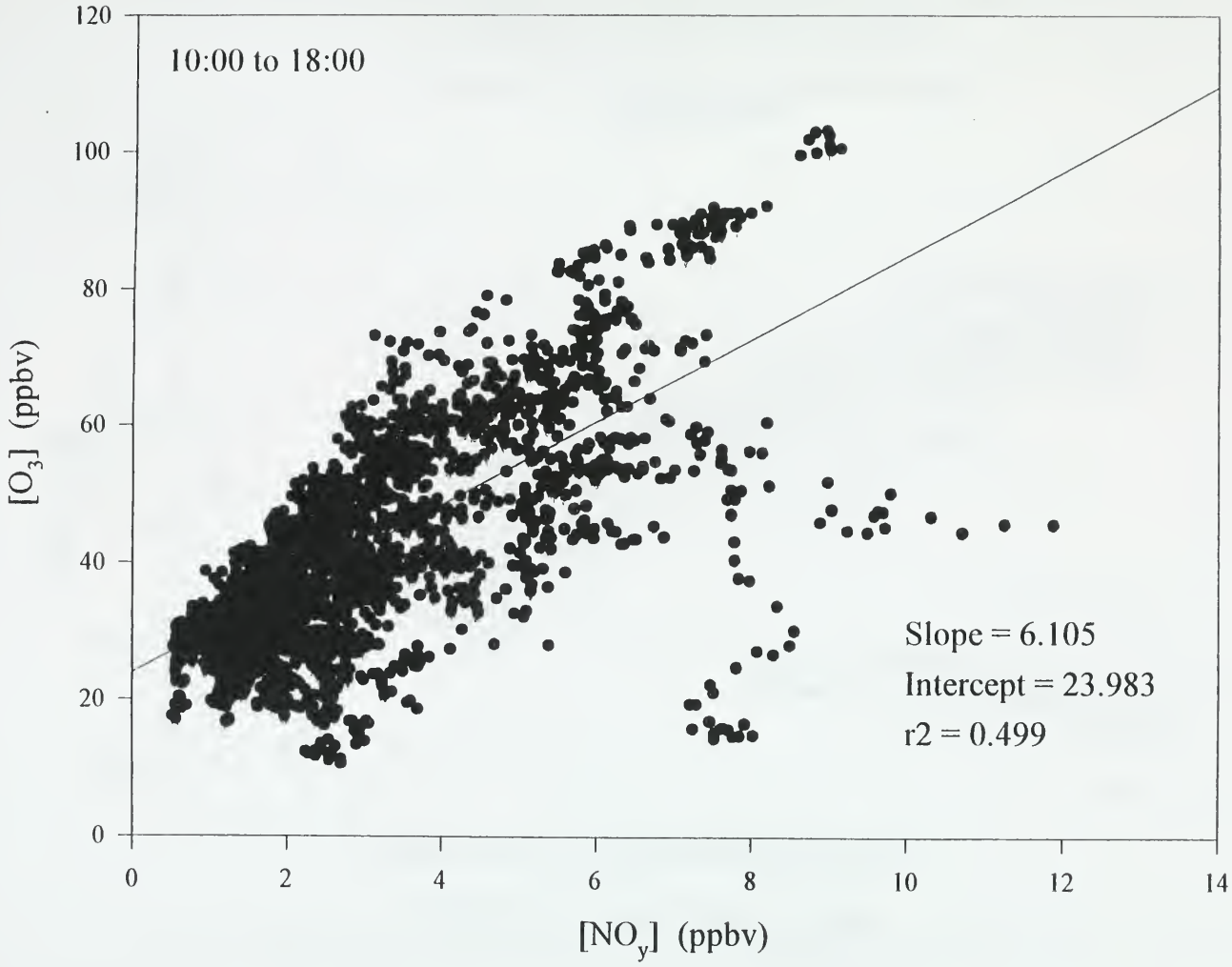

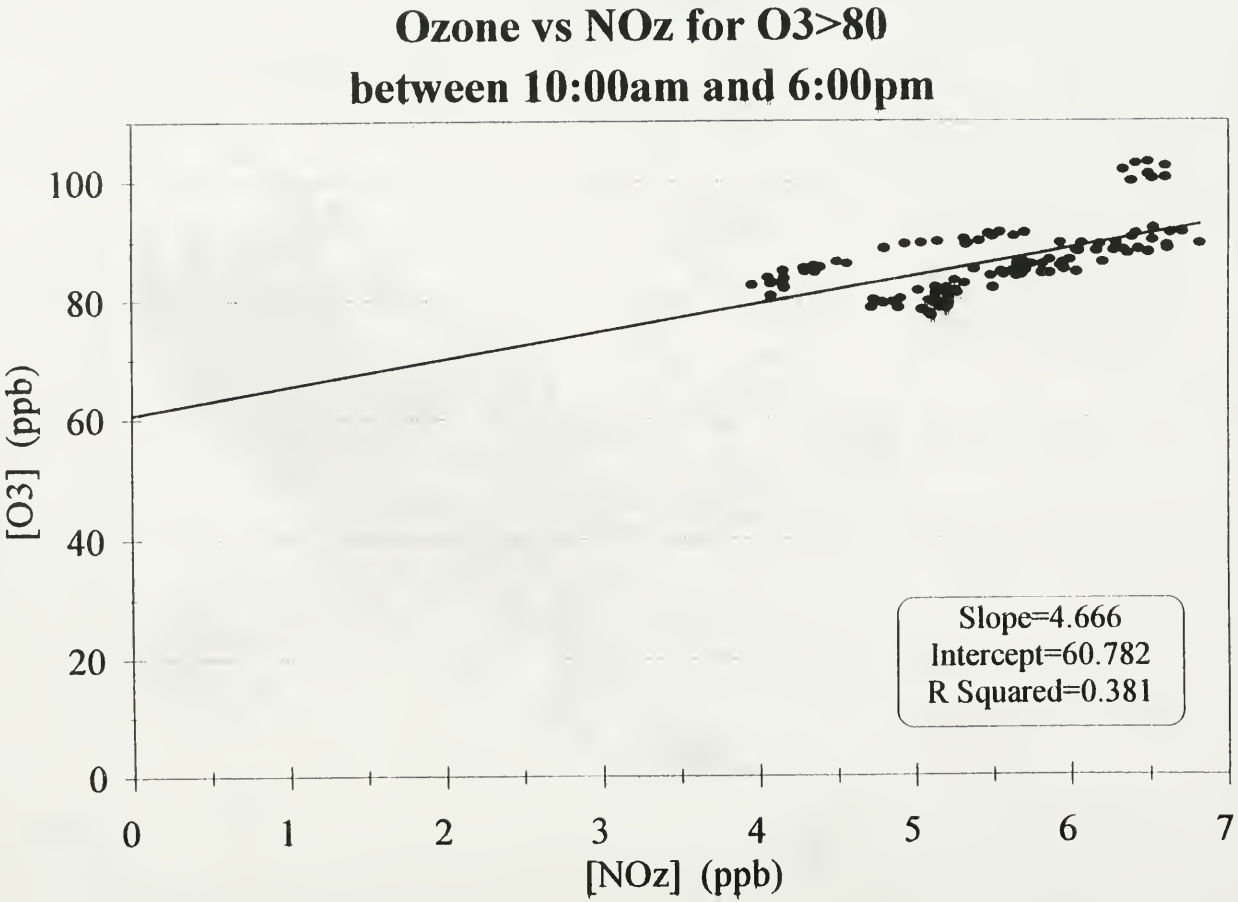

Figure 5a. Plot of O_3 against NO_z (NO_y-NO_x) for the daytime (10am-6pm) in 1993 when $O_3 > 80$.

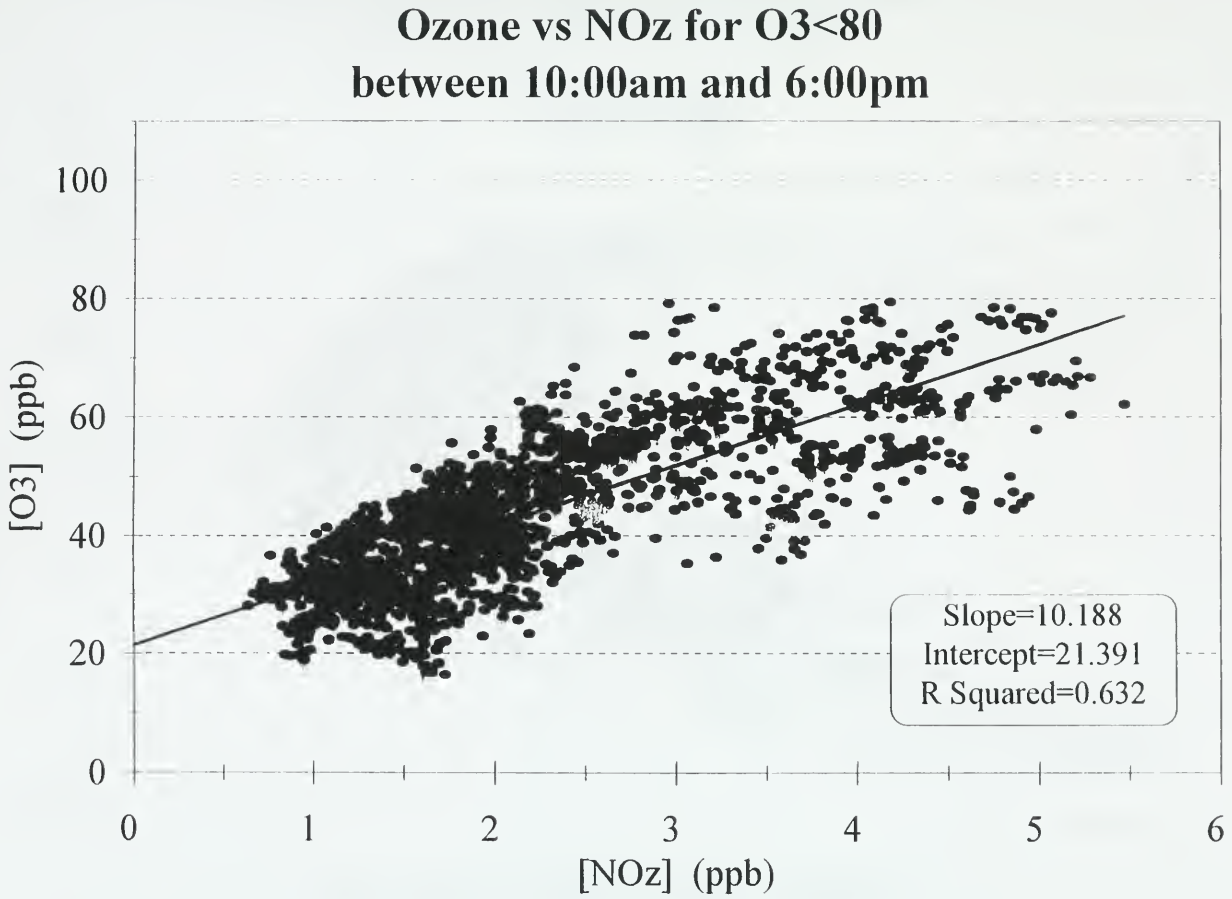

Figure 5b. Plot of O_3 against NO_z (NO_y-NO_x) for the daytime (10am-6pm) for 1993 when $O_3 < 80$.

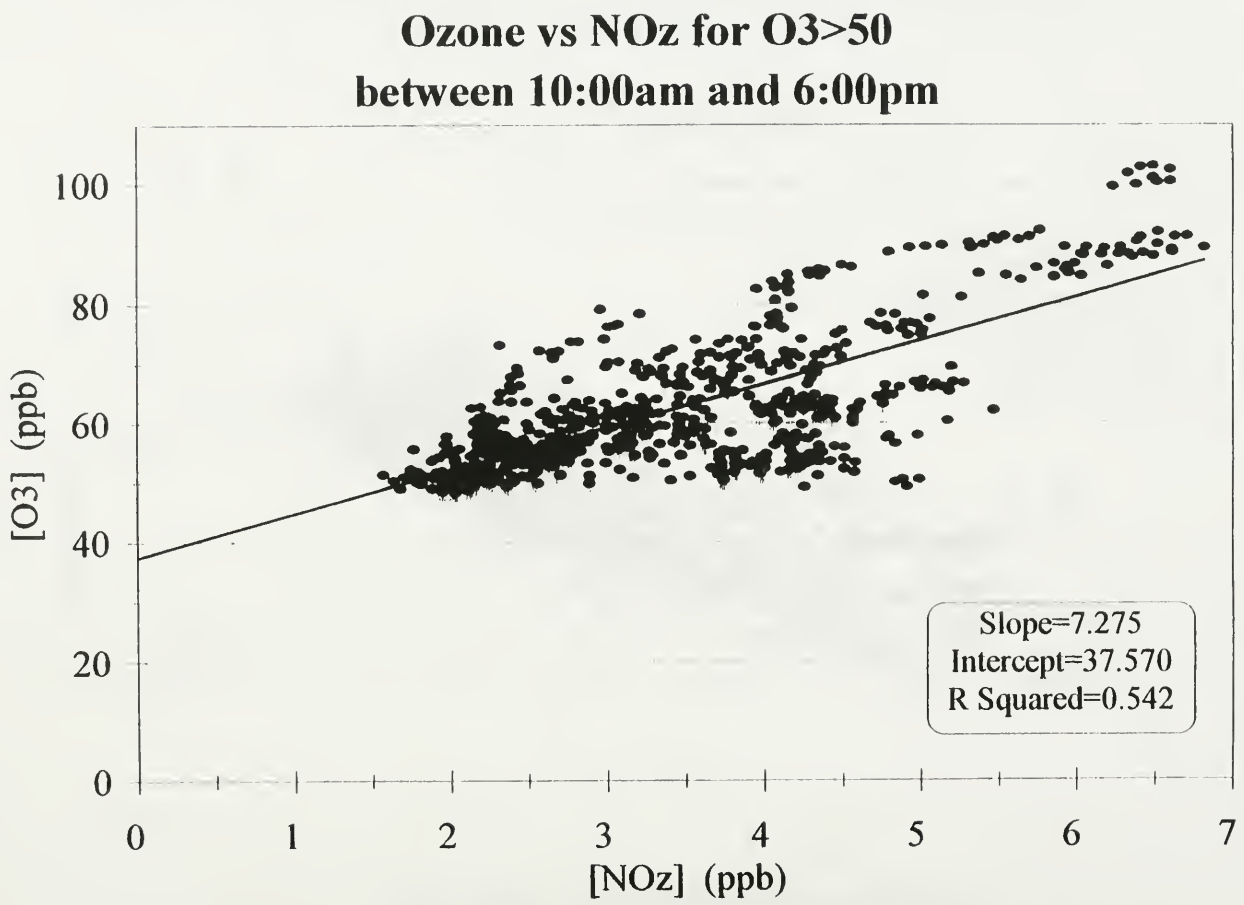

Figure 5c. Plot of O_3 against NO_z (NO_y-NO_x) for the daytime (10am-6pm) for 1993 when $O_3 > 50$.

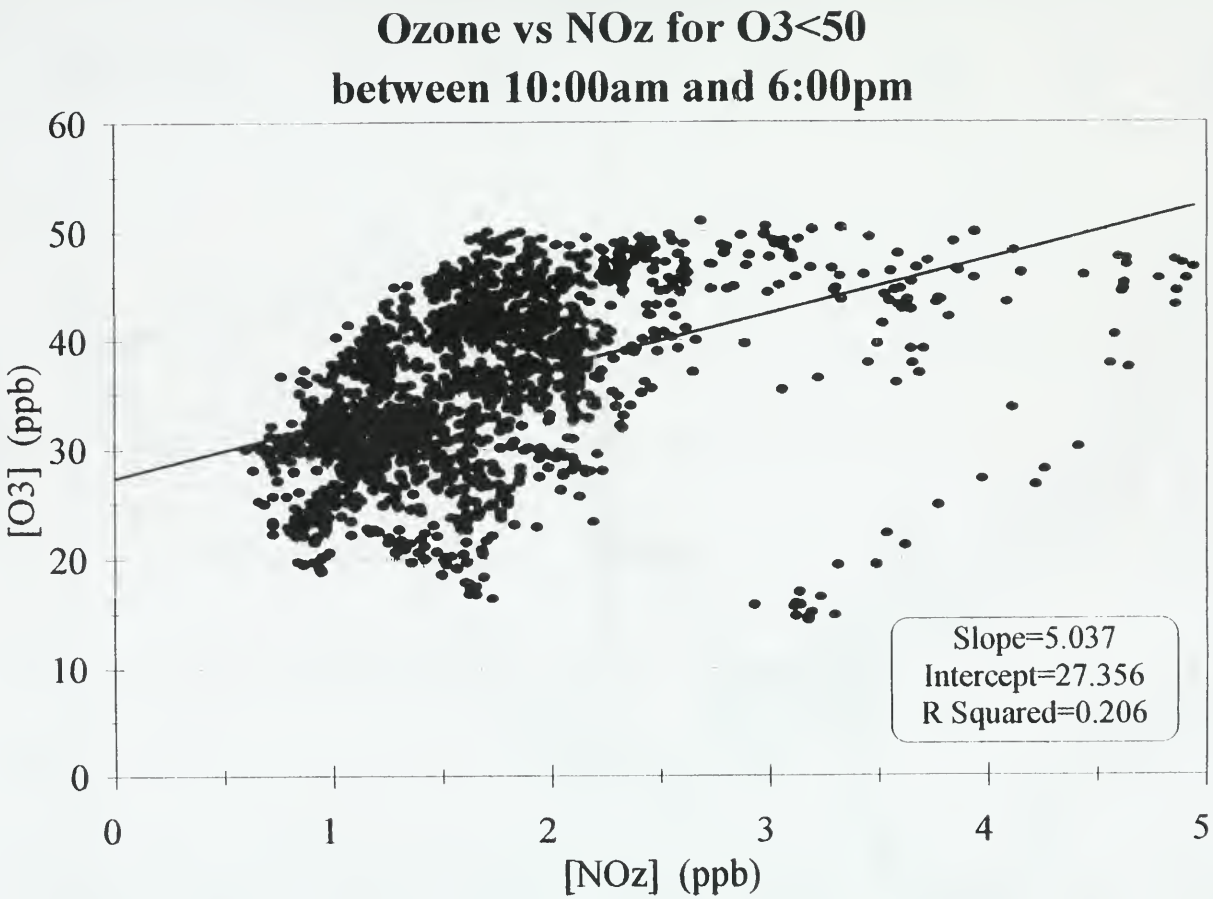

Figure 5d. Plot of O_3 against NO_z (NO_y-NO_x) for the daytime (10am-6pm) for 1993 when $O_3 < 50$.

Figure 6a.i. Ozone data on Aug 1st when there was an incursion of polluted air in the late afternoon.

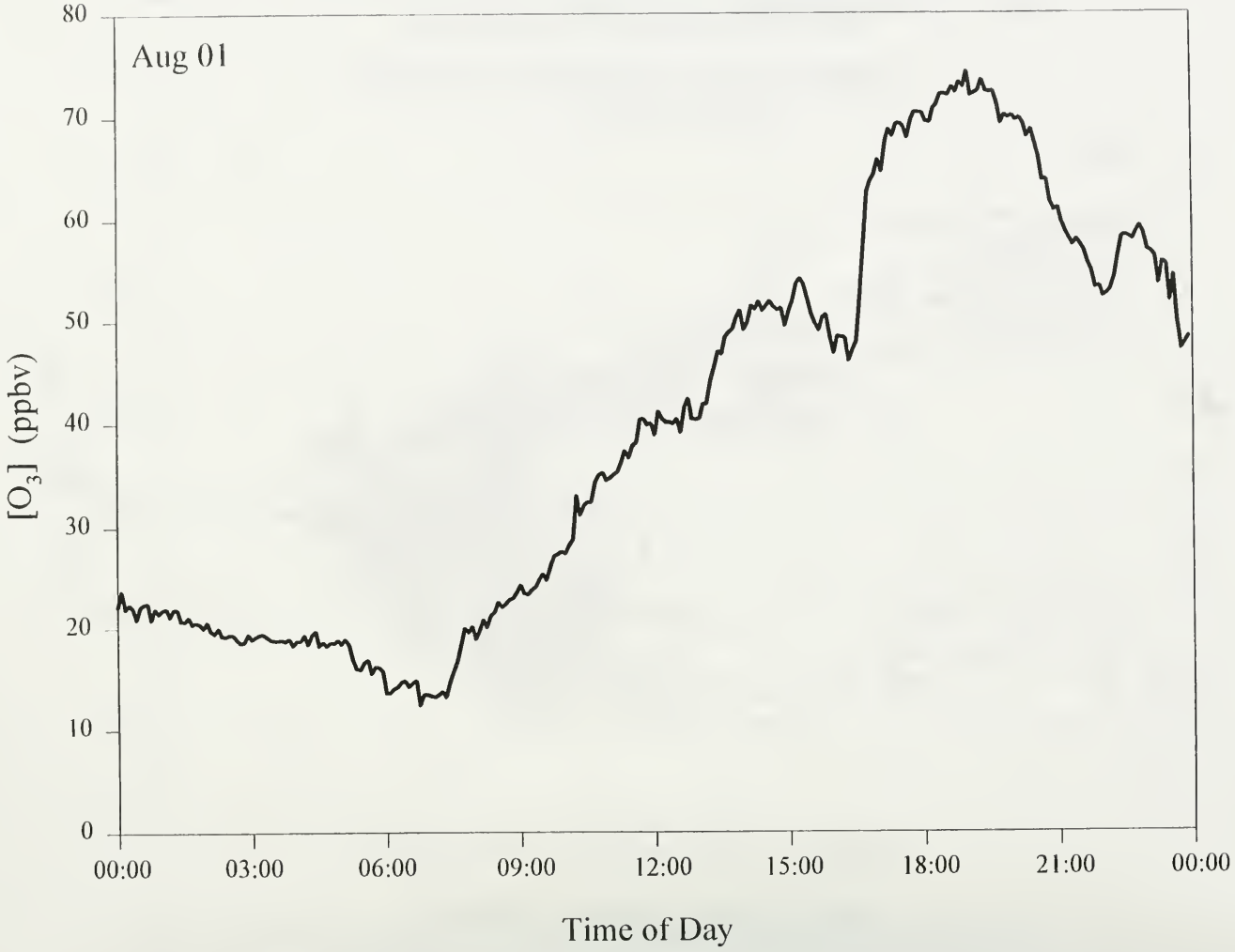

Figure 6a.ii. NO_x data on Aug 1st when there was an incursion of polluted air in the late afternoon.

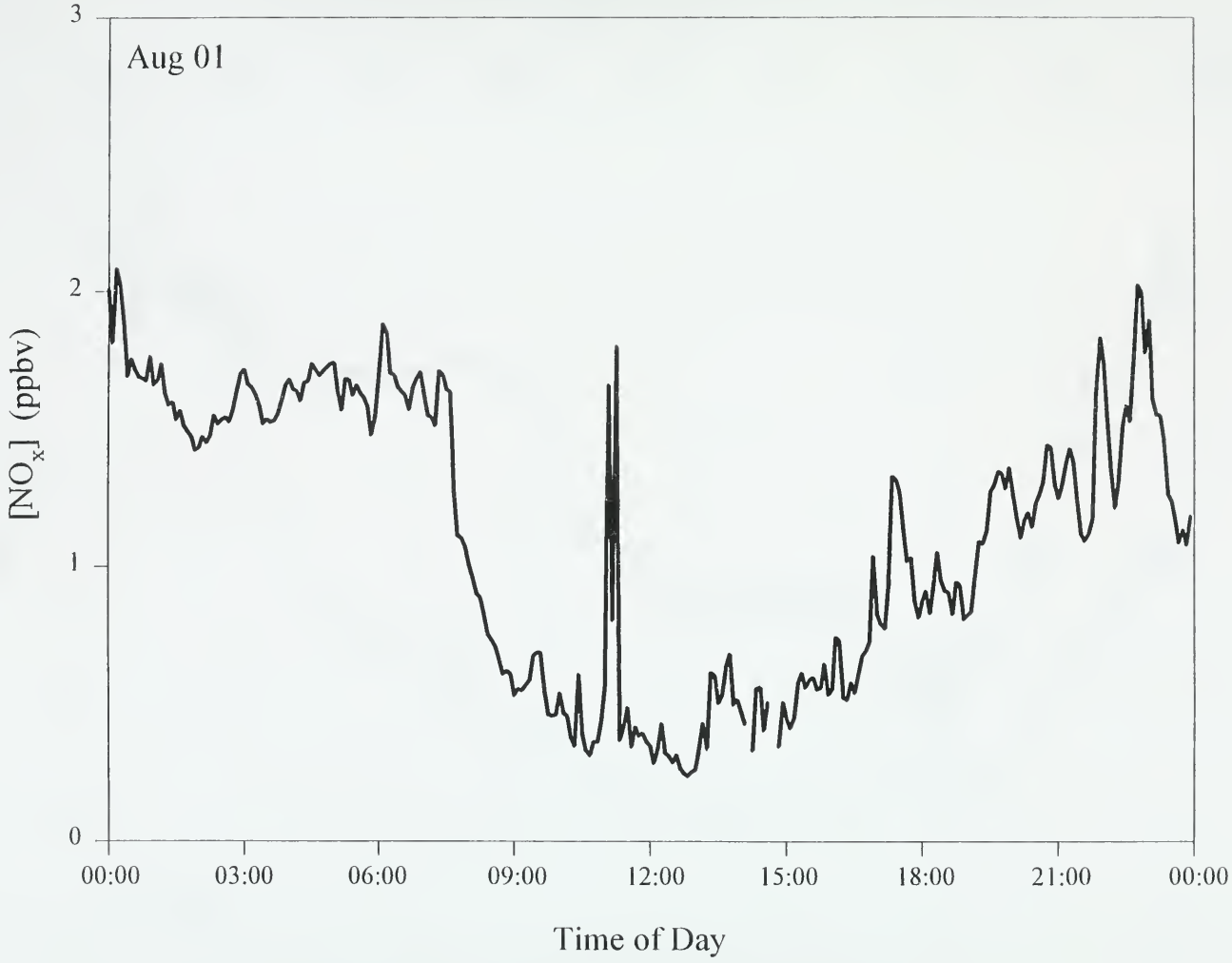

Figure 6a.iii. Ozone data on Aug 8th when there was an incursion of polluted air in the late afternoon.

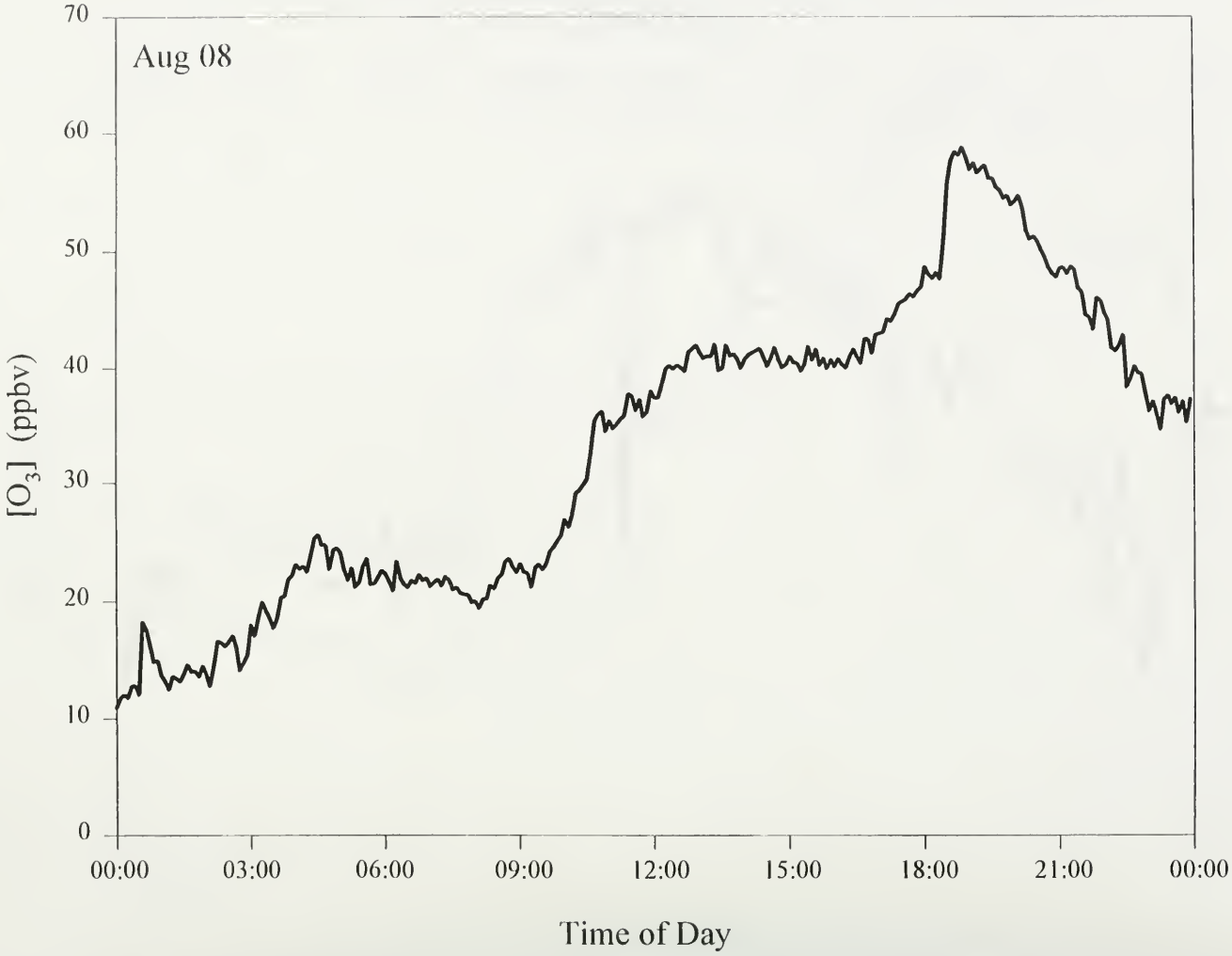

Figure 6a.iv. NO_x data on Aug 8th when there was an incursion of polluted air in the late afternoon.

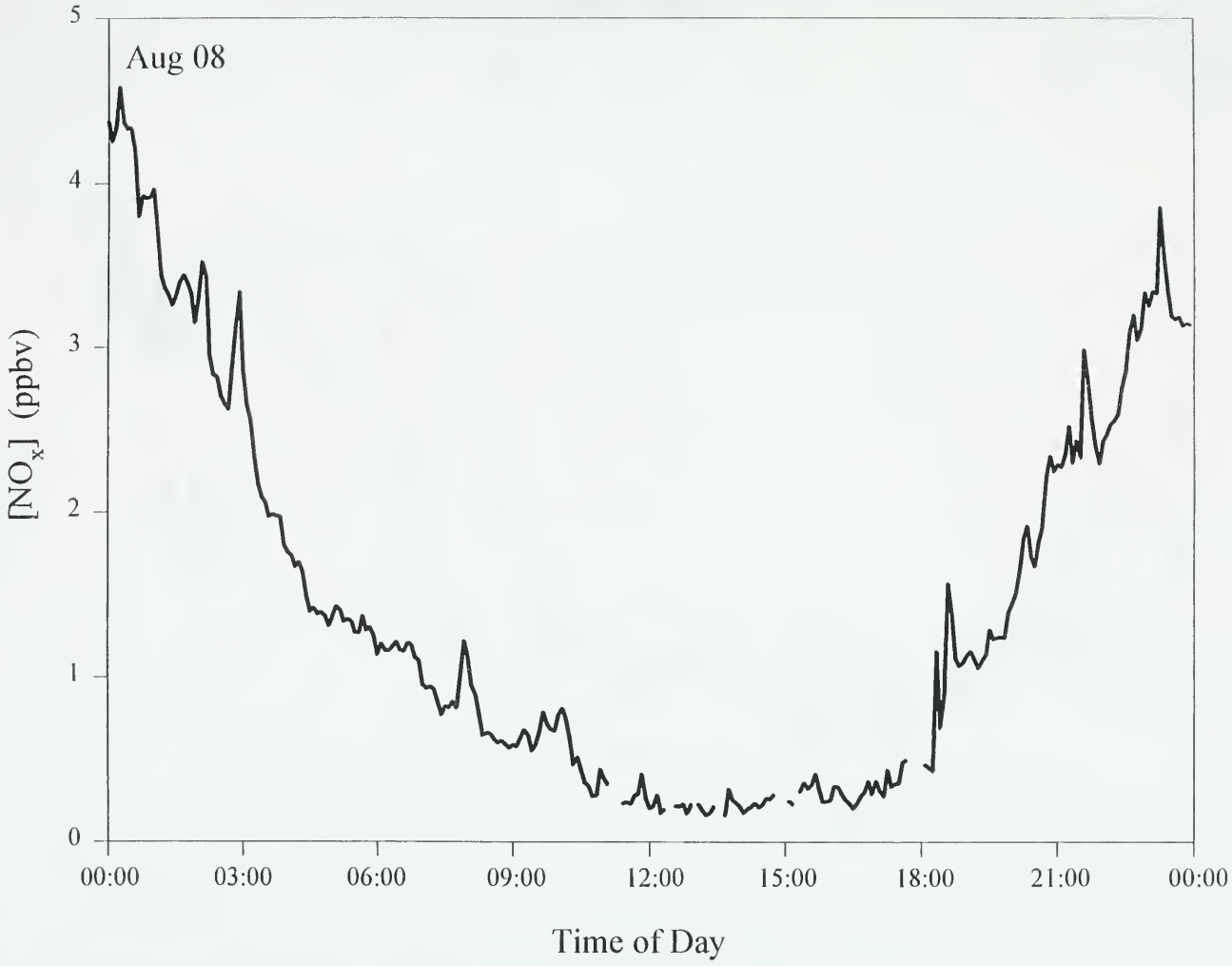

Figure 6a.v. Ozone data on Aug 15th when there was an incursion of polluted air in the late afternoon.

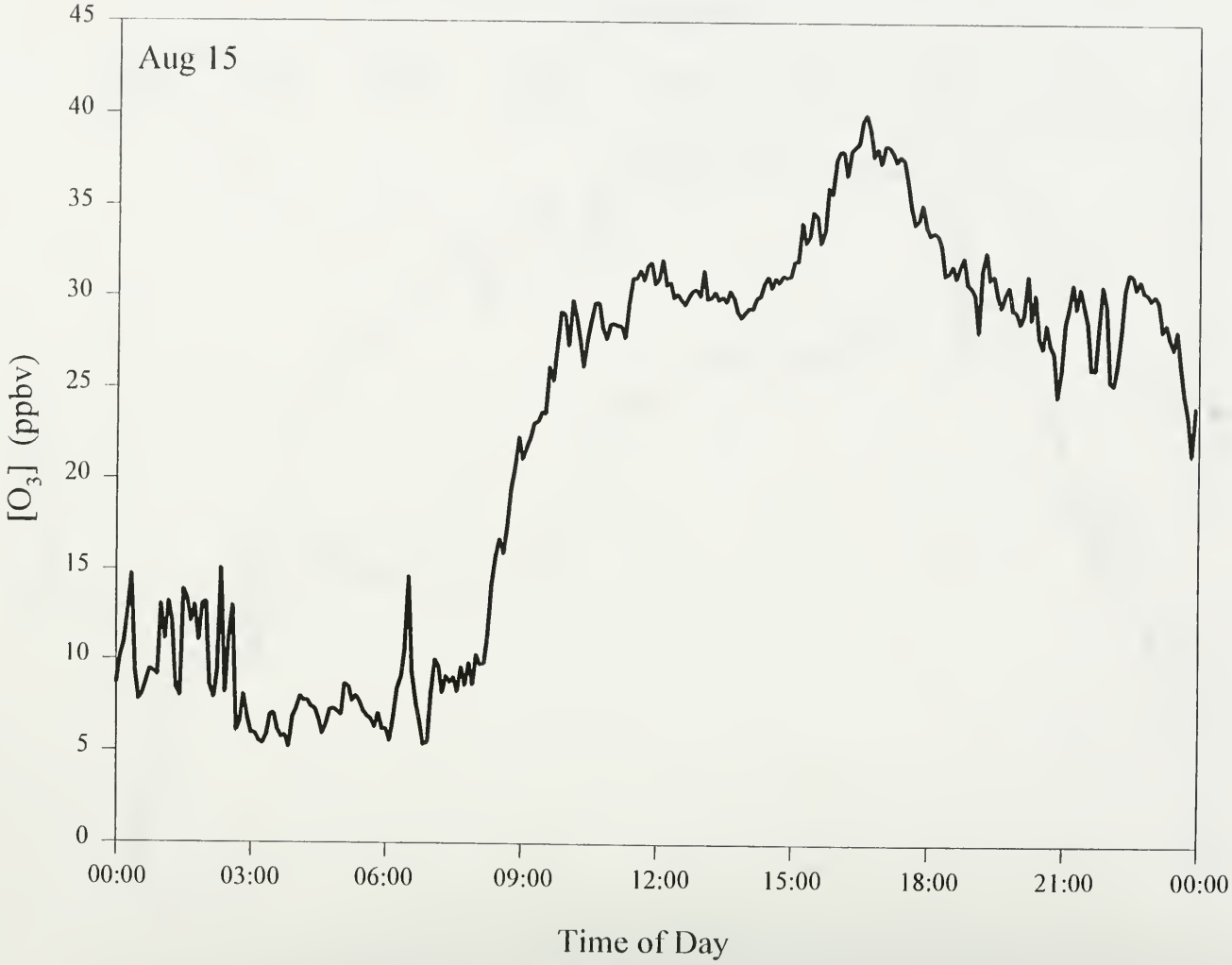

Figure 6a.vi. NO_x data on Aug 15th when there was an incursion of polluted air in the late afternoon.

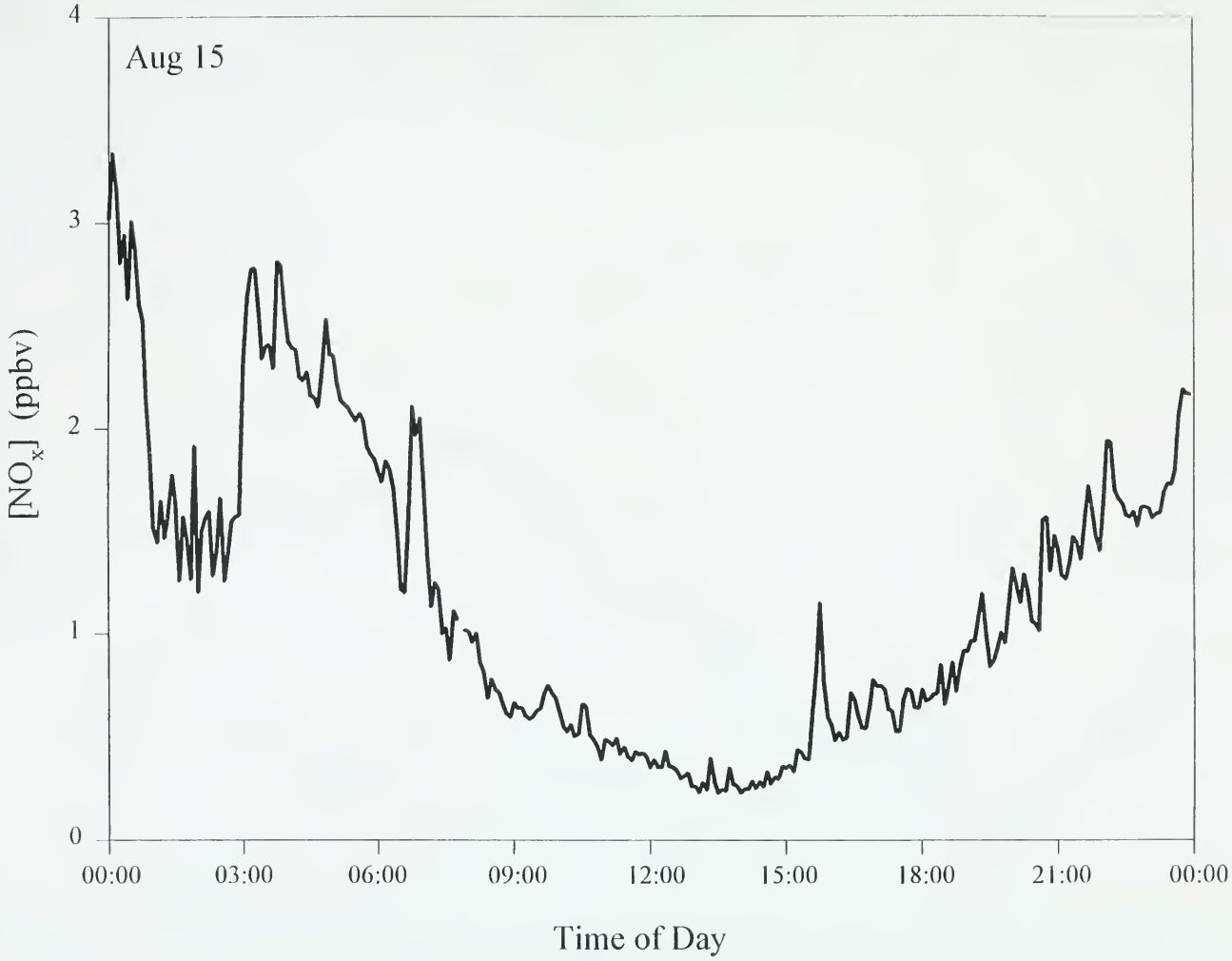

Figure 6a.vii. Ozone data on Aug 18th when there was an incursion of polluted air in the late afternoon.

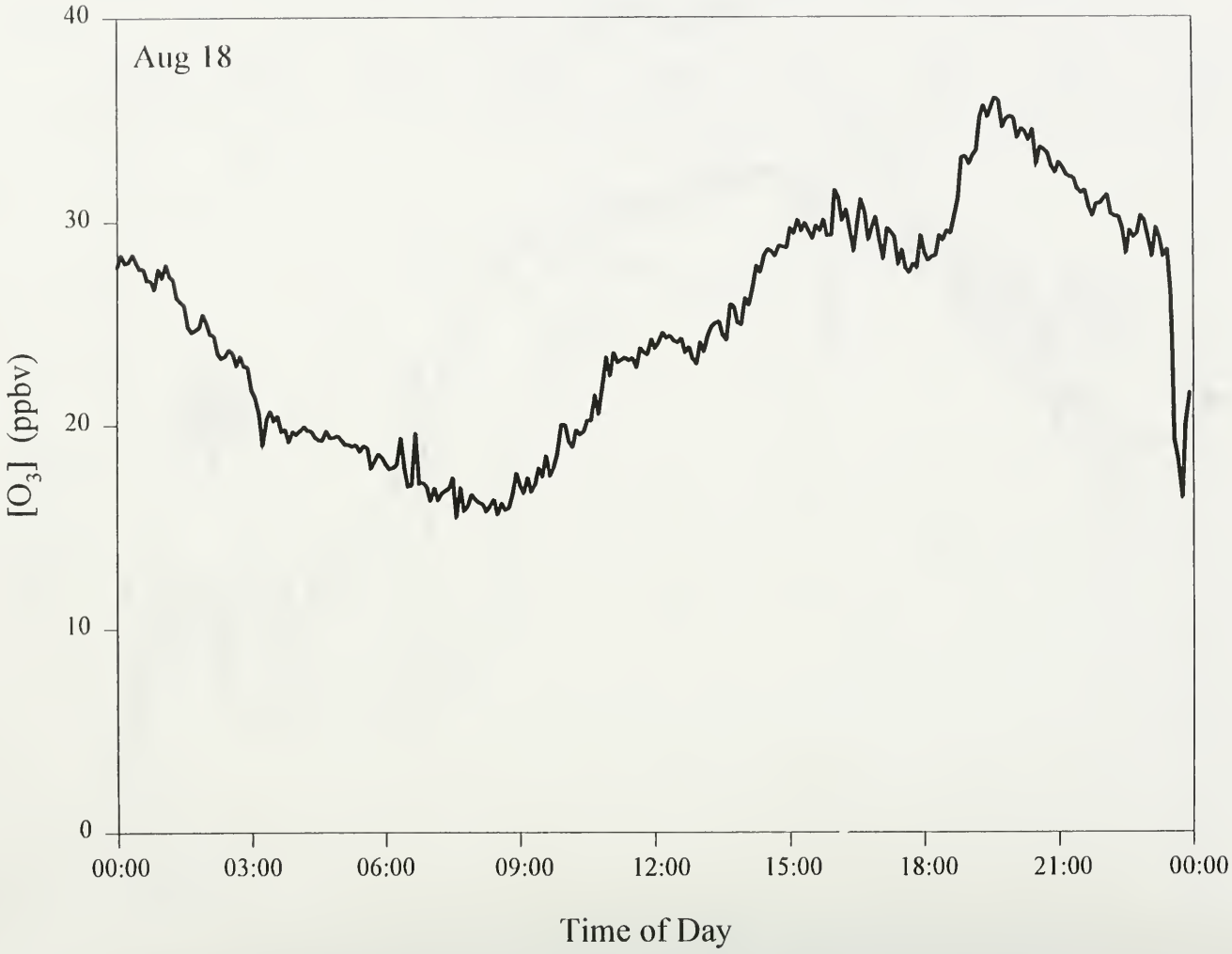

Figure 6a.viii. NO_x data on Aug 18th when there was an incursion of polluted air in the late afternoon.

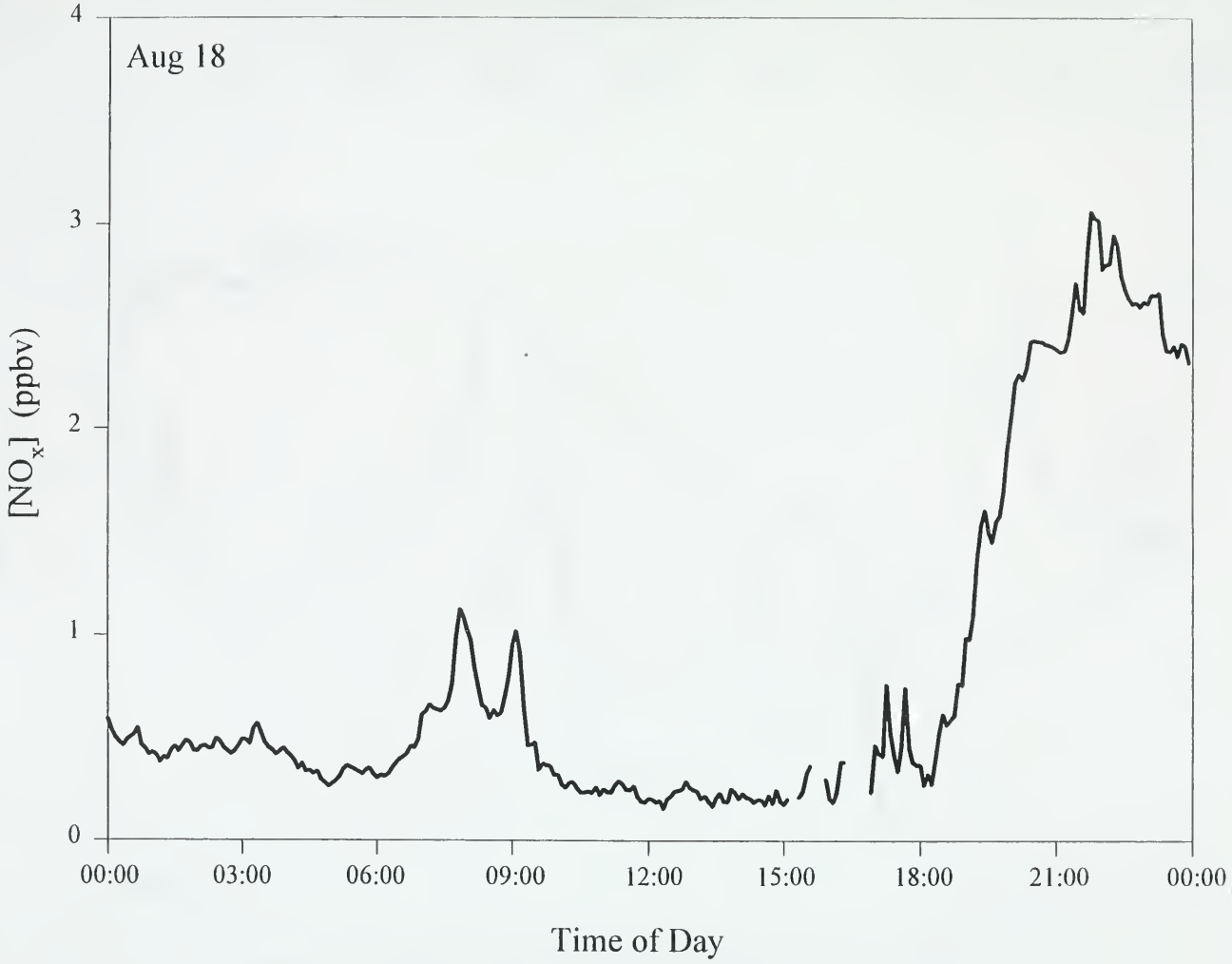

Figure 6a.ix. Ozone data on Aug 26th when there was an incursion of polluted air in the late afternoon.

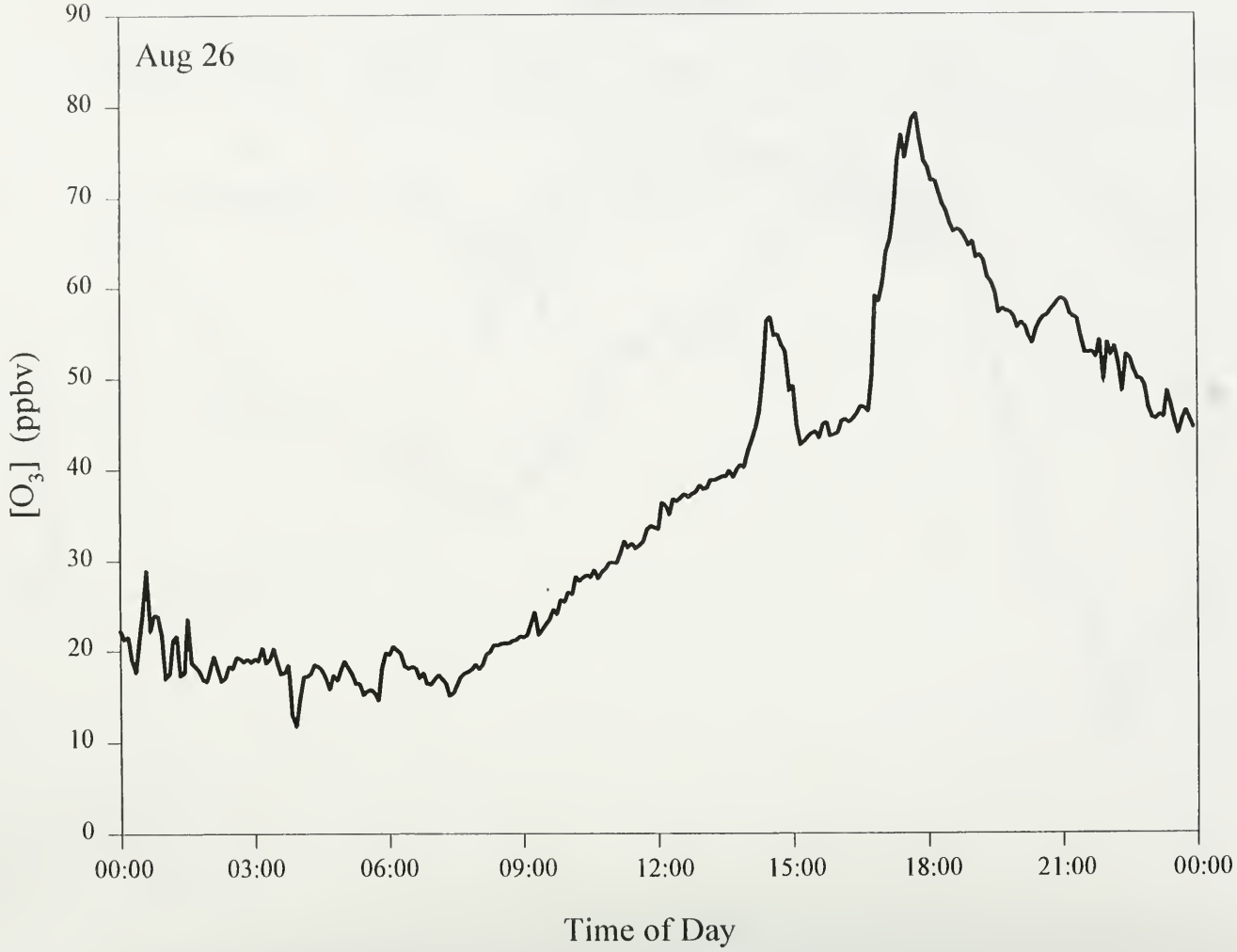

Figure 6a.x. NO_x data on Aug 26th when there was an incursion of polluted air in the late afternoon.

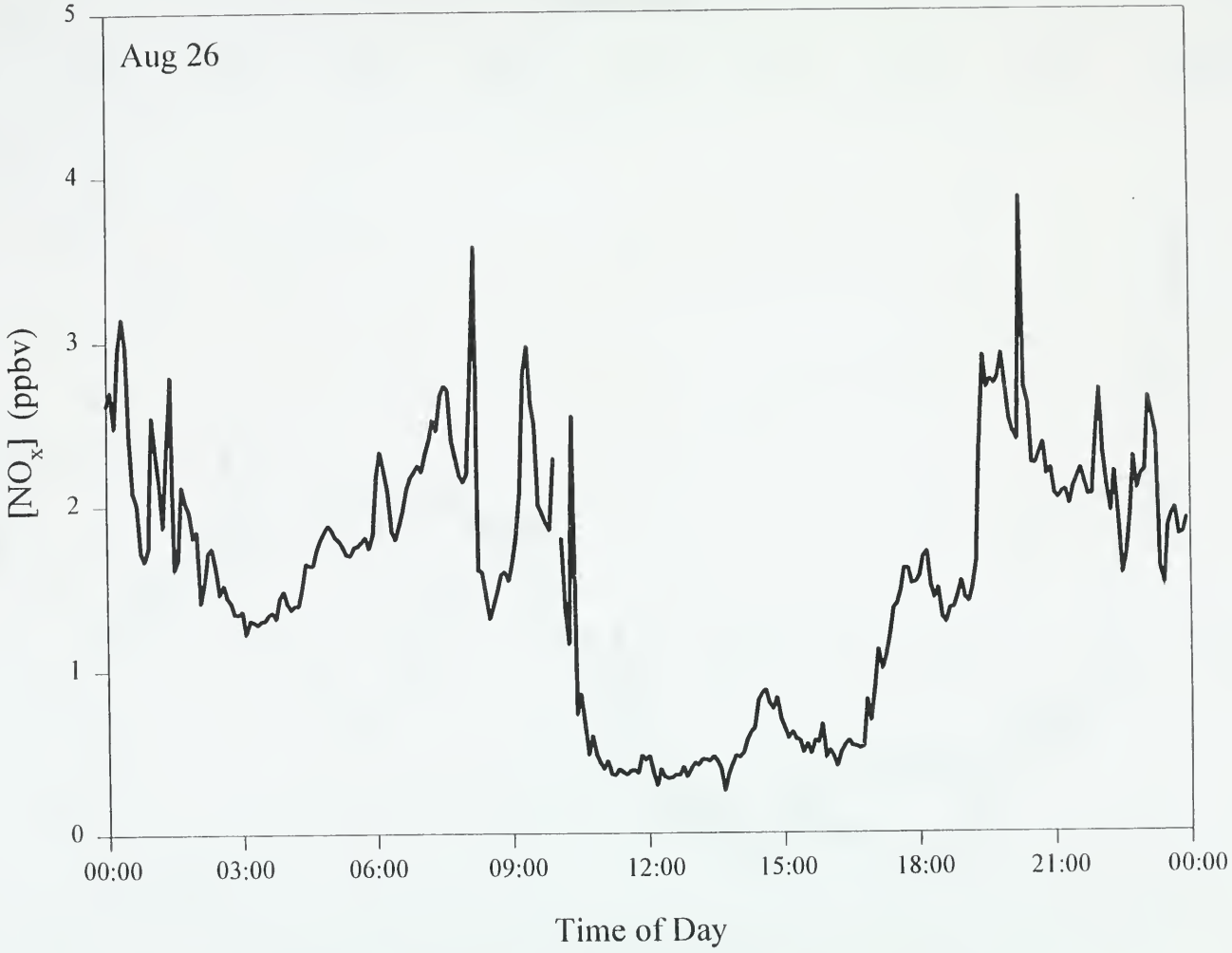

Figure 6b.i. Ozone data on Aug 5th when there was no incursion of polluted air in the late afternoon.

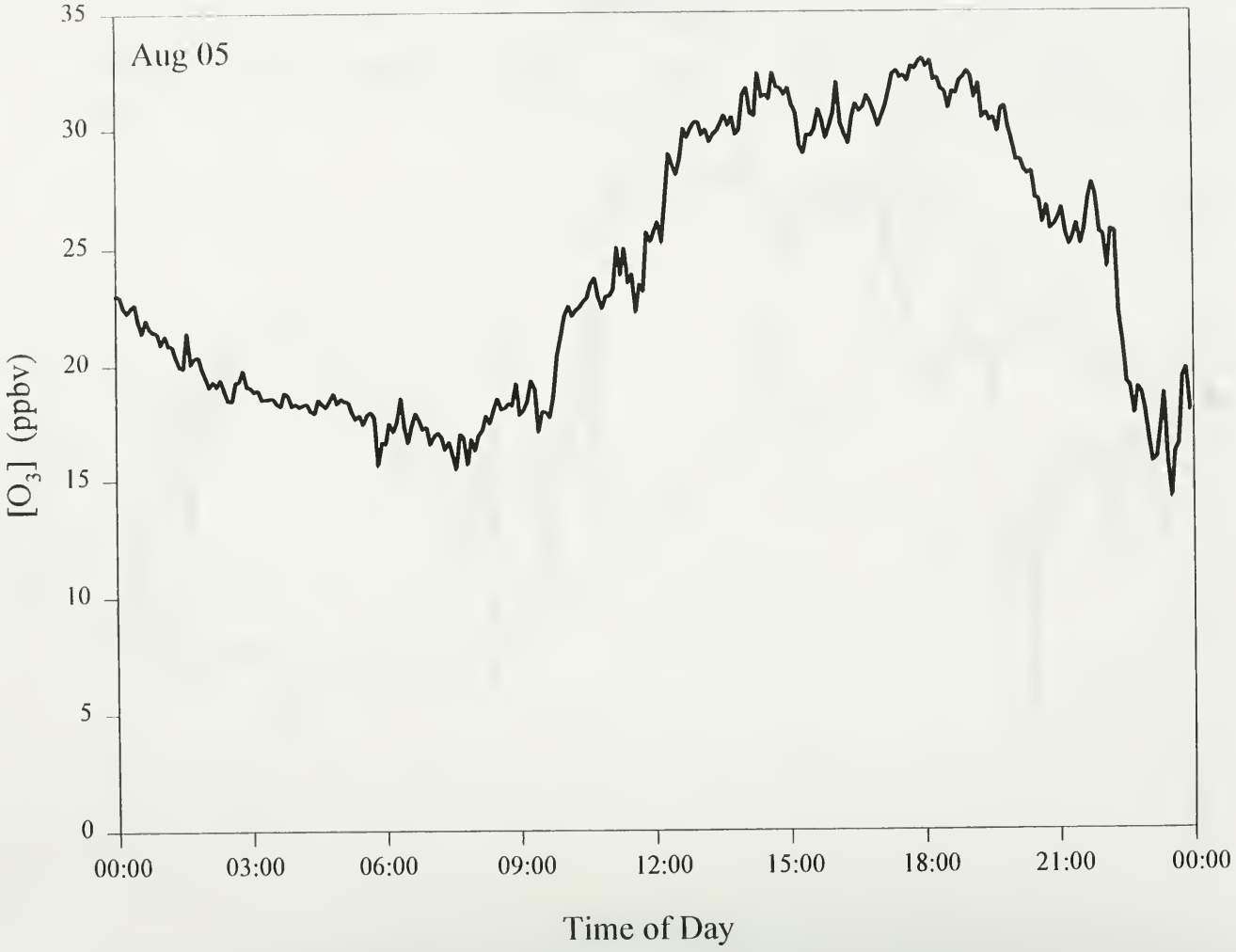

Figure 6b.ii. NO_x data on Aug 5th when there was no incursion of polluted air in the late afternoon.

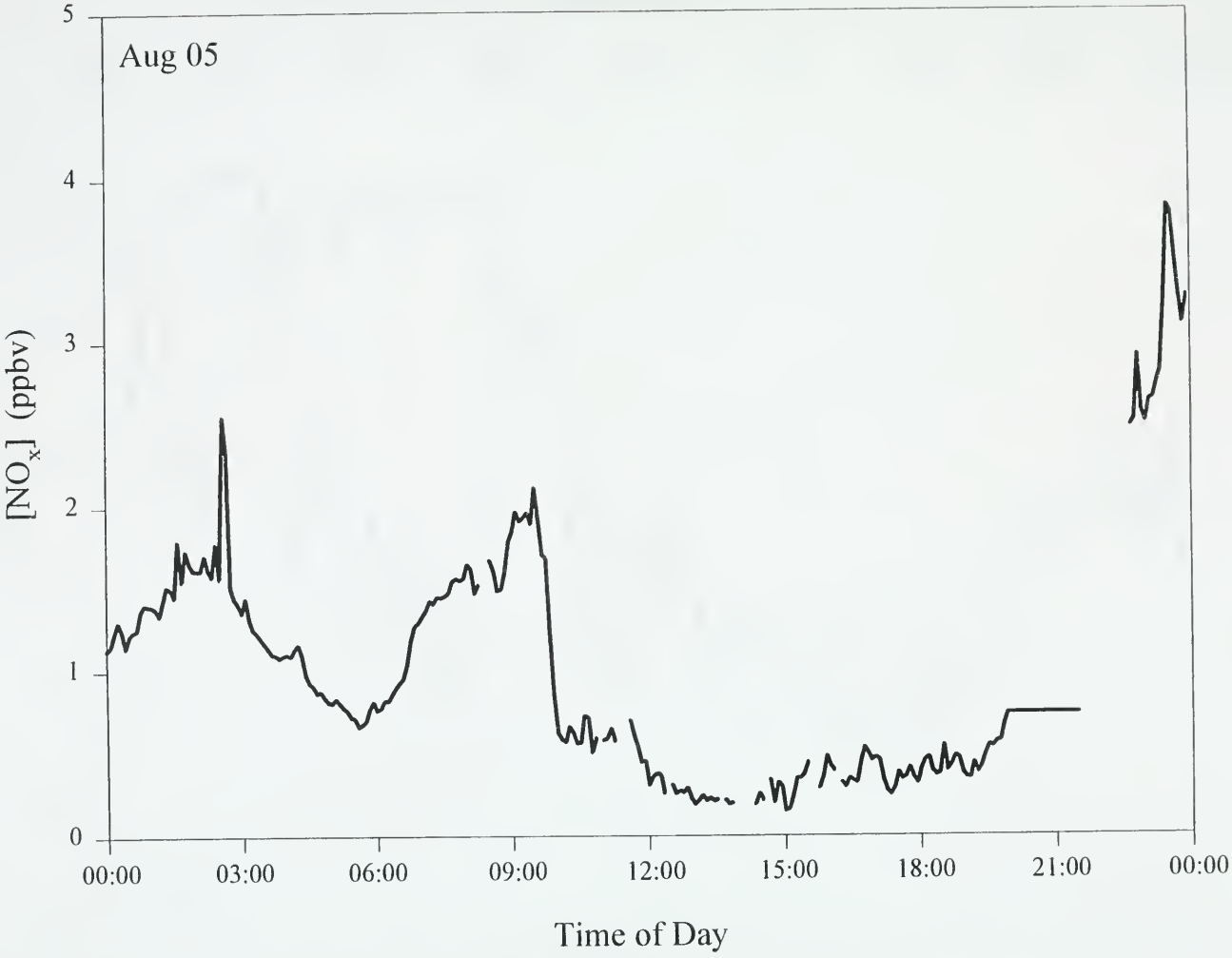

Figure 6b.iii. Ozone data on Aug 22nd when there was no incursion of polluted air in the late afternoon.

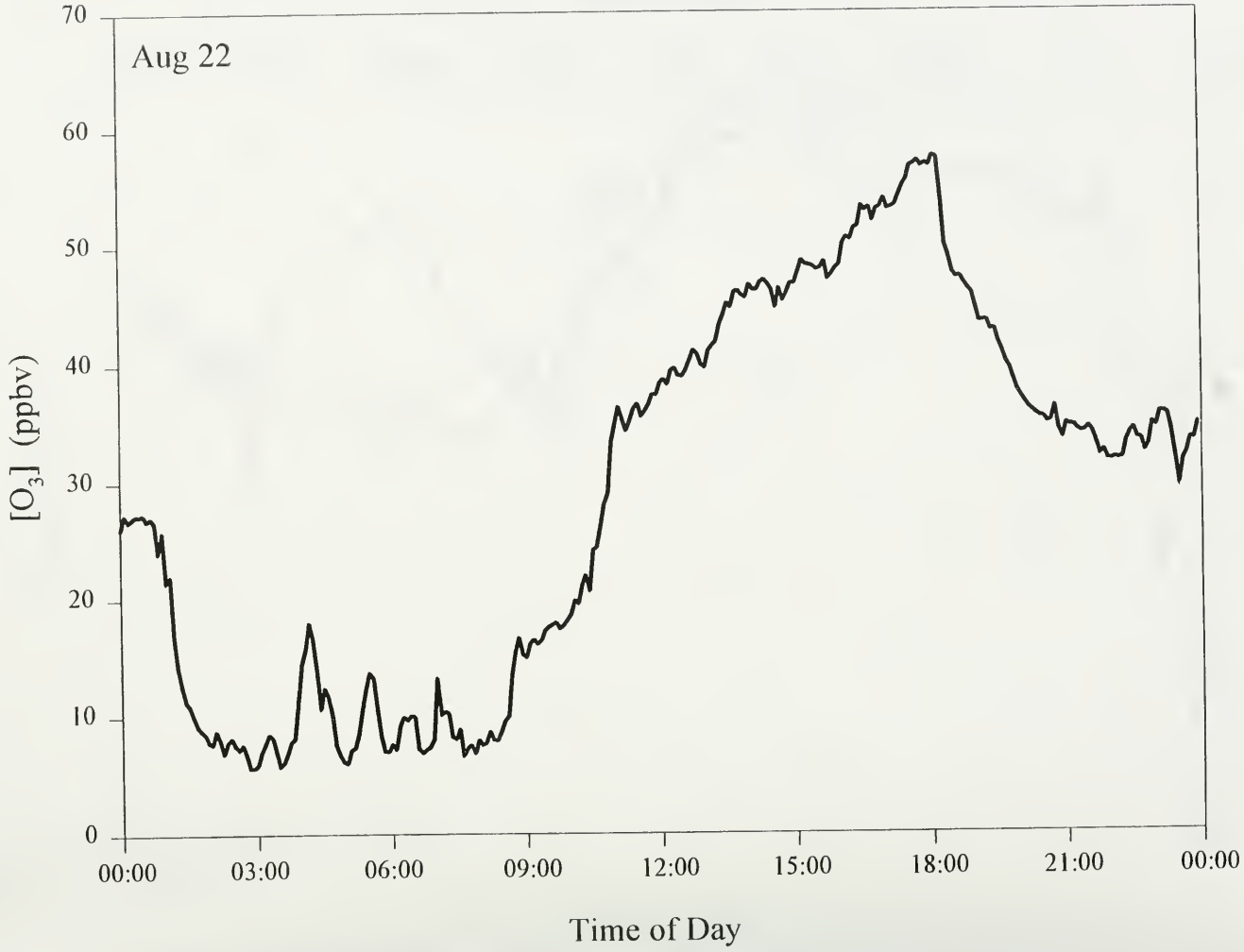

Figure 6b.iv. NO_x data on Aug 22 nd when there was no incursion of polluted air in the late afternoon.

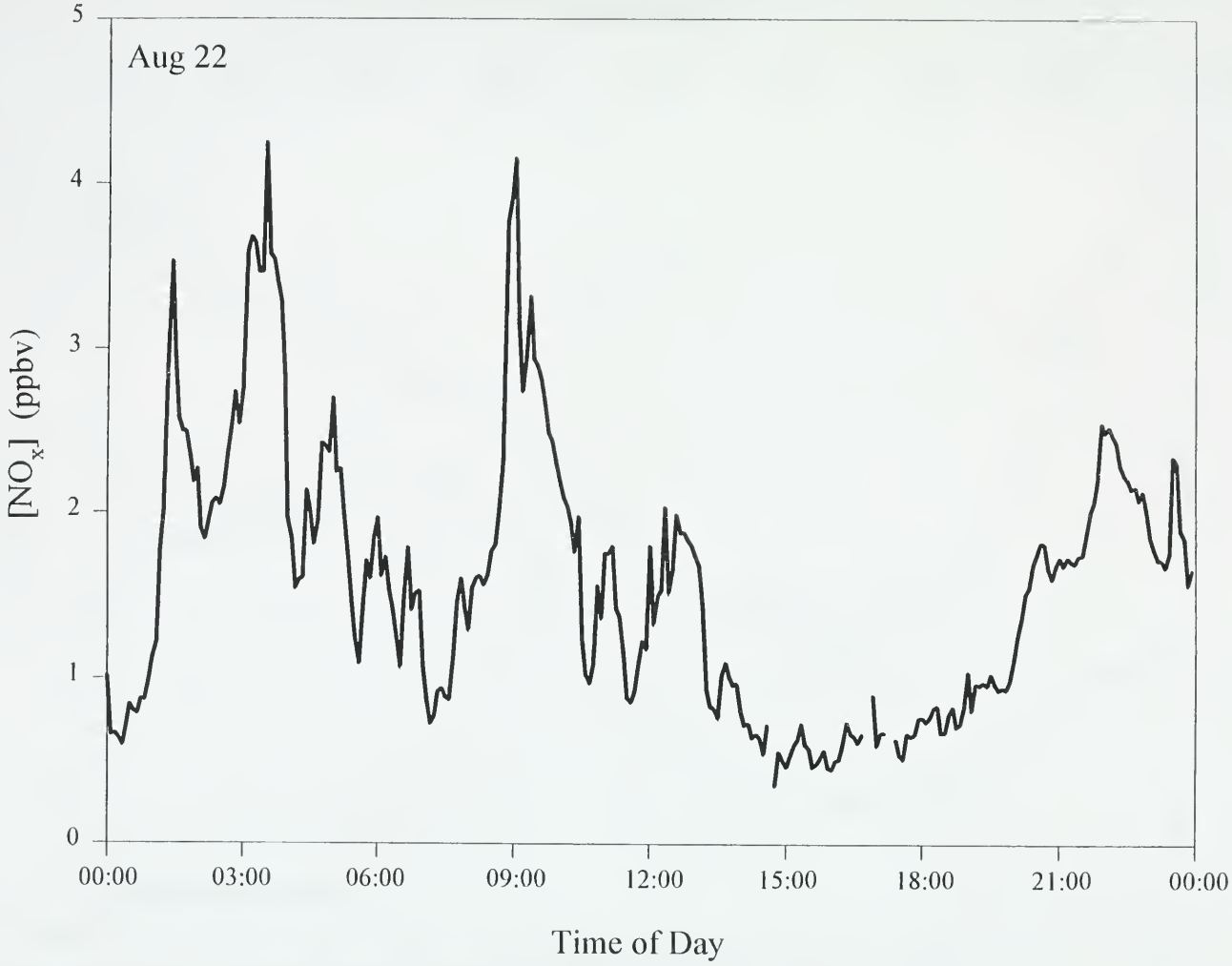

Figure 6b.v. Summer average of Ozone data showing no incursion of polluted air in the late afternoon.

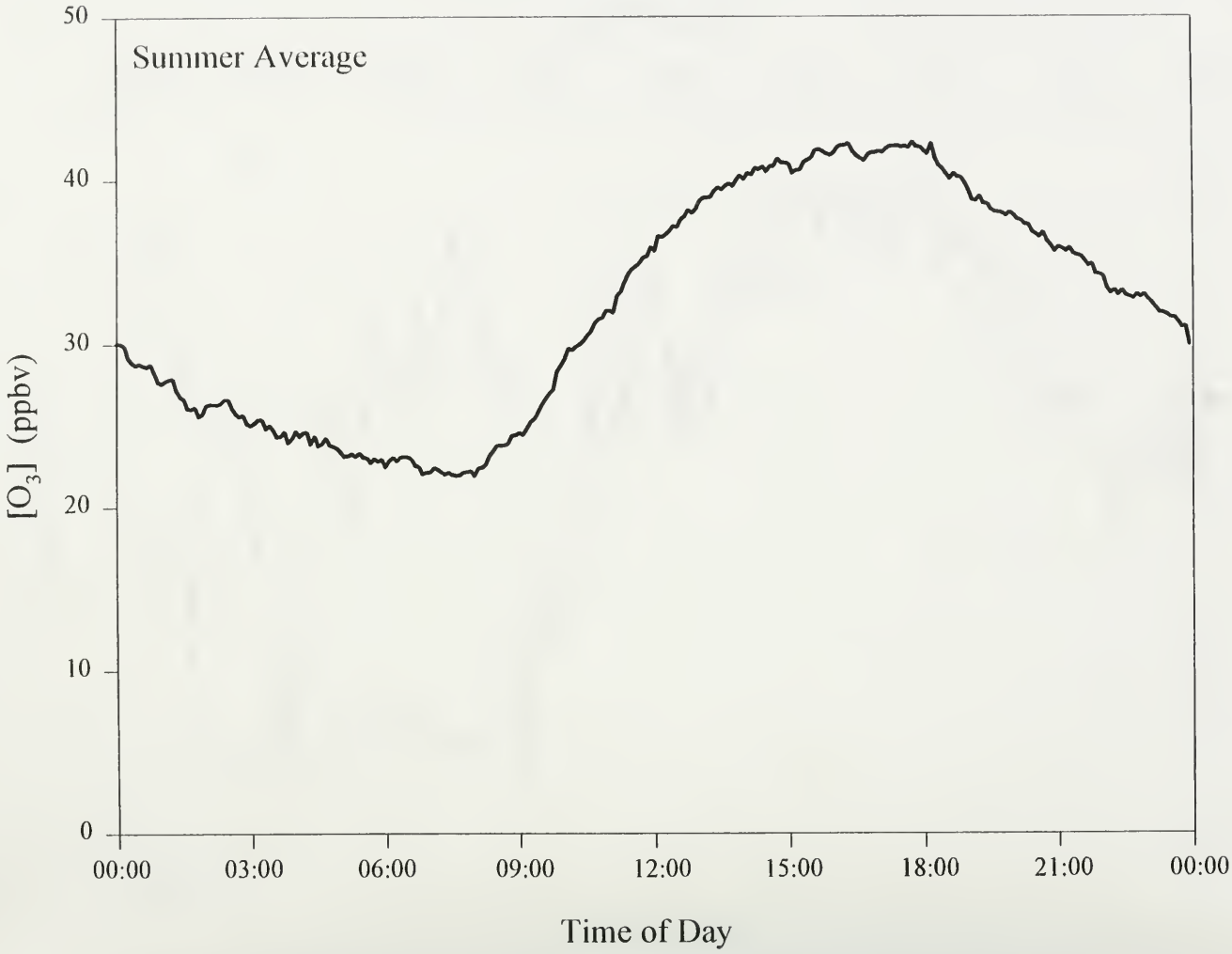

Figure 6b.vi. Summer average of NO_x data showing no incursion of polluted air in the late afternoon.

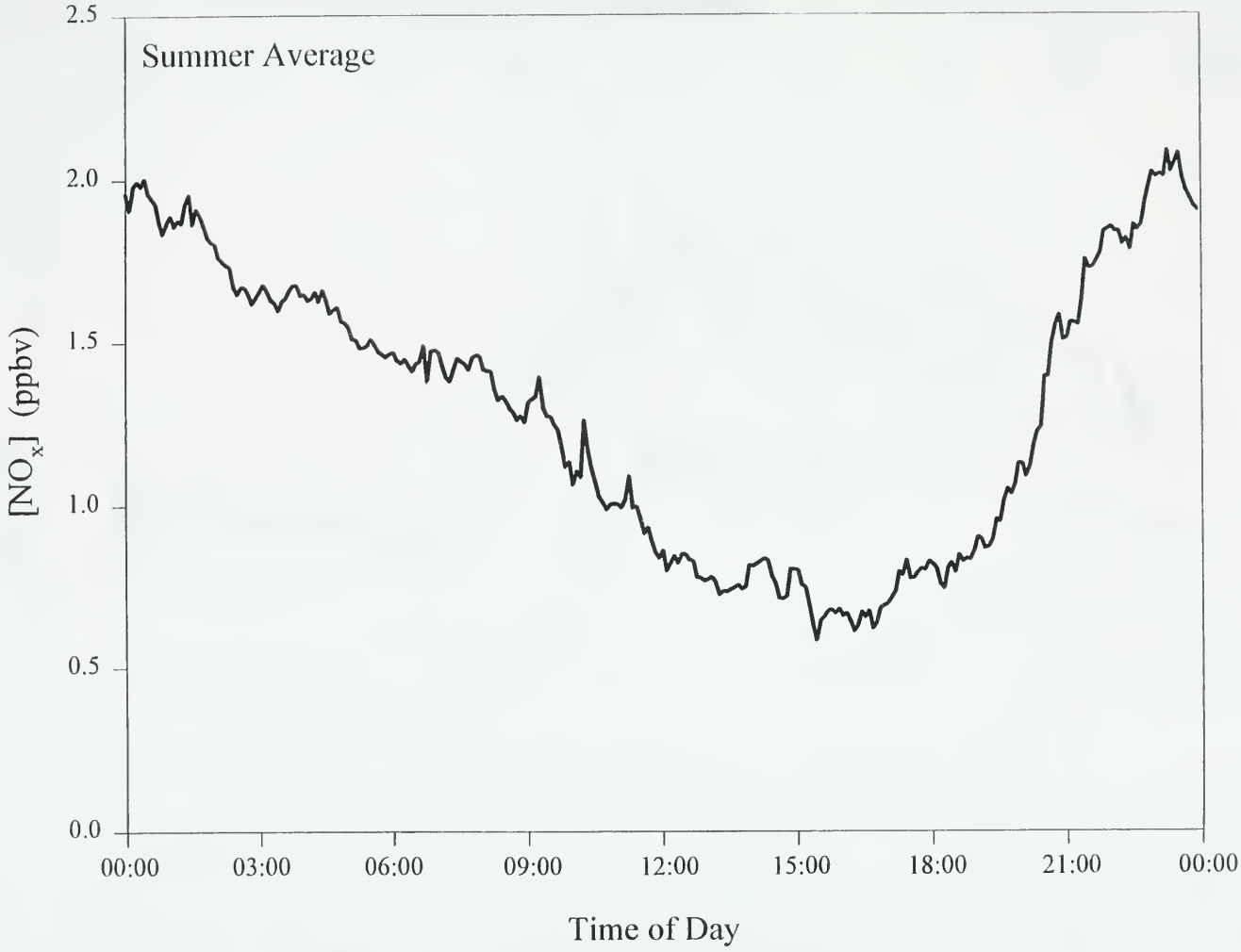

Figure 7a.i. NO_x/NO_y data on Aug 1st when there was an incursion of polluted air in the late afternoon.

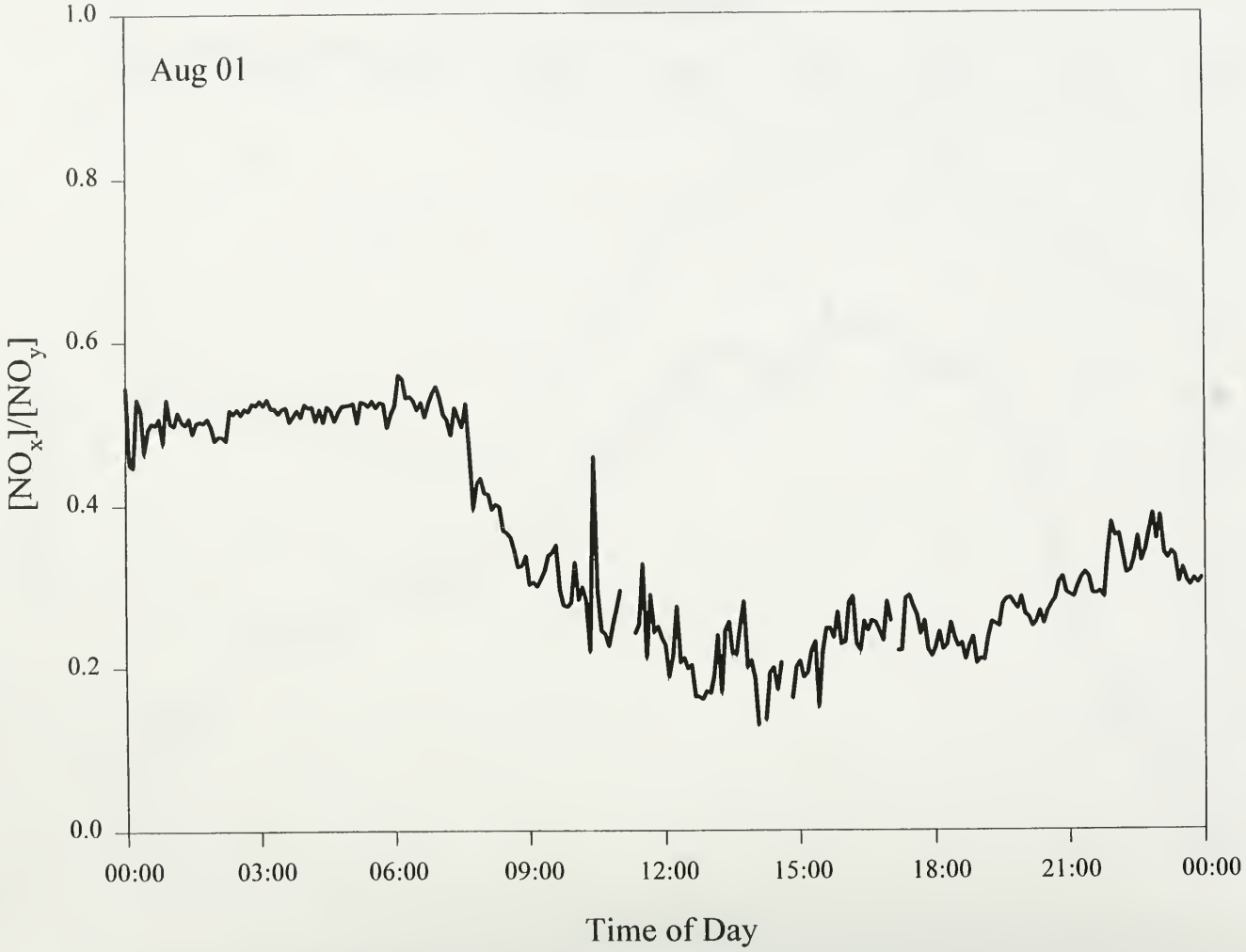

Figure 7a.ii. O_3/NO_z data on Aug 1st when there was an incursion of polluted air in the late afternoon.

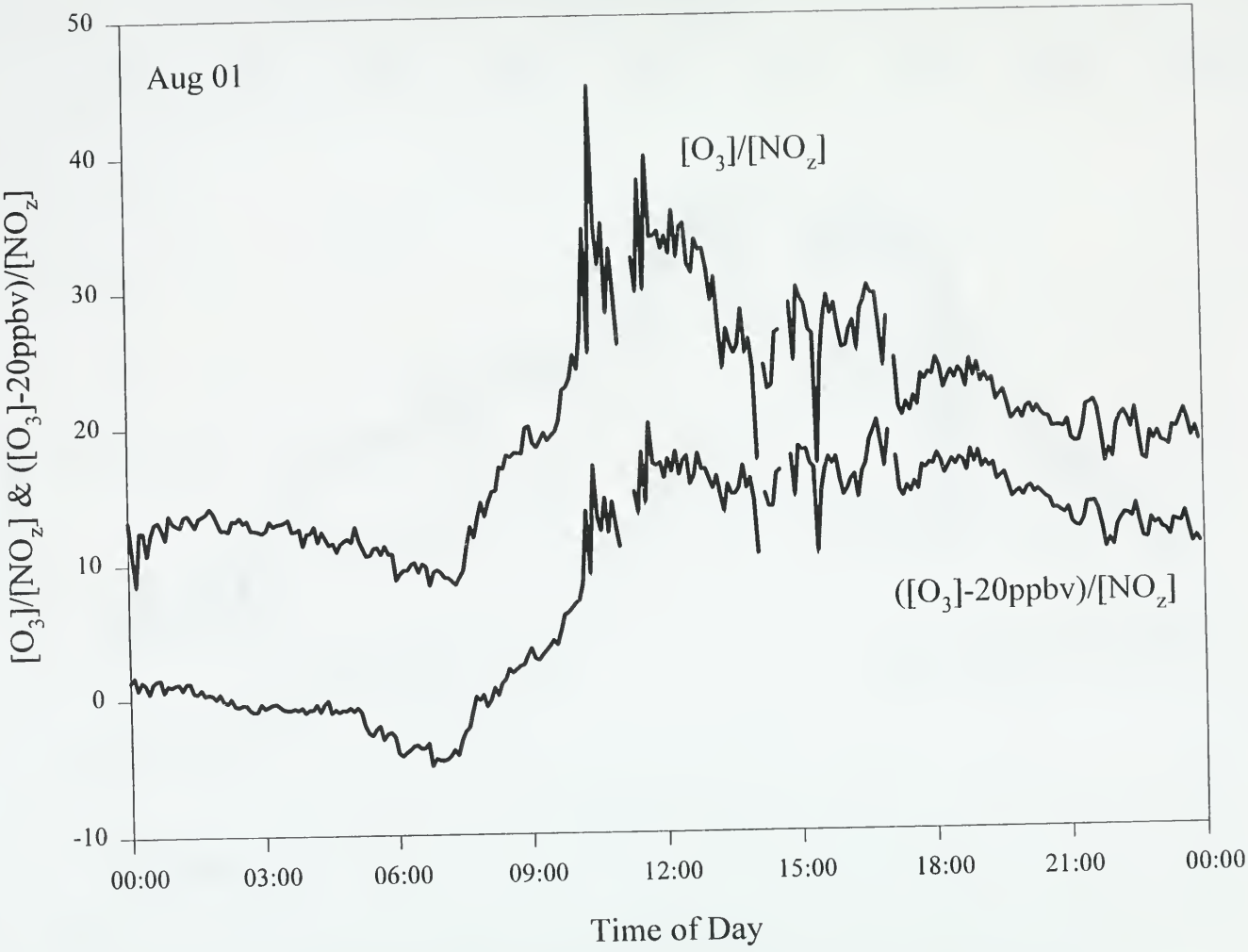

Figure 7a.iii. NO_x/NO_y data on Aug 8th when there was an incursion of polluted air in the late afternoon.

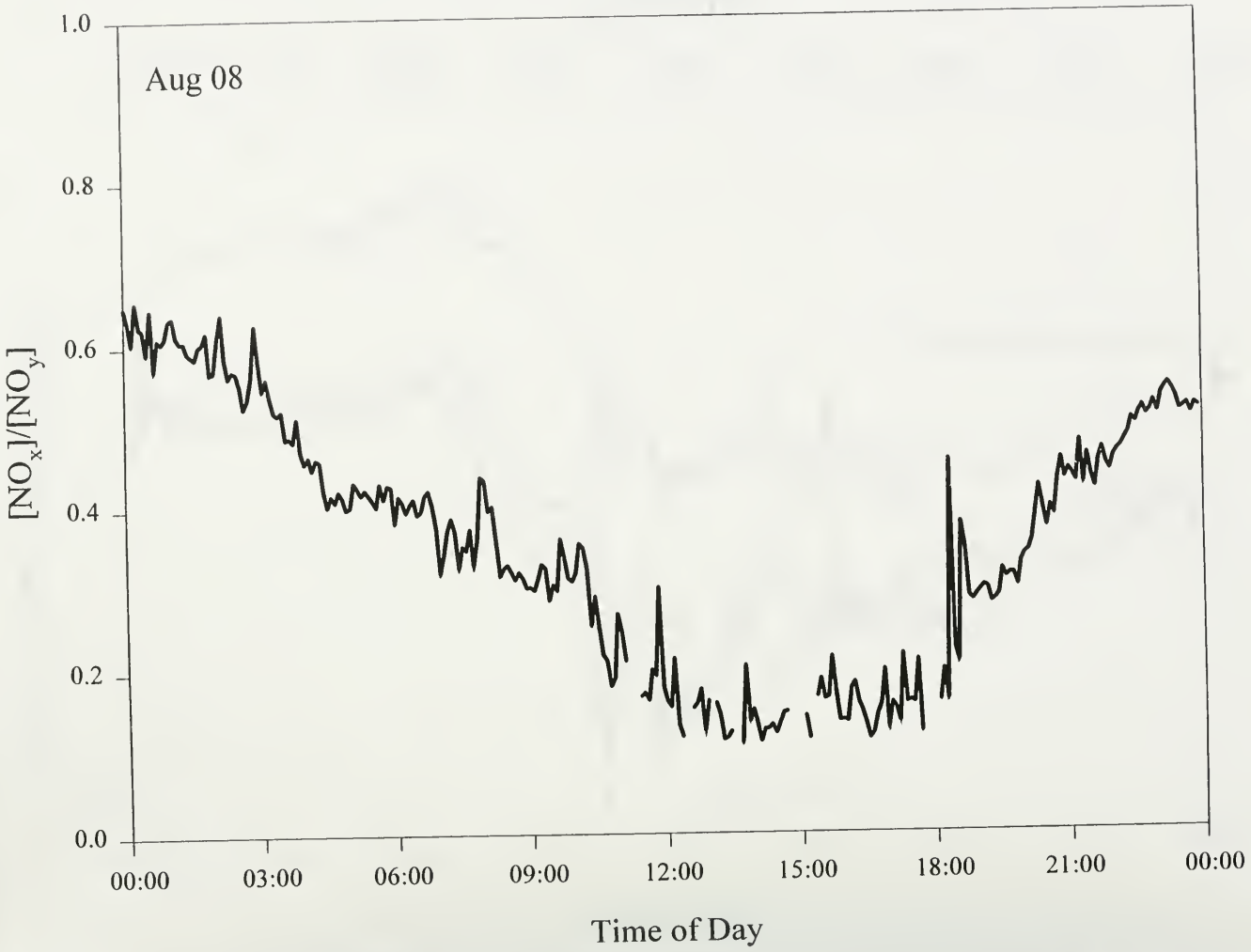

Figure 7a.iv. O_3/NO_z data on Aug 8th when there was an incursion of polluted air in the late afternoon.

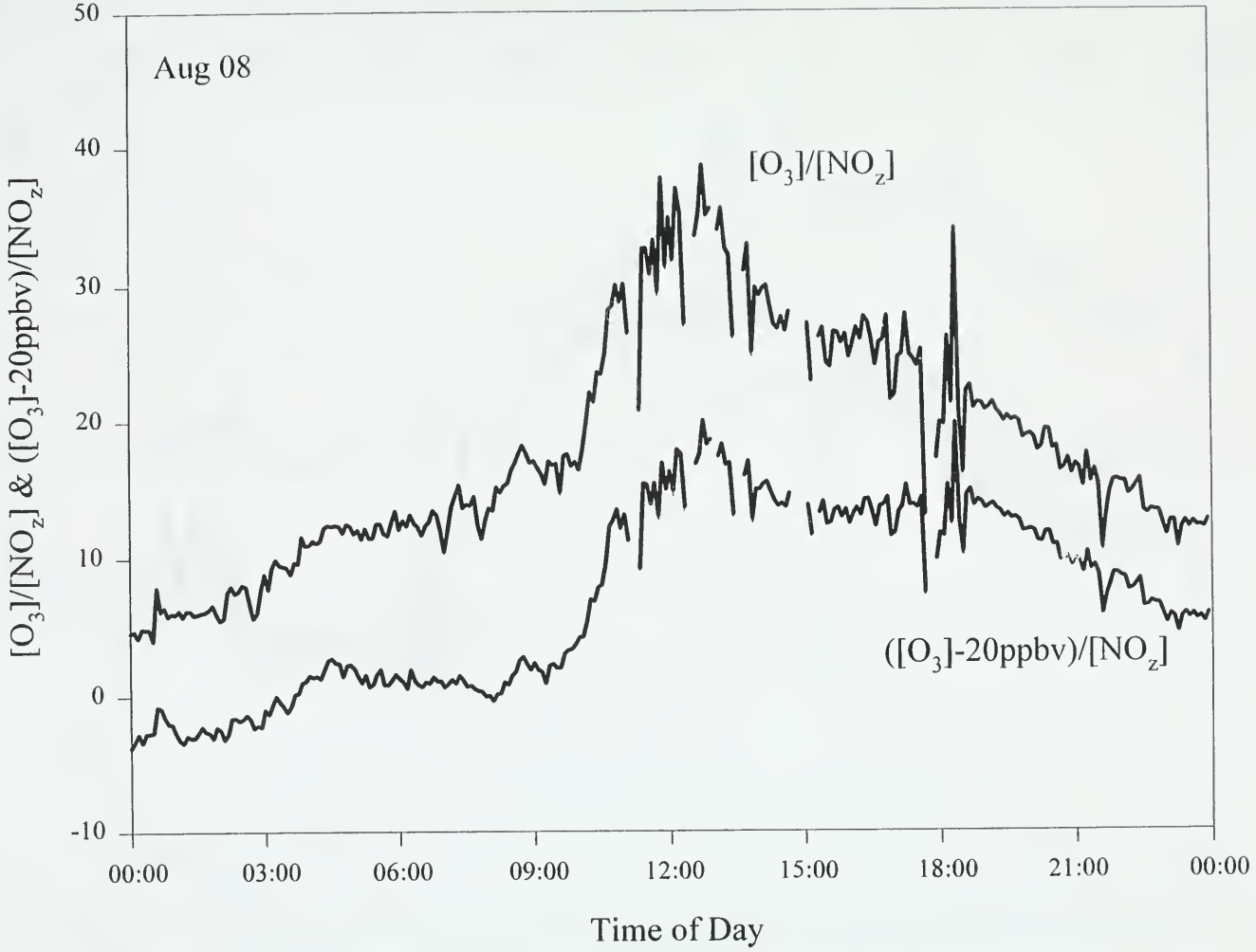

Figure 7a.v. NO /NO data on Aug 15 when there was an incur

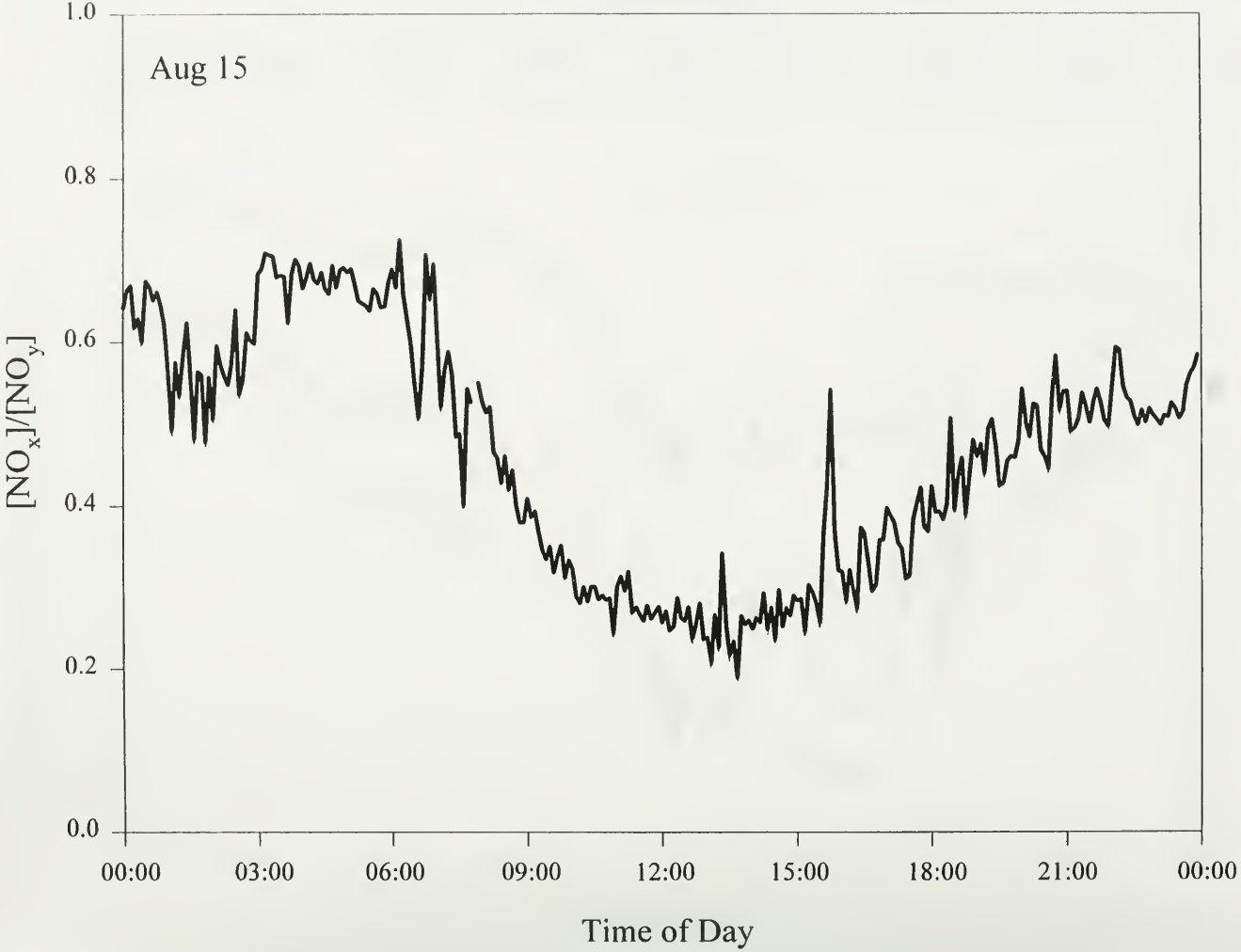

Figure 7a.vi. O_3/NO_z data on Aug 15th when there was an incursion of polluted air in the late afternoon.

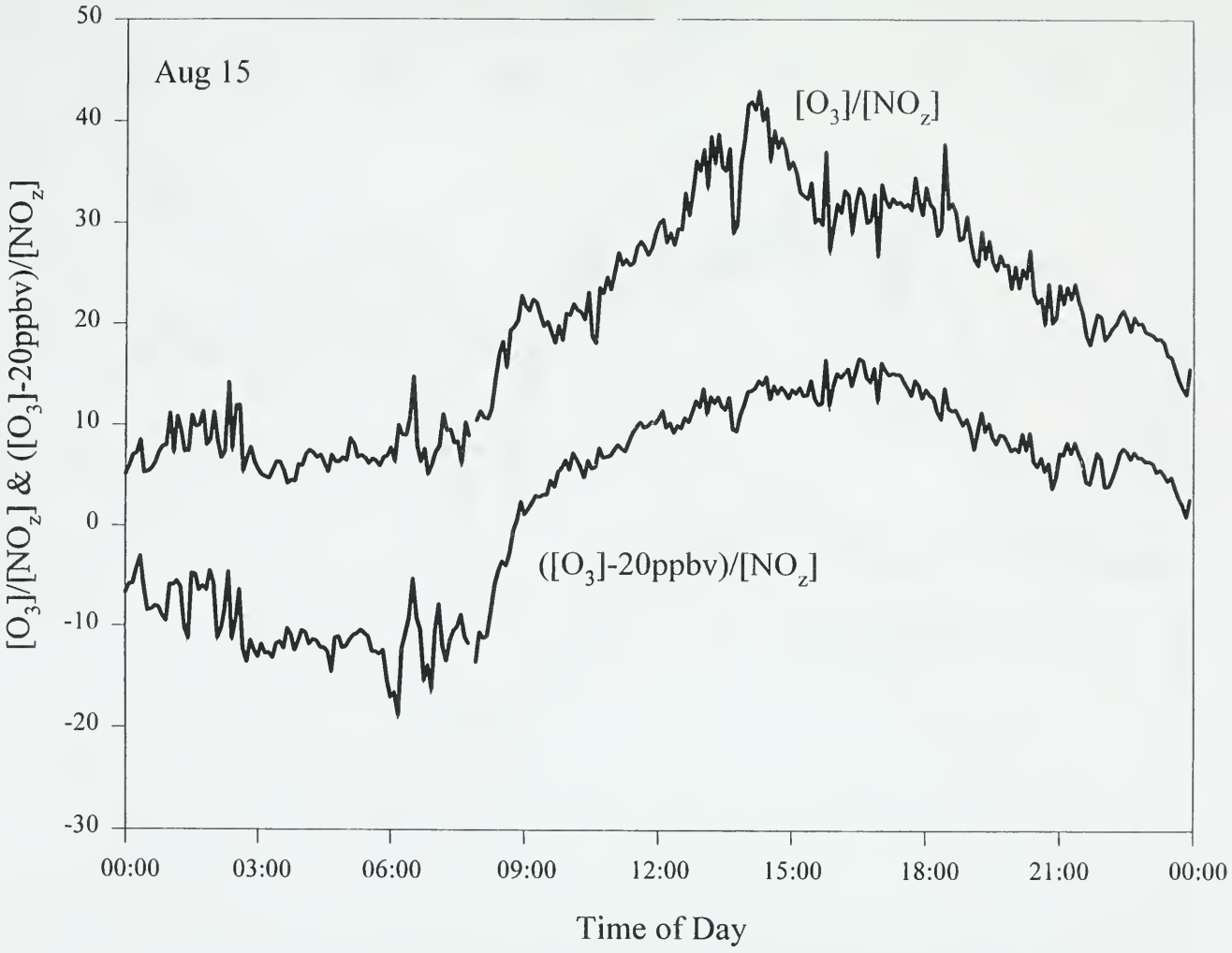

Figure 7a.vii. NO_x/NO_y data on Aug 18th when there was an incursion of polluted air in the late afternoon.

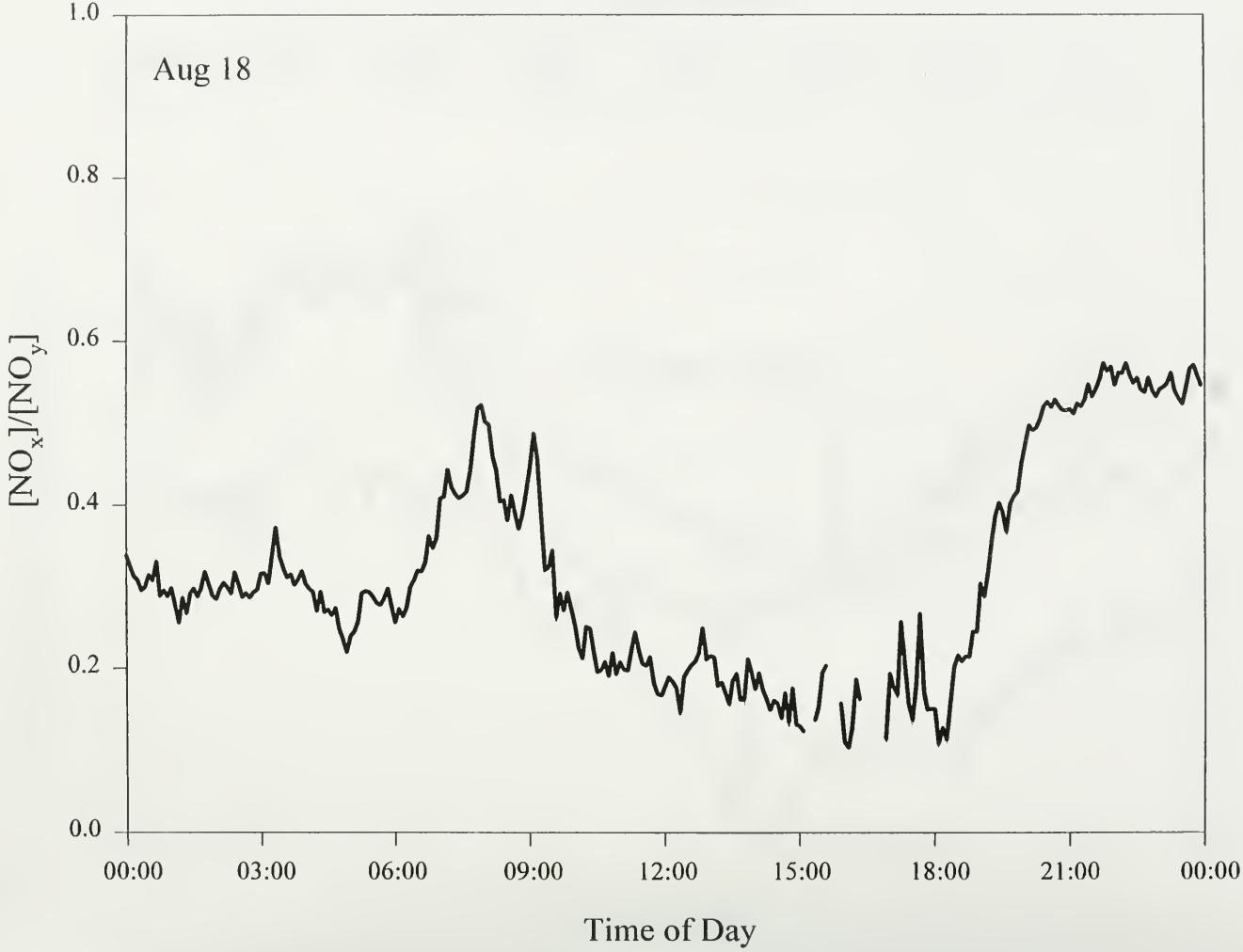

Figure 7a.viii. O_3/NO_z data on Aug 18th when there was an incursion of polluted air in the late afternoon.

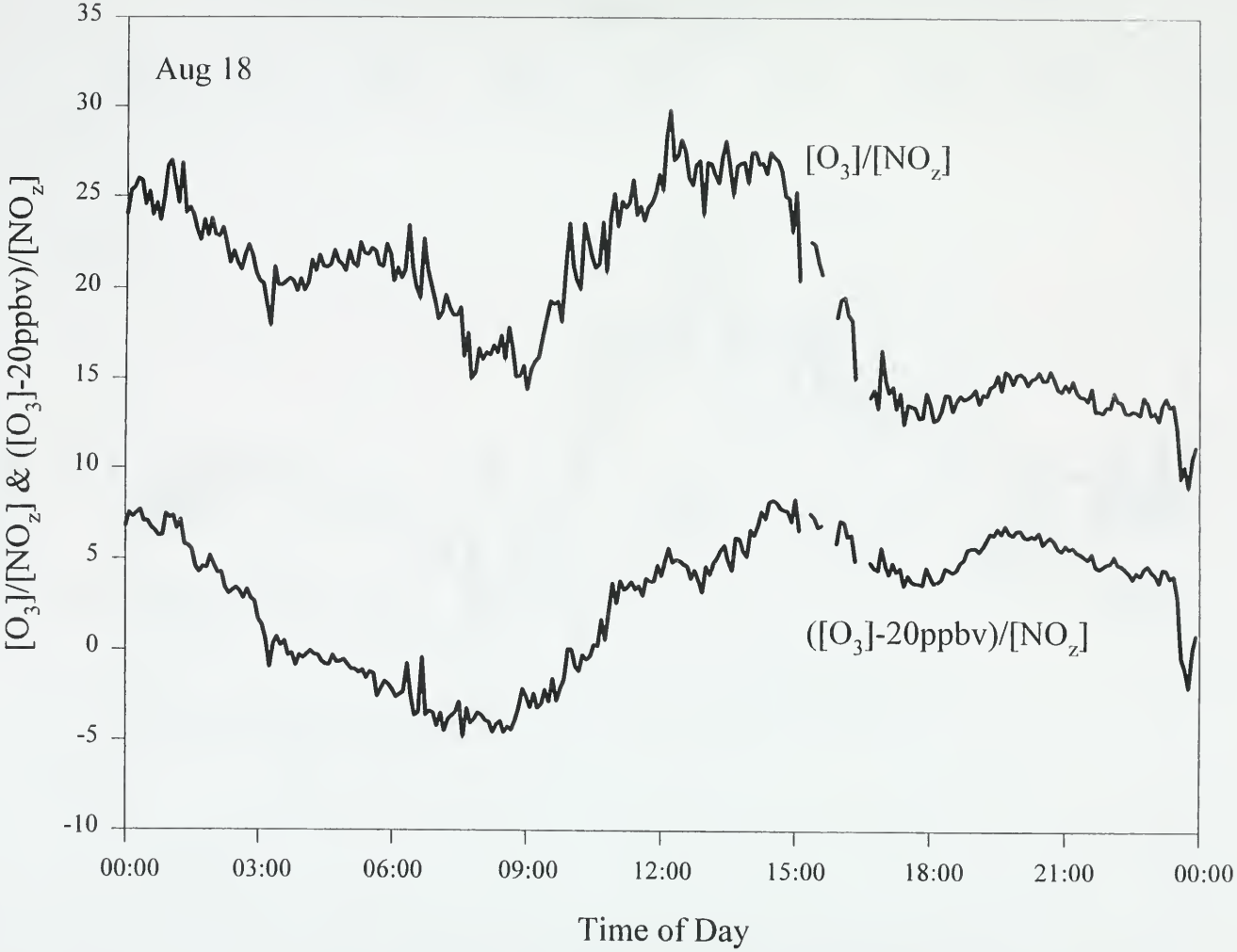

Figure 7a.ix. NO_x/NO_y data on Aug 26th when there was an incursion of polluted air in the late afternoon.

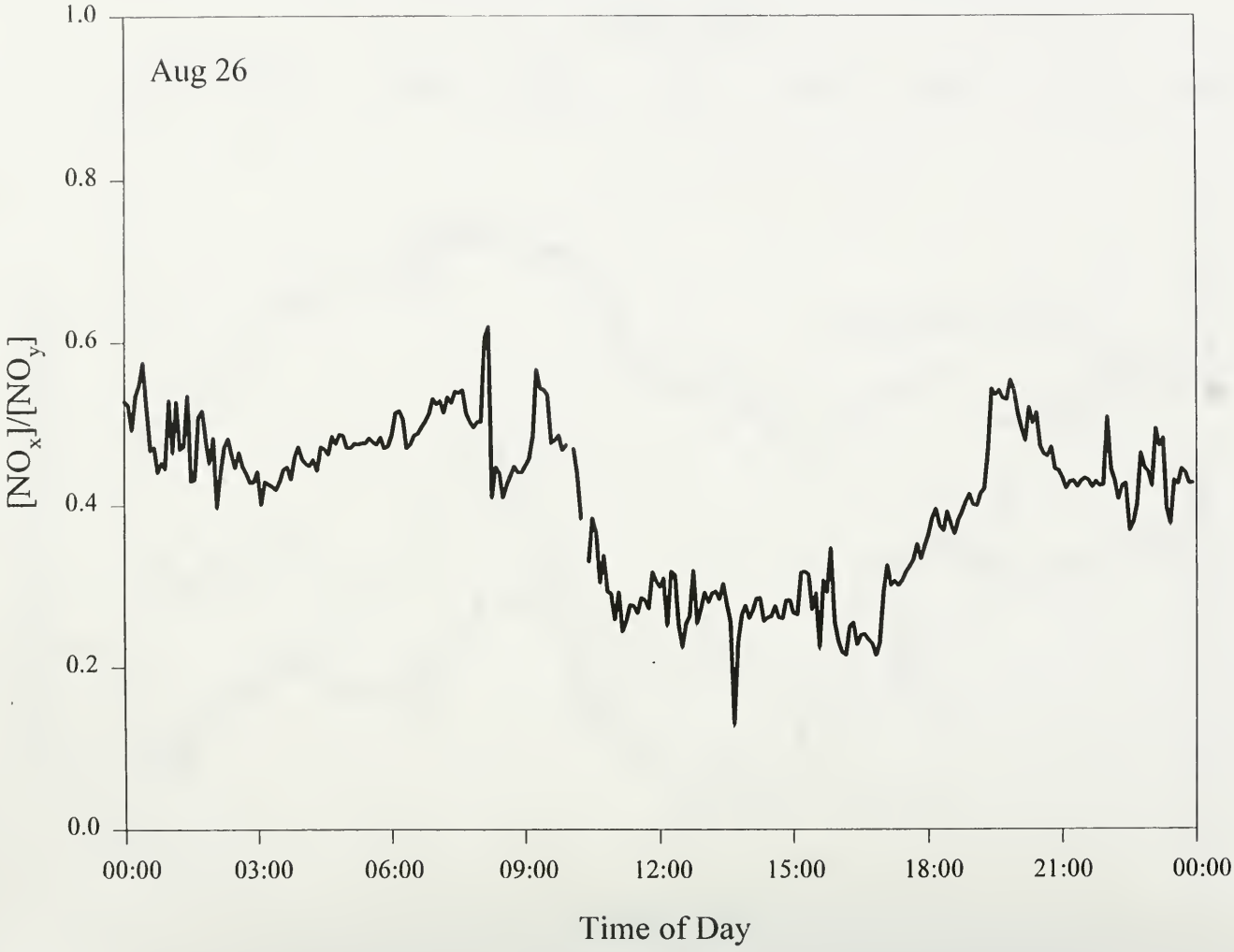

Figure 7a.x. O_3/NO_z data on Aug 26th when there was an incursion of polluted air in the late afternoon.

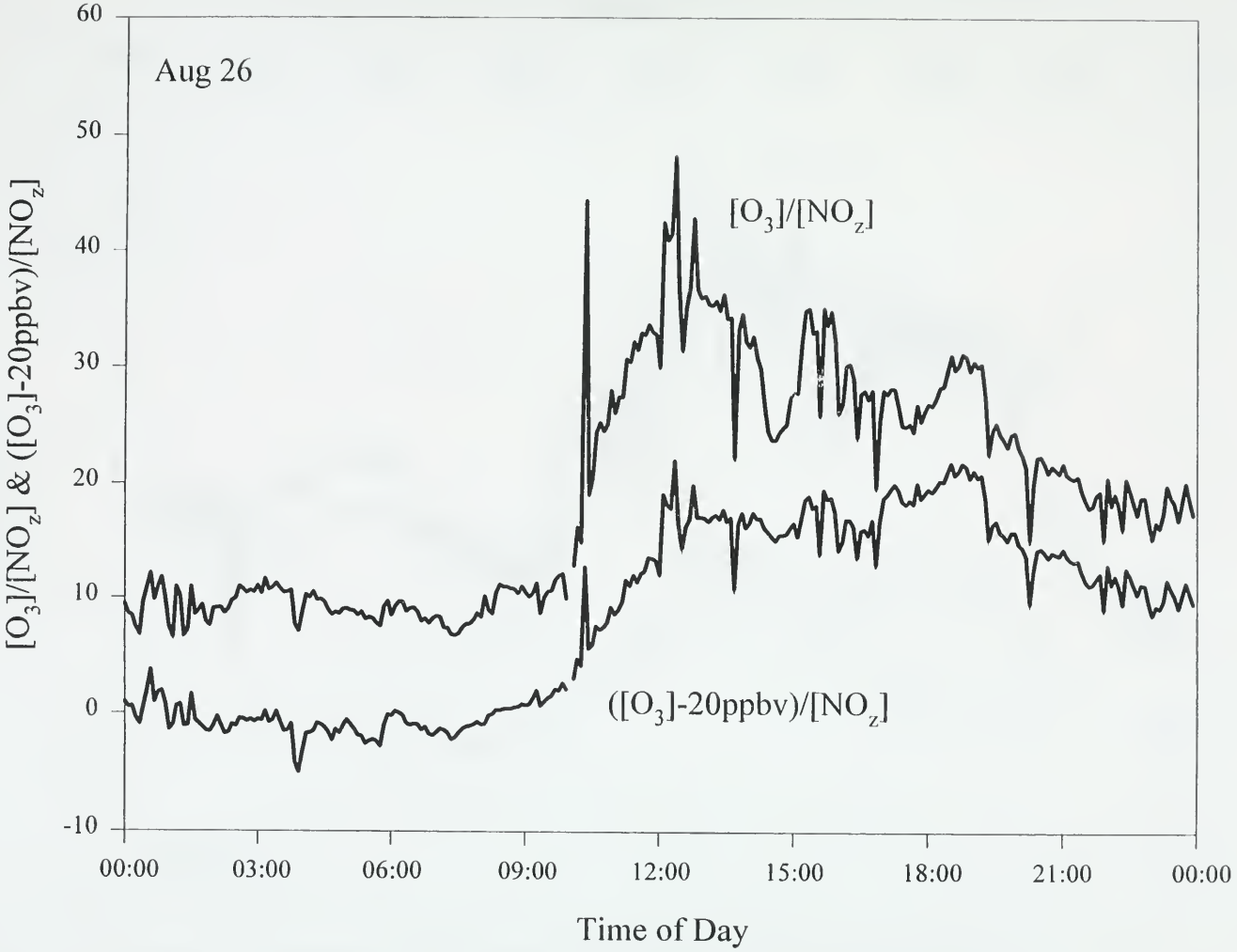

Figure 7b.i. NO_x/NO_y data on Aug 5th when there was no incursion of polluted air in the late afternoon.

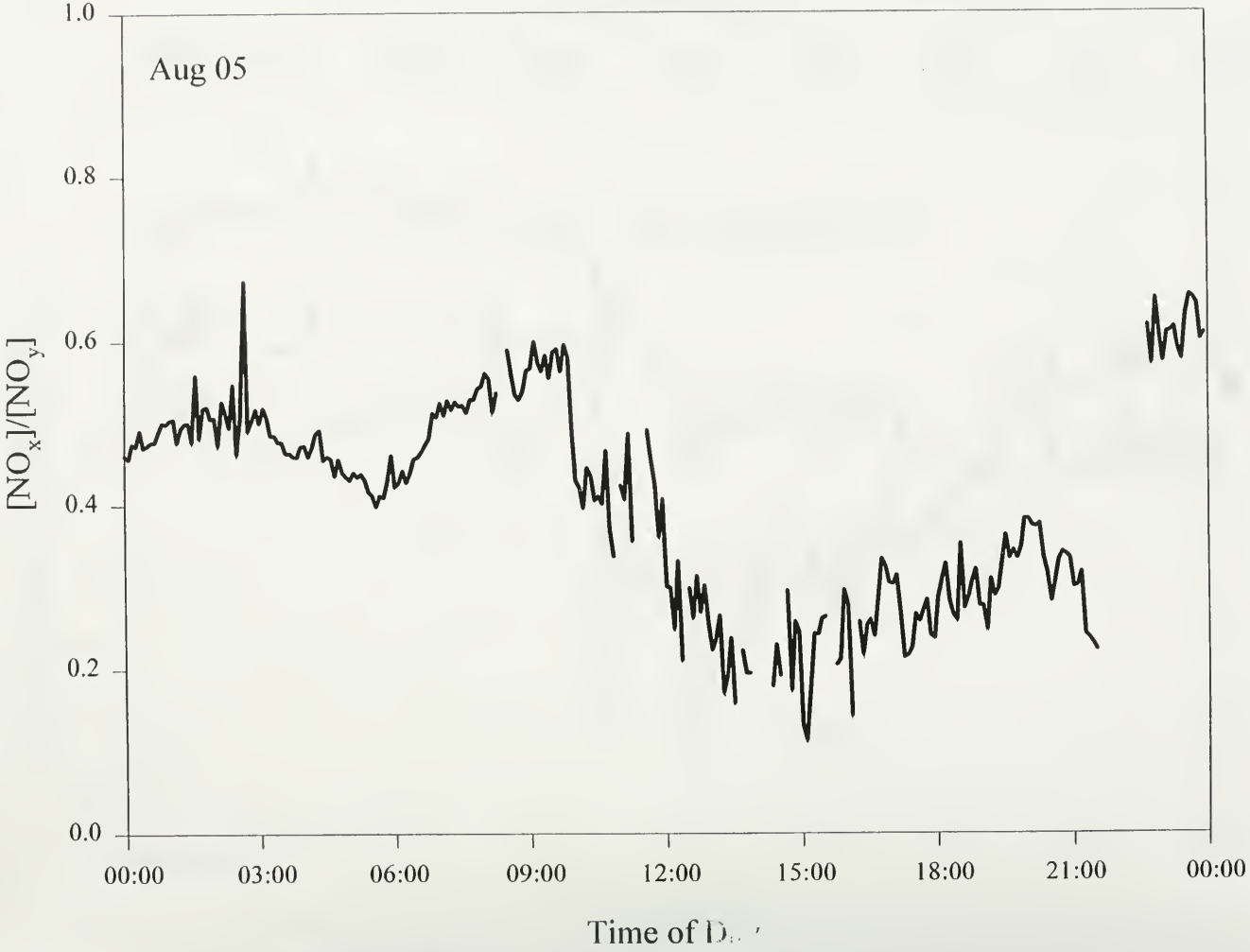

Figure 7b.ii. O_3/NO_z data on Aug 5th when there was no incursion of polluted air in the late afternoon.

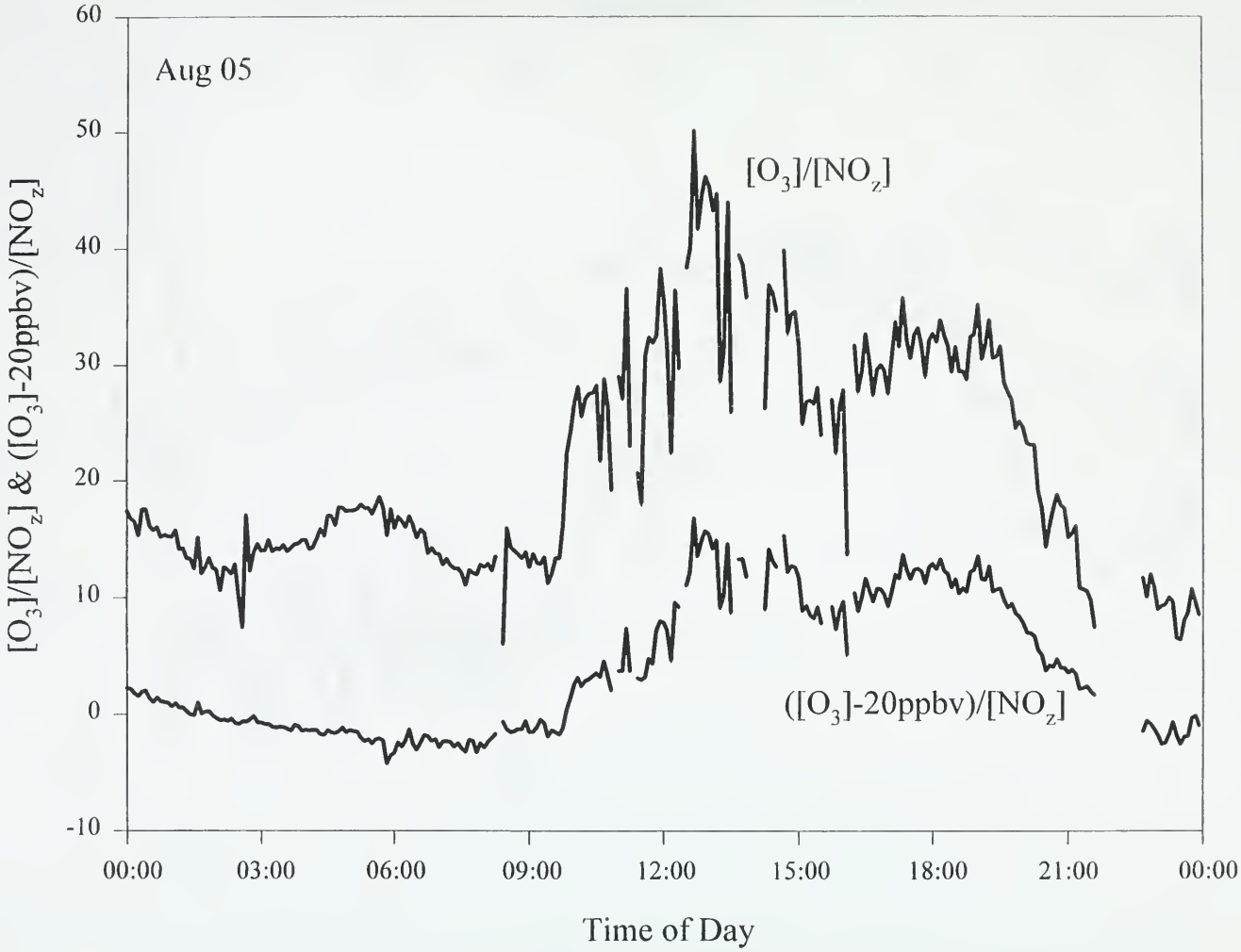

Figure 7b.iii. NO_x/NO_y data on Aug 22nd when there was no incursion of polluted air in the late afternoon.

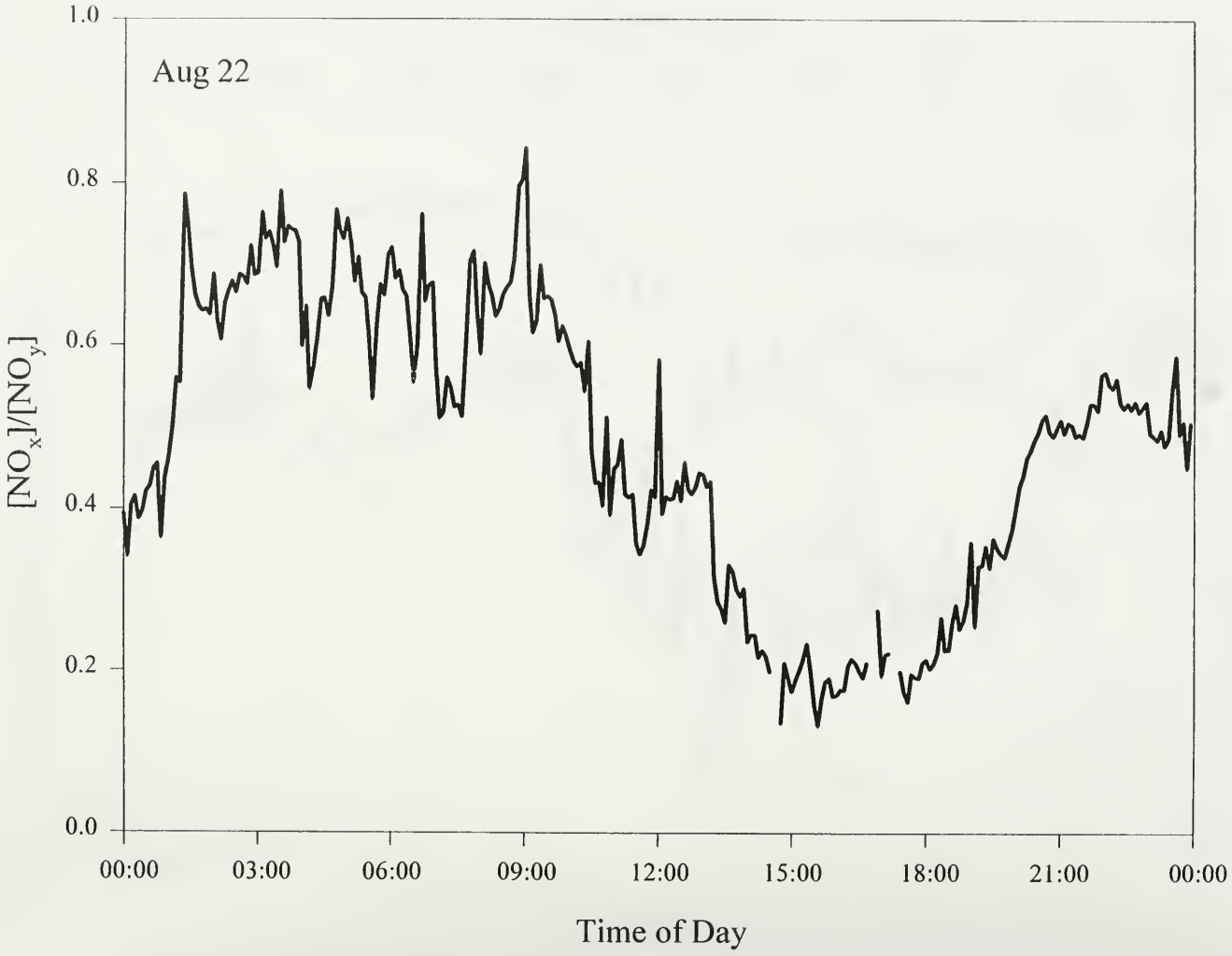

Figure 7b.iv. O_3/NO_z data on Aug 22 nd when there was no incursion of polluted air in the late afternoon.

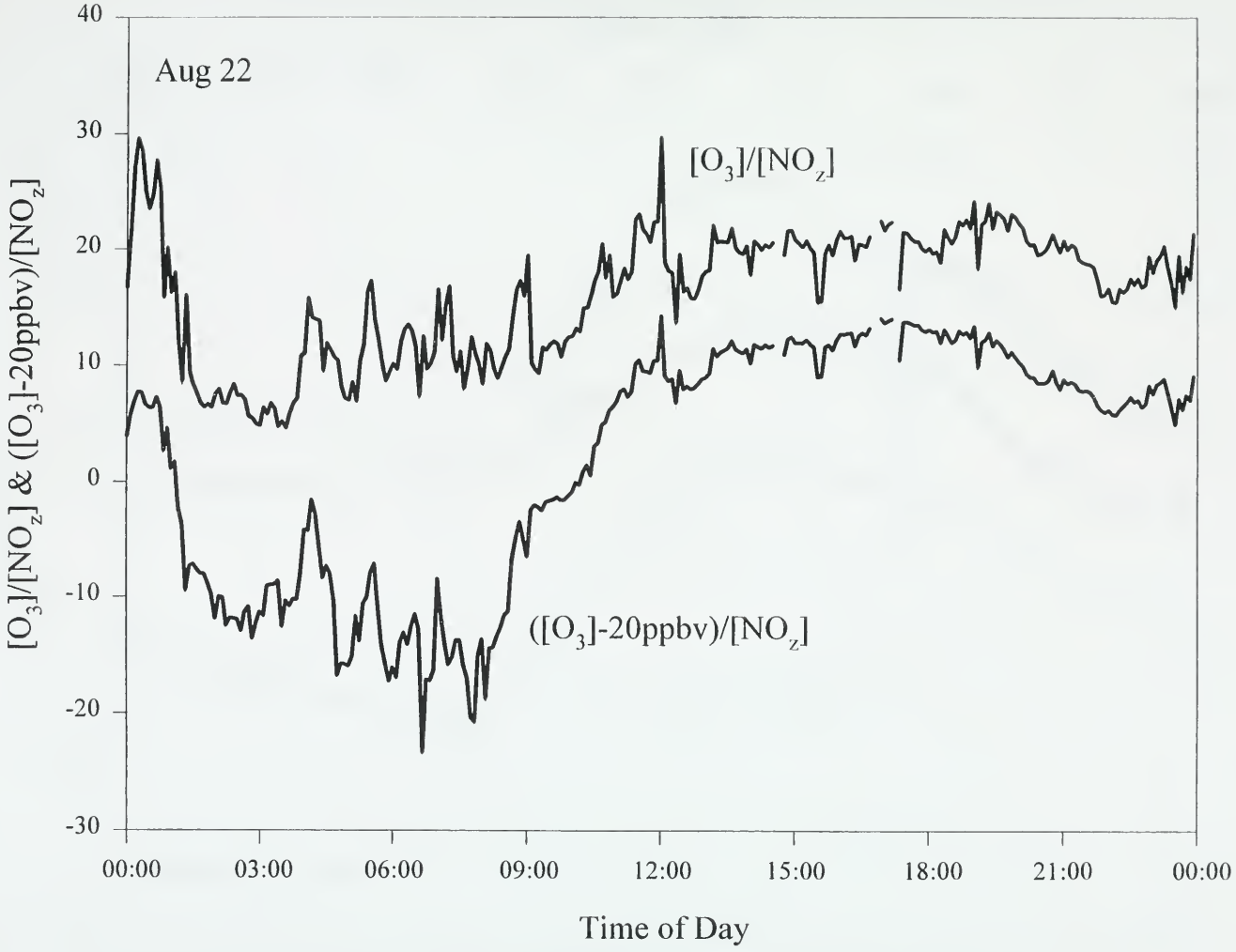

Figure 7b.v. Summer average of NO_x/NO_y data showing no incursion of polluted air in the late afternoon.

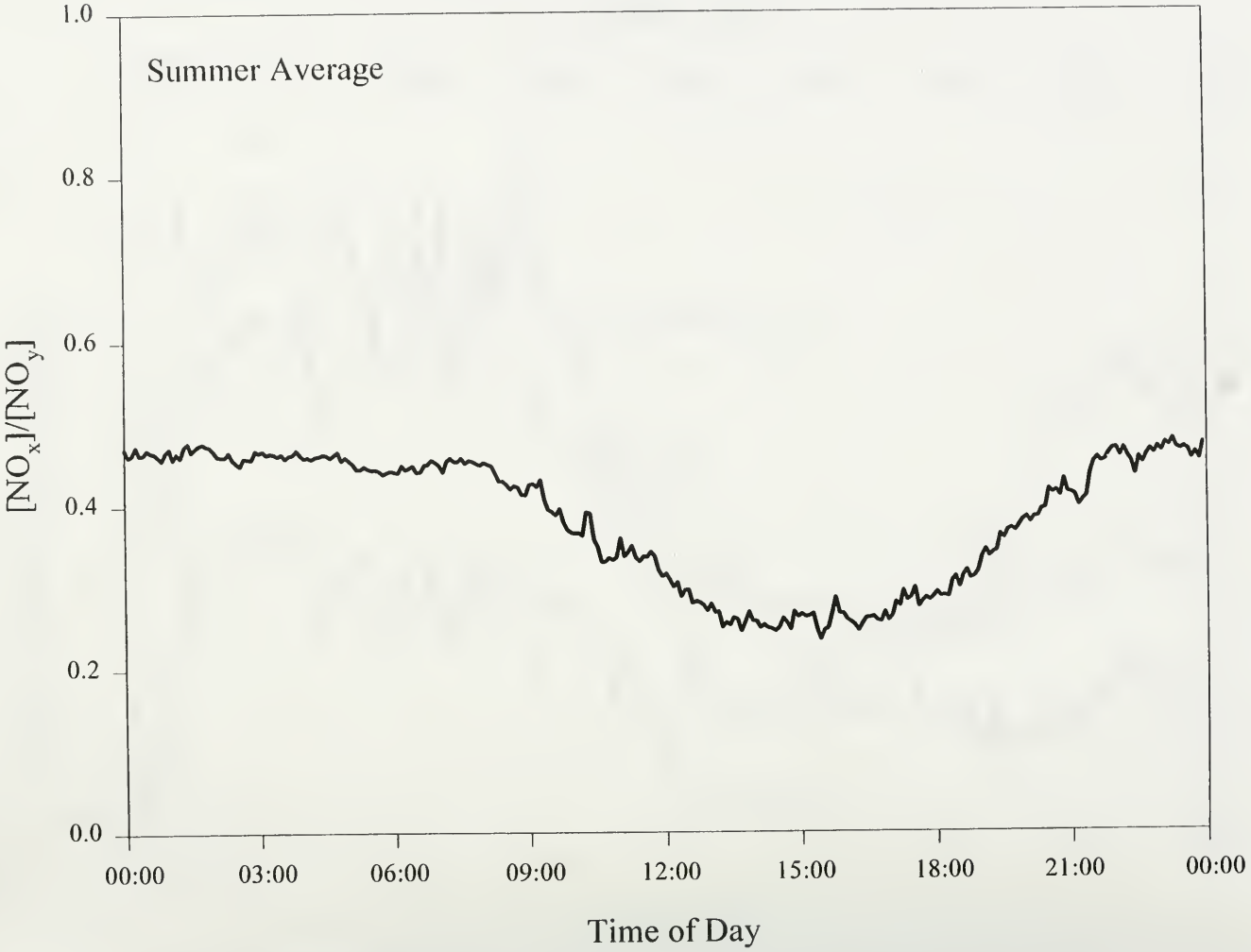

Figure 7b.vi. Summer average of O_3/NO_z data showing no incursion of polluted air in the late afternoon.

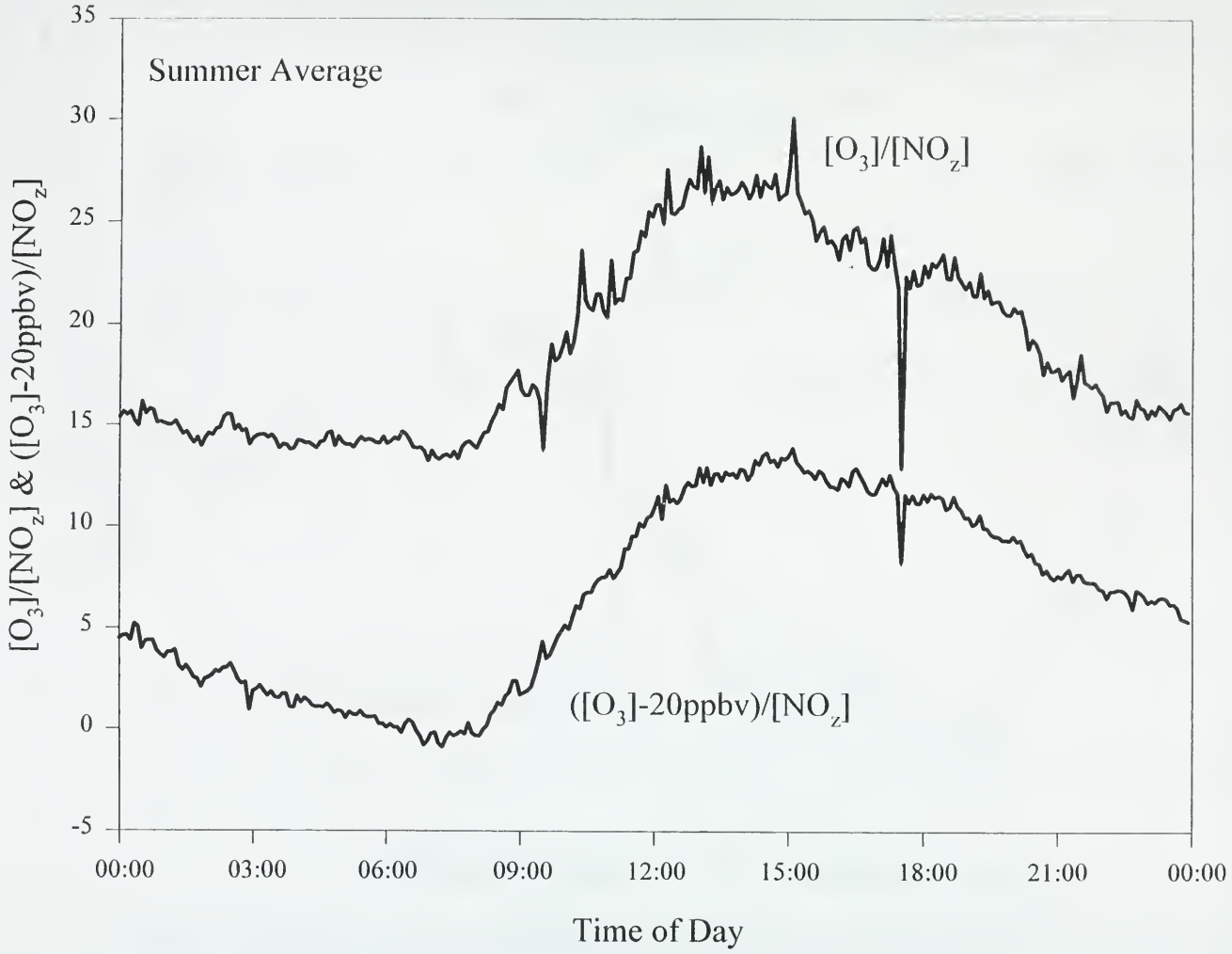

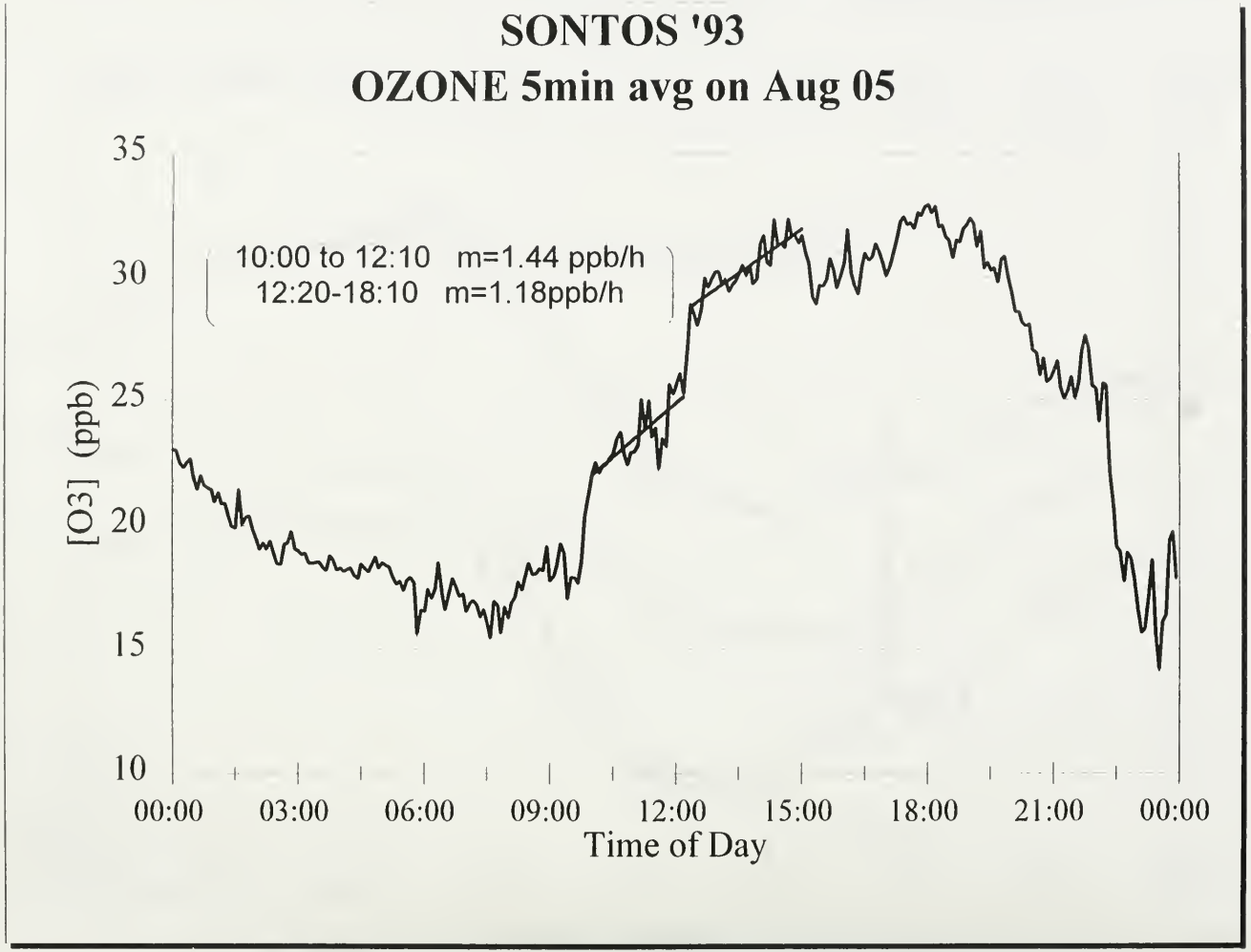

Figure 8a.i. Diurnal plot of Ozone on Aug 5th used to determine observed Ozone production rates.

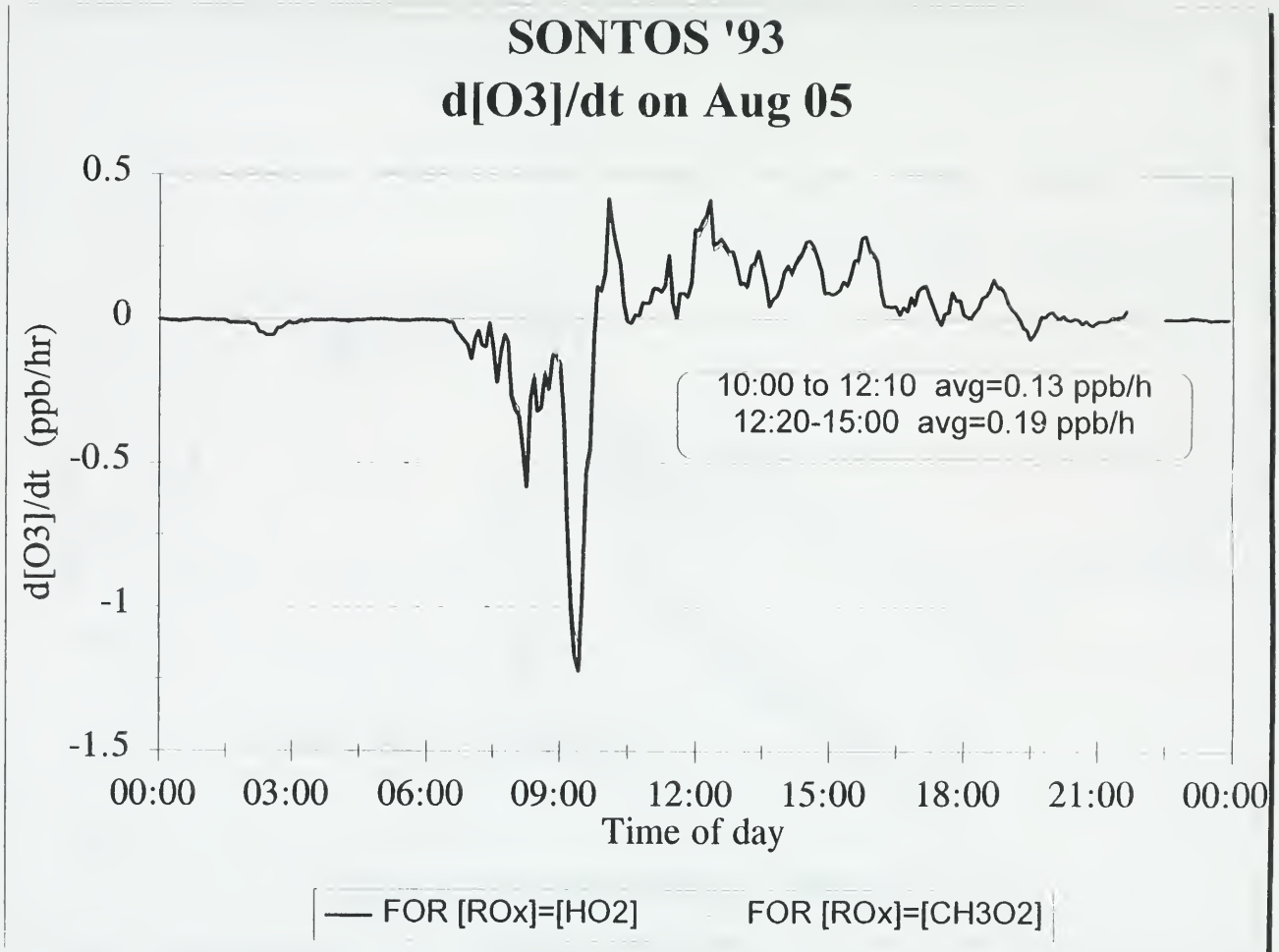

Figure 8b.i. Diurnal plot of the Ozone production rate calculated from the radical data on Aug 5th.

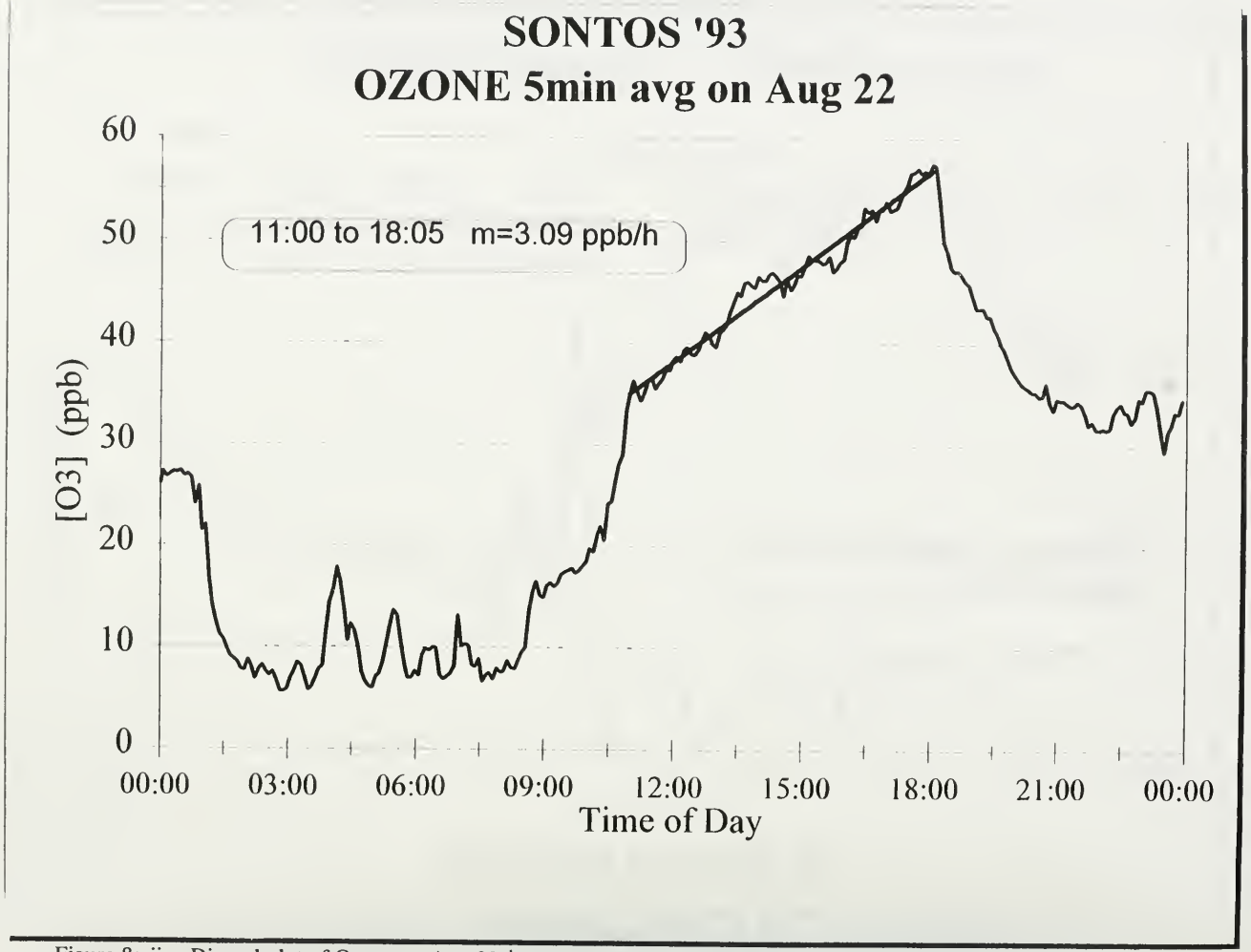

Figure 8a.ii. Diurnal plot of Ozone on Aug 22nd used to determine observed Ozone production rates.

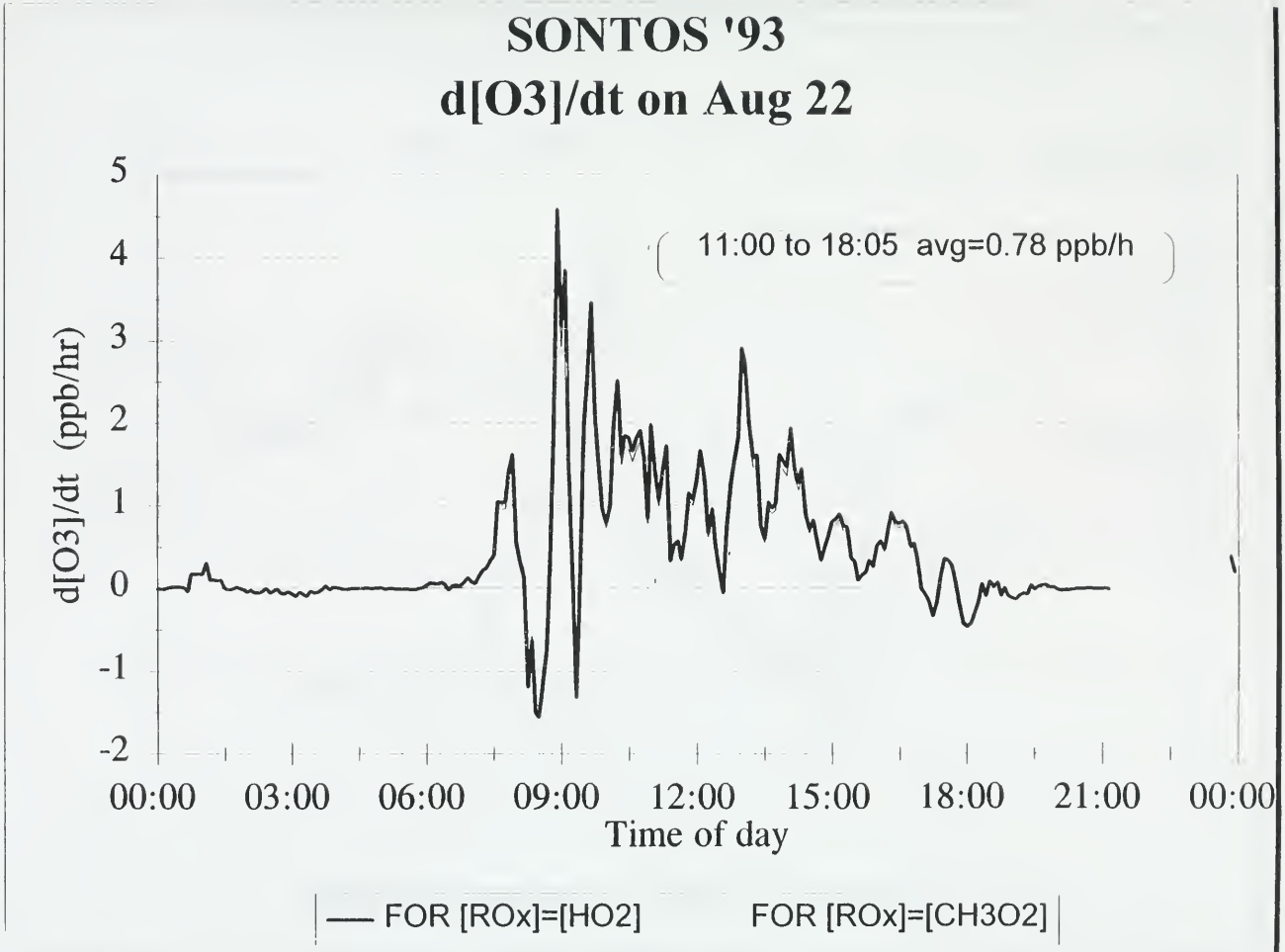

Figure 8b.ii. Diurnal plot of the Ozone production rate calculated from the radical data on Aug 22nd.

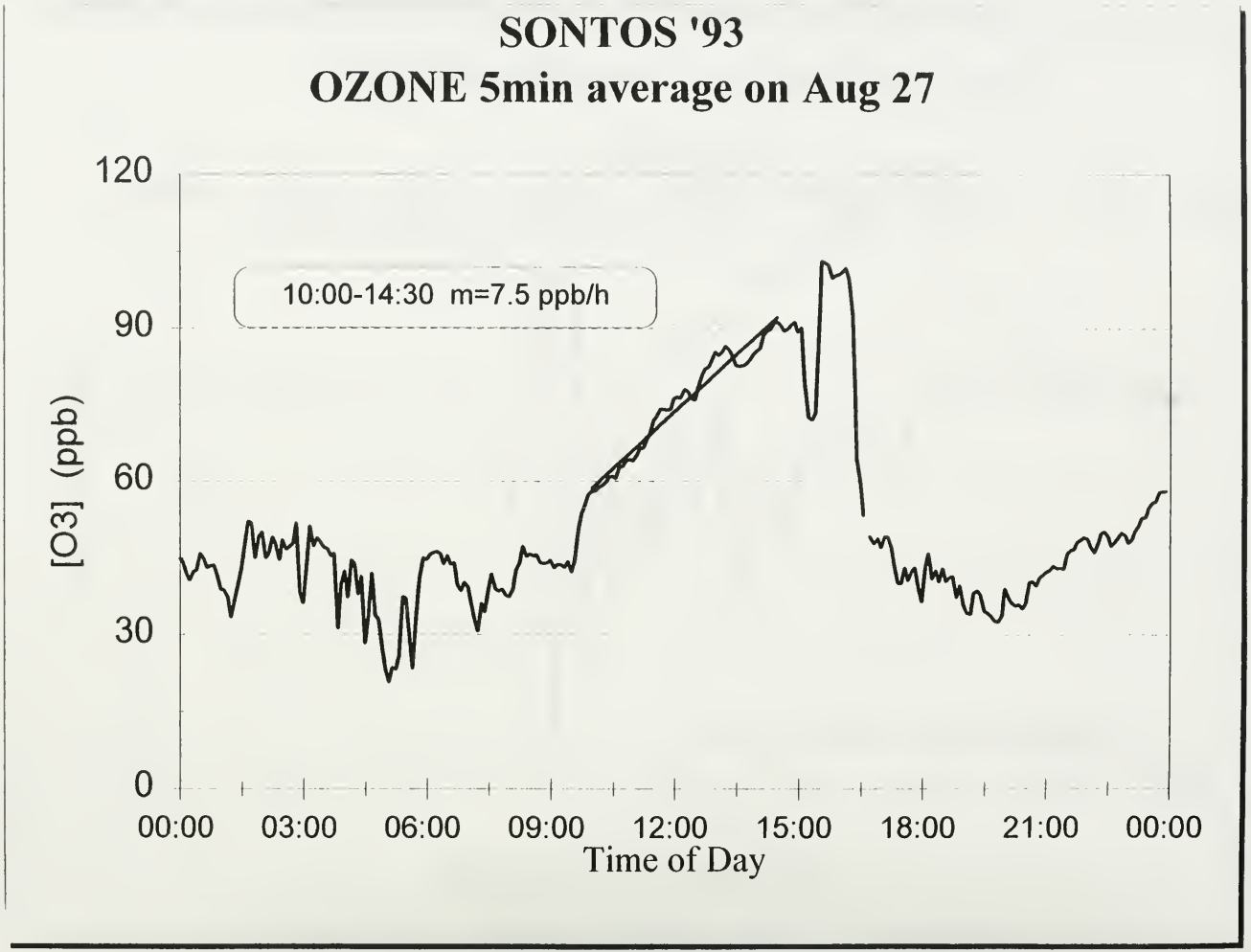

Figure 8a.iii. Diurnal plot of Ozone on Aug 27th used to determine observed Ozone production rates.

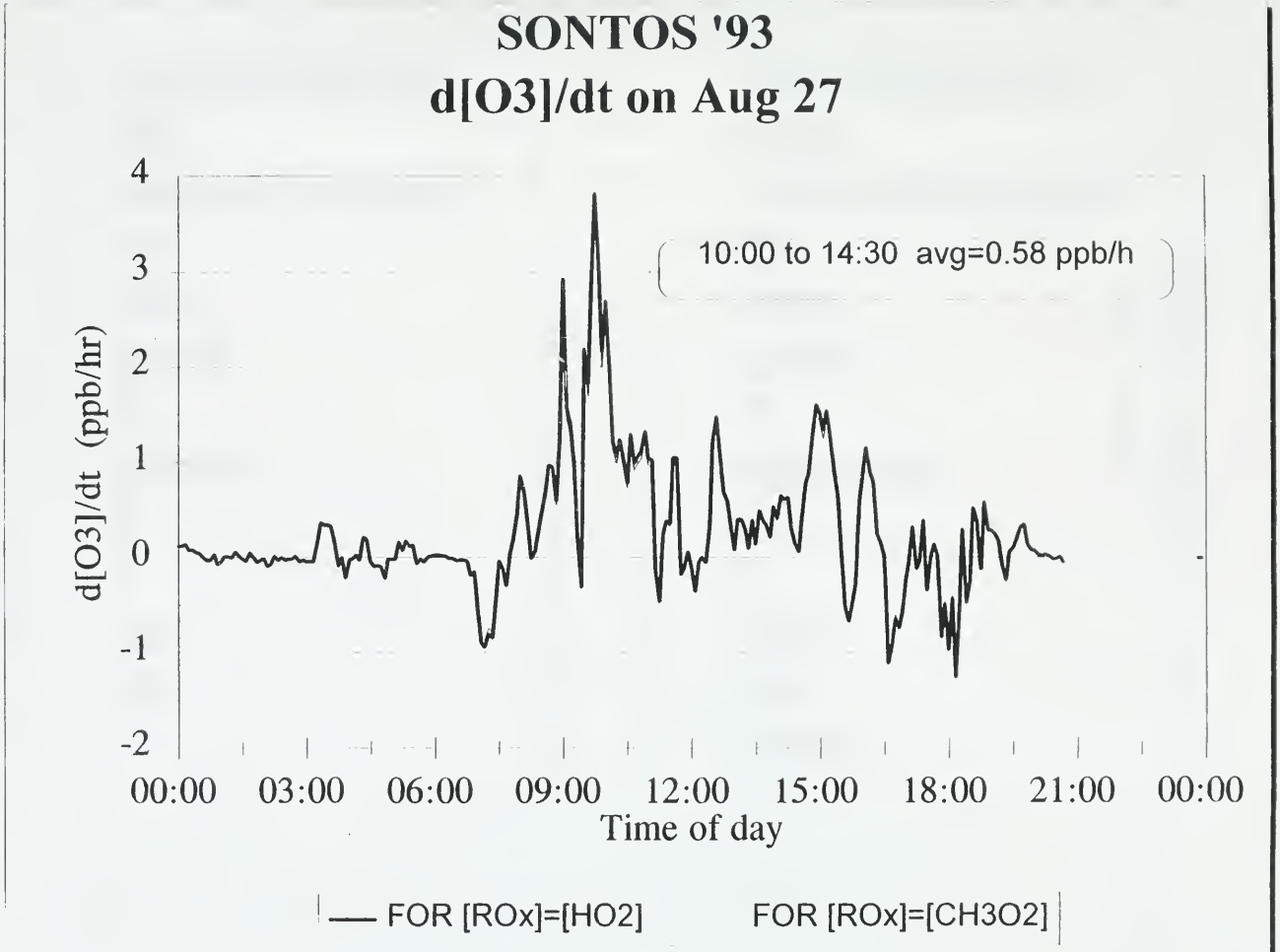

Figure 8b.iii. Diurnal plot of the Ozone production rate calculated from the radical data on Aug 27th.

Figure 9. Plot of acetone against 2-propyl nitrate.

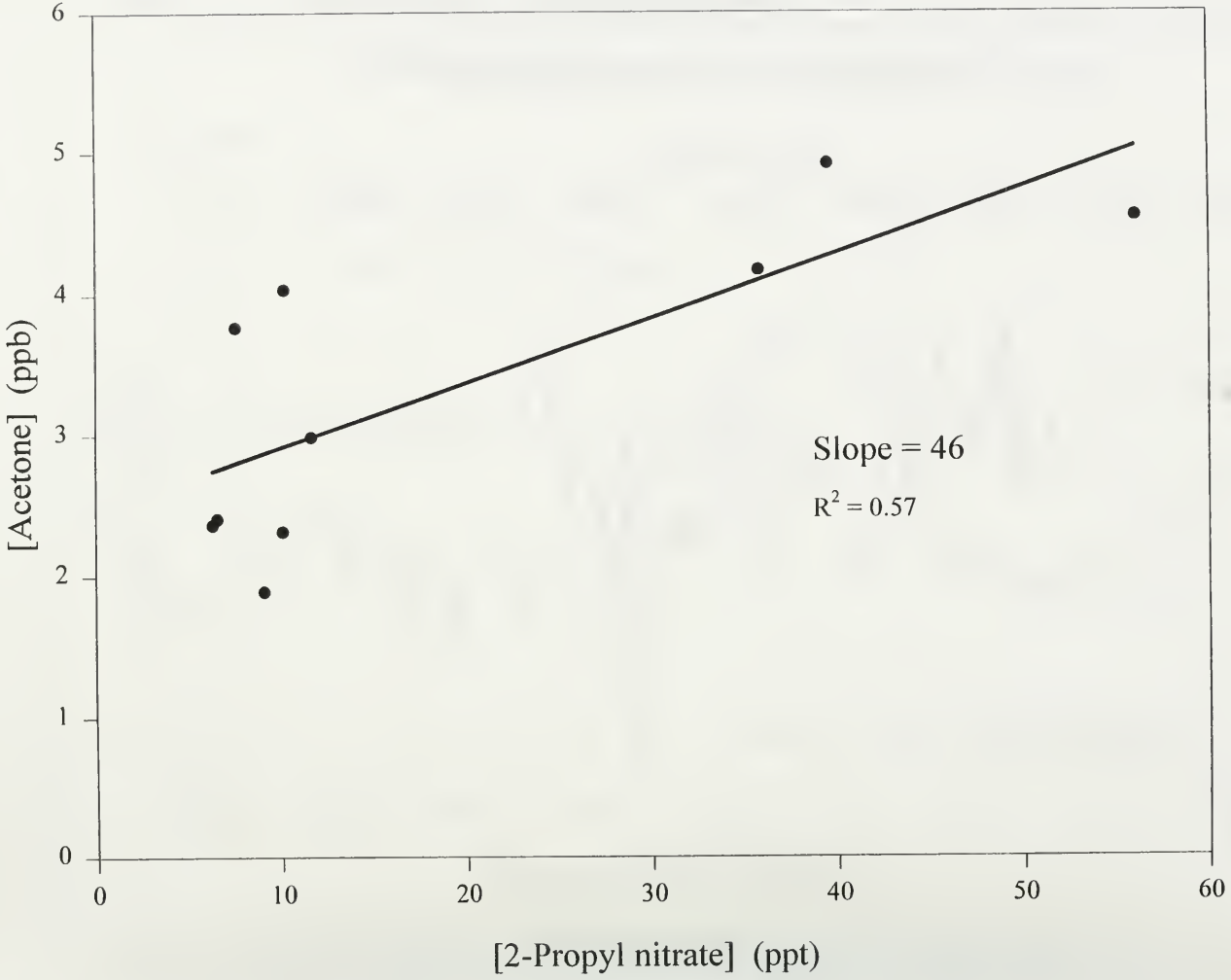

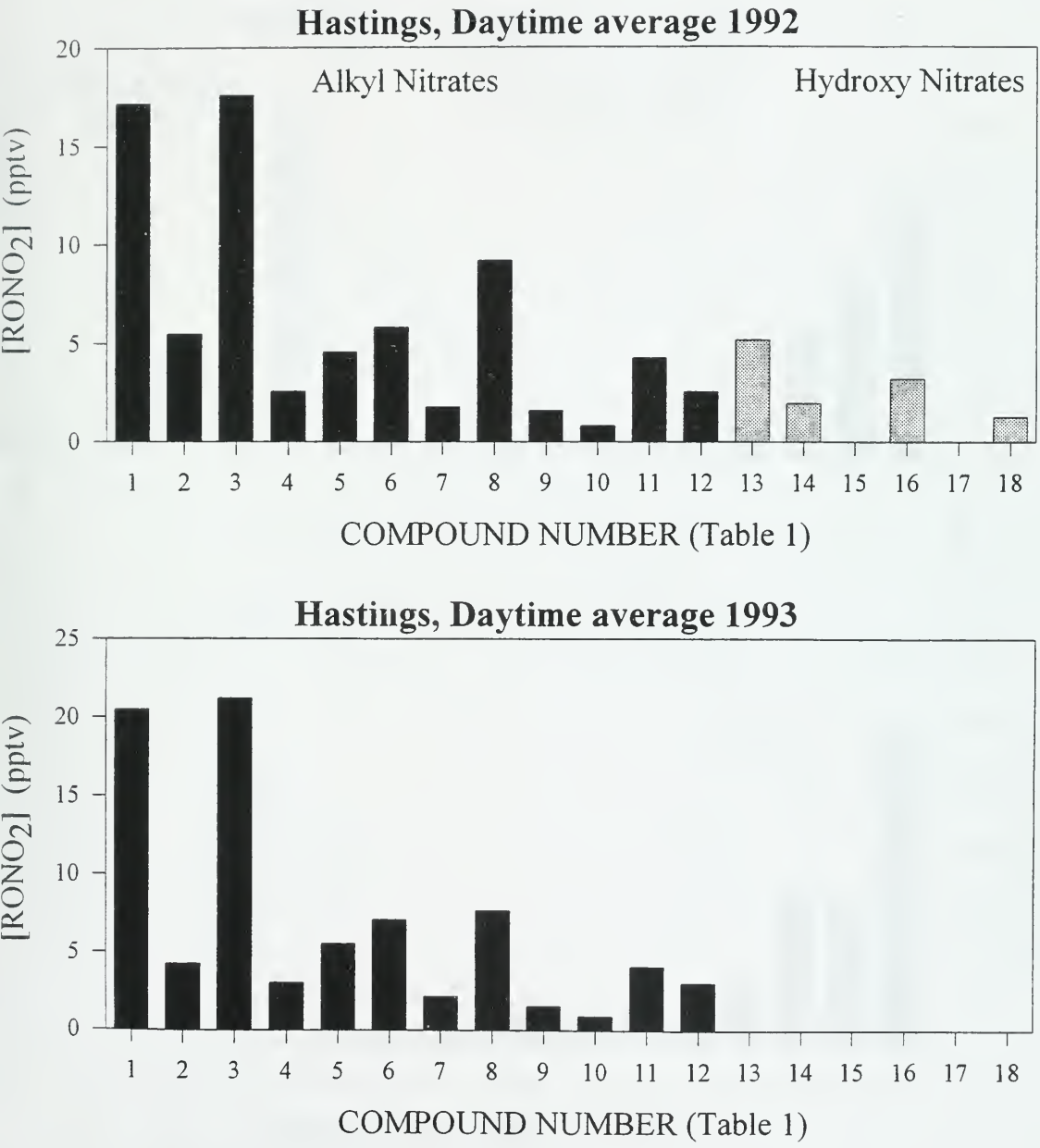

Figure 10. Concentrations of organic nitrates for the 1992 and 1993 field studies.

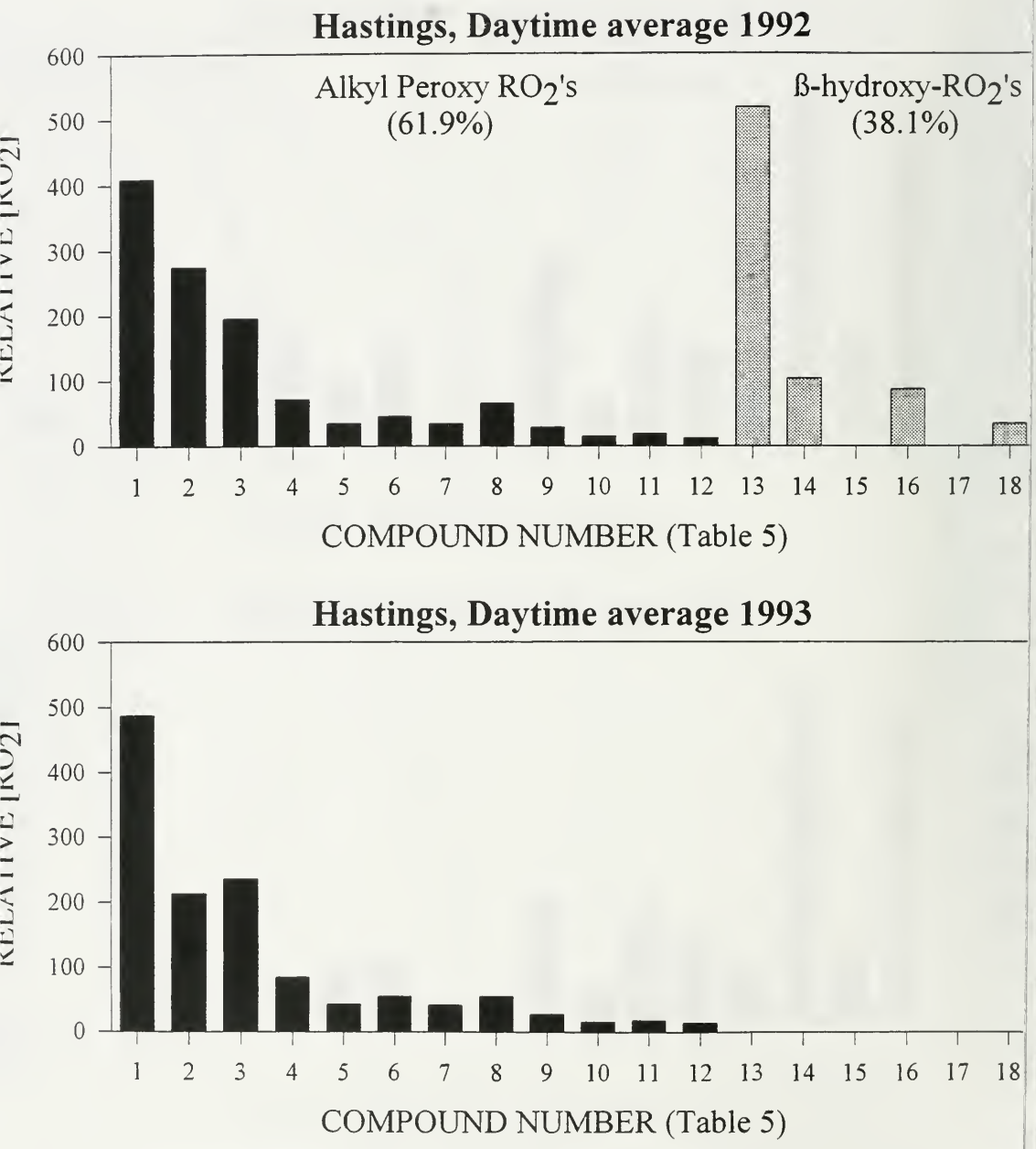

Figure 11. Relative abundances of the peroxy radicals, obtained from the organic nitrate measurements.

Figure 12. Plot of organic nitrate concentration against ozone. The slope is the average branching ratio for the reaction of the peroxy radical with NO.

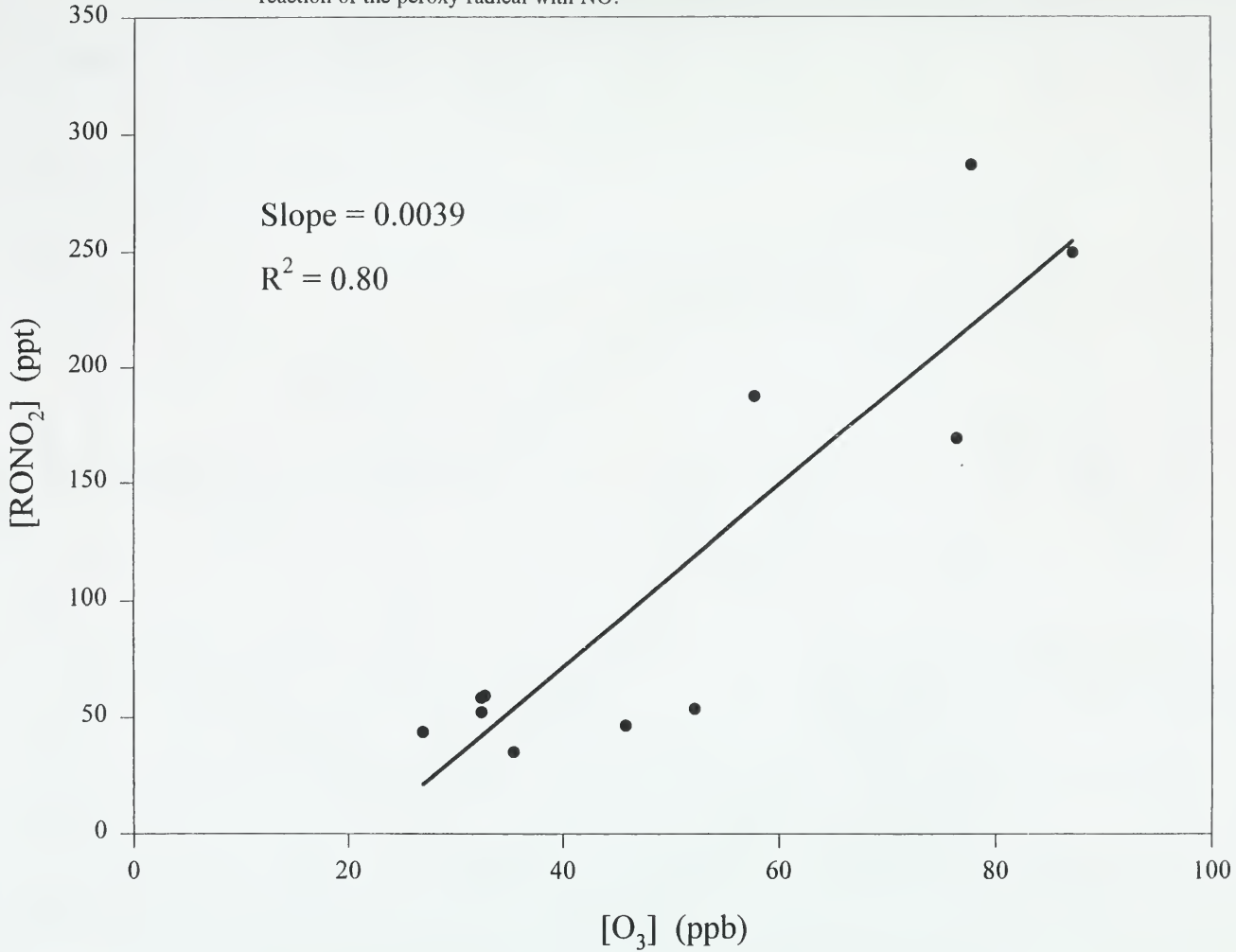

Figure 13. Average ratios of NO_x, PAN, HNO_3, and their sum, to NO_y

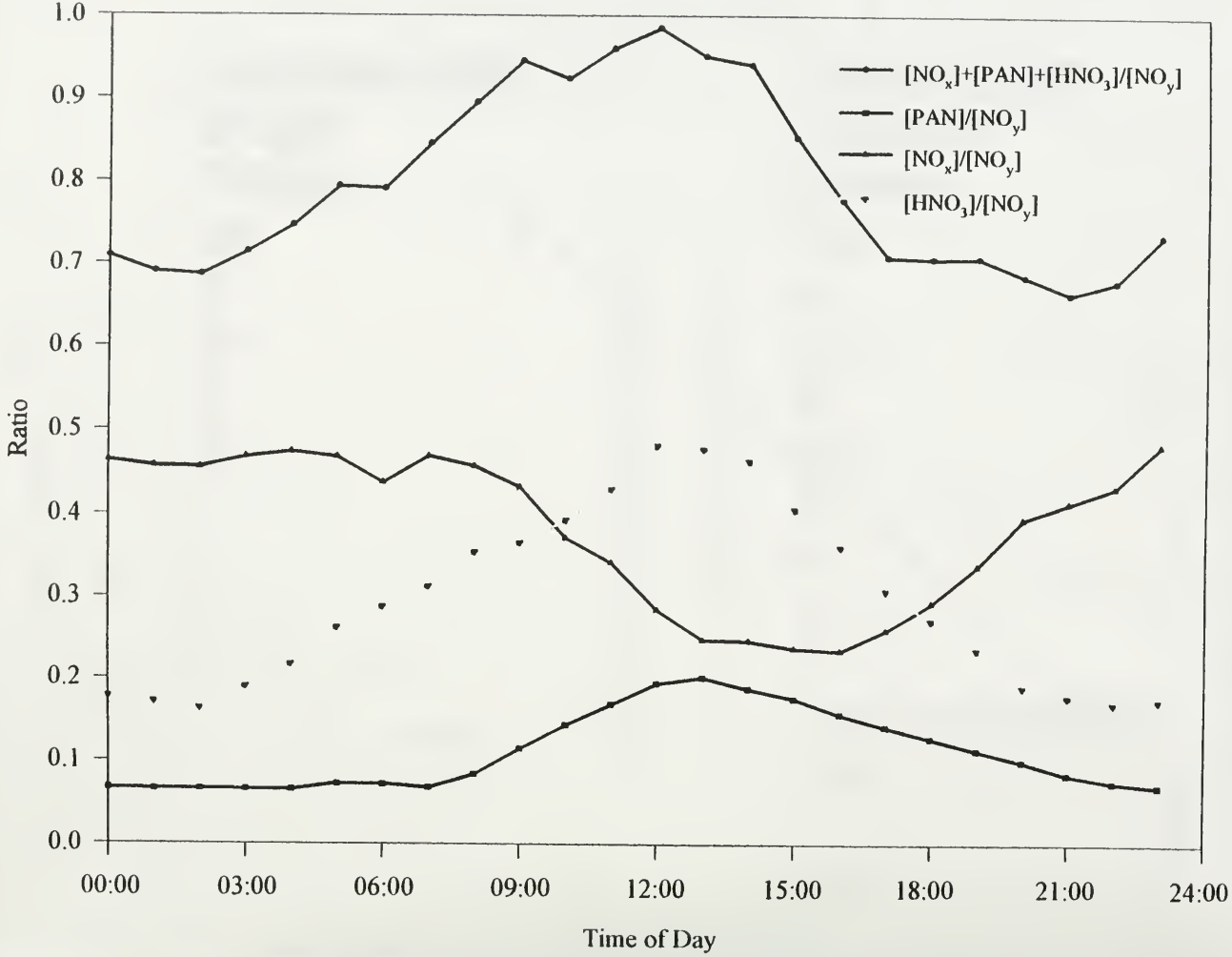

Figure 14. Contribution of organic nitrates to the total NO_y for 3 days during the 1993 field study.

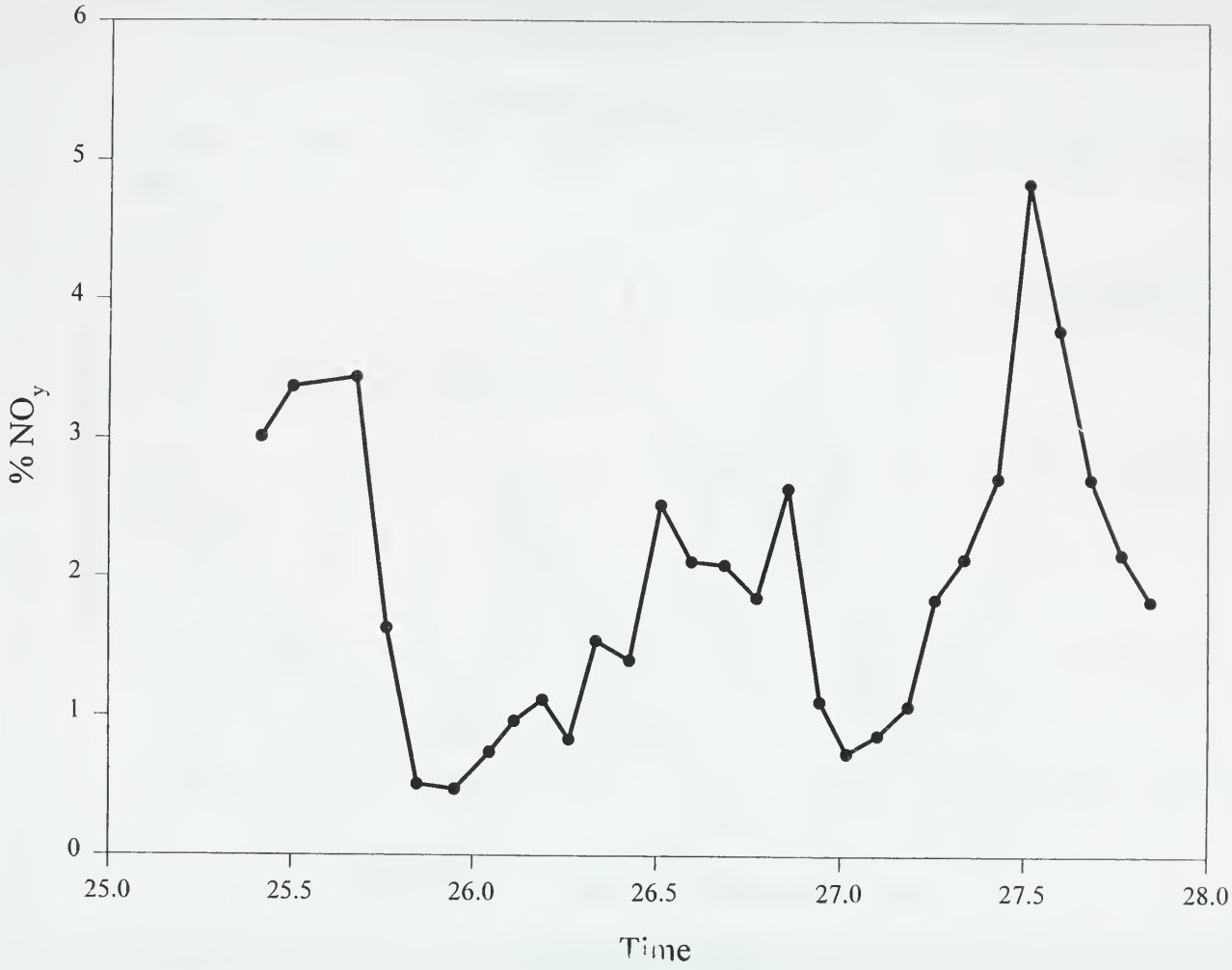

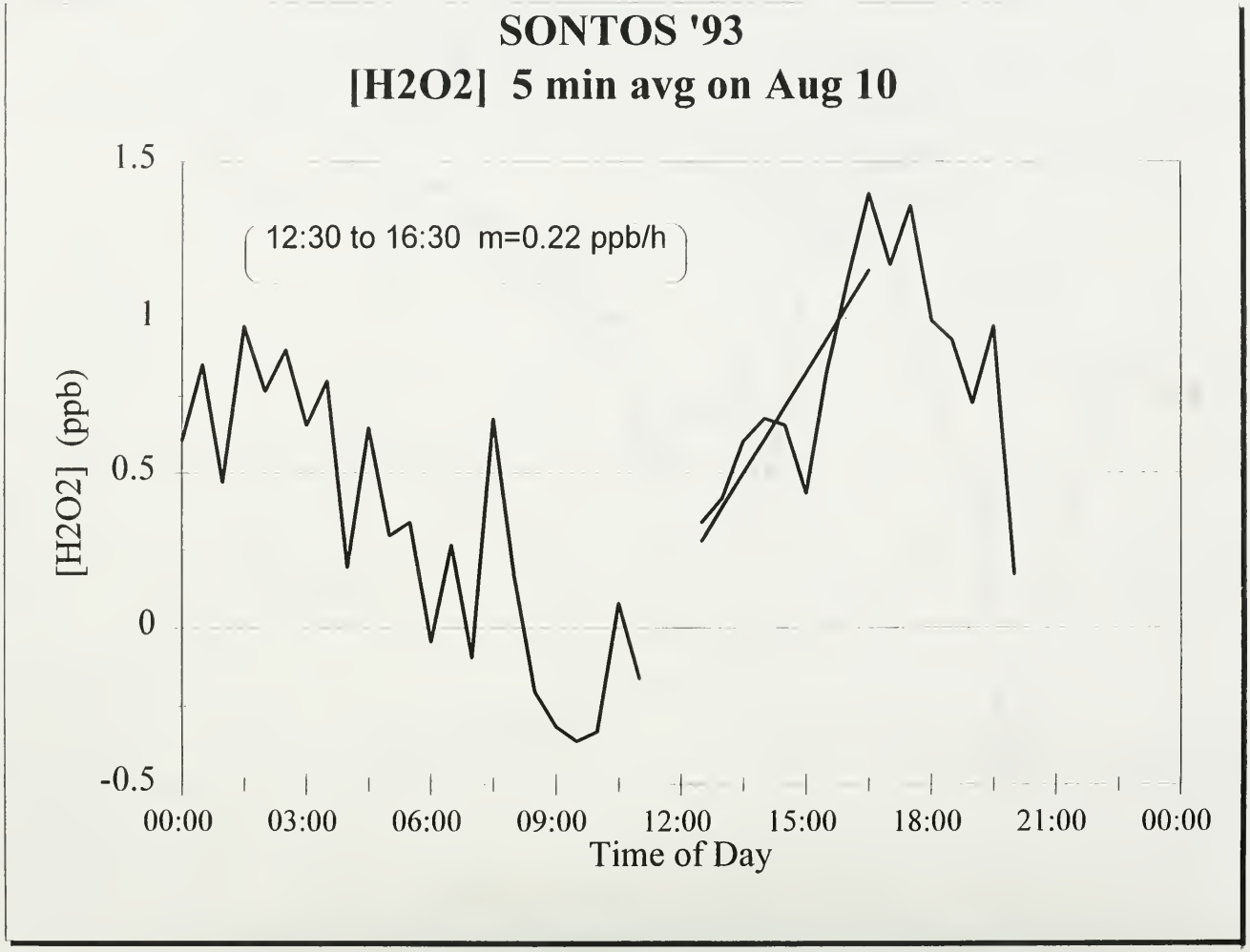

Figure 15a.i. Diurnal plot of H_2O_2 on Aug 10th used to determine the observed H_2O_2 production rates.

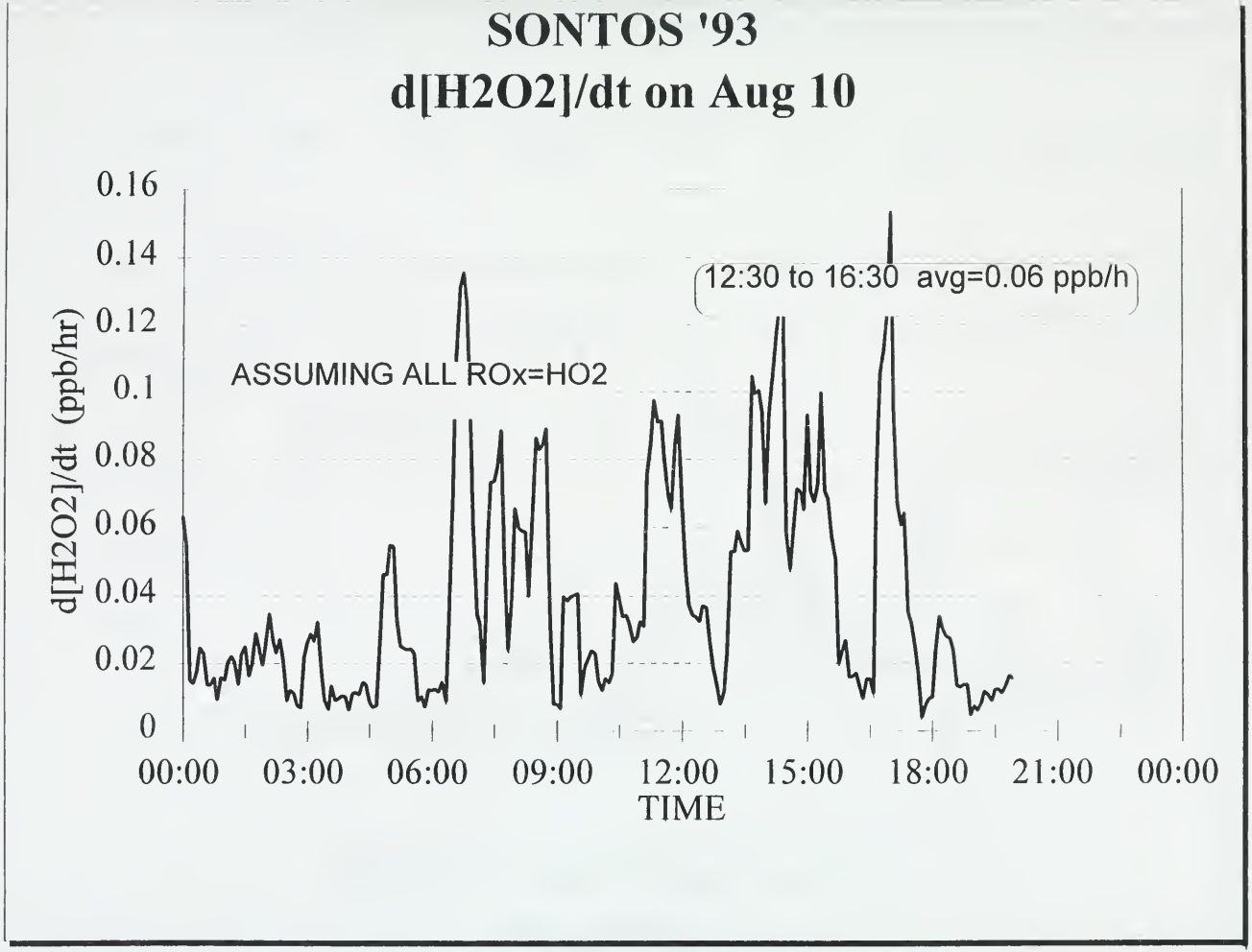

Figure 15b.i. Diurnal plot of the H_2O_2 production rate calculated from the radical data on Aug 10th.

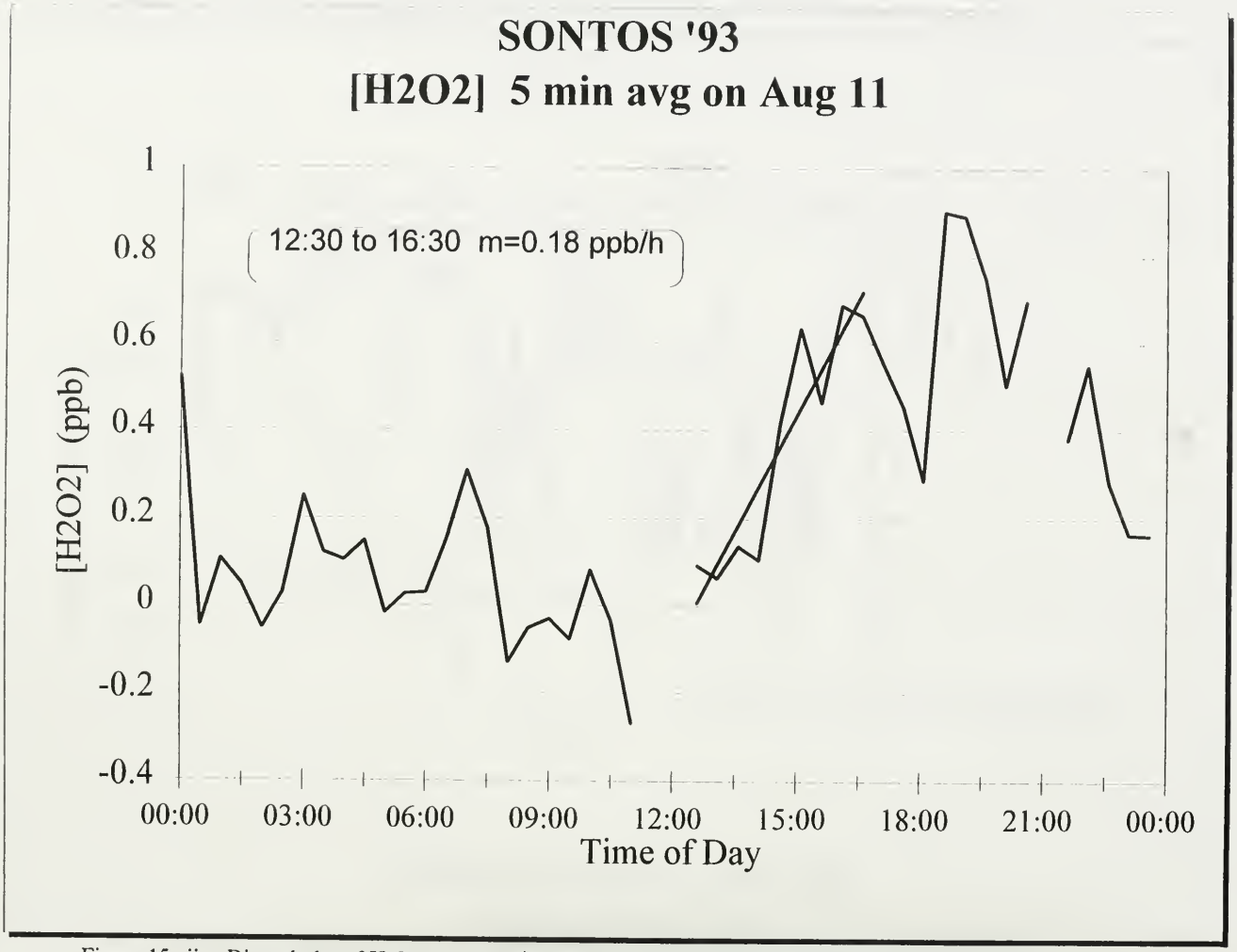

Figure 15a.ii. Diurnal plot of H_2O_2 on Aug 11th used to determine the observed H_2O_2 production rates.

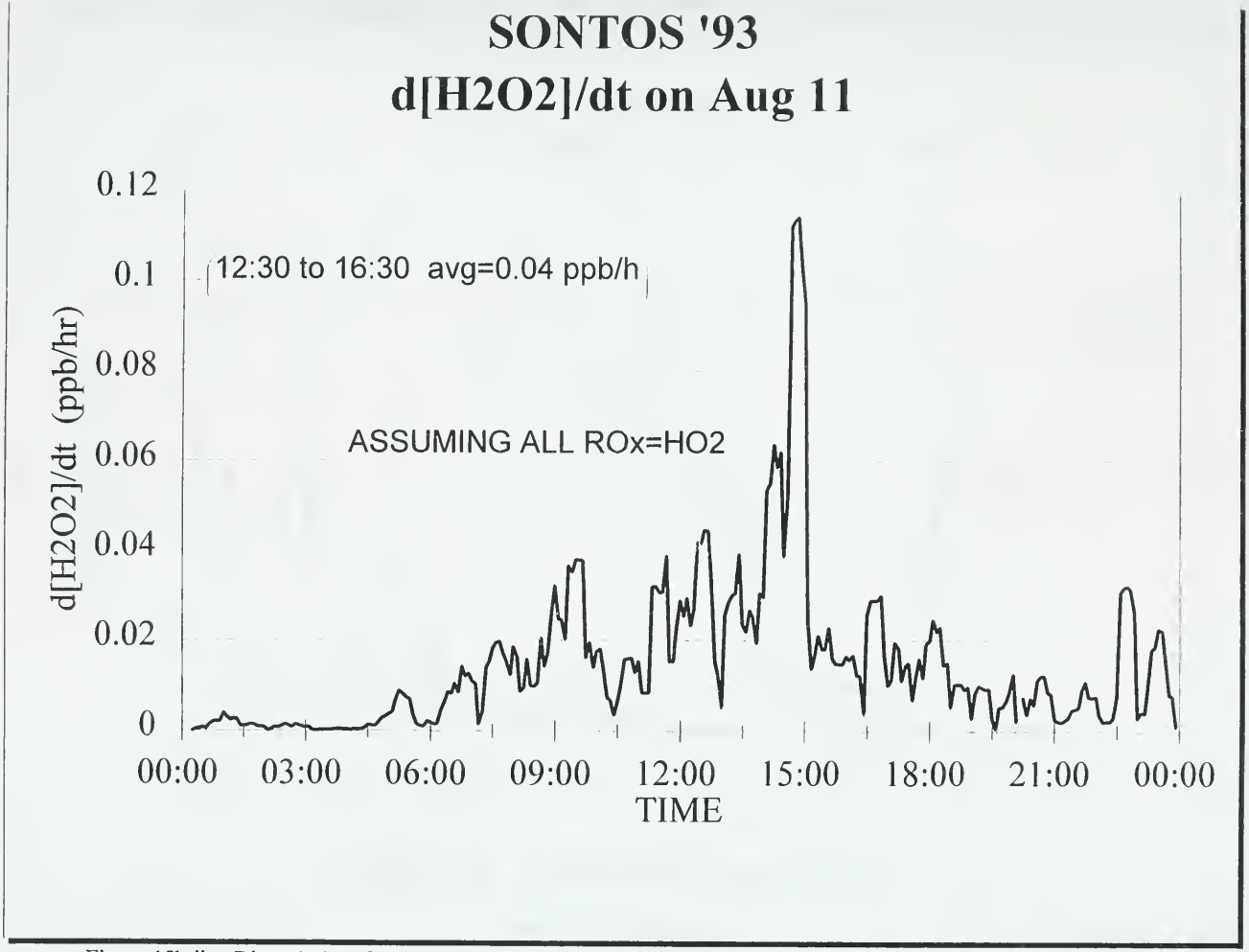

Figure 15b.ii. Diurnal plot of the H_2O_2 production rate calculated from the radical data on Aug 11th.

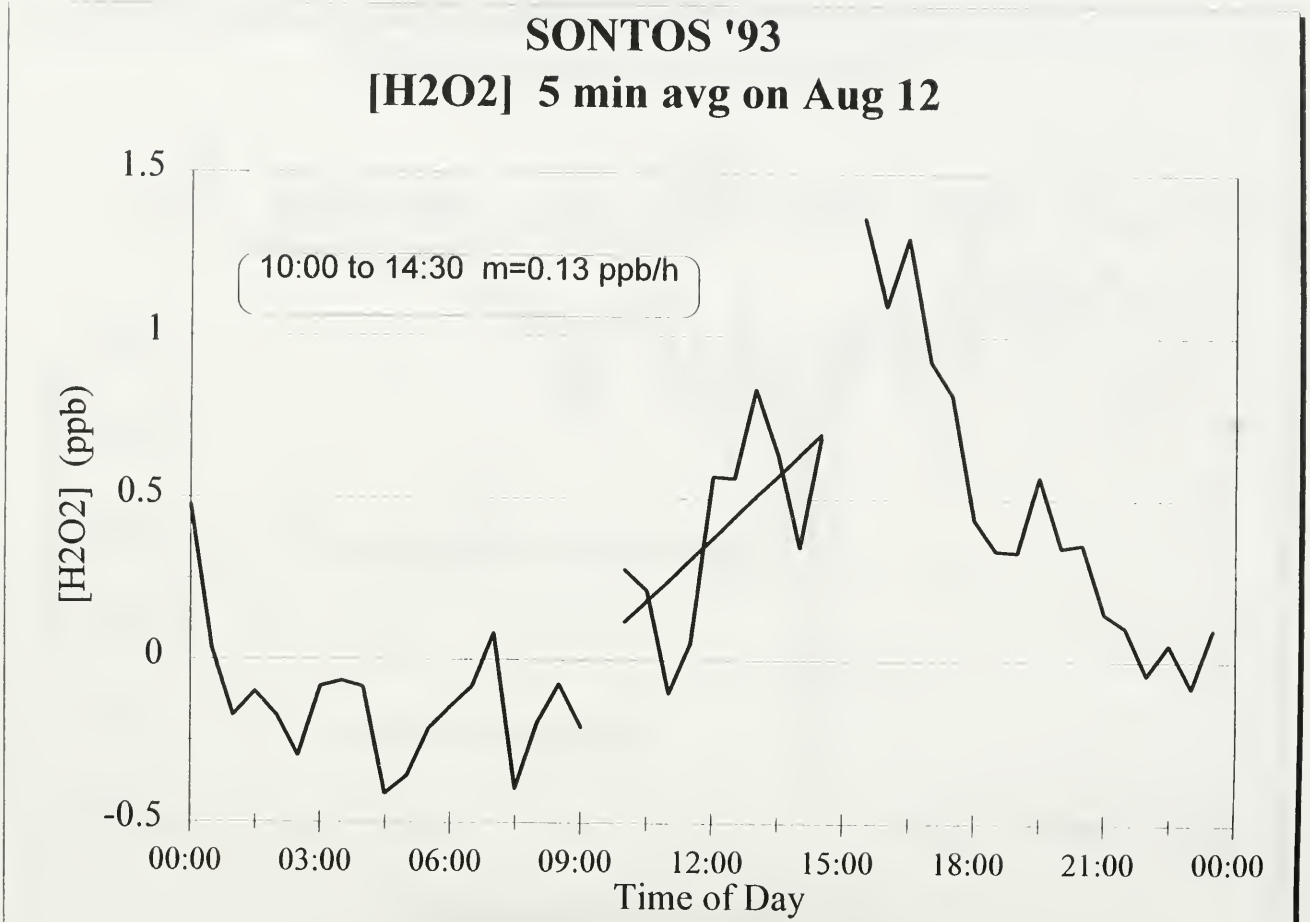

Figure 15a.iii. Diurnal plot of H_2O_2 on Aug 12th used to determine the observed H_2O_2 production rates.

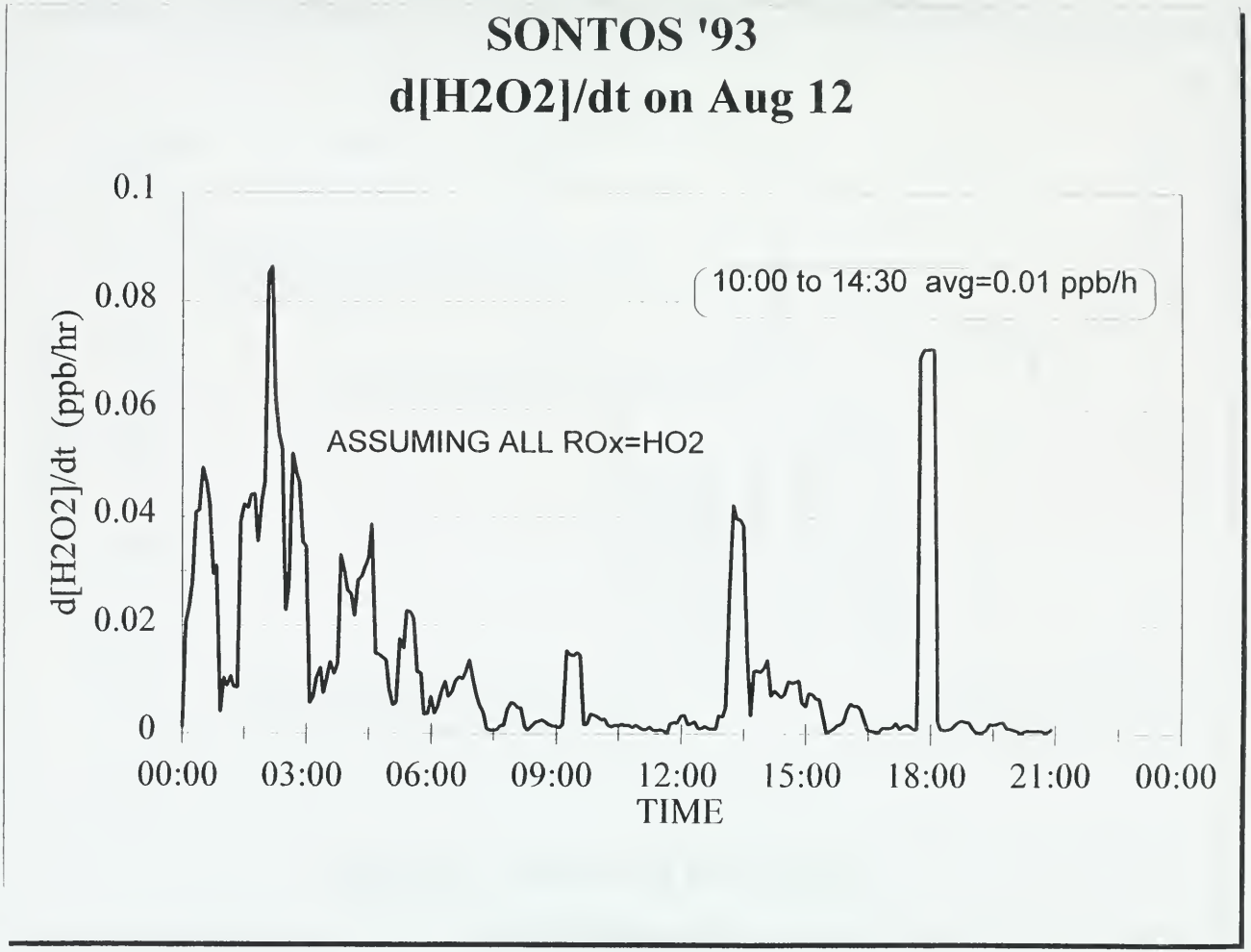

Figure 15b.iii. Diurnal plot of the H_2O_2 production rate calculated from the radical data on Aug 12th.

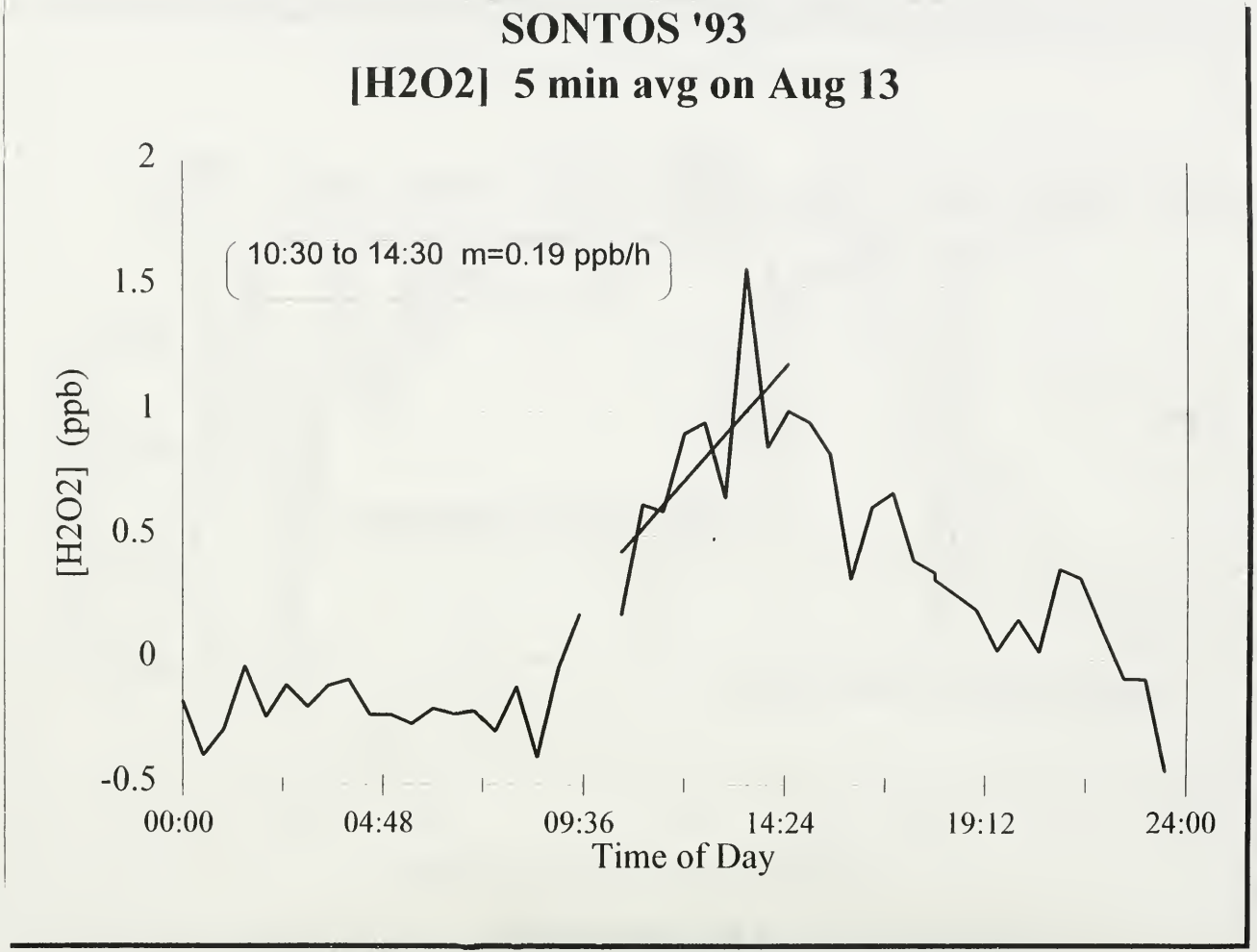

Figure 15a.iv. Diurnal plot of H_2O_2 on Aug 13th used to determine the observed H_2O_2 production rates.

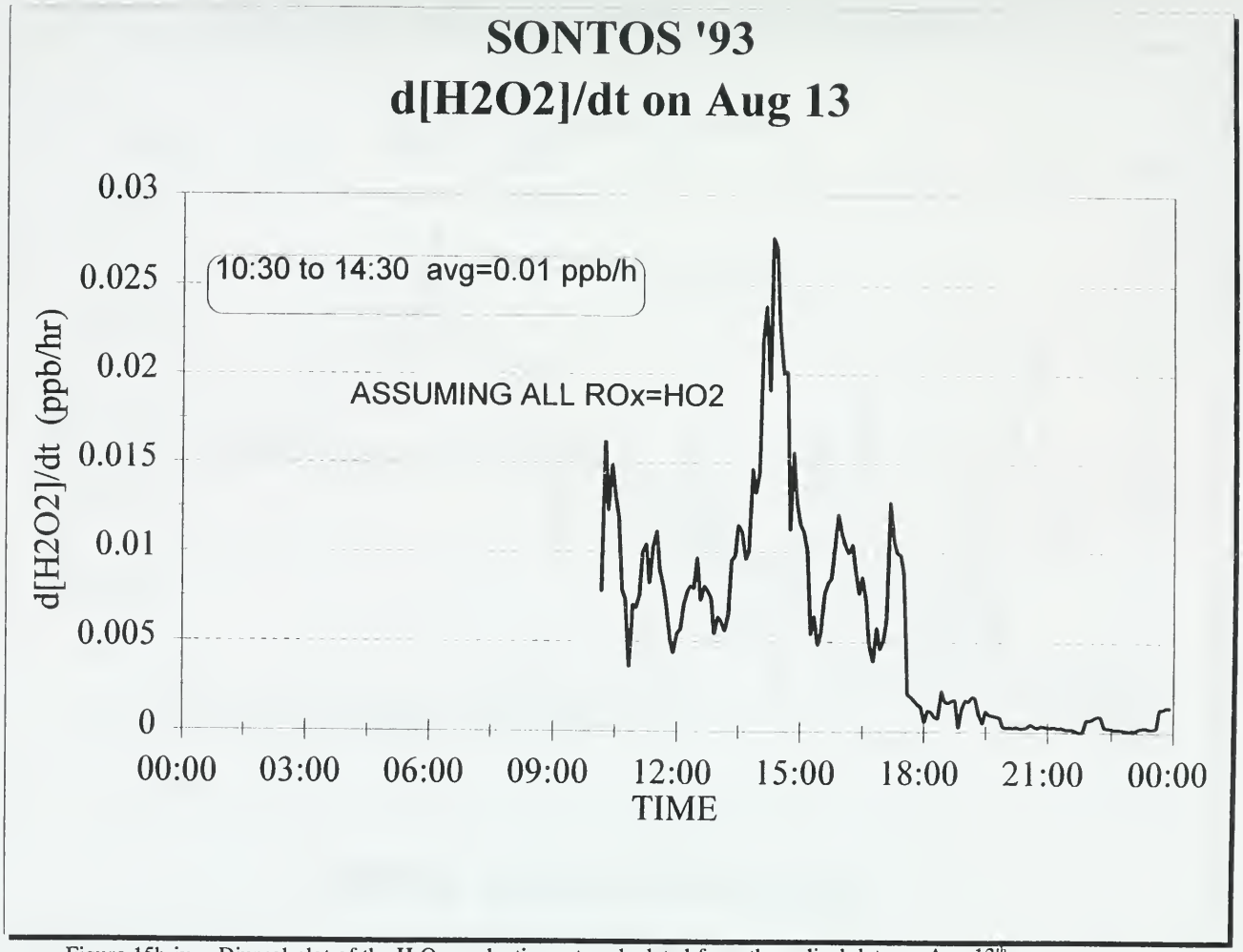

Figure 15b.iv. Diurnal plot of the H_2O_2 production rate calculated from the radical data on Aug 13th.

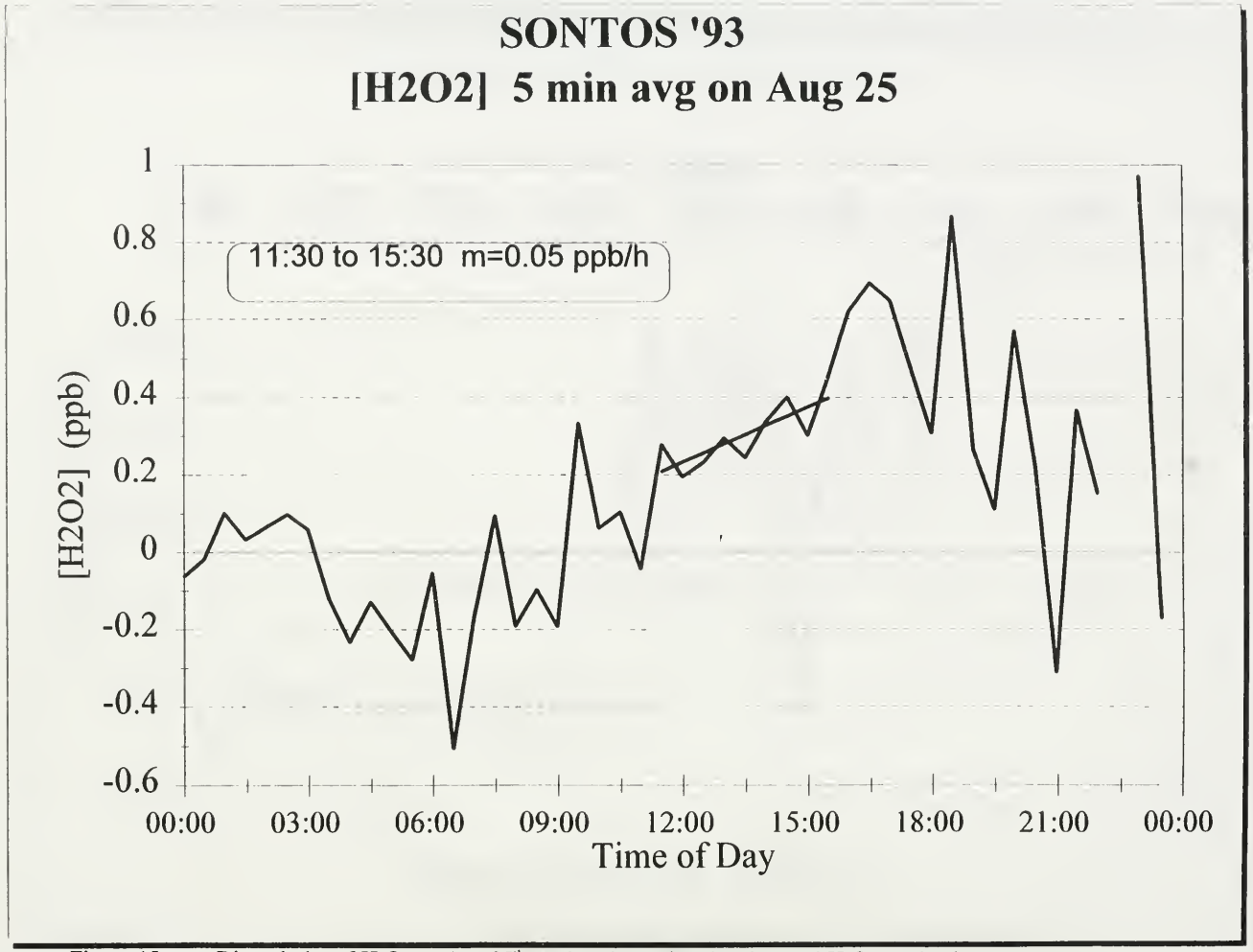

Figure 15a.v. Diurnal plot of H_2O_2 on Aug 25th used to determine the observed H_2O_2 production rates.

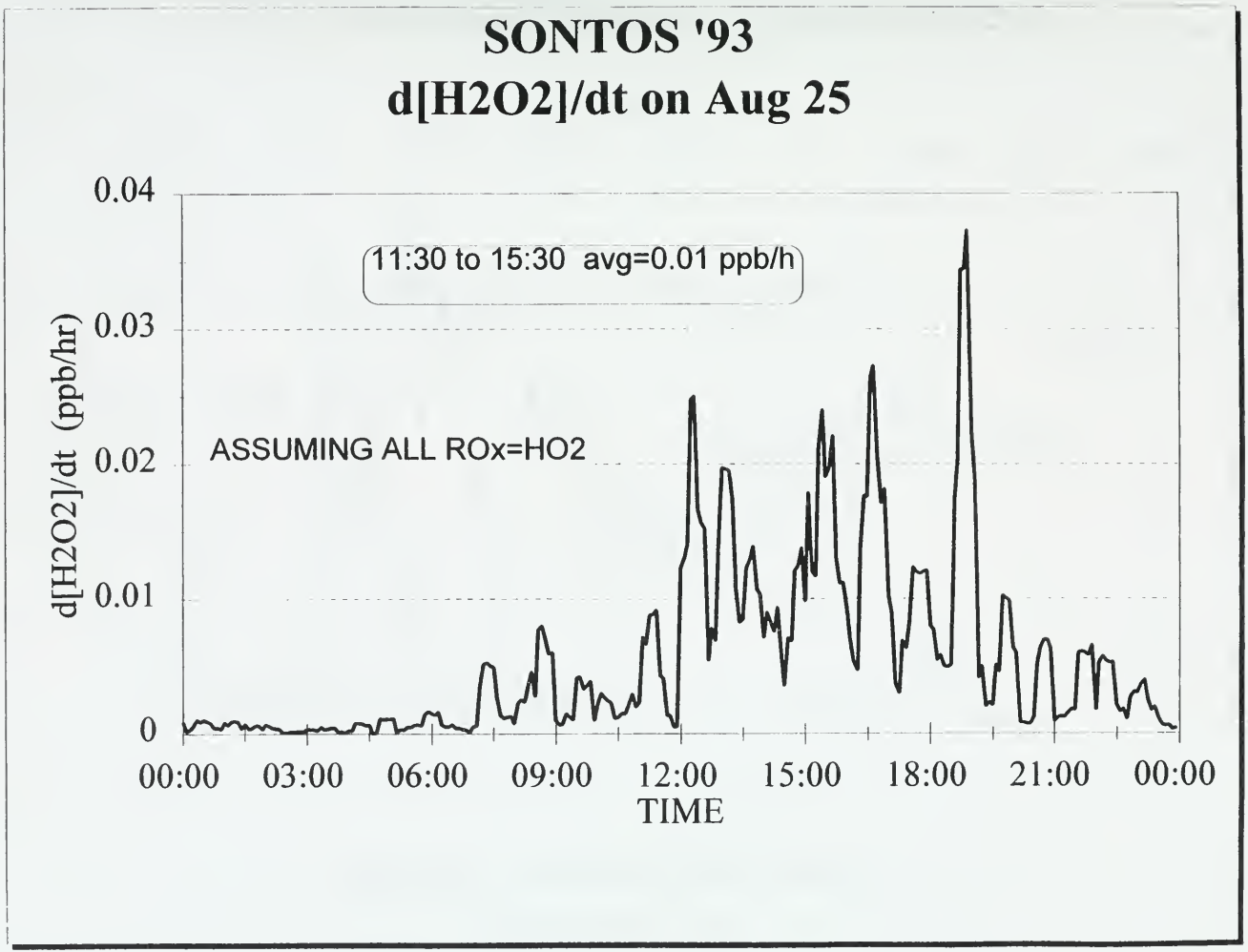

Figure 15b.v. Diurnal plot of the H_2O_2 production rate calculated from the radical data on Aug 25th.

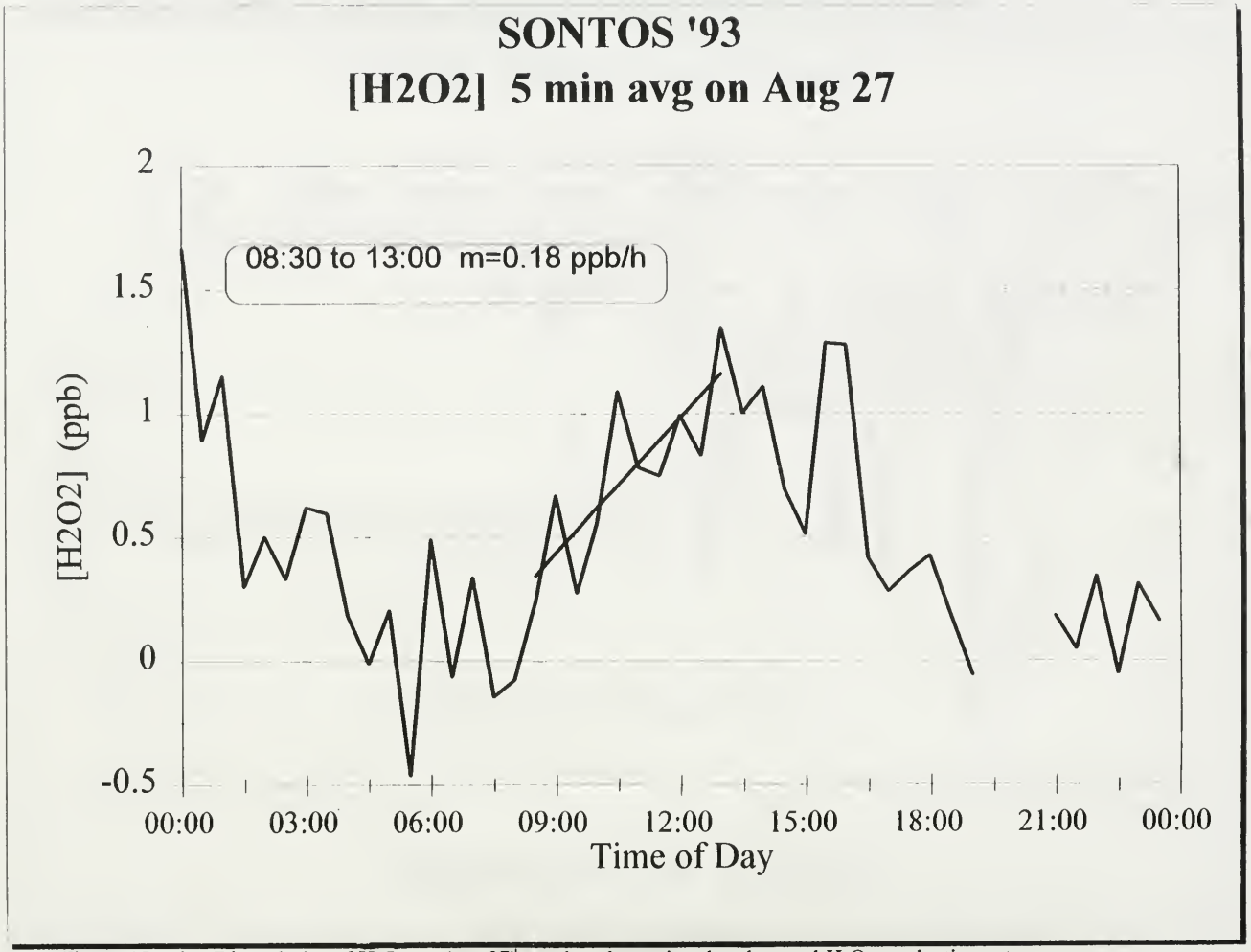

Figure 15a.vi. Diurnal plot of H_2O_2 on Aug 27th used to determine the observed H_2O_2 production rates.

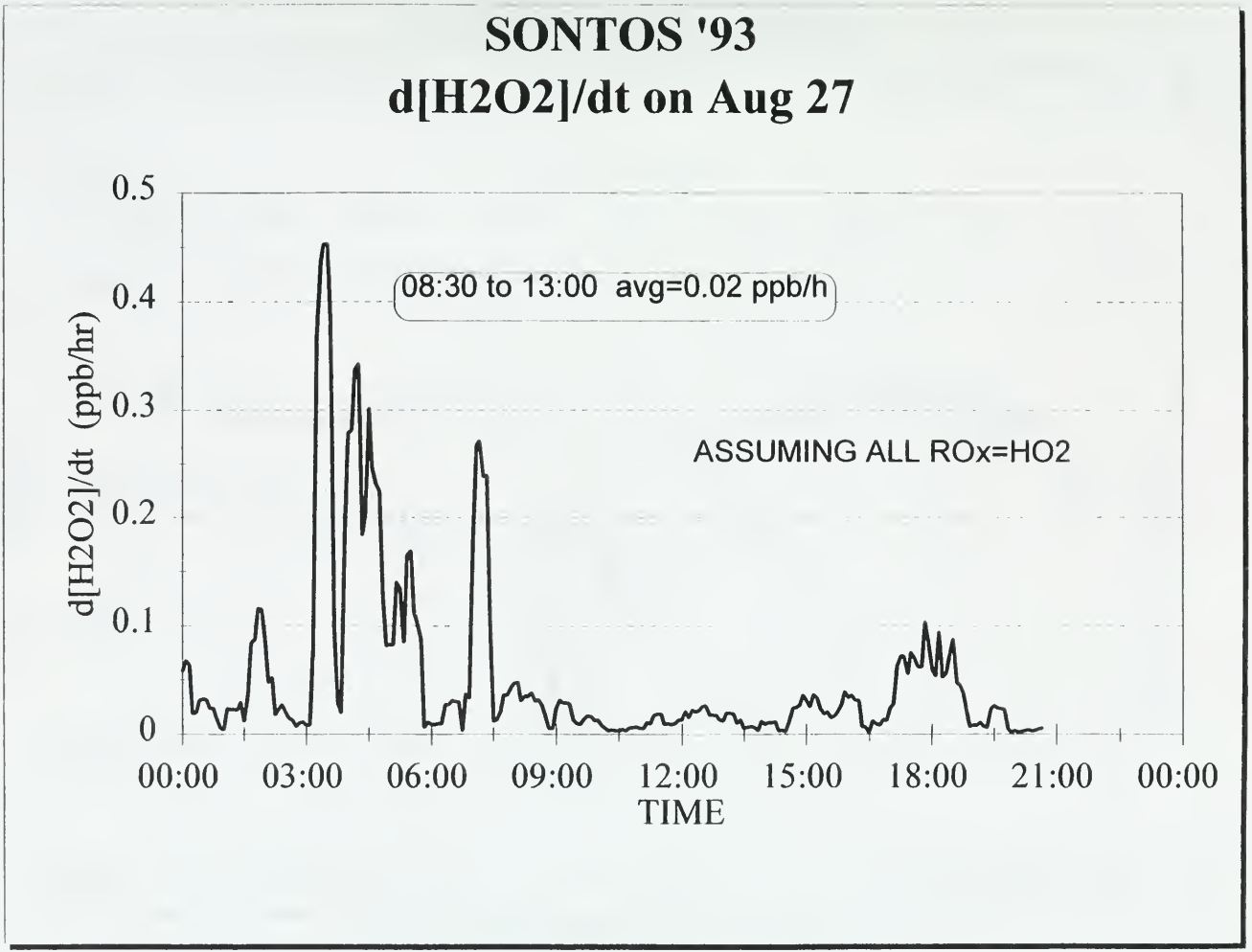

Figure 15b.vi. Diurnal plot of the H_2O_2 production rate calculated from the radical data on Aug 27th.

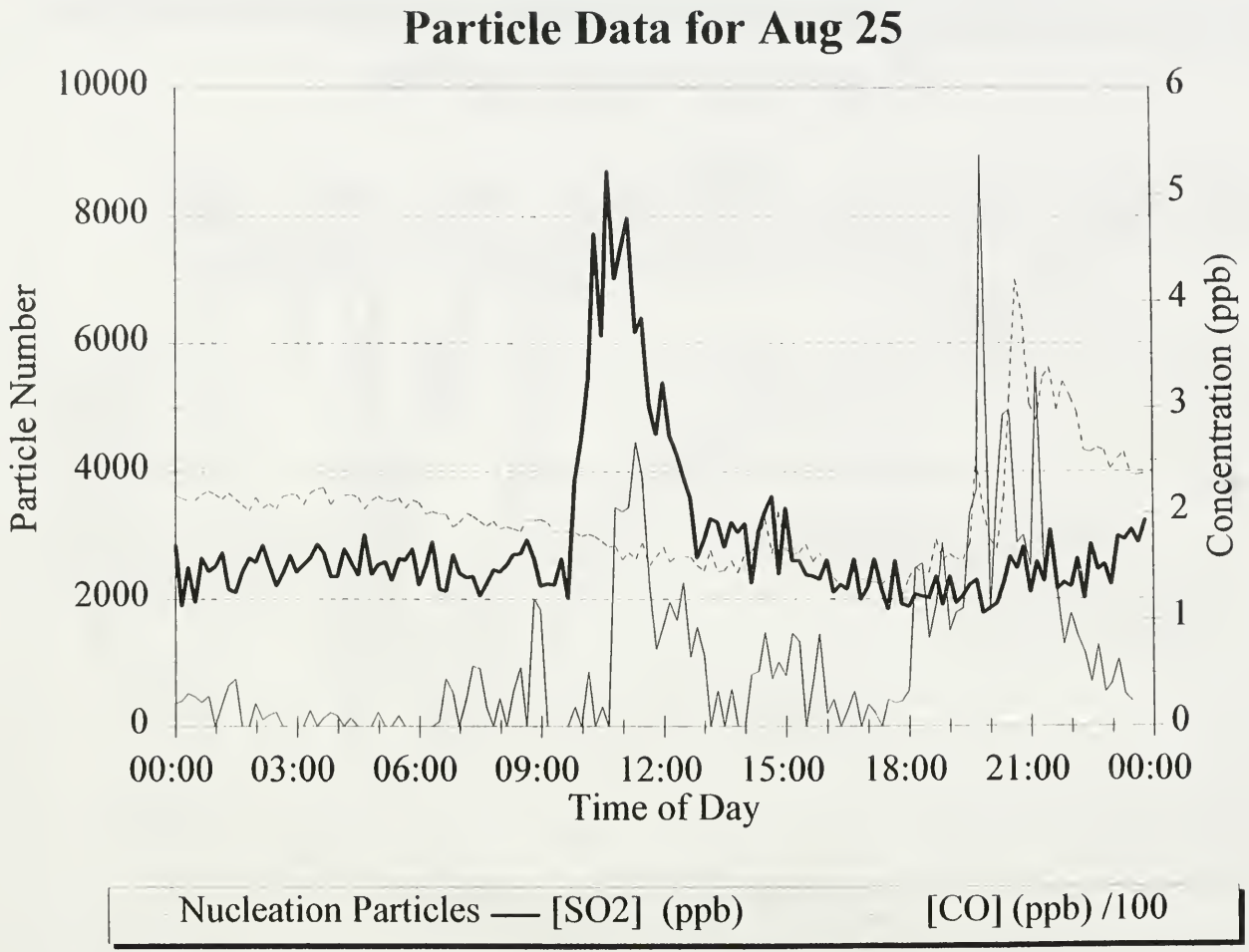

Figure 16a.i. Nucleation particle data with SO_2 and CO concentrations for Aug 25th.

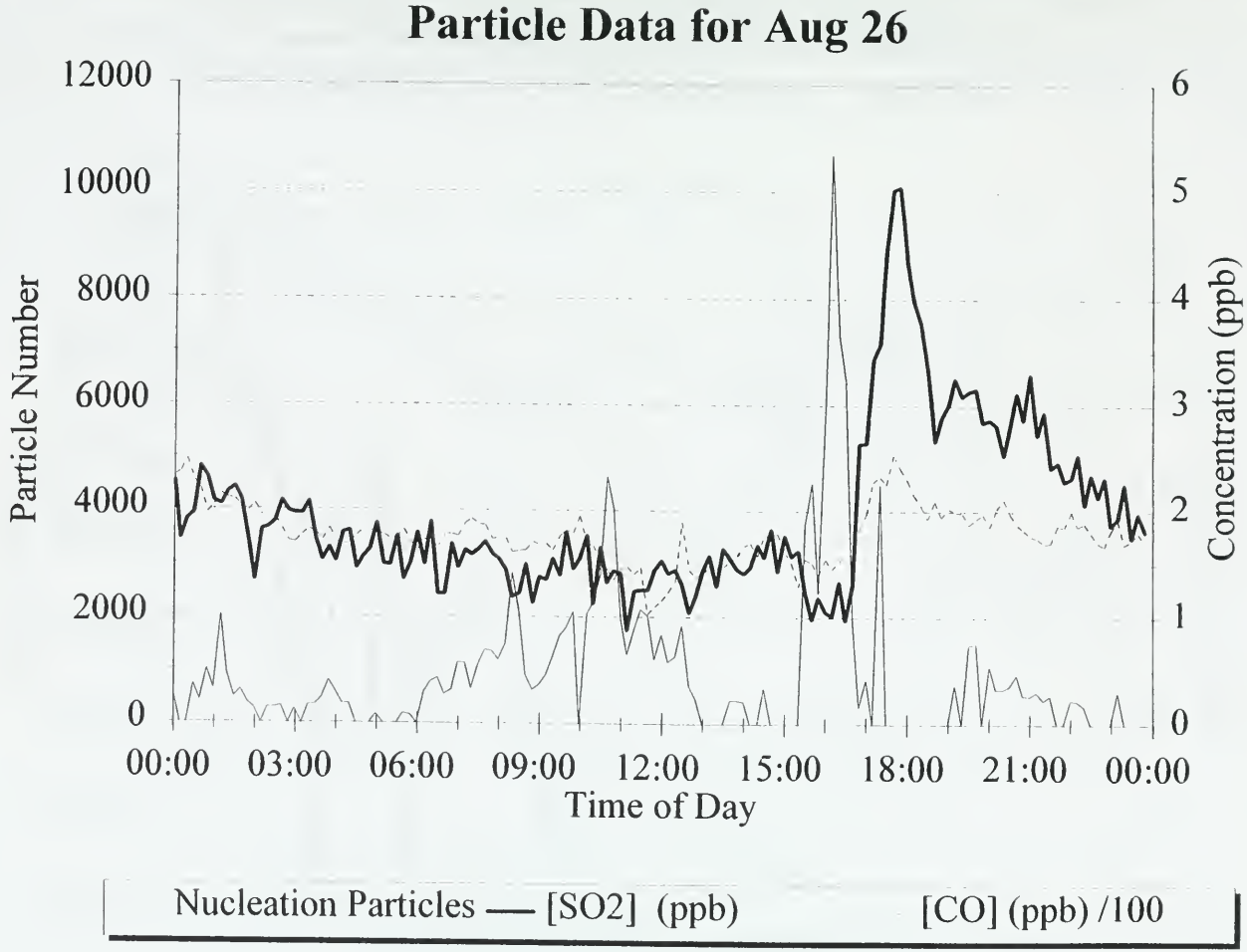

Figure 16a.ii. Nucleation particle data with SO_2 and CO concentrations for Aug 26th.

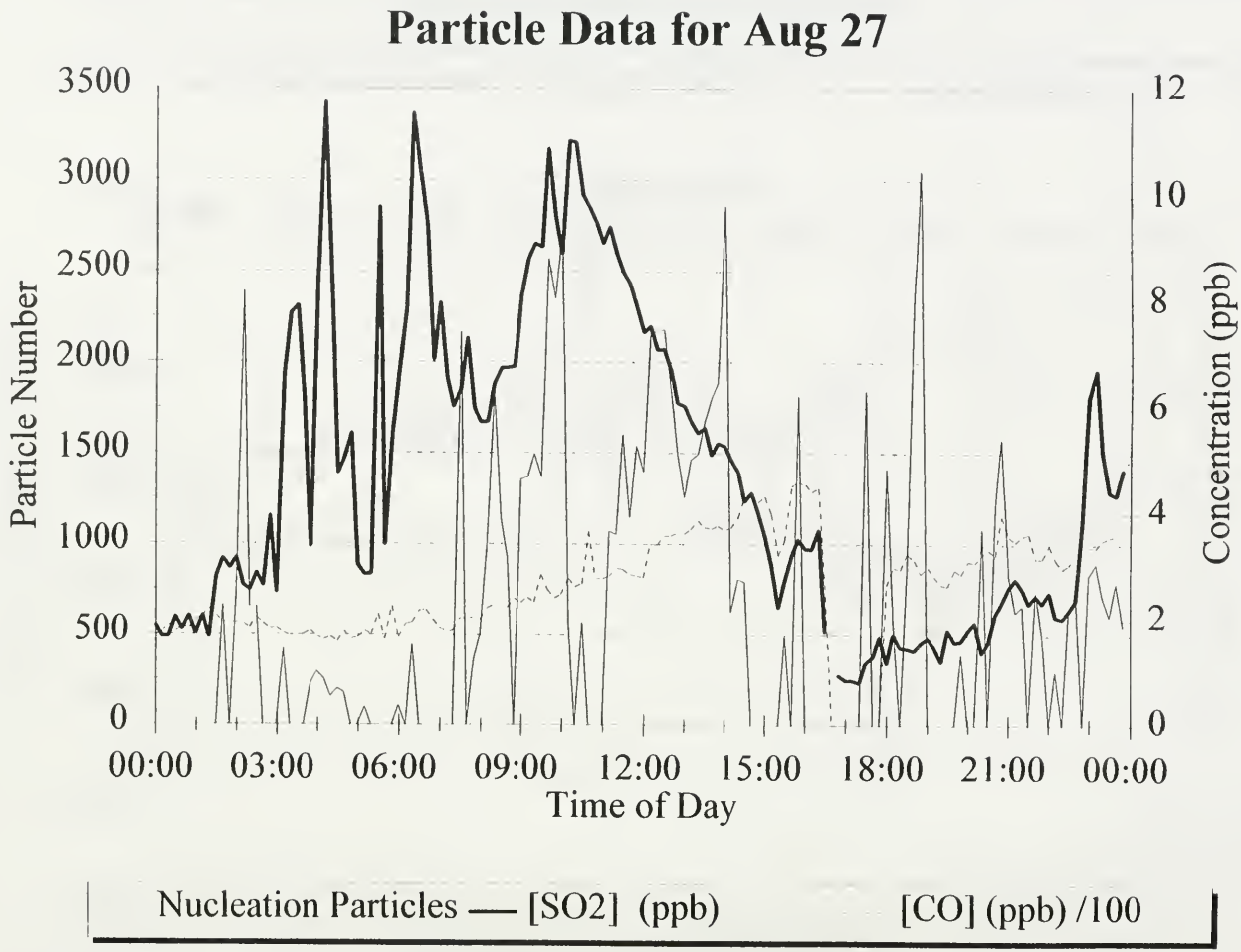

Figure 16a.iii. Nucleation particle data with SO_2 and CO concentrations for Aug 27th.

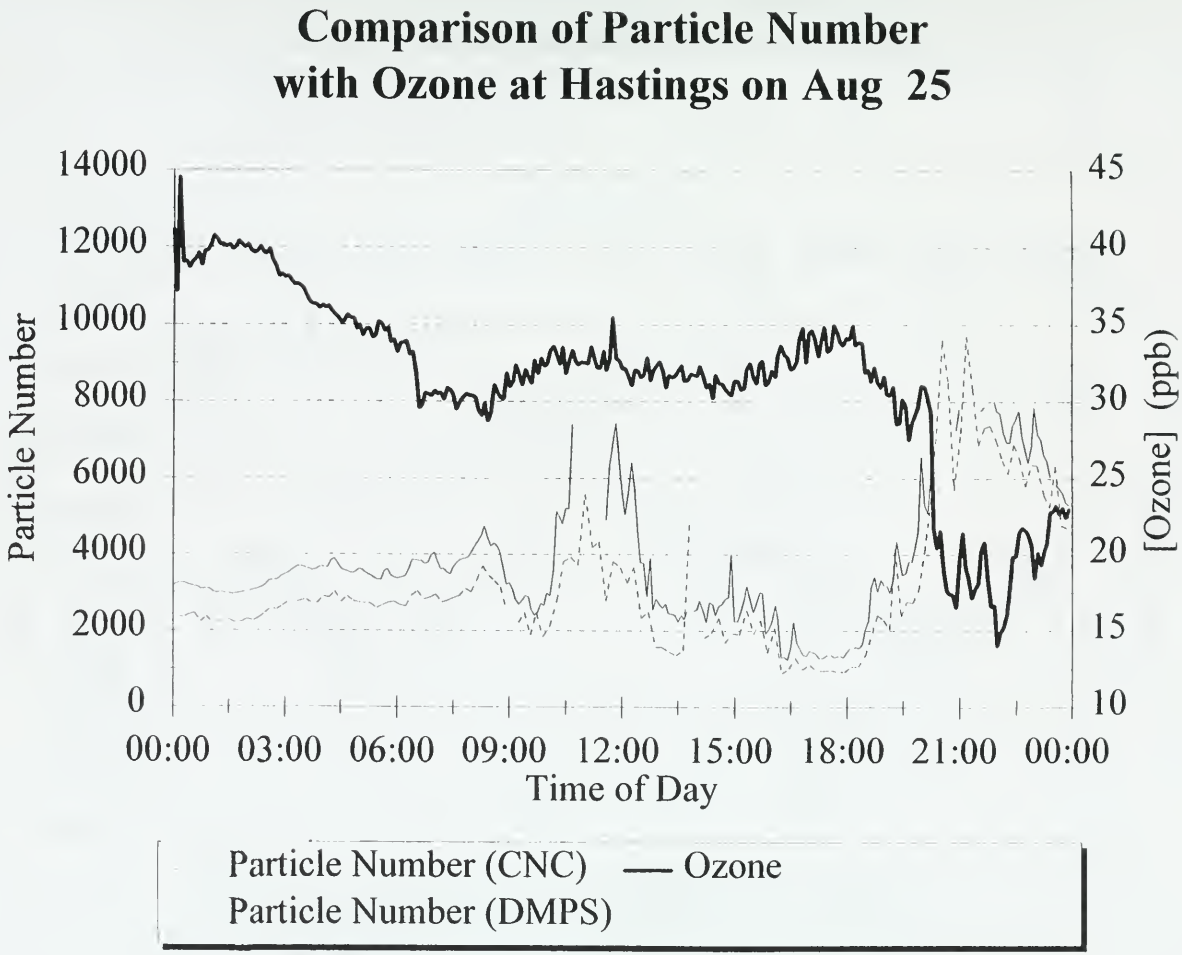

Figure 16b.i. Particle number from two instruments with Ozone concentrations for Aug 25th.

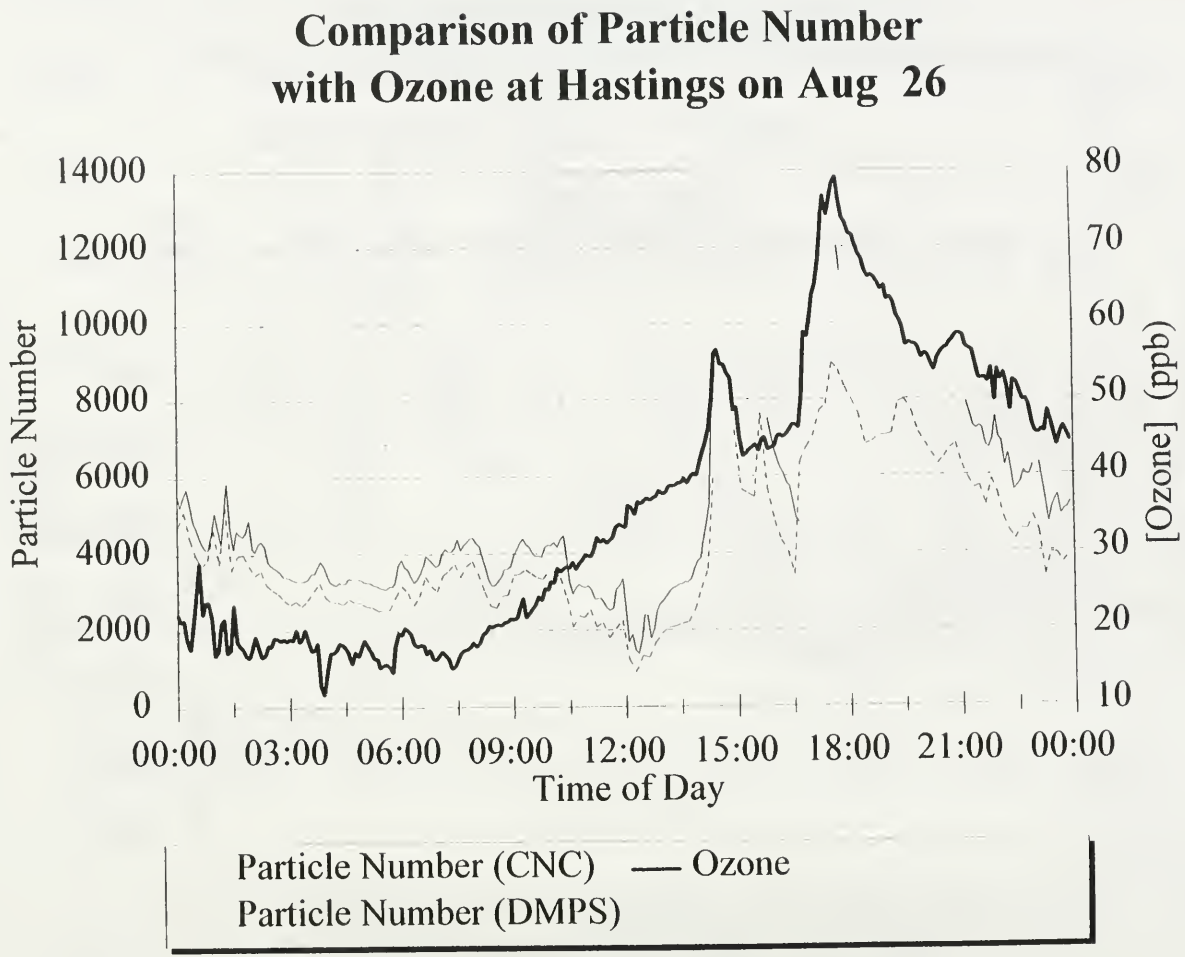

Figure 16b.ii. Particle number from two instruments with Ozone concentrations for Aug 26th.

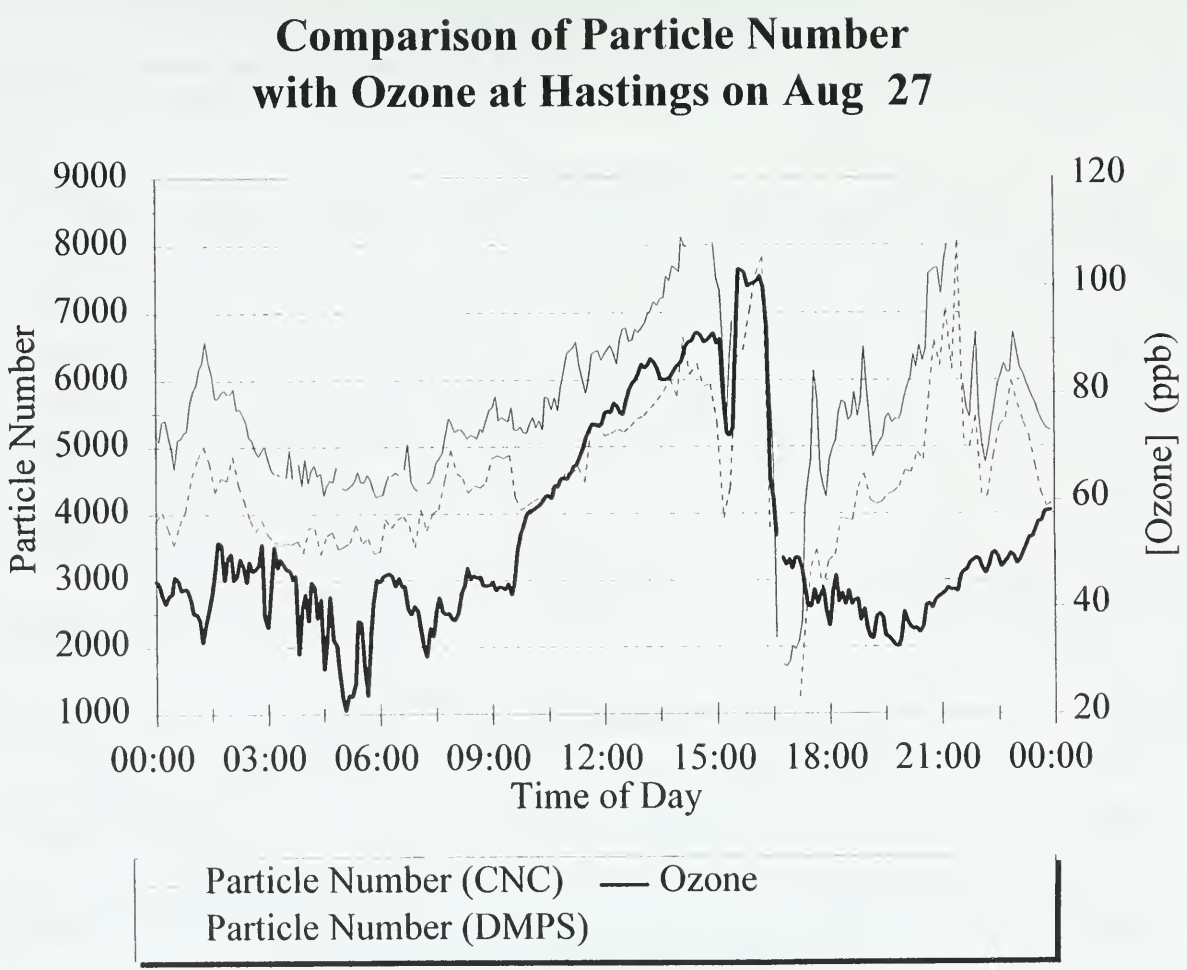

Figure 16b.iii. Particle number from two instruments with Ozone concentrations for Aug 27th.

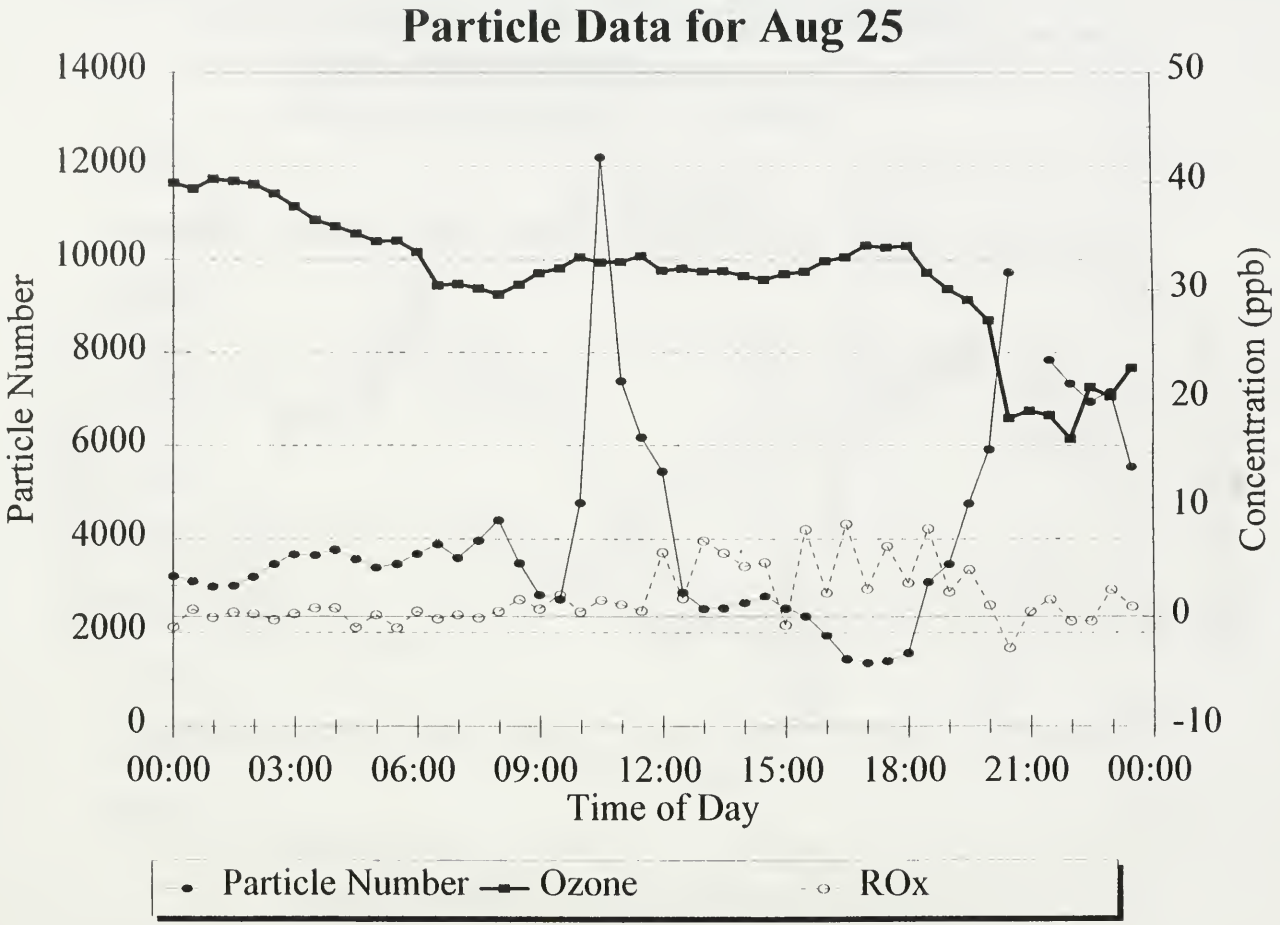

Figure 16c.i. Particle number with O_3 and RO_x concentrations for Aug 25th.

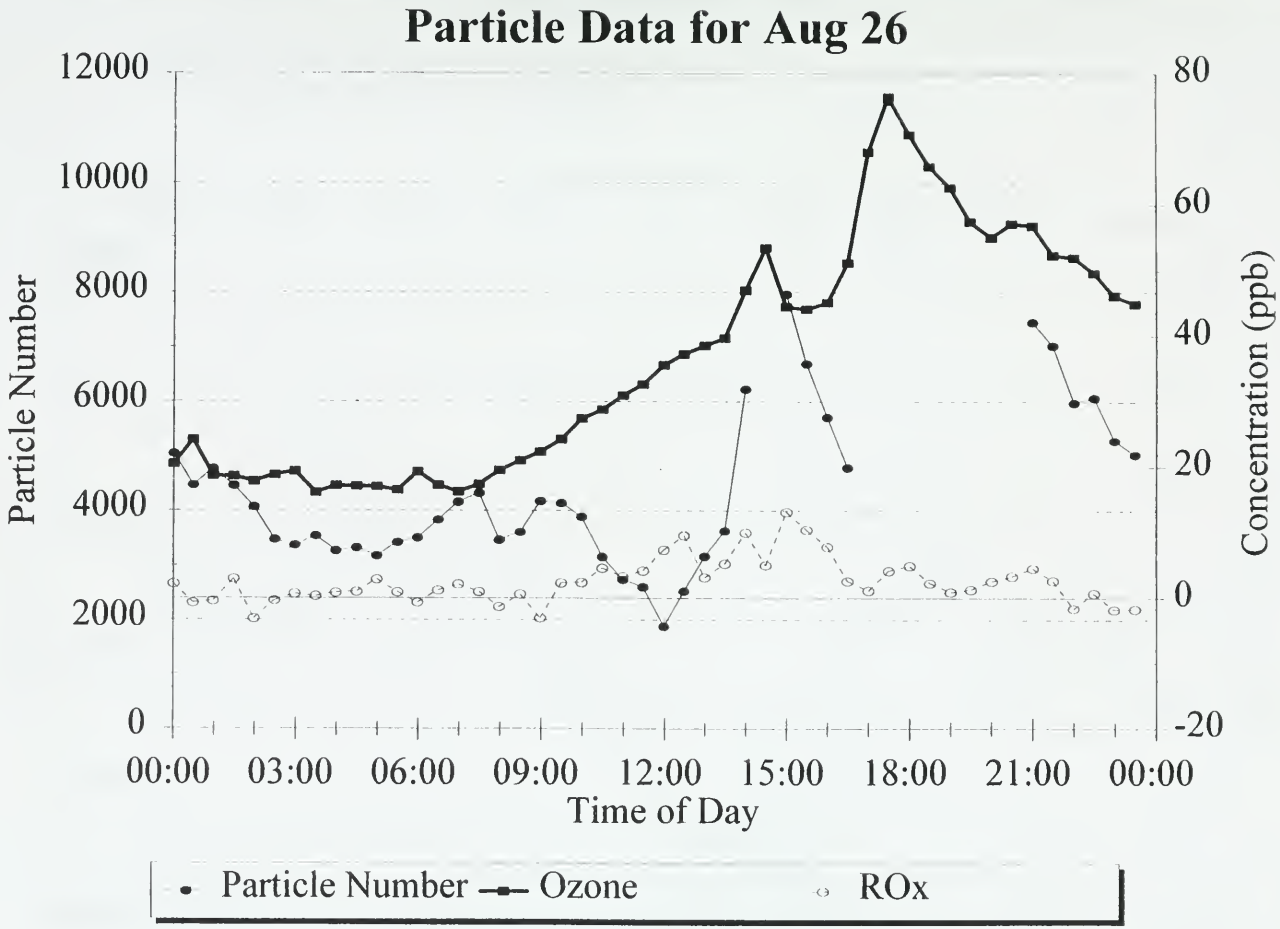

Figure 16c.ii. Particle number with O_3 and RO_x concentrations for Aug 26th.

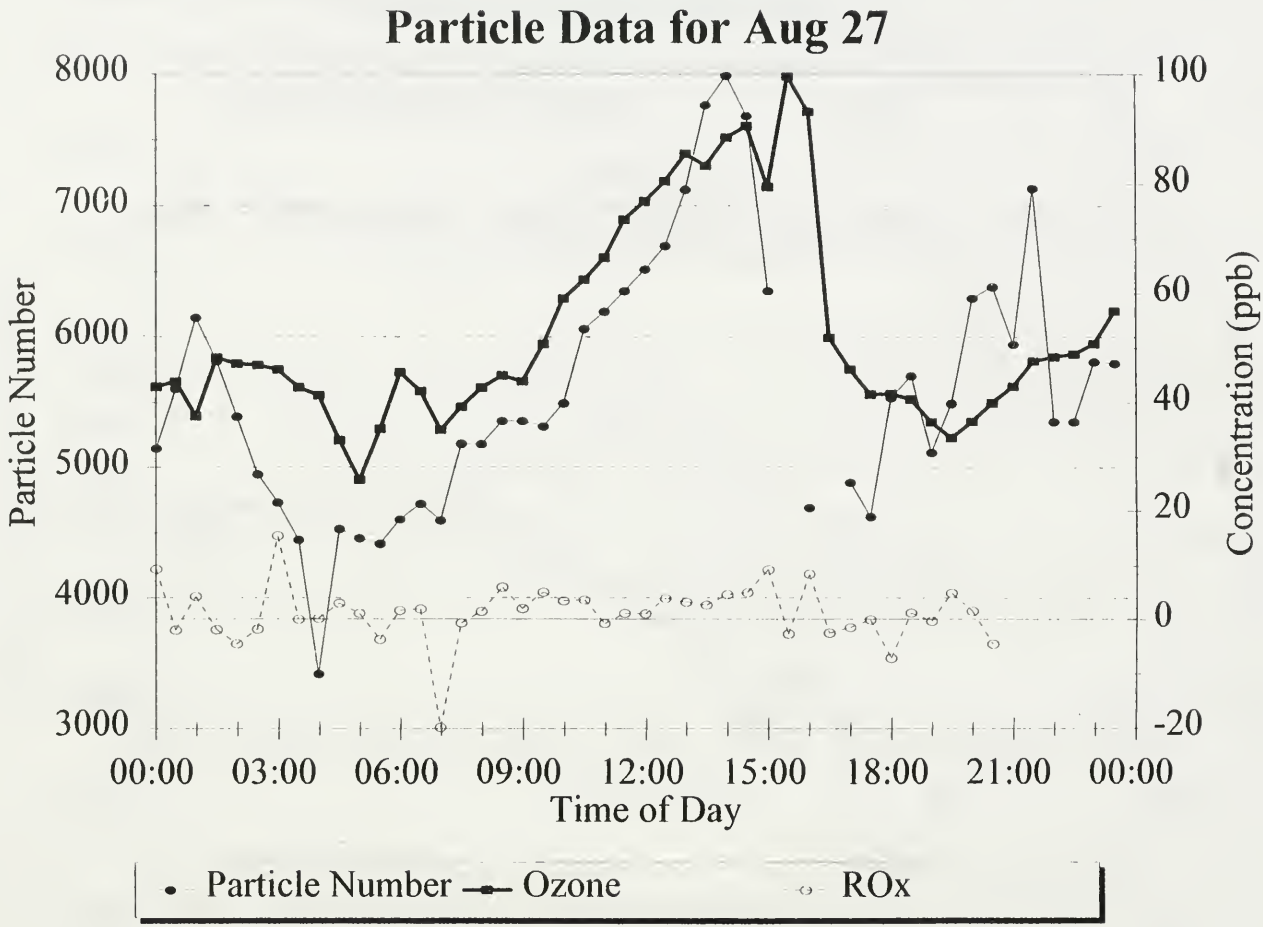

Figure 16c.iii. Particle number with O_3 and RO_x concentrations for Aug 27th.

Figure 16d.i. Correlation of particle number with radical concentrations for Aug 25th.

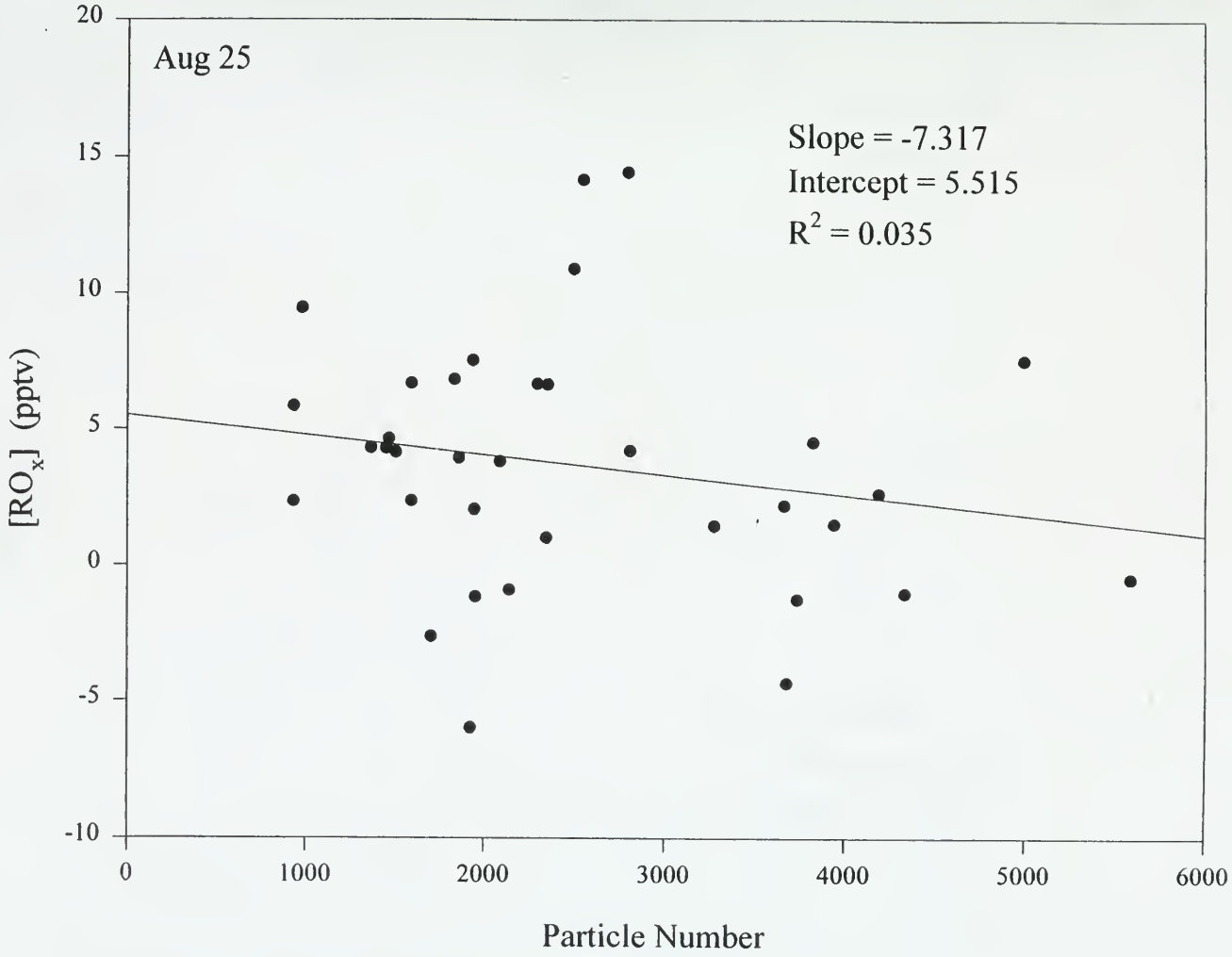

Figure 16d.ii. Correlation of particle number with radical concentrations for Aug 26th.

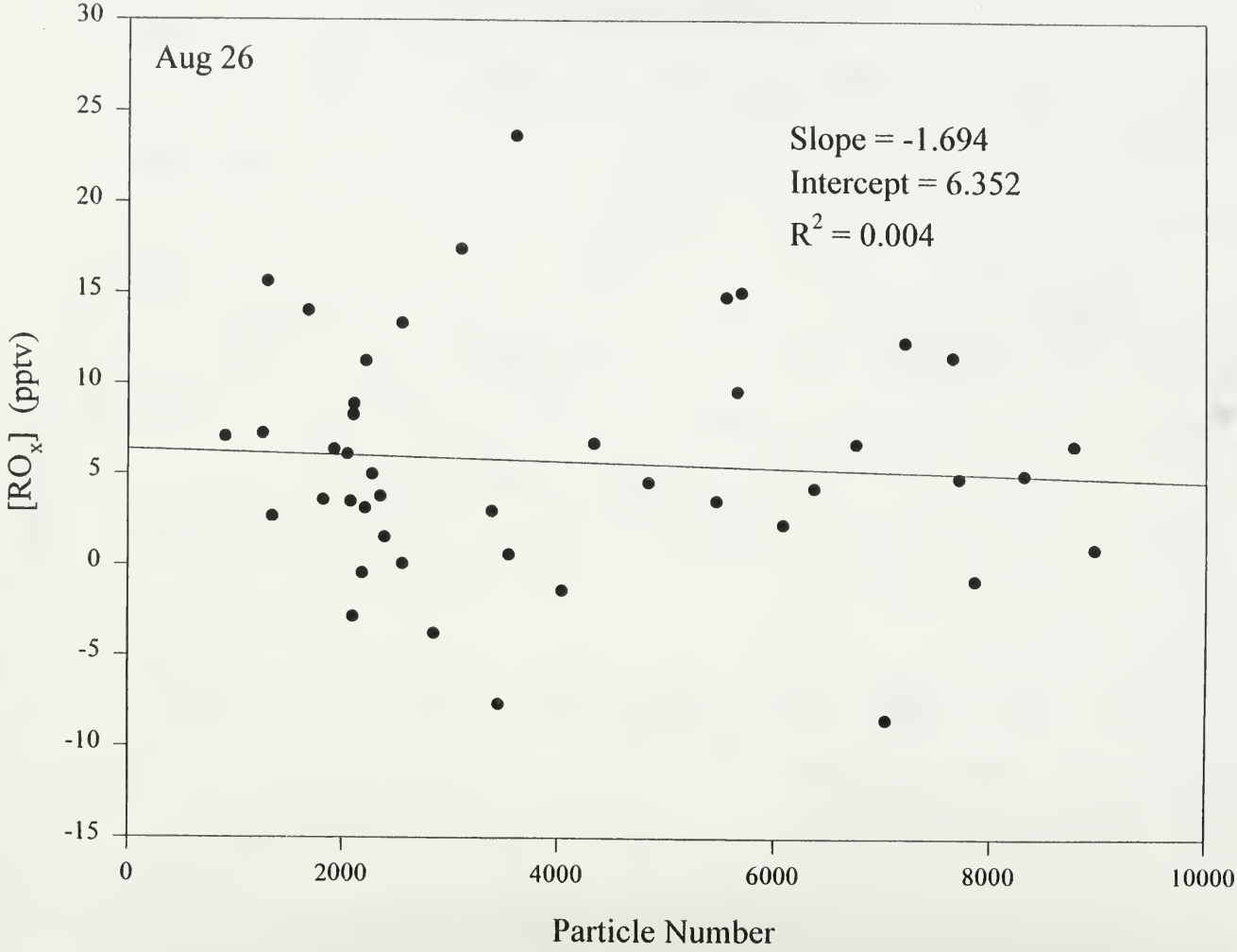

Figure 16d.iii. Correlation of particle number with radical concentrations for Aug 27th.

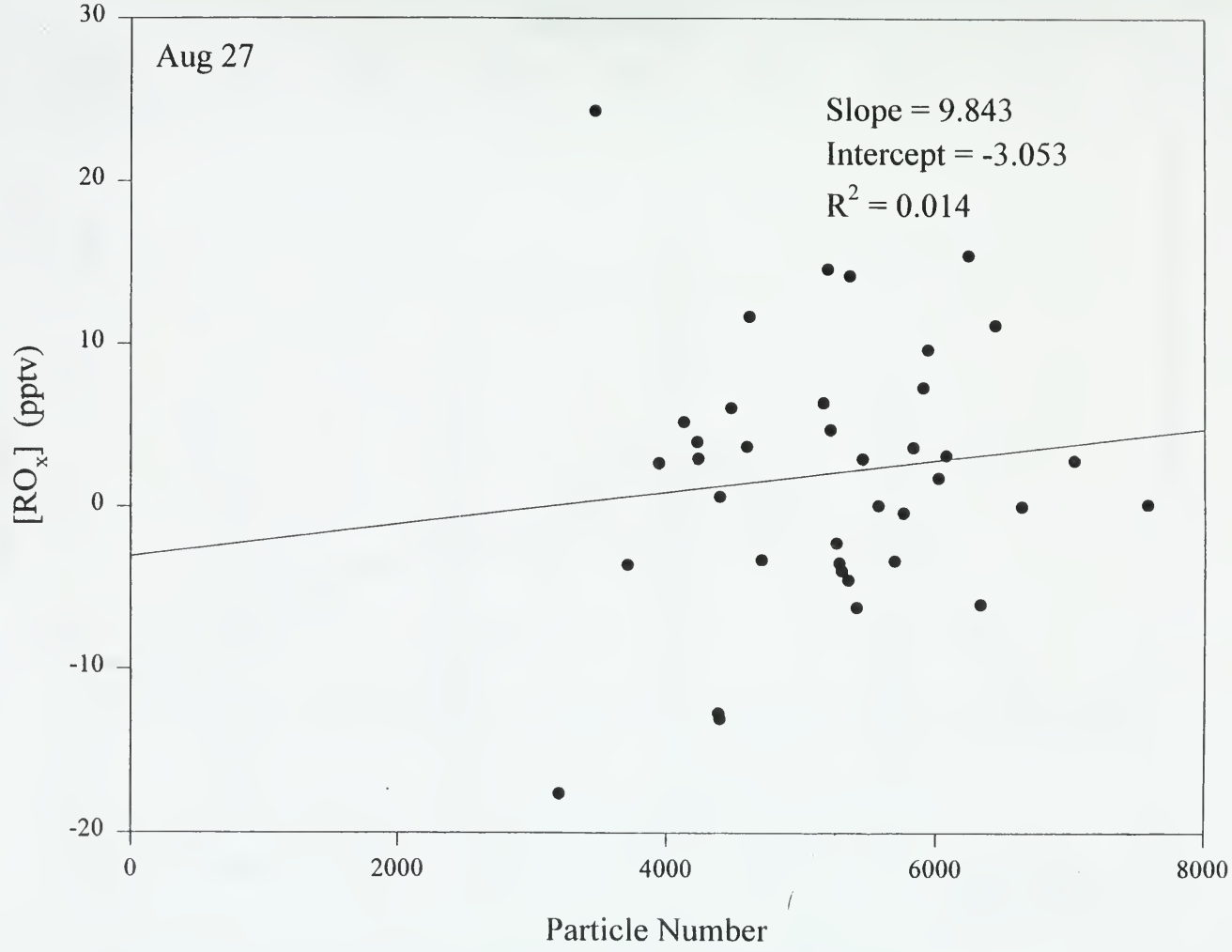

Figure 17a. Average diurnal plot of NO_y indicating Sillman threshold of $NO_y < 20$ppbv.

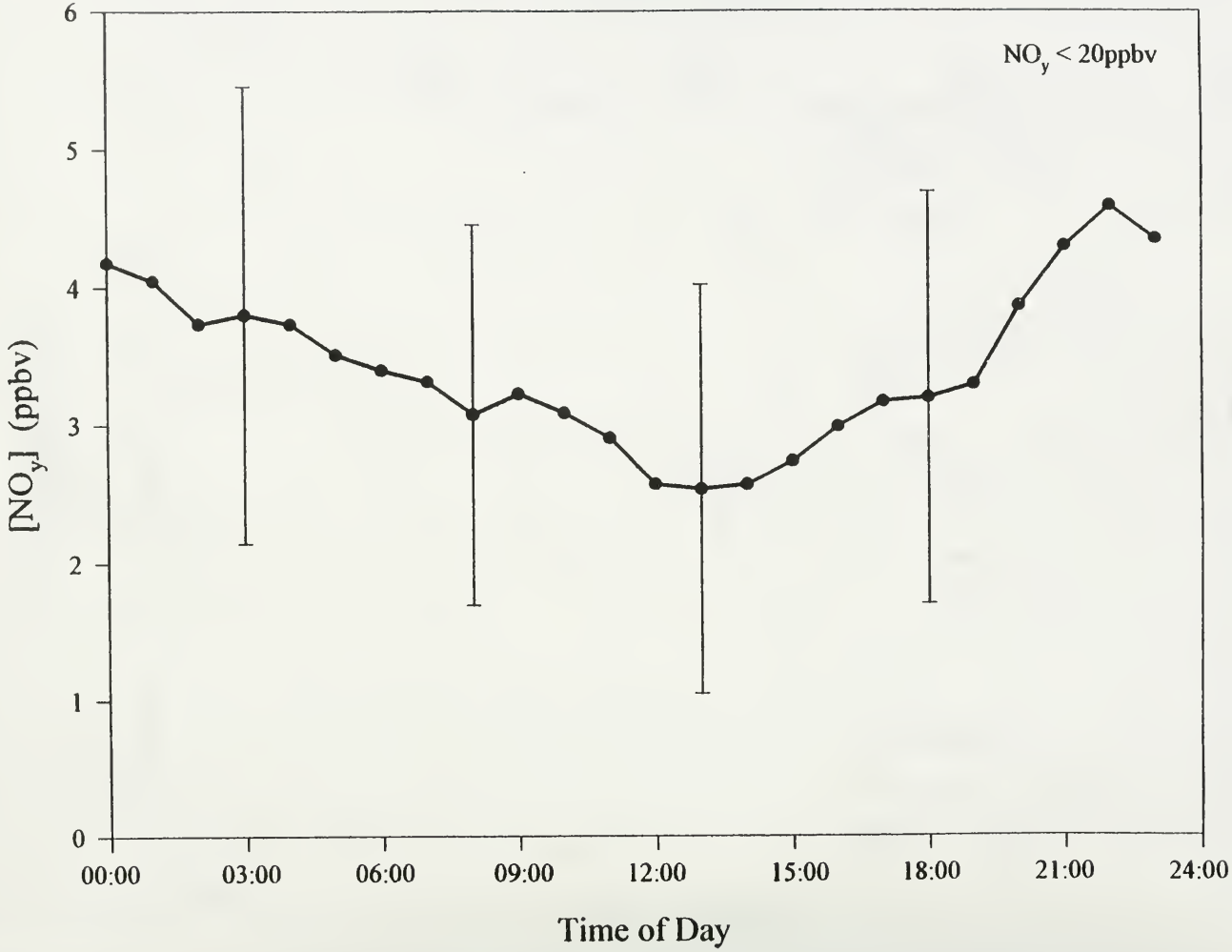

Figure 17b. Average diurnal plot of CH_2O/NO_y indicating Sillman threshold for a change in sensitivity.

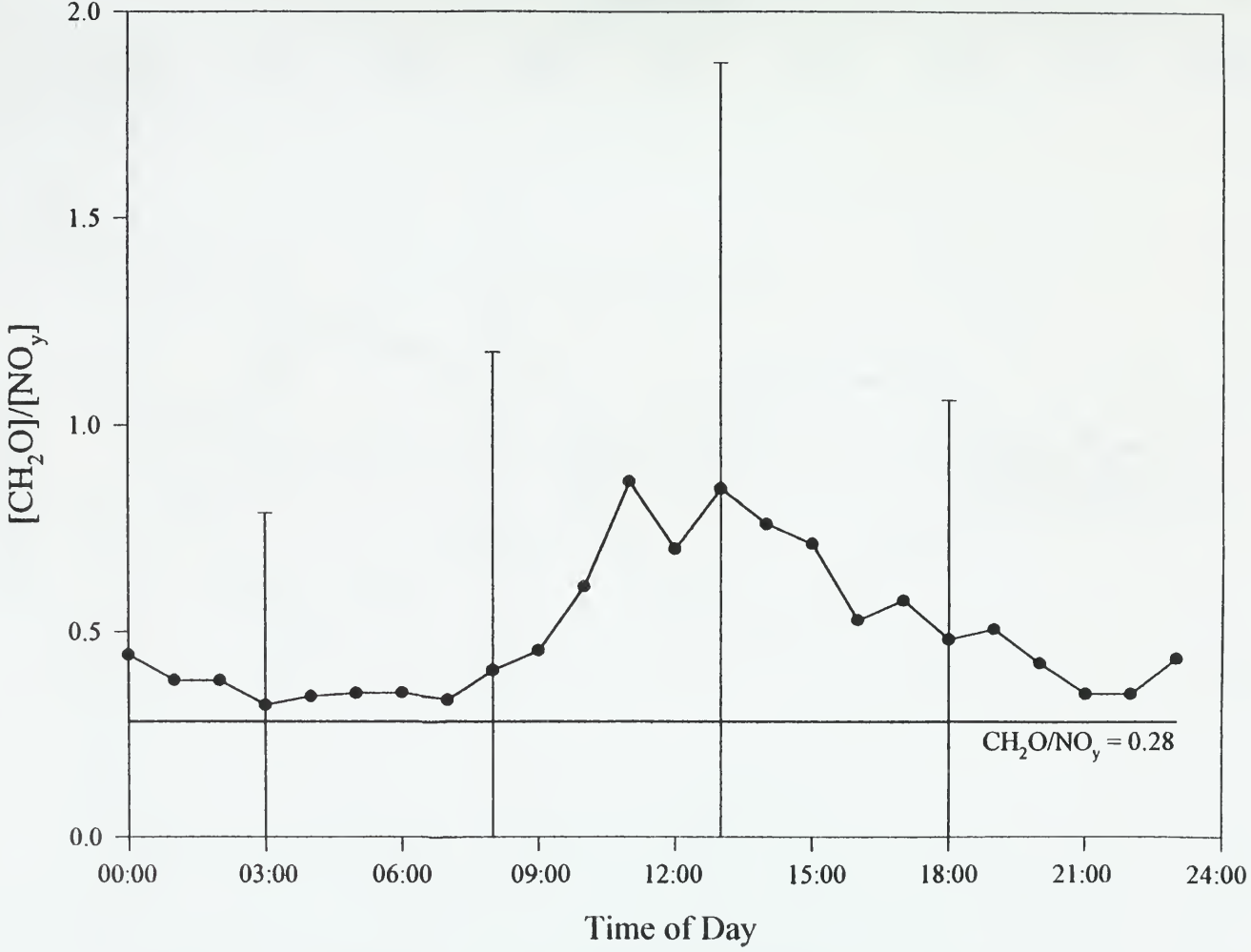

Figure 17c. Average diurnal plot of H_2O_2/NO_y indicating Sillman threshold for a change in sensitivity.

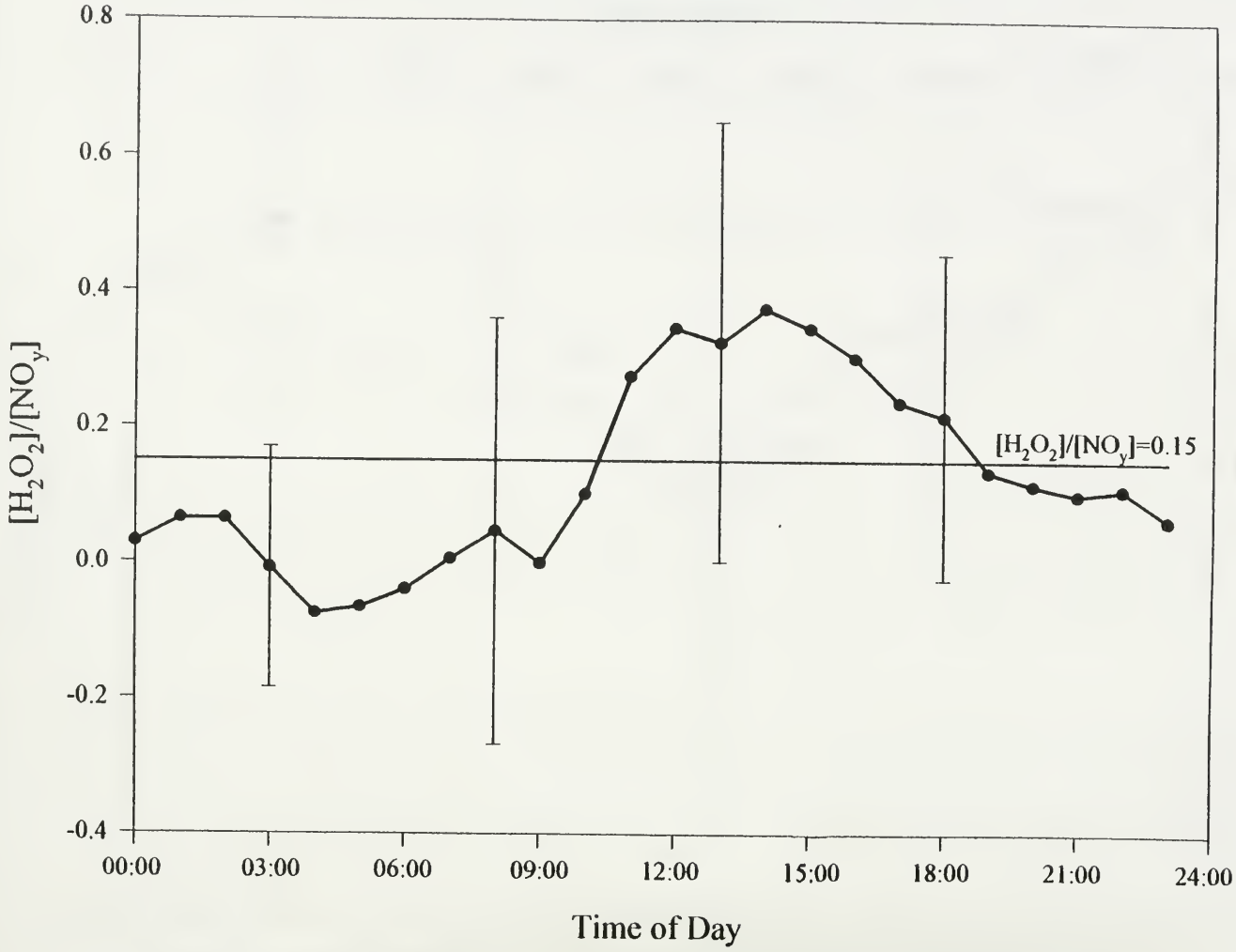

Figure 17d. Average diurnal plot of H_2O_2/HNO_3 indicating Sillman threshold for a change in sensitivity.

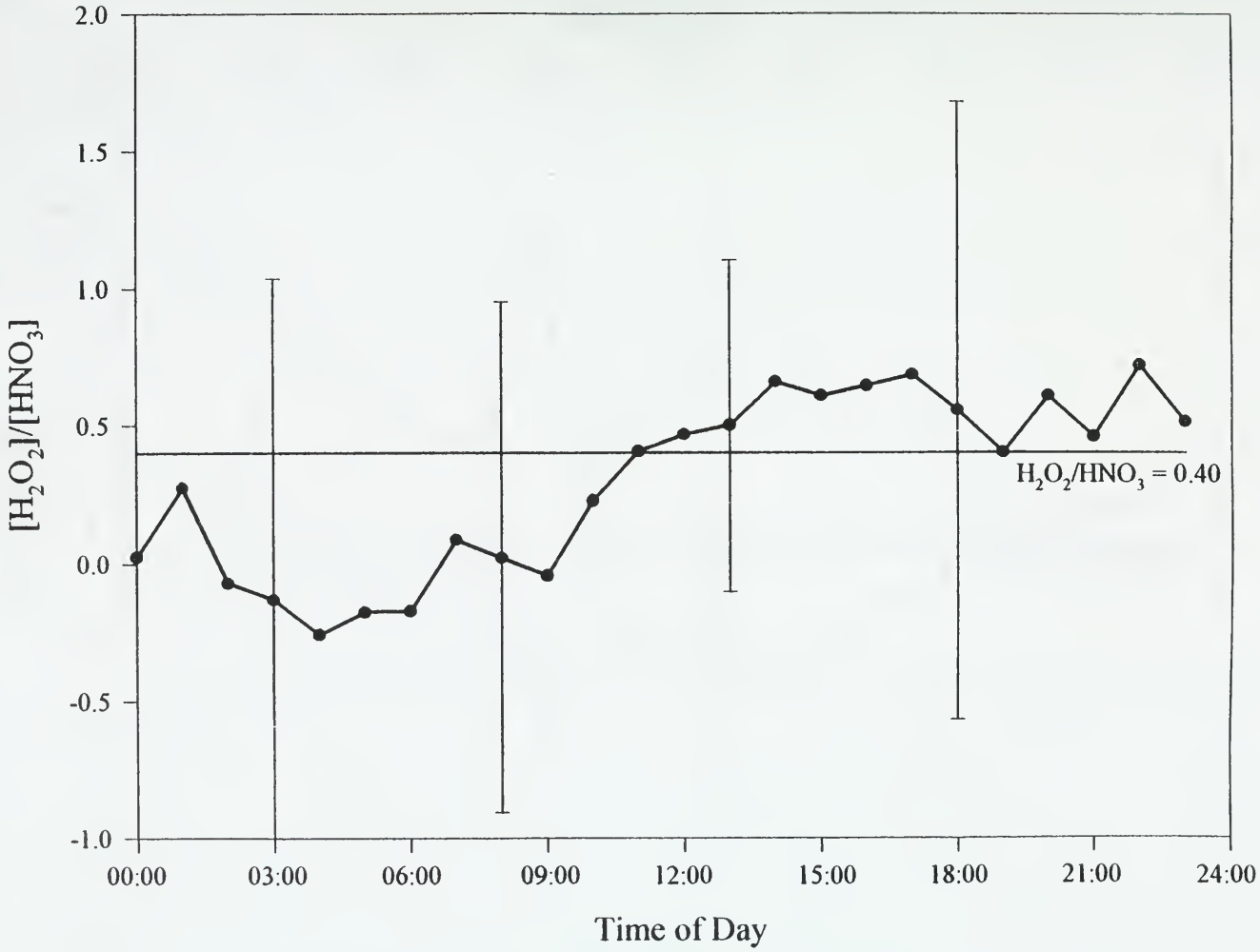

Figure 17e. Average diurnal plot of H_2O_2/NO_z indicating Sillman threshold for a change in sensitivity.

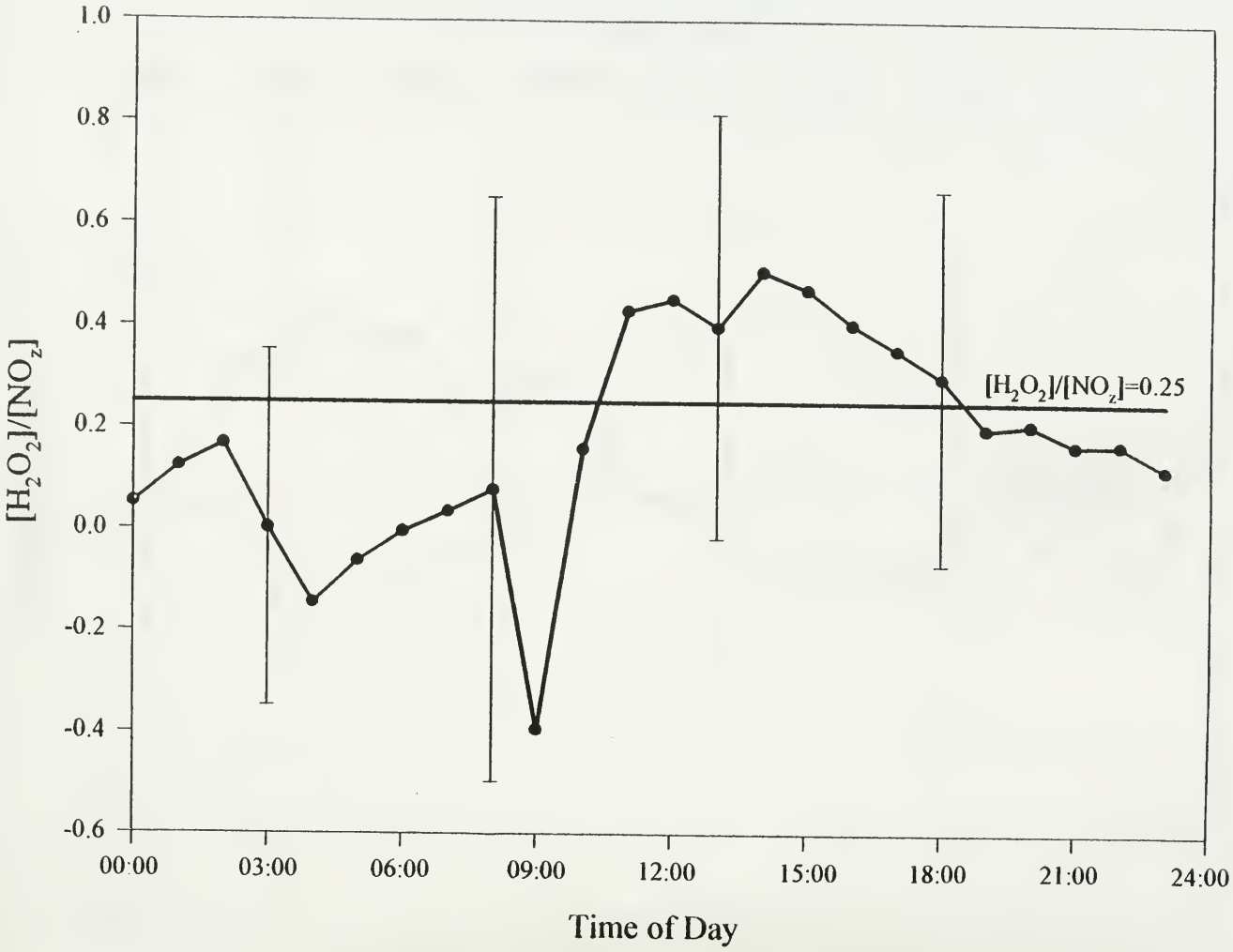

Figure 17f. Average diurnal plot of O_3/NO_z indicating Sillman threshold for a change in sensitivity.

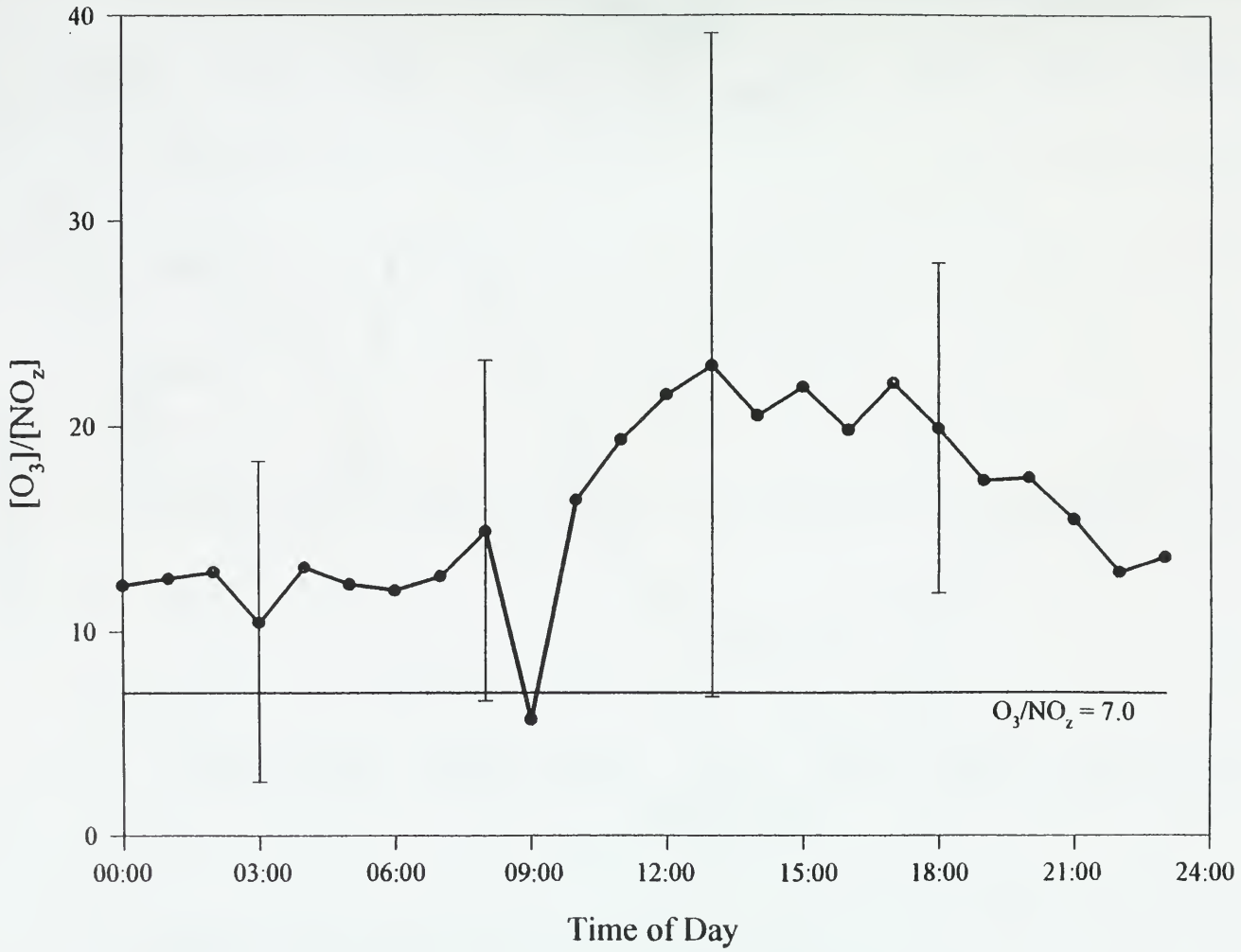

Figure 17g. Average diurnal plot of (O_3-20ppb)/NO_z indicating Sillman threshold for a change in sensitivity.

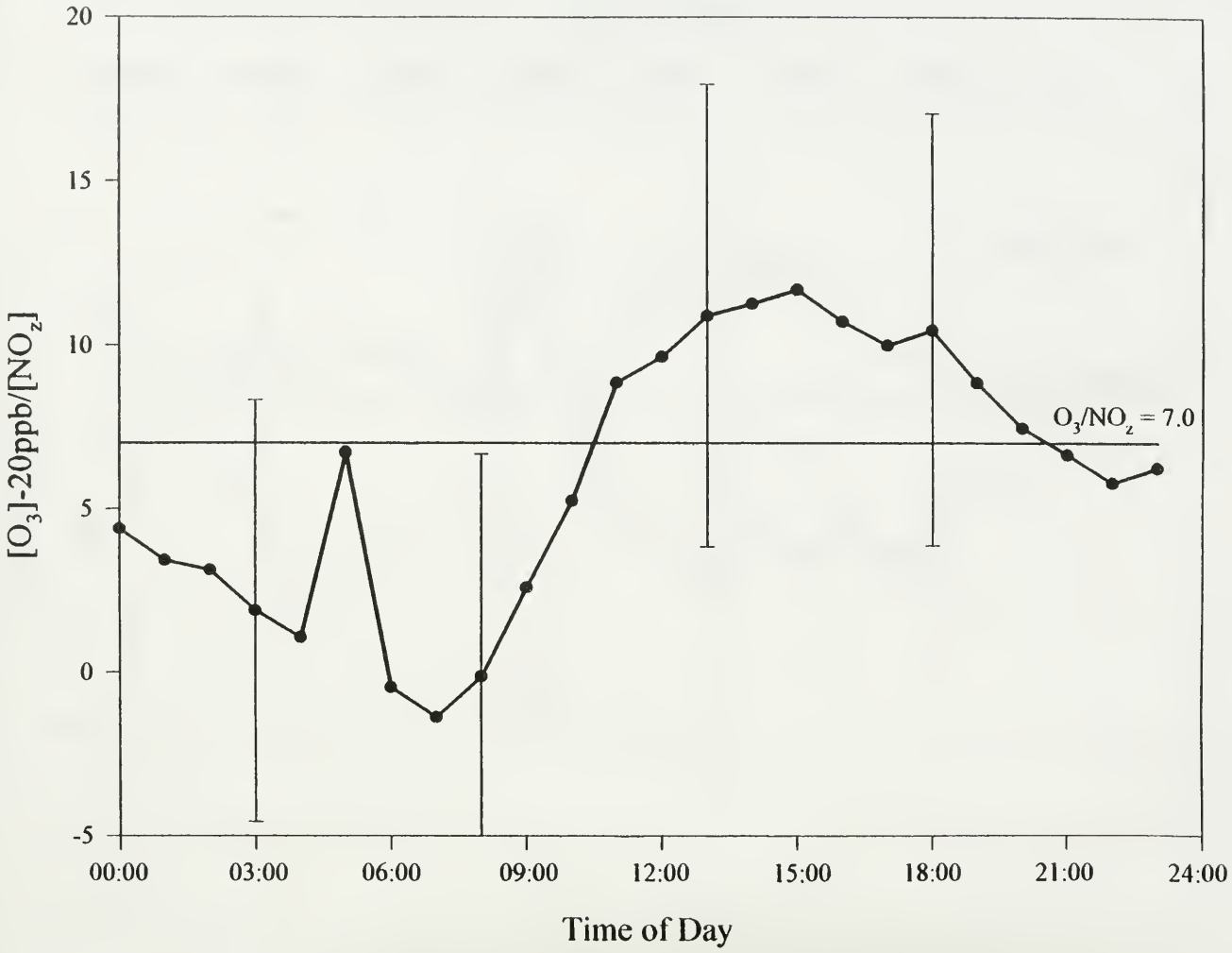

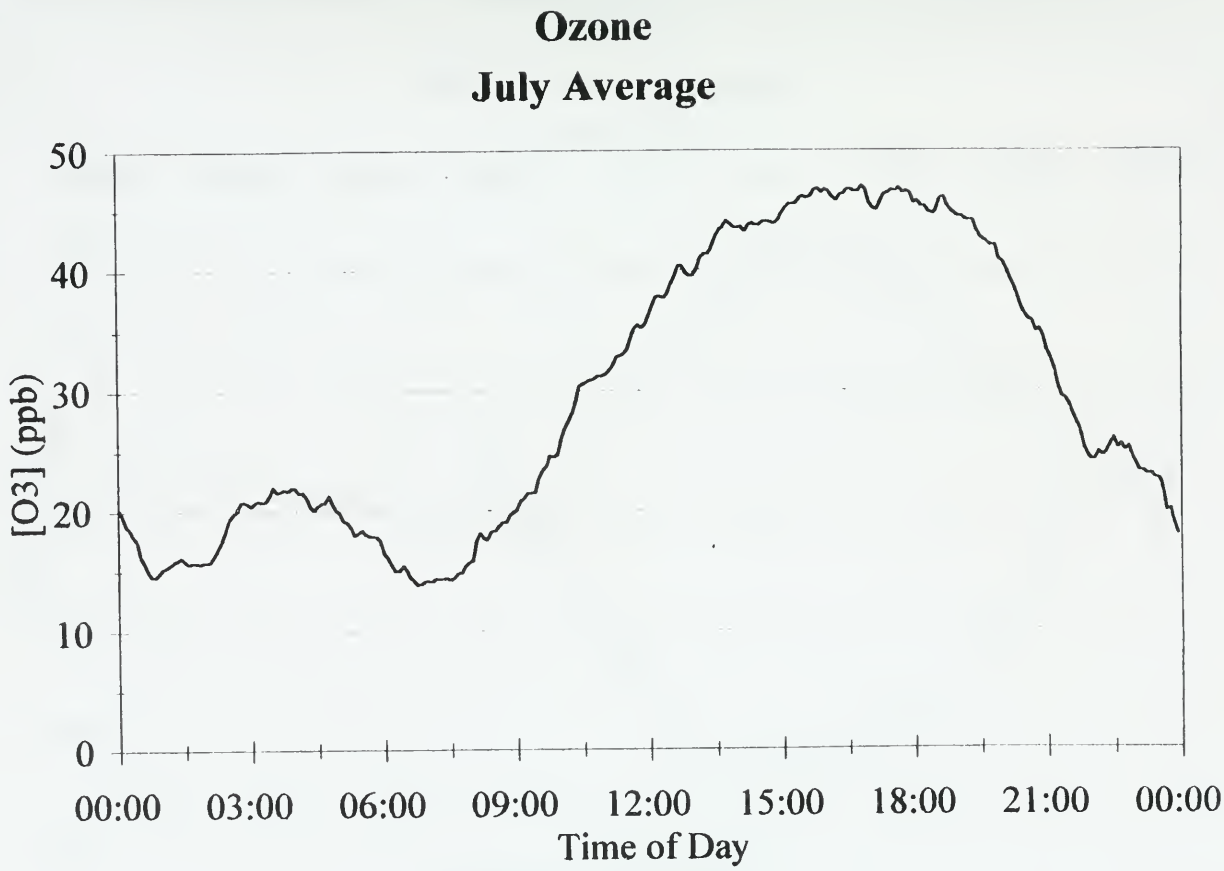

Figure 18a. Average diurnal variation of O_3 at York University in July.

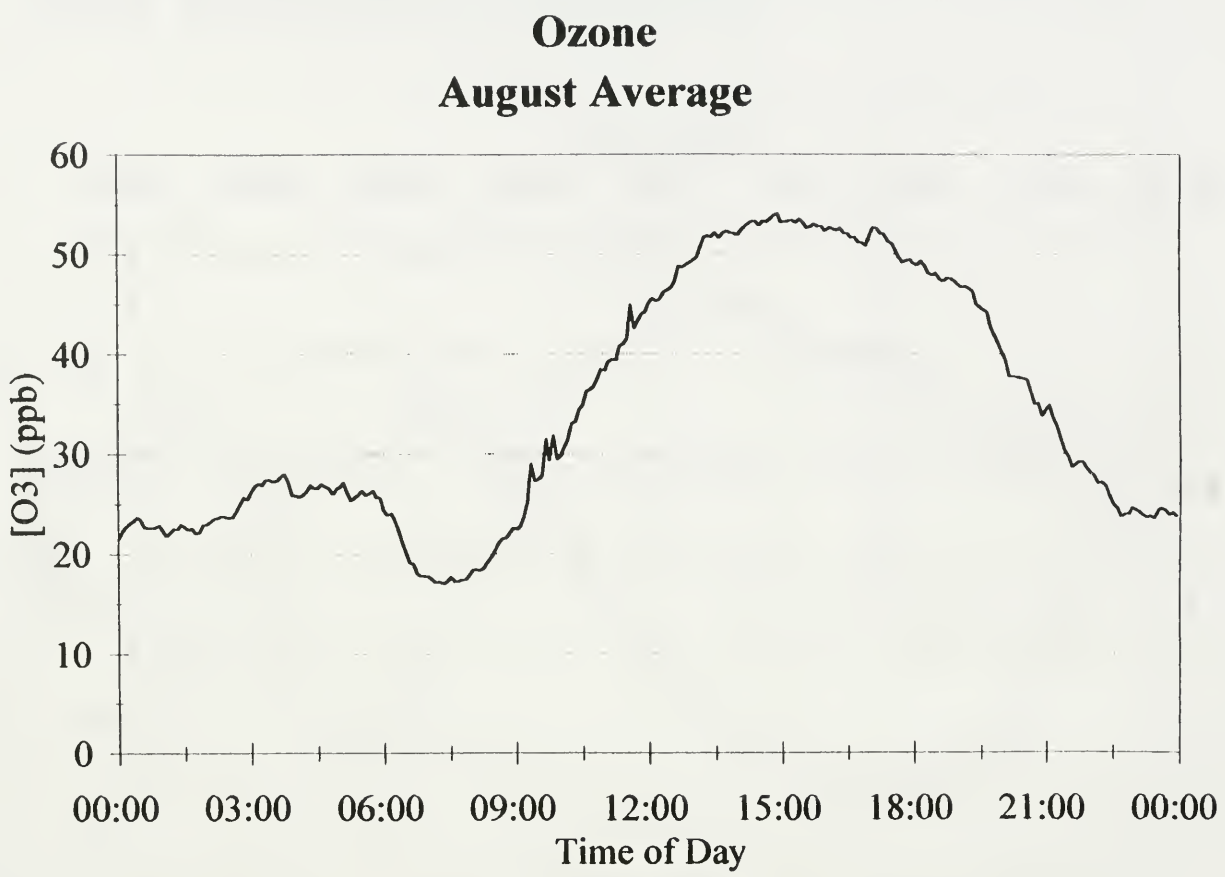

Figure 18b. Average diurnal variation of O_3 at York University in August.

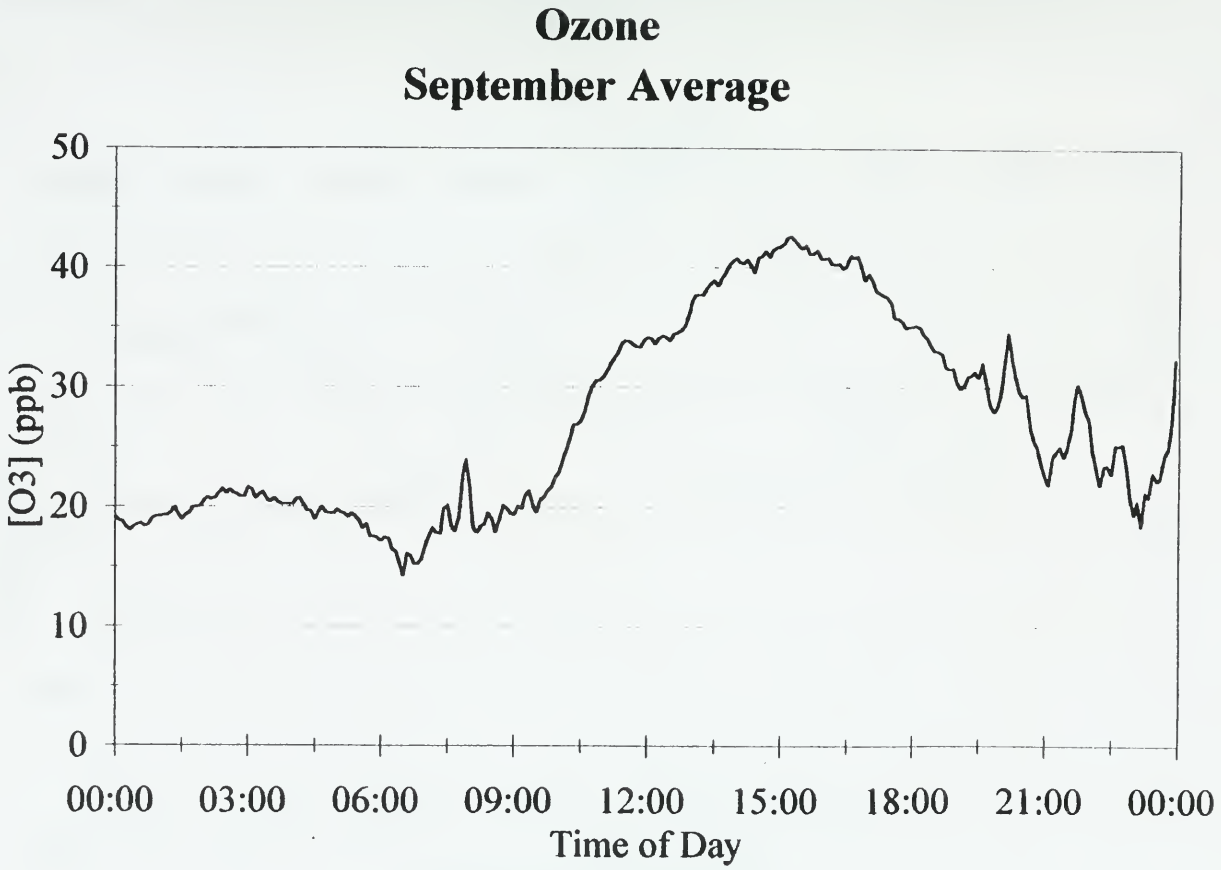

Figure 18c. Average diurnal variation of O_3 at York University in September.

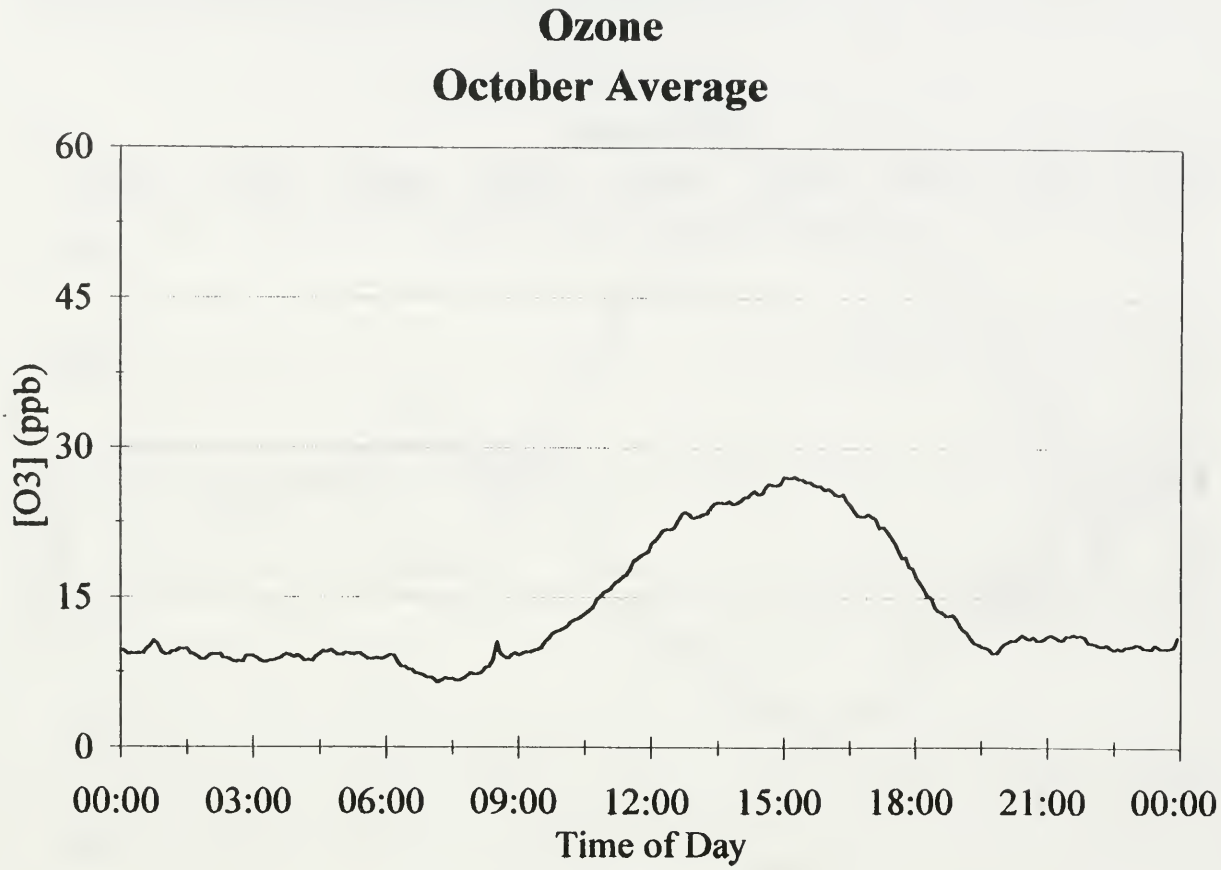

Figure 18d. Average diurnal variation of O_3 at York University in October.

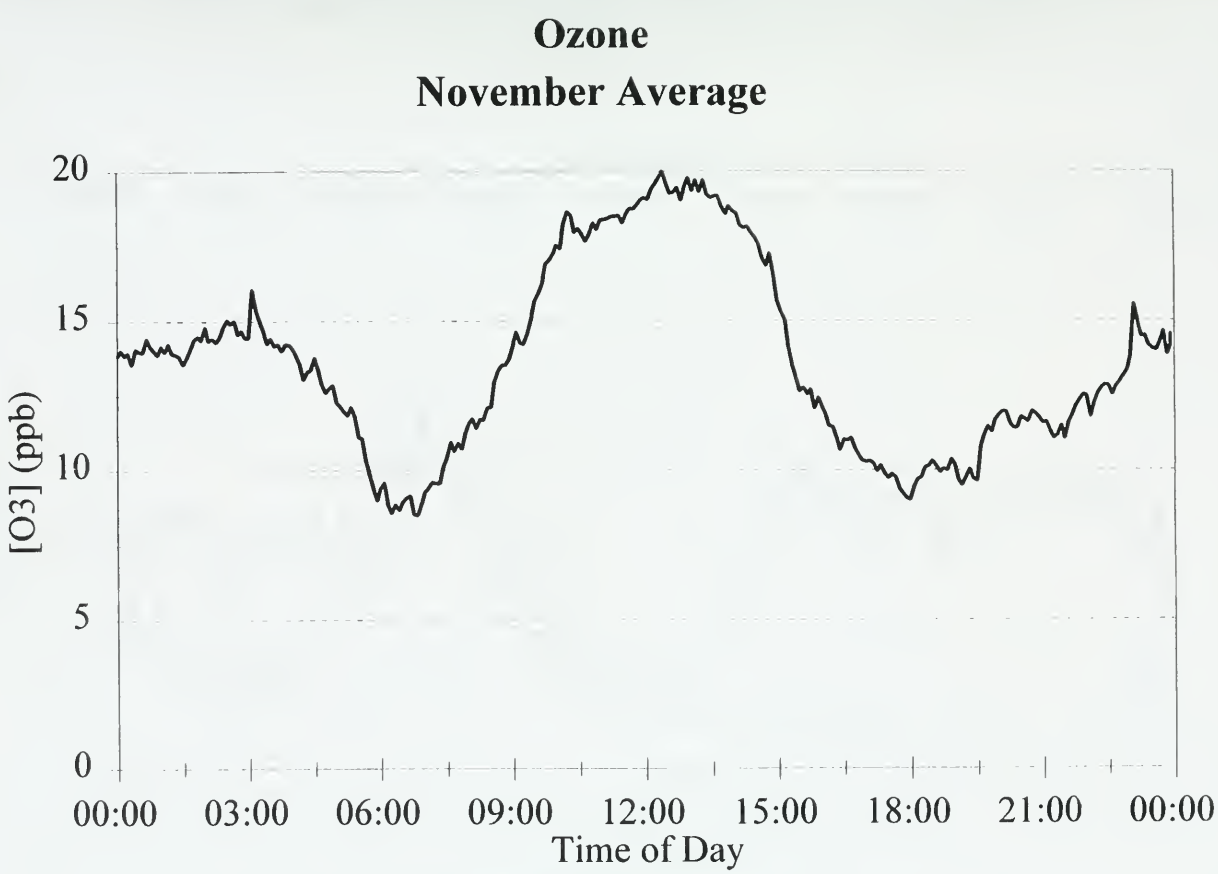

Figure 18e. Average diurnal variation of O_3 at York University in November.

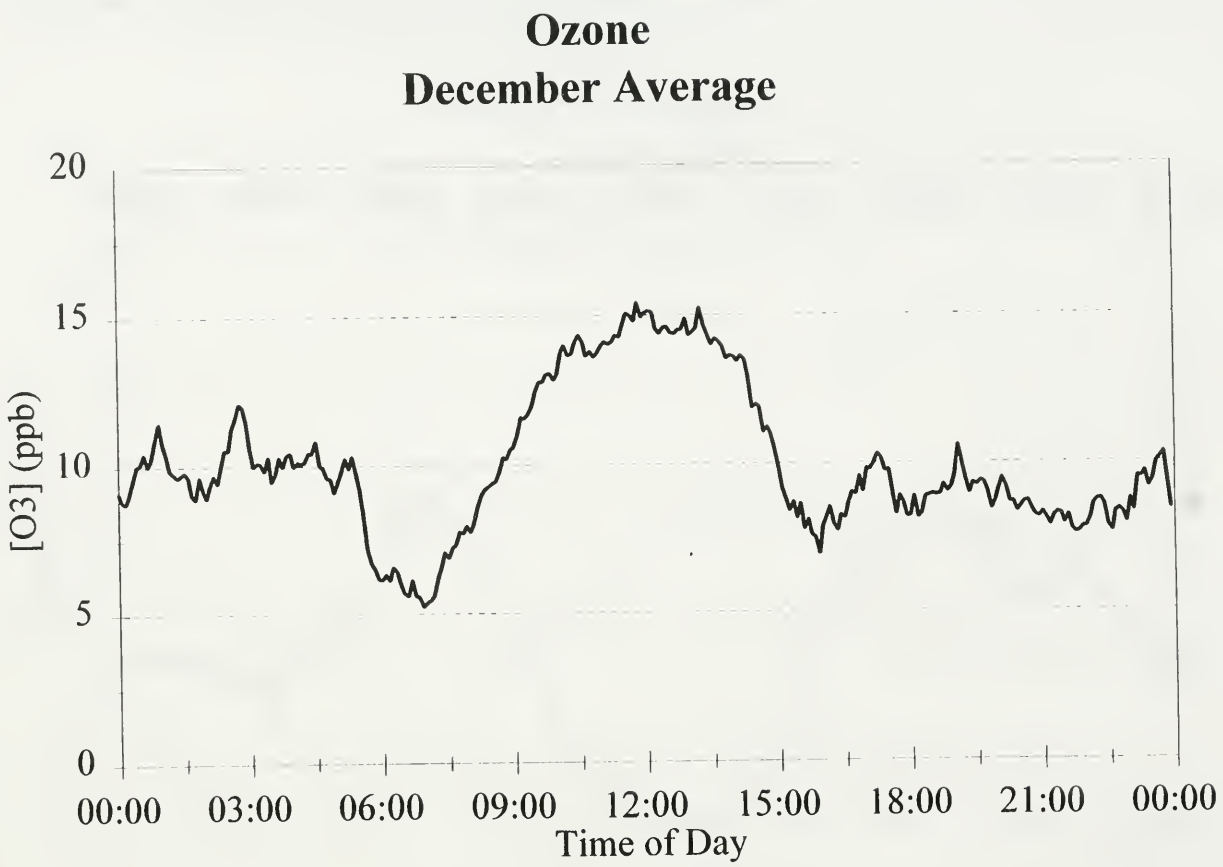

Figure 18f. Average diurnal variation of O_3 at York University in December.

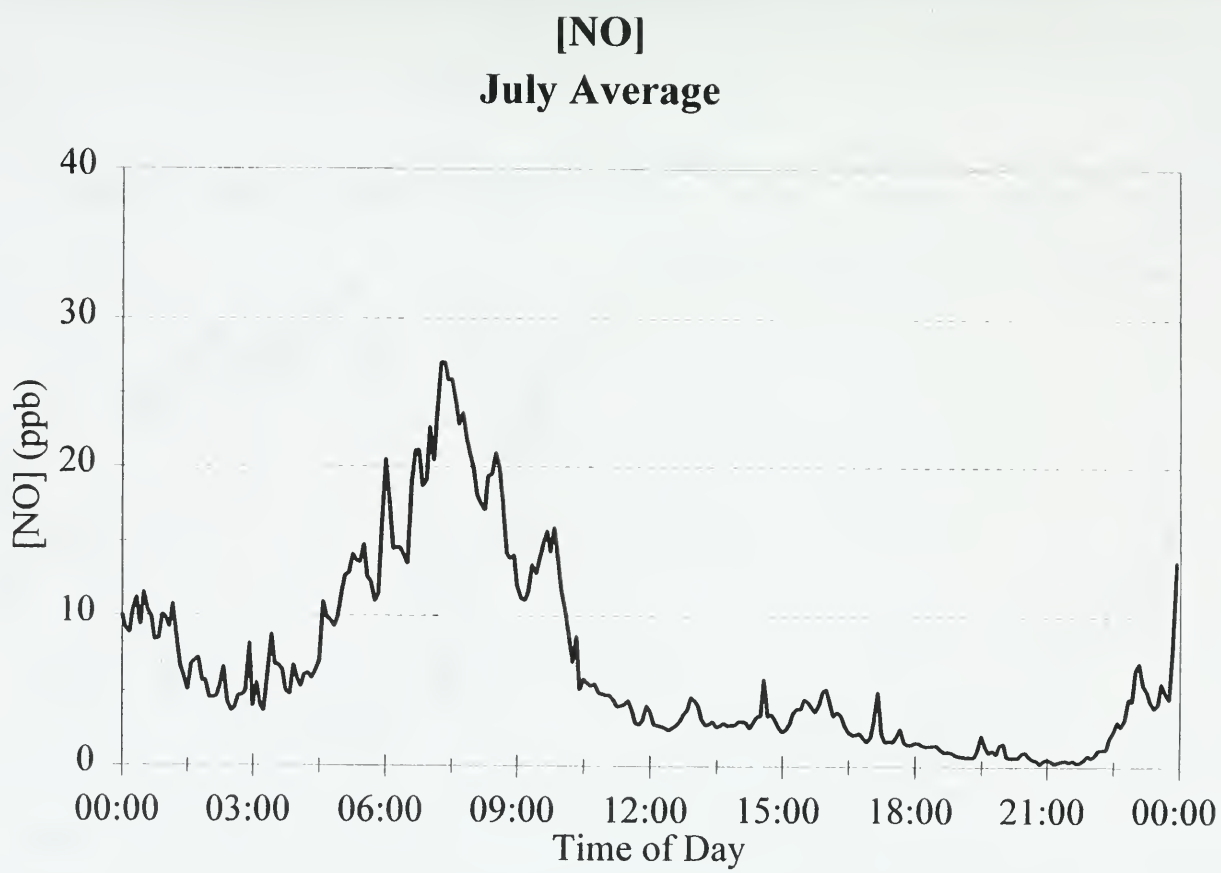

Figure 19a. Average diurnal variation of NO at York University in July.

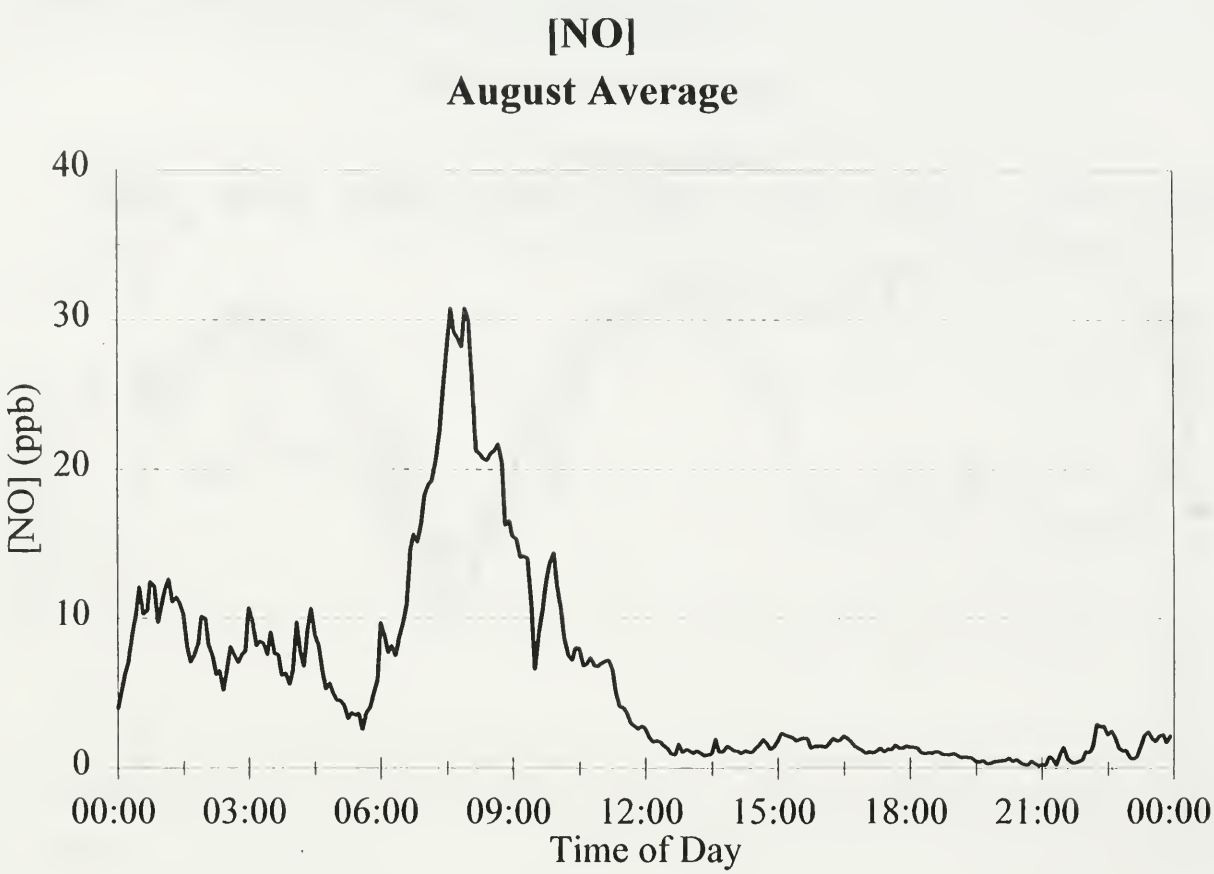

Figure 19b. Average diurnal variation of NO at York University in August.

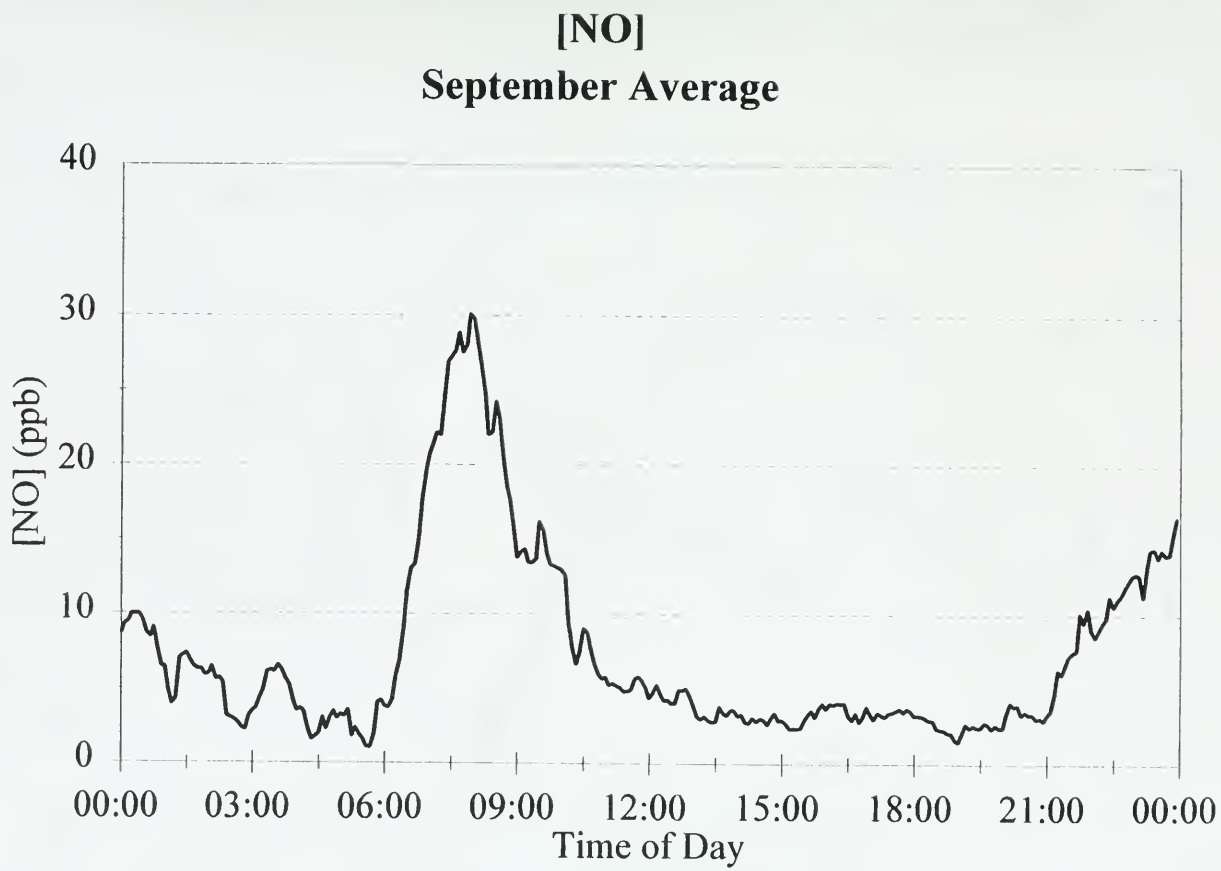

Figure 19c. Average diurnal variation of NO at York University in September.

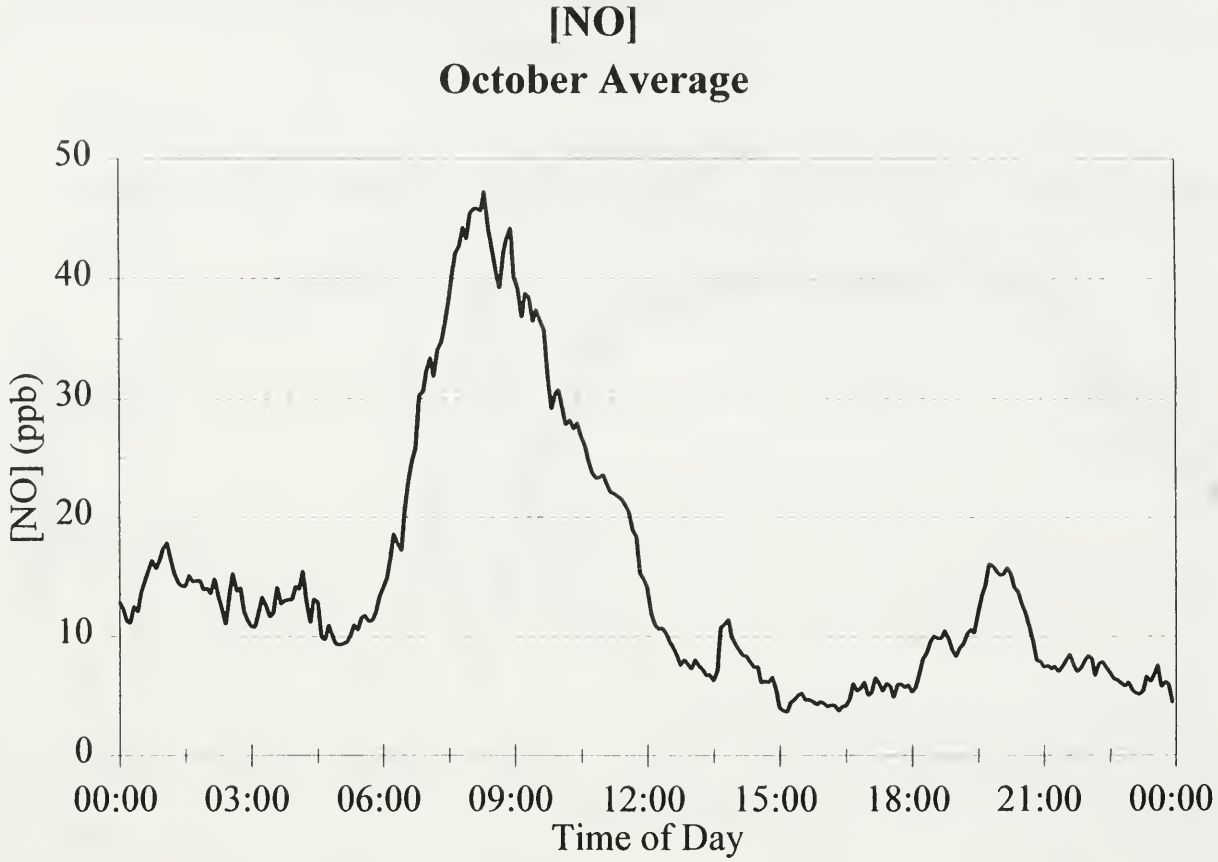

Figure 19d. Average diurnal variation of NO at York University in October.

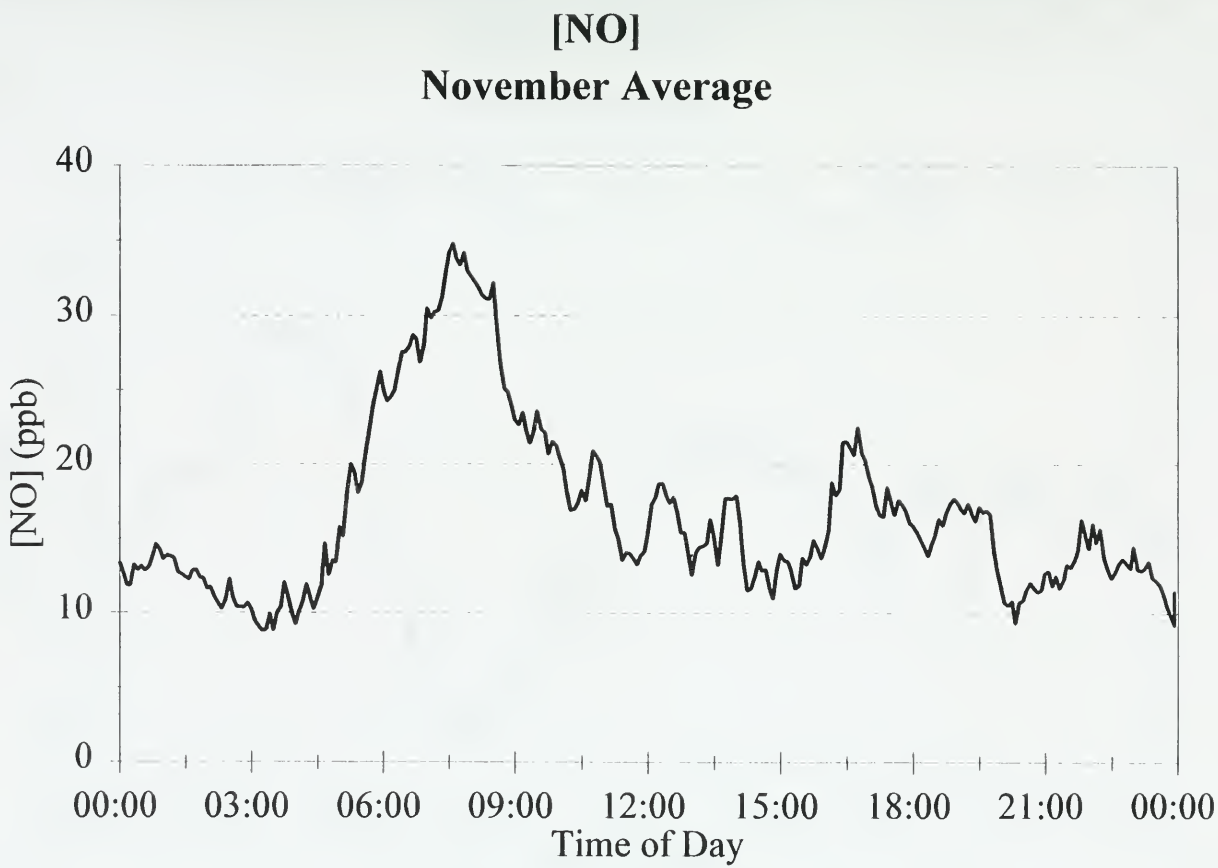

Figure 19e. Average diurnal variation of NO at York University in November.

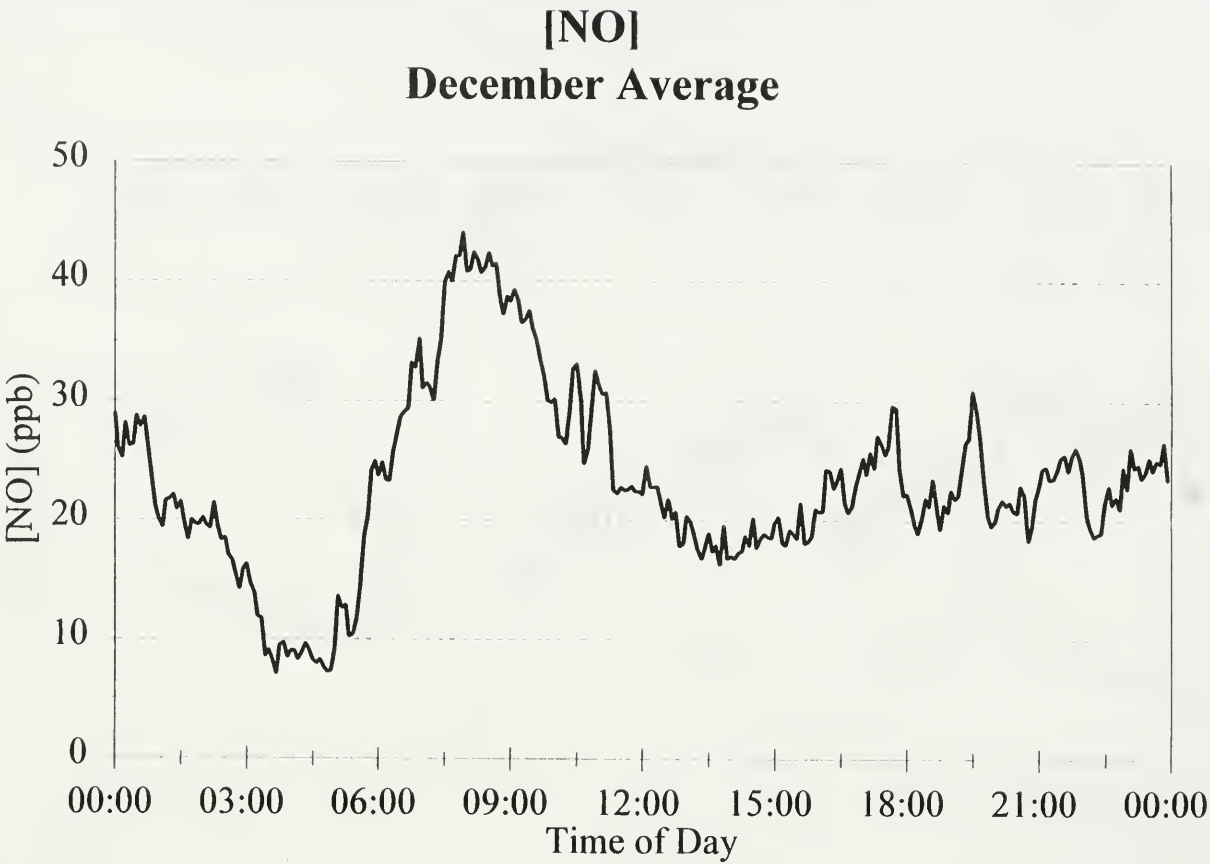

Figure 19f. Average diurnal variation of NO at York University in December.

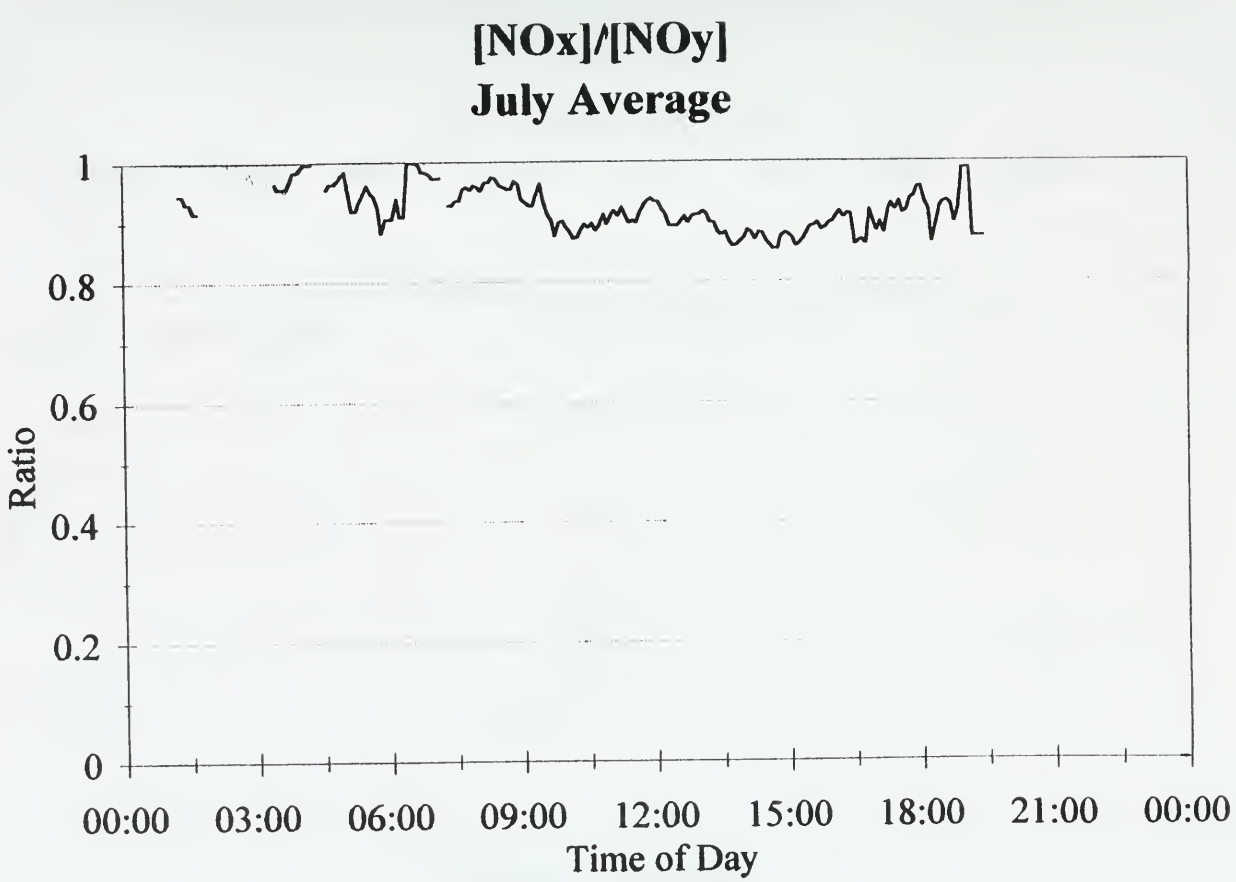

Figure 20a. Average diurnal variation of NO_x/NO_y at York University in July.

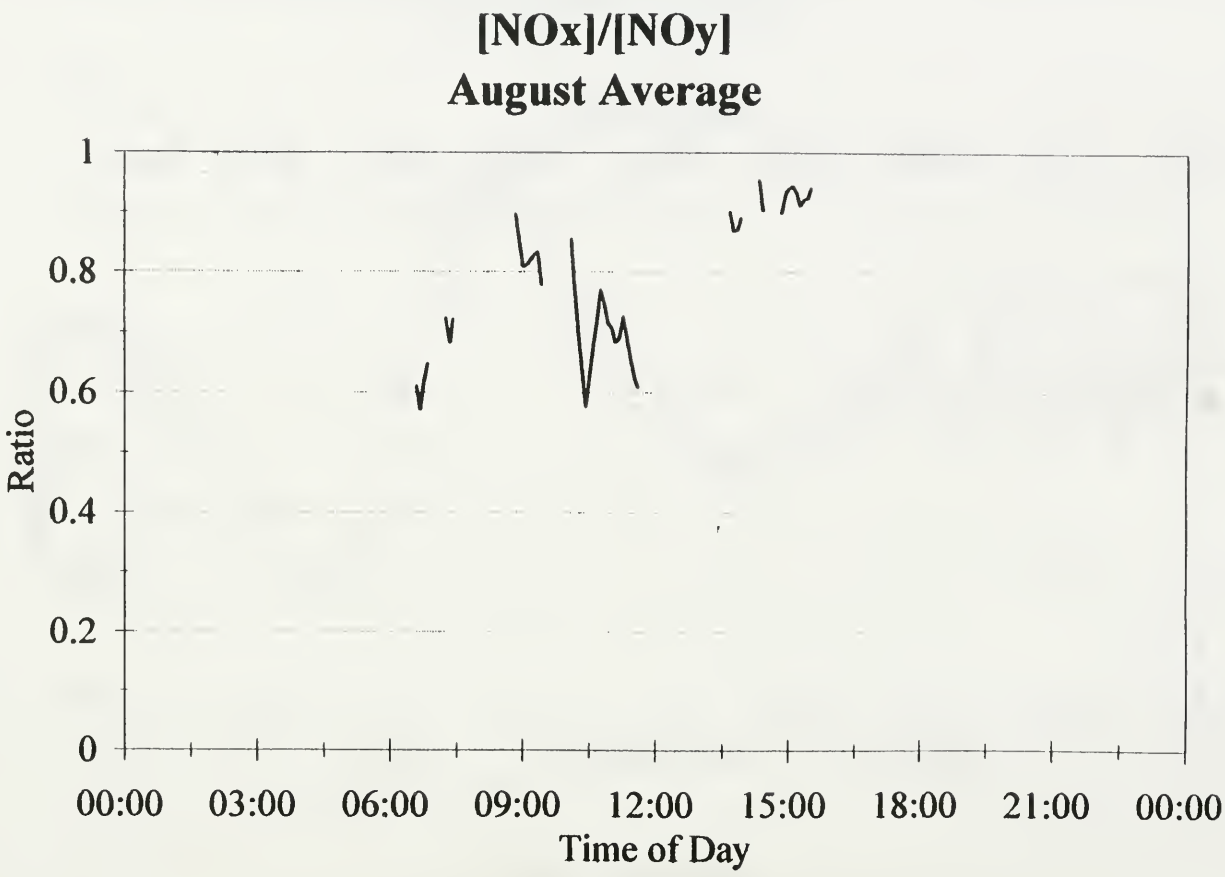

Figure 20b. Average diurnal variation of NO_x/NO_y at York University in August.

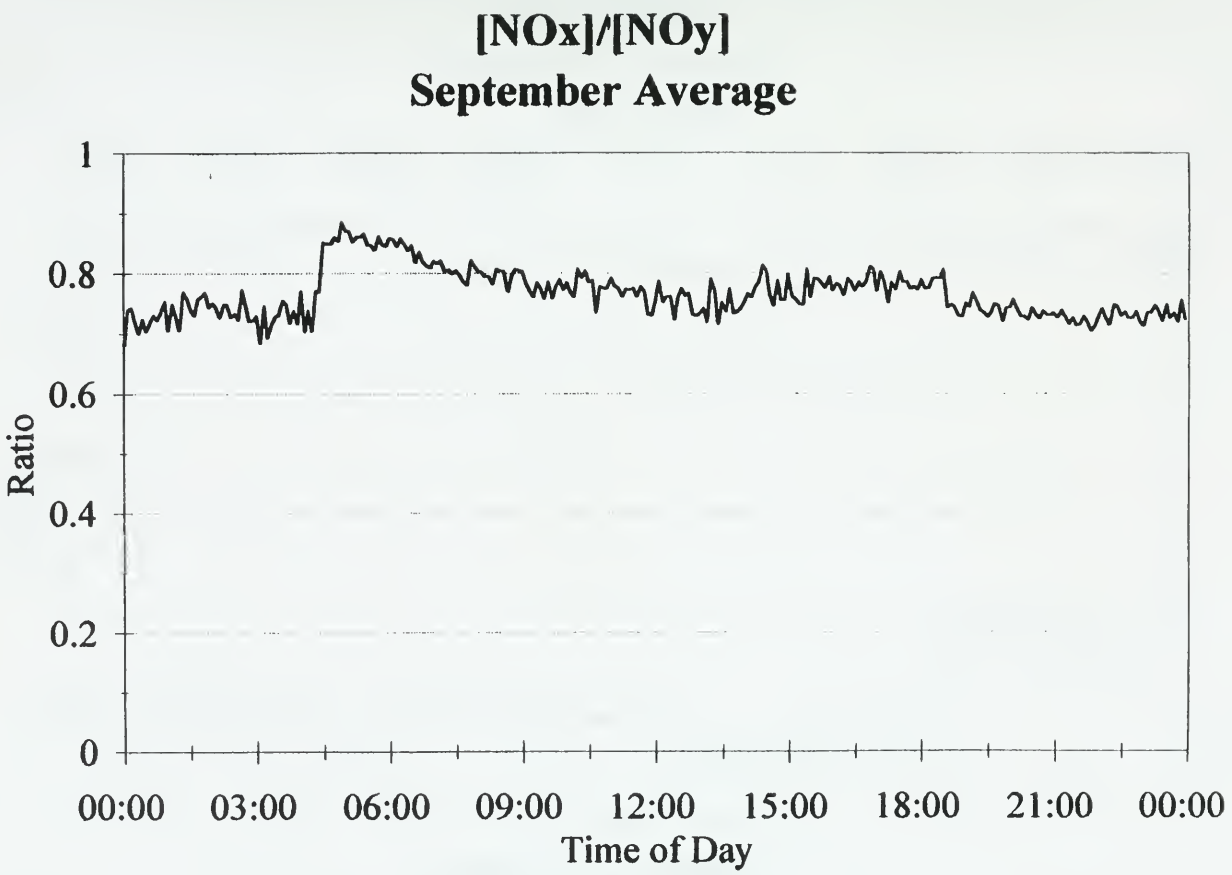

Figure 20c. Average diurnal variation of NO_x/NO_y at York University in September.

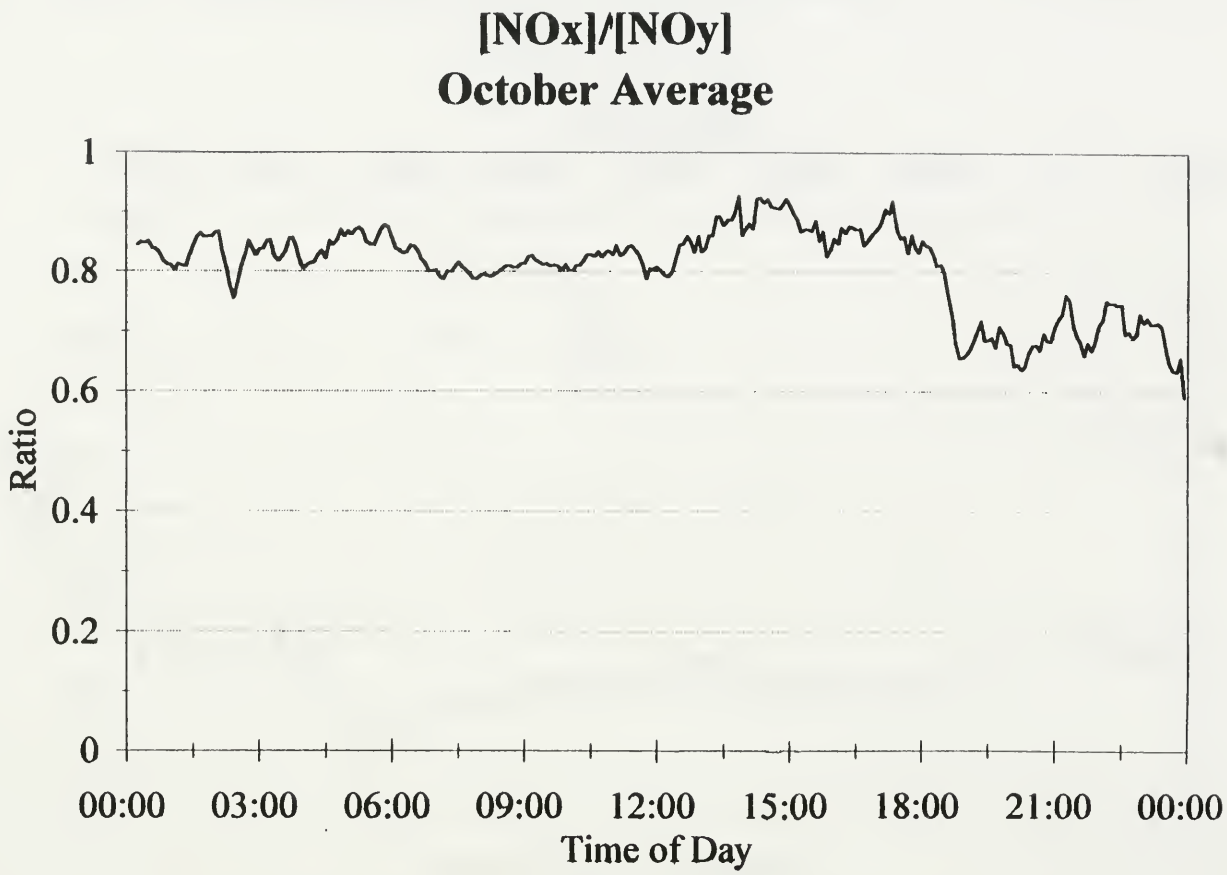

Figure 20d. Average diurnal variation of NO_x/NO_y at York University in October.

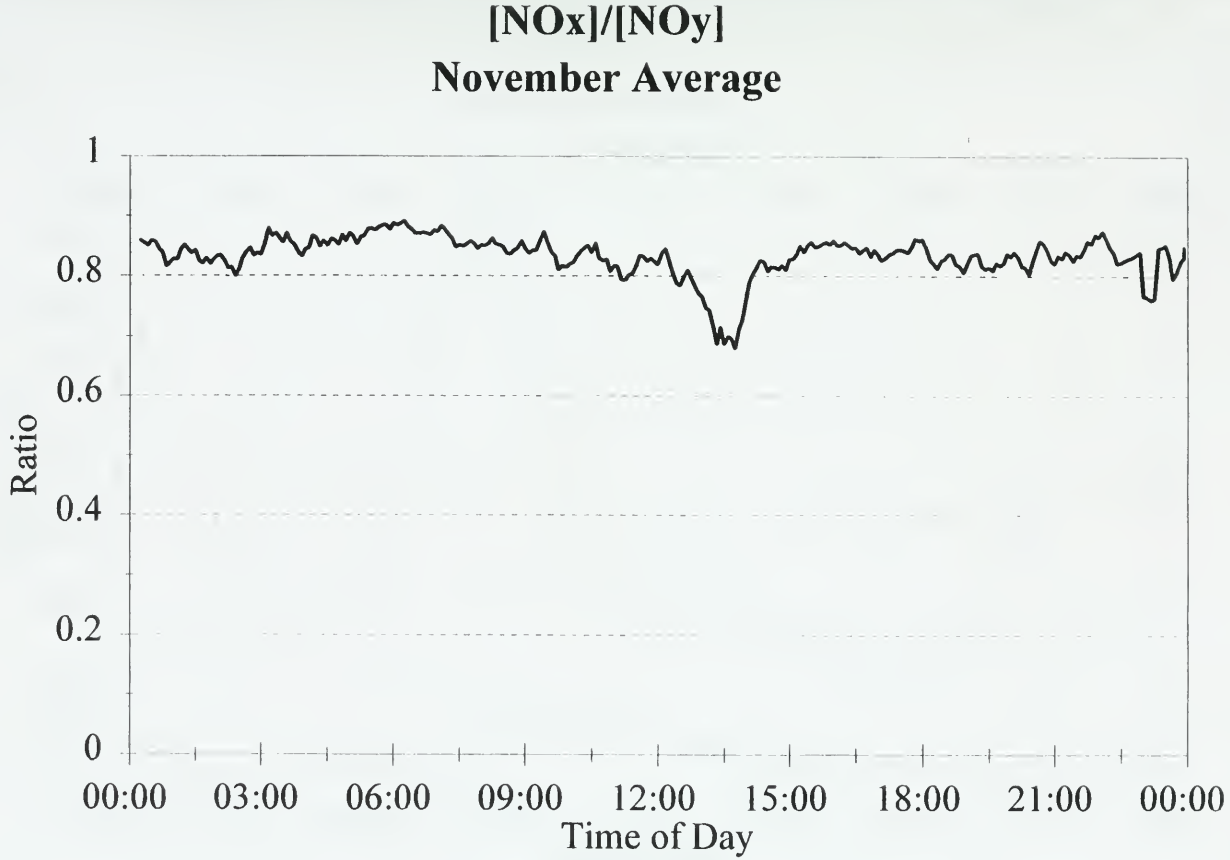

Figure 20e. Average diurnal variation of NO_x/NO_y at York University in November.

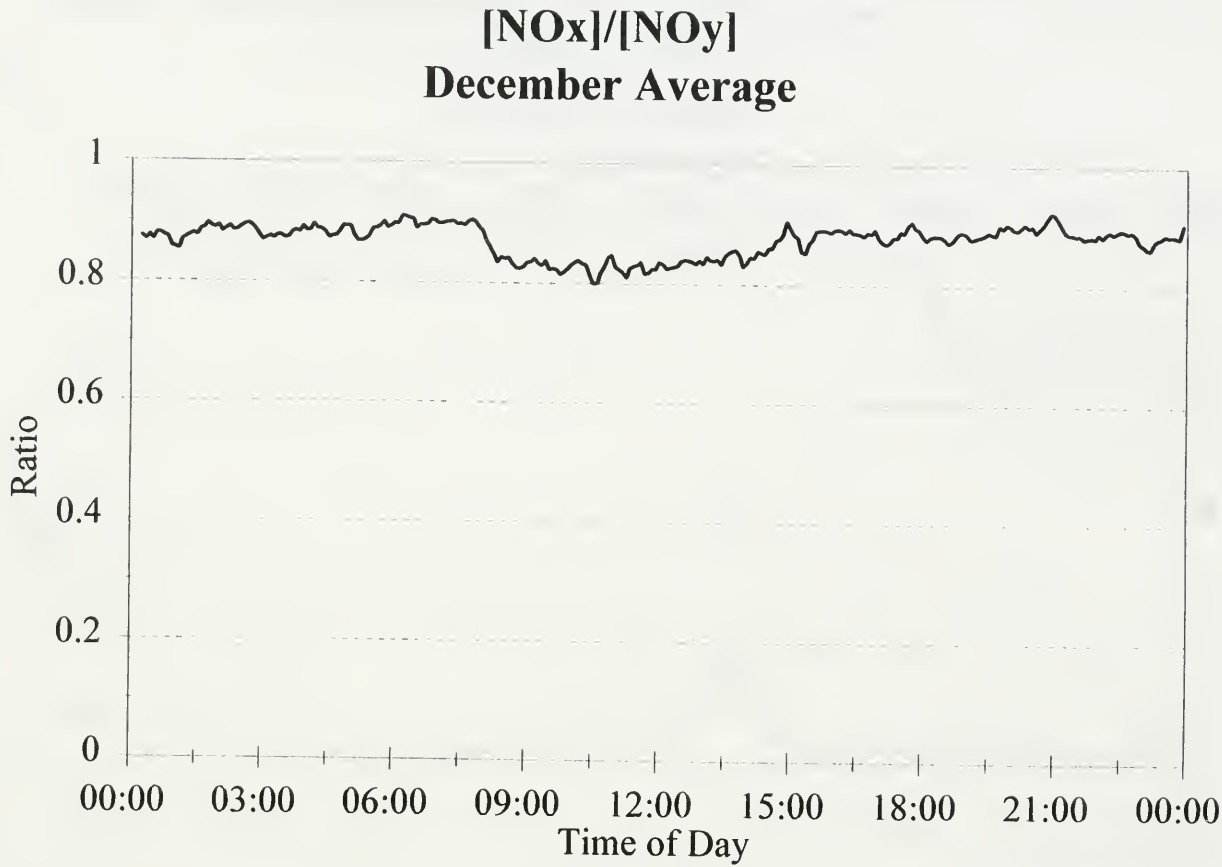

Figure 20f. Average diurnal variation of NO_x/NO_y at York University in December.

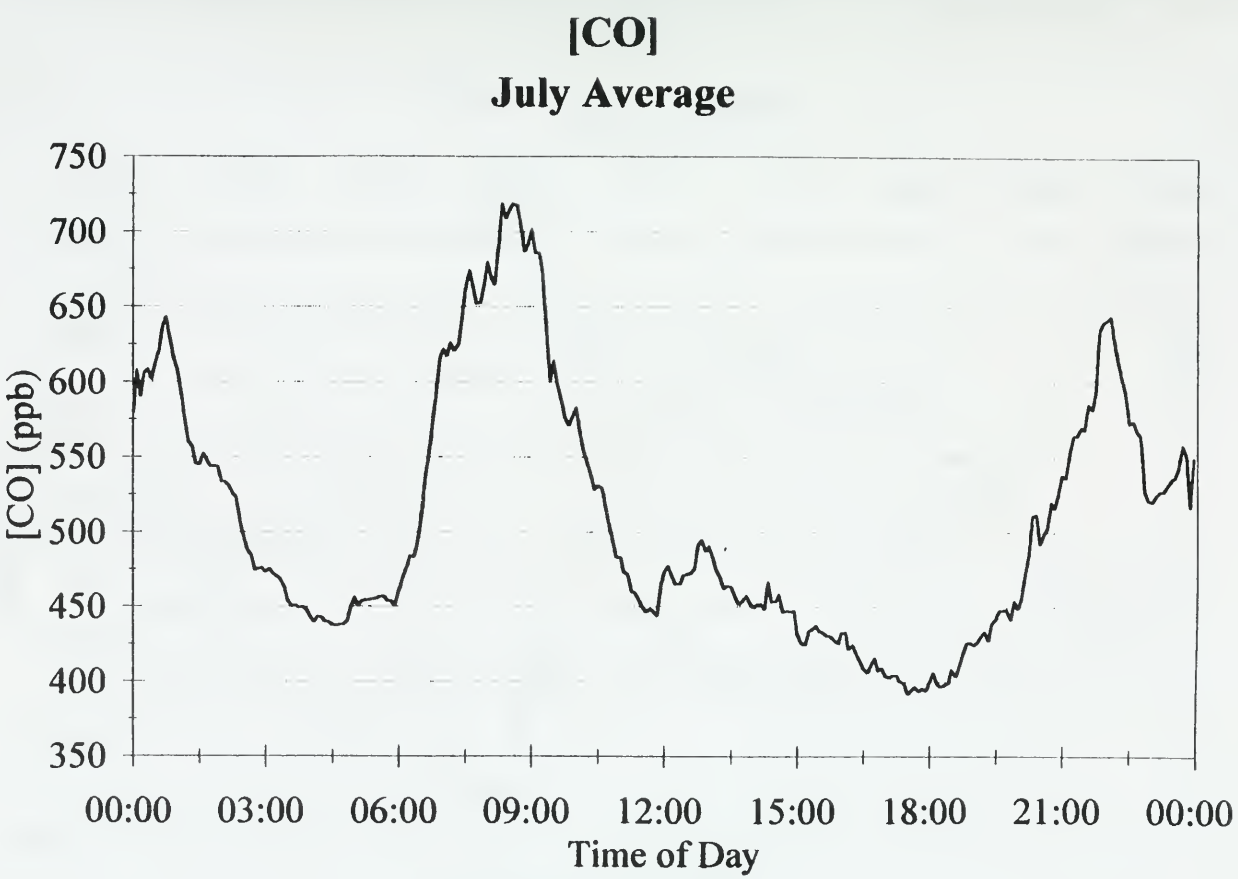

Figure 21a. Average diurnal variation of CO at York University in July.

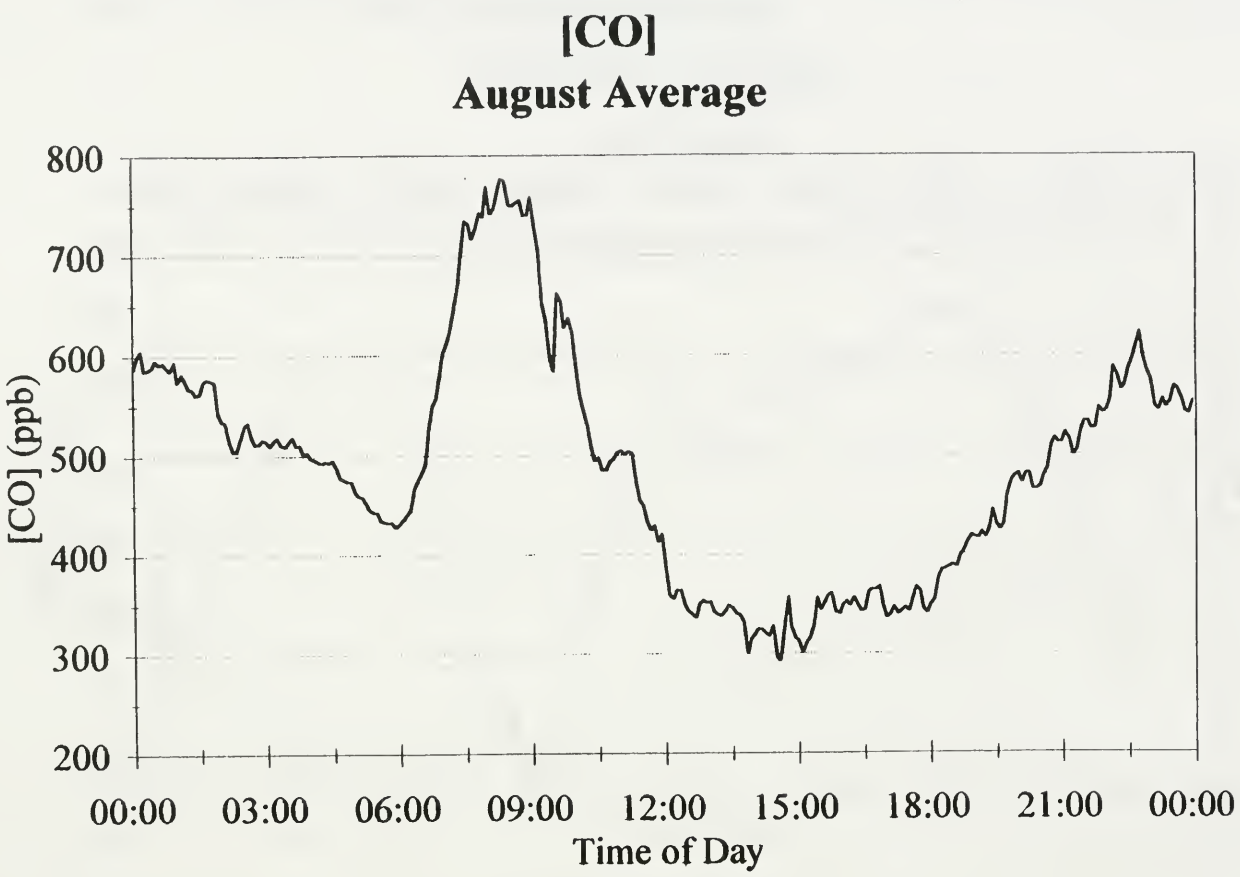

Figure 21b. Average diurnal variation of CO at York University in August.

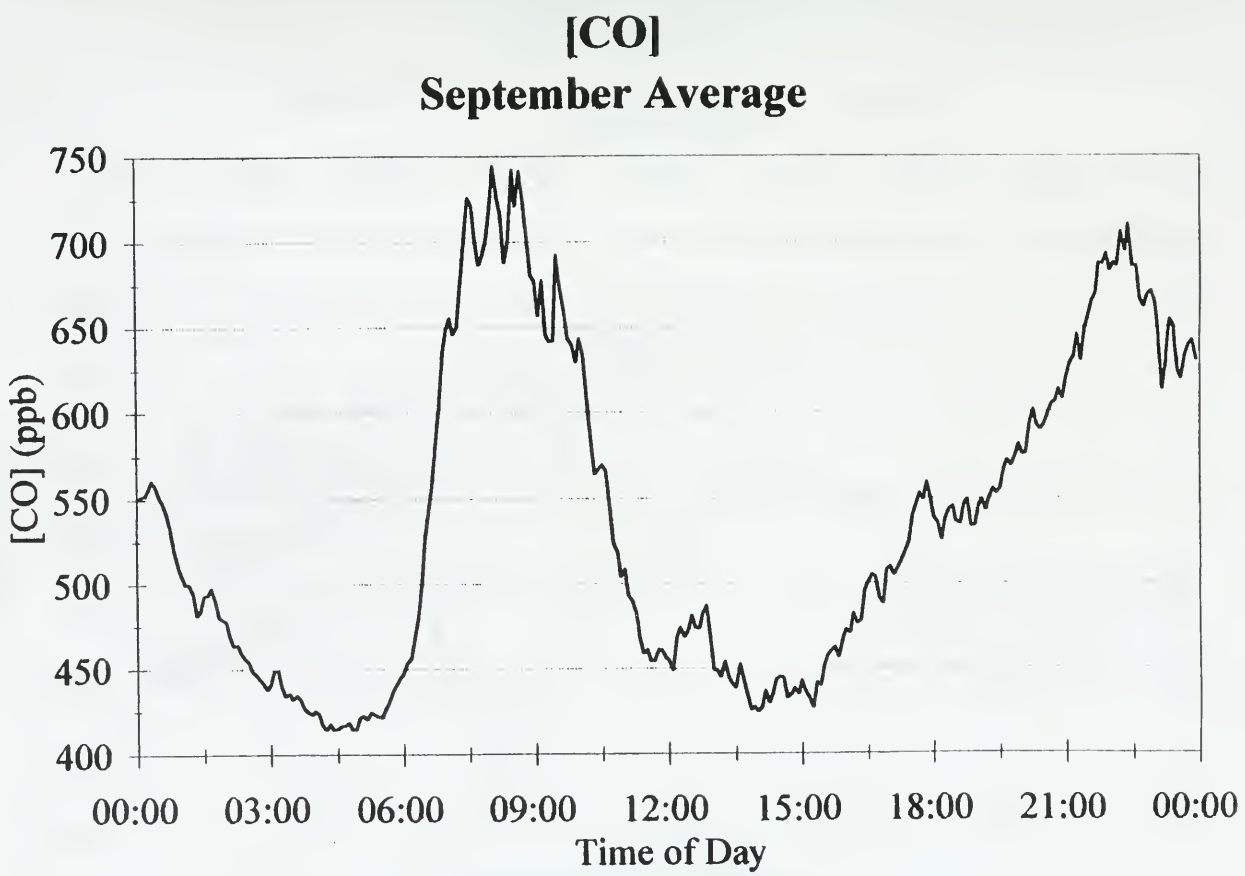

Figure 21c. Average diurnal variation of CO at York University in September.

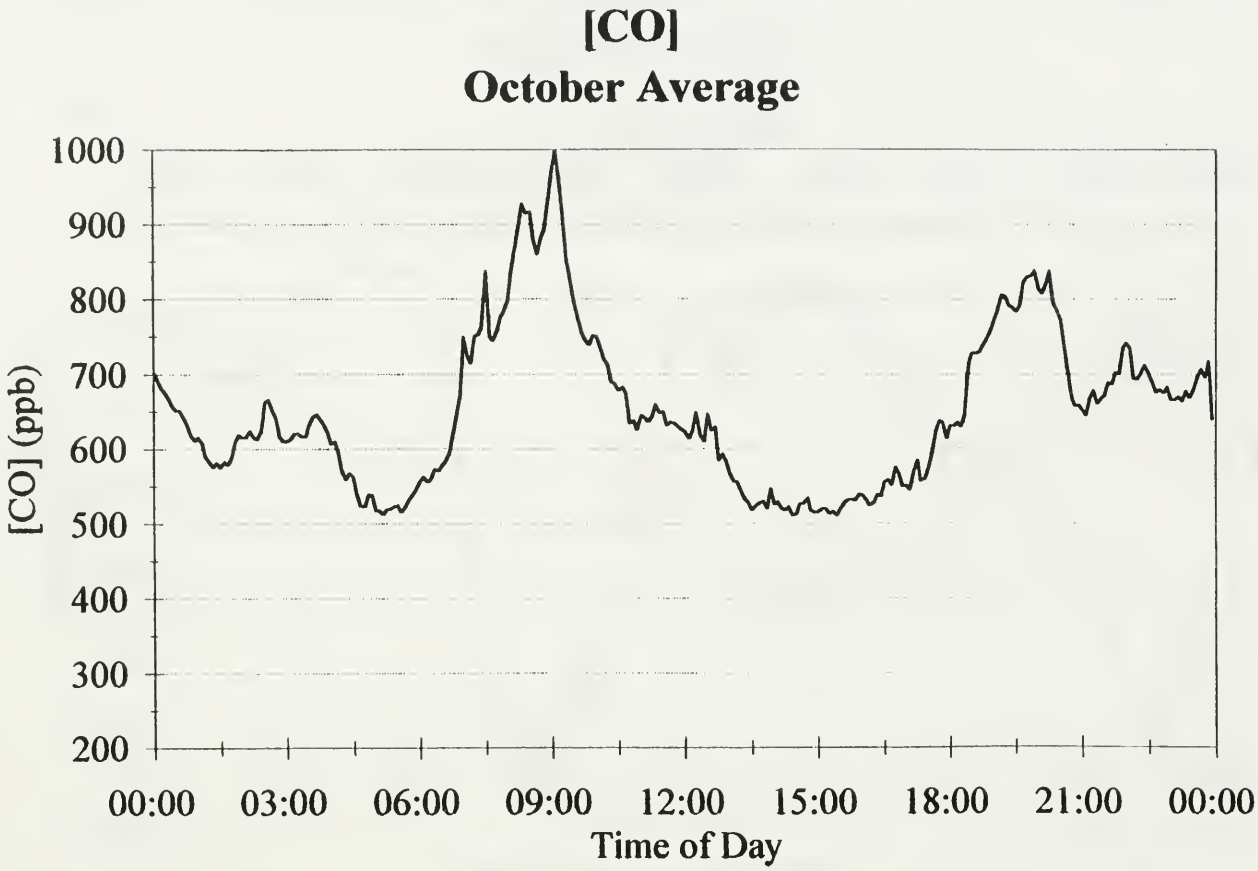

Figure 21d. Average diurnal variation of CO at York University in October.

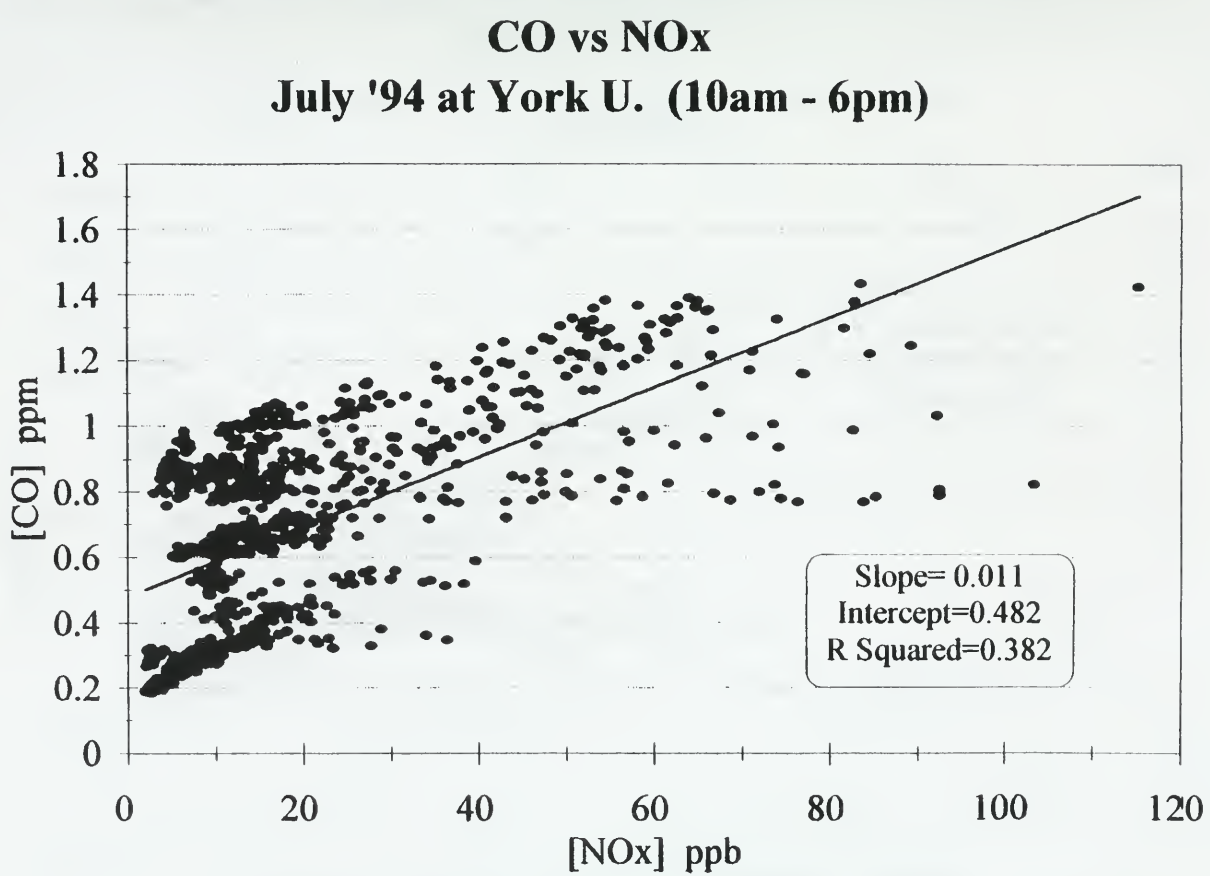

Figure 22a. Daytime plot of CO against NO_x at York University in July.

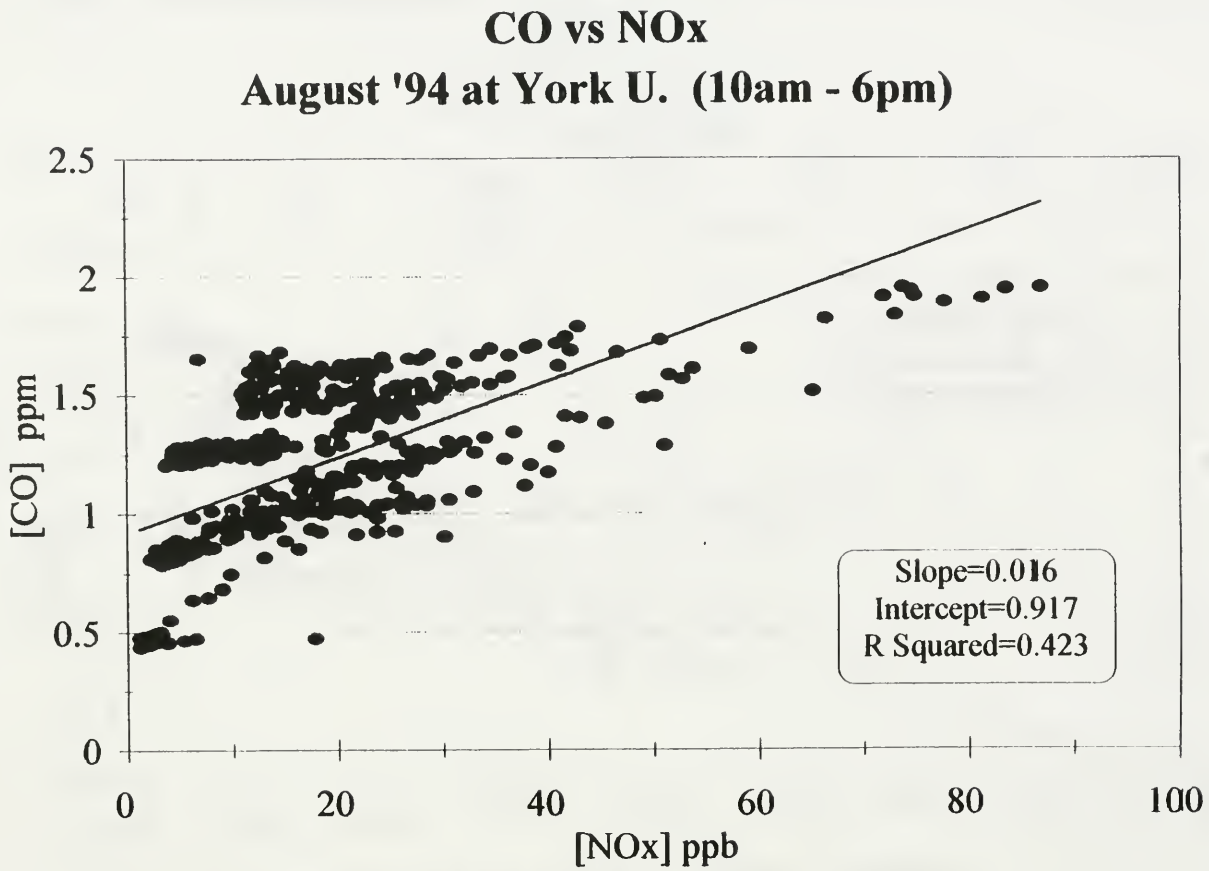

Figure 22b. Daytime plot of CO against NO_x at York University in August.

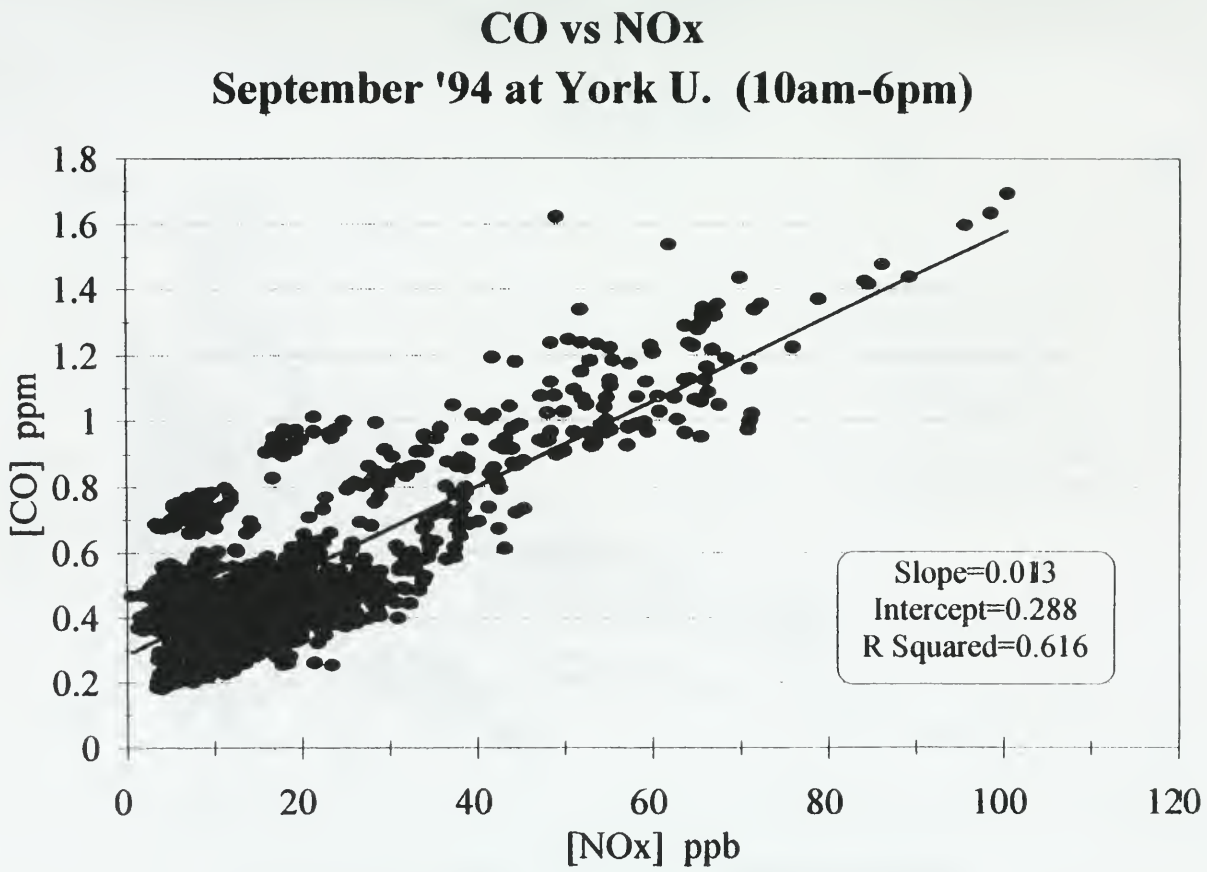

Figure 22c. Daytime plot of CO against NO_x at York University in September.

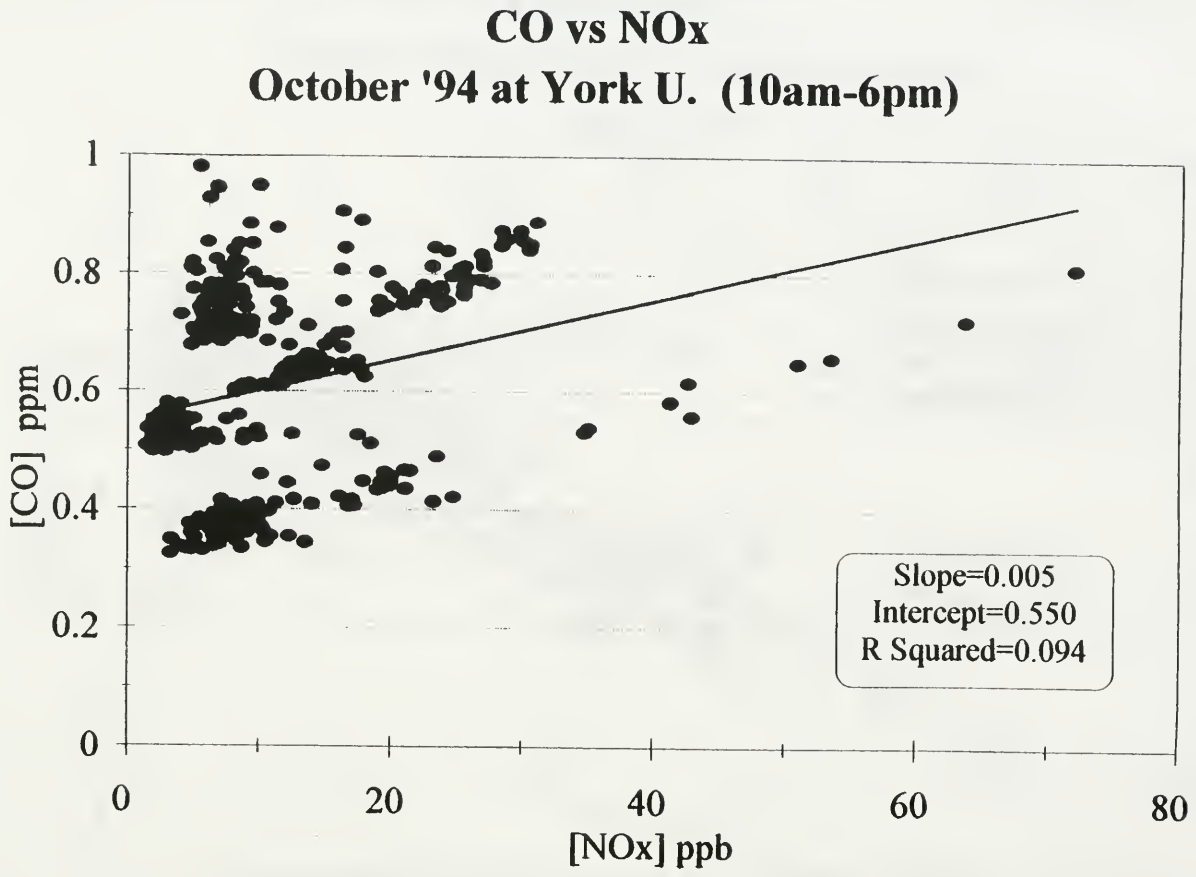

Figure 22d. Daytime plot of CO against NO_x at York University in October.

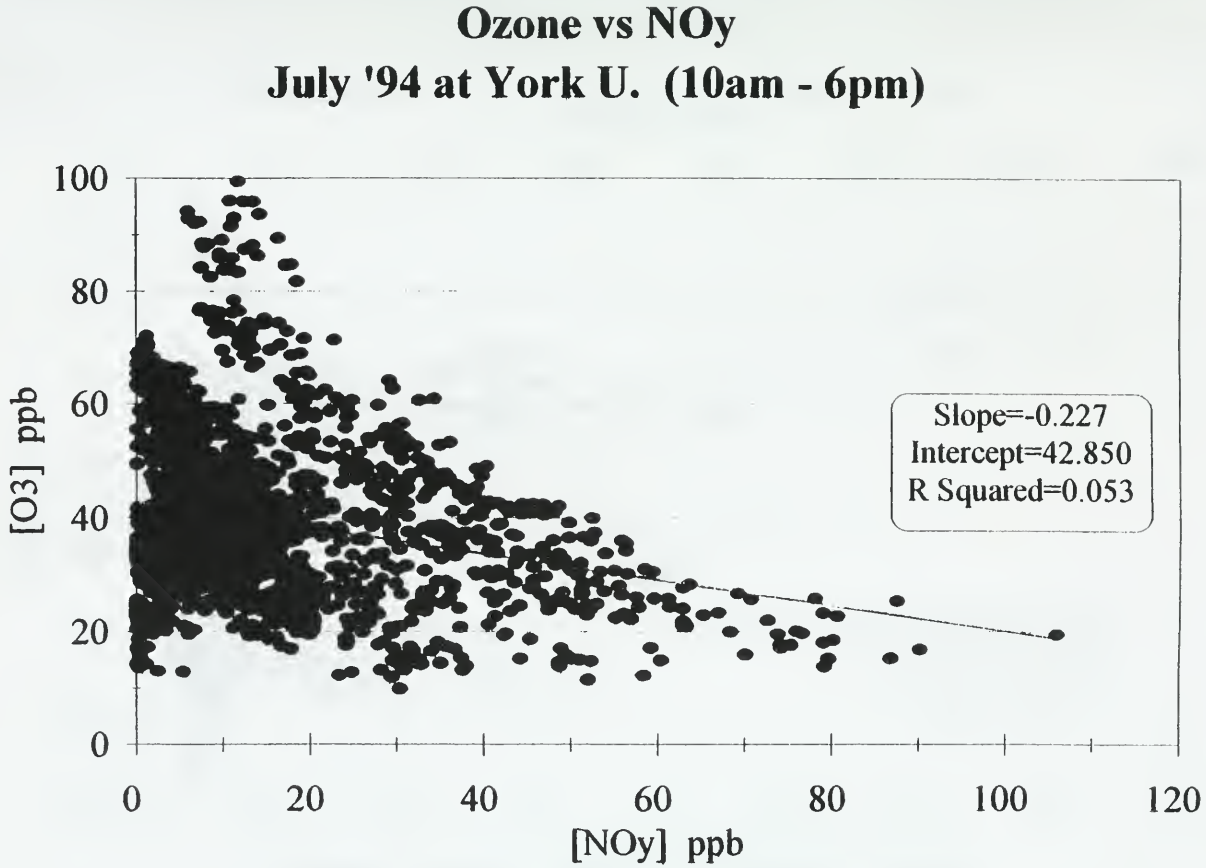

Figure 23a. Daytime plot of O_3 against NO_y at York University in July.

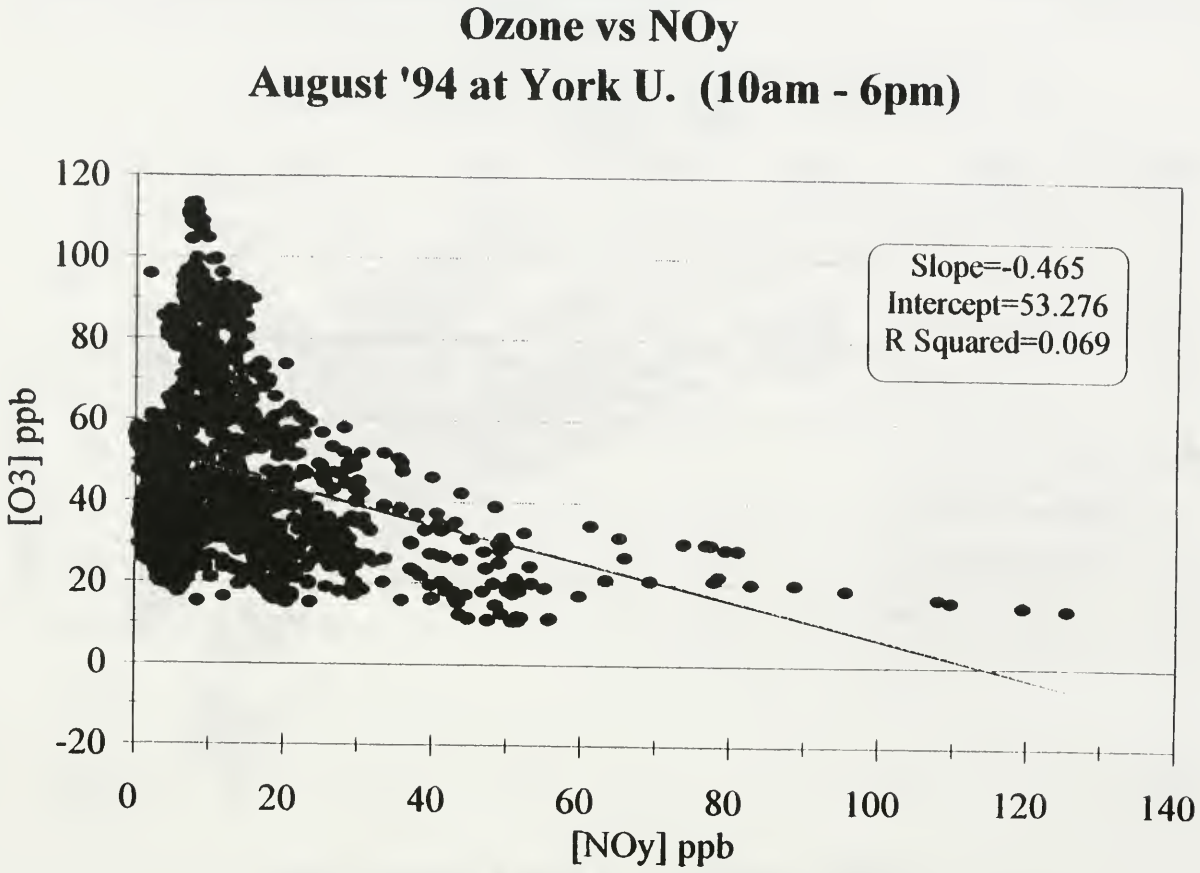

Figure 23b. Daytime plot of O_3 against NO_y at York University in August.

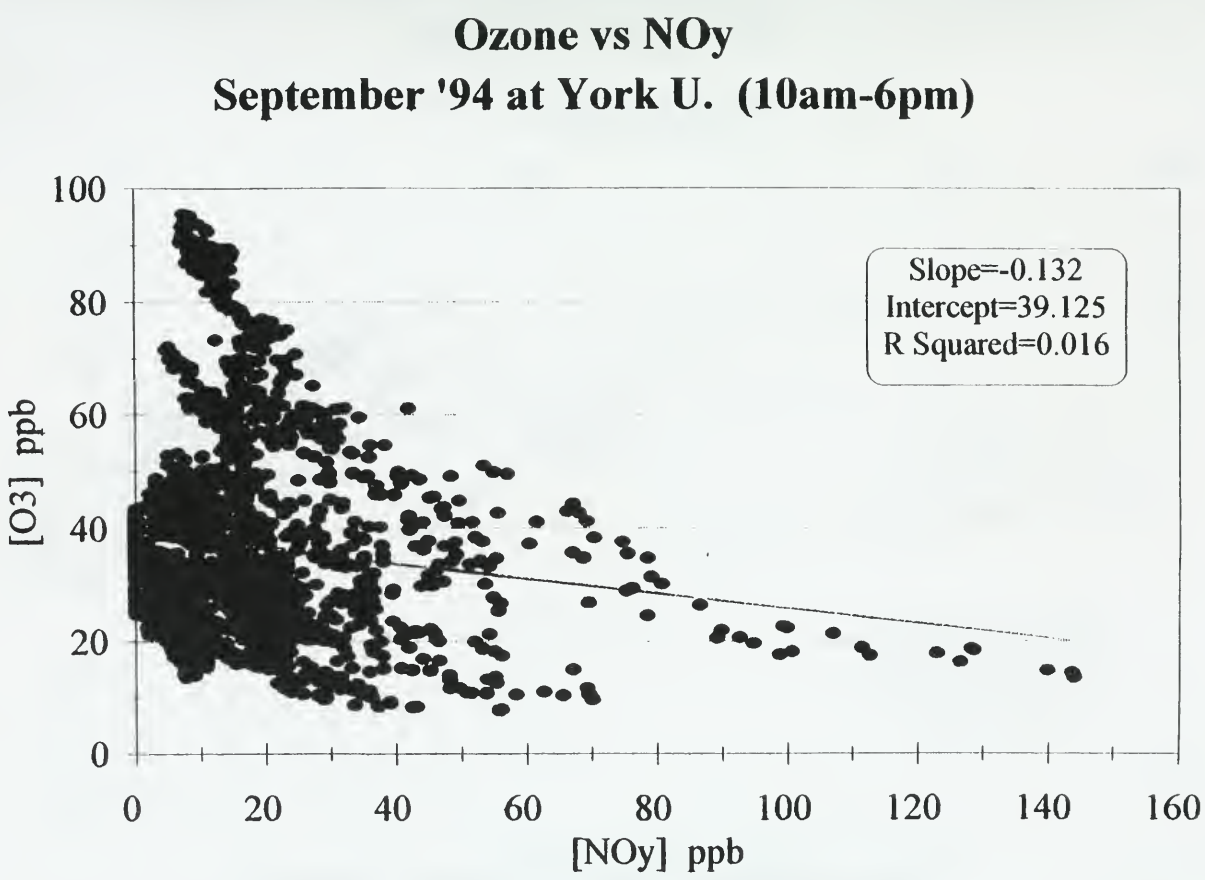

Figure 23c. Daytime plot of O_3 against NO_y at York University in September.

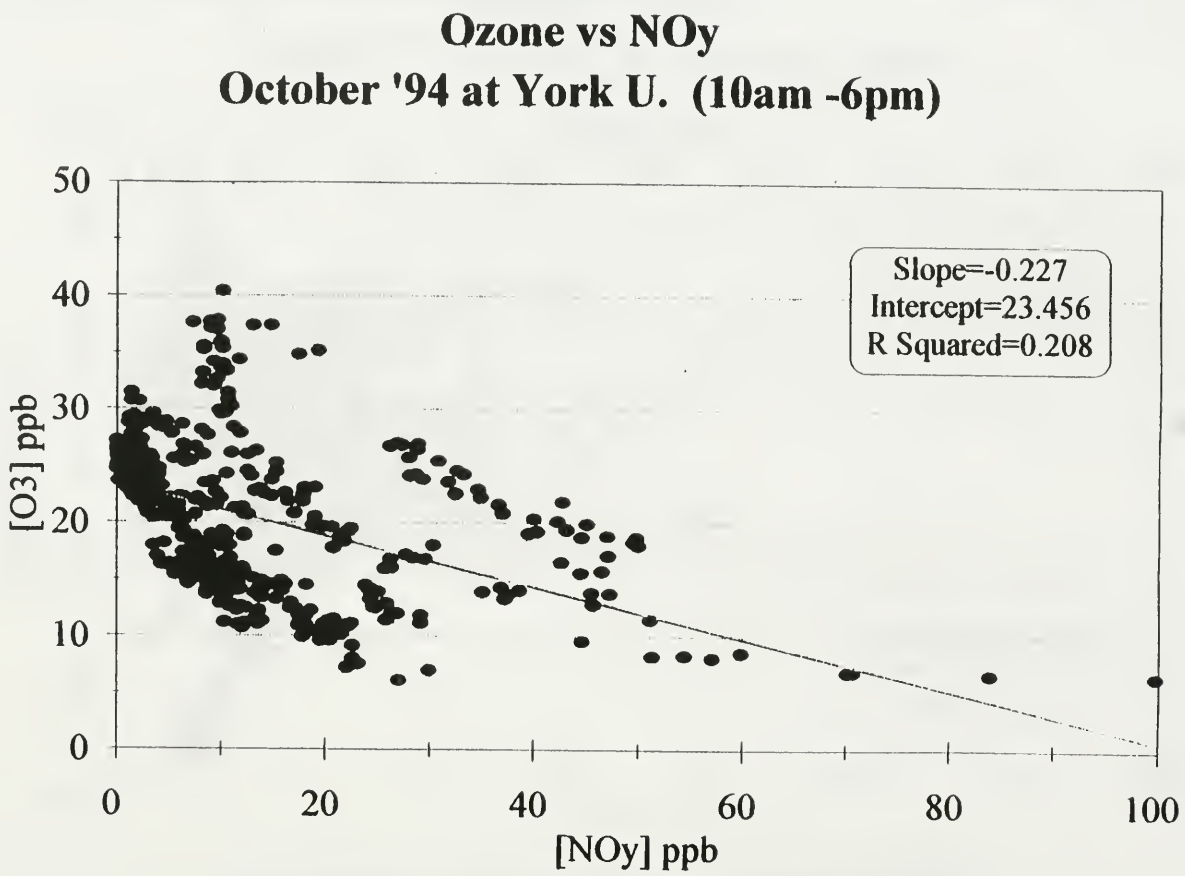

Figure 23d. Daytime plot of O_3 against NO_y at York University in October.

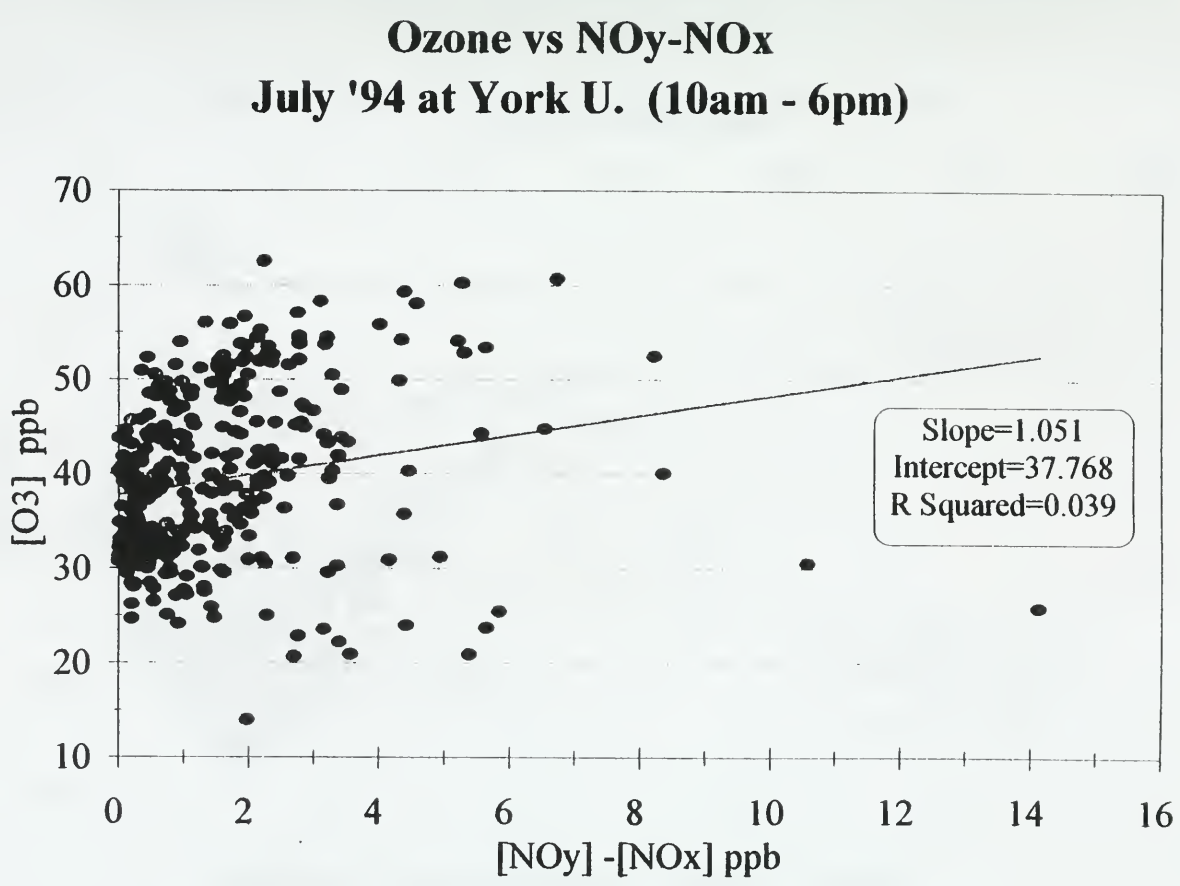

Figure 24a. Daytime plot of O_3 against NO_z at York University in July.

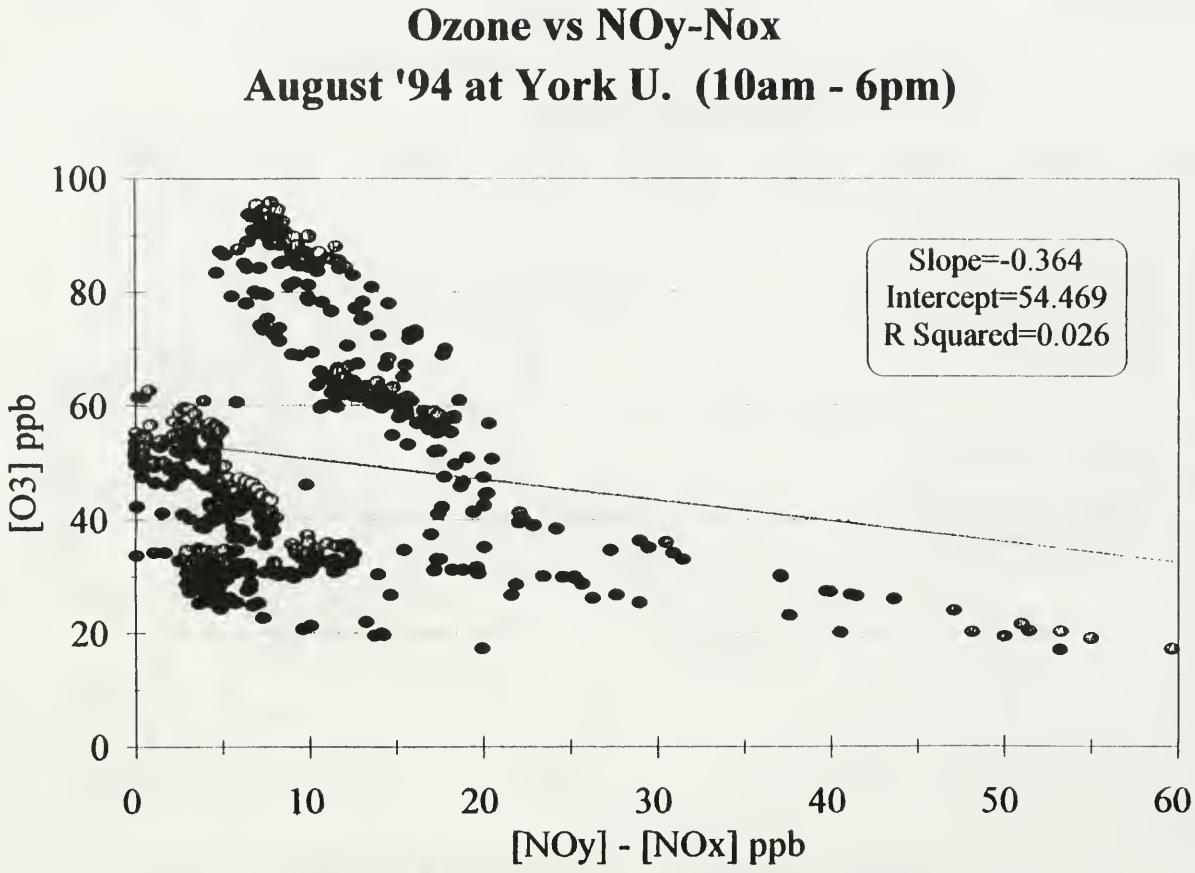

Figure 24b. Daytime plot of O_3 against NO_z at York University in August.

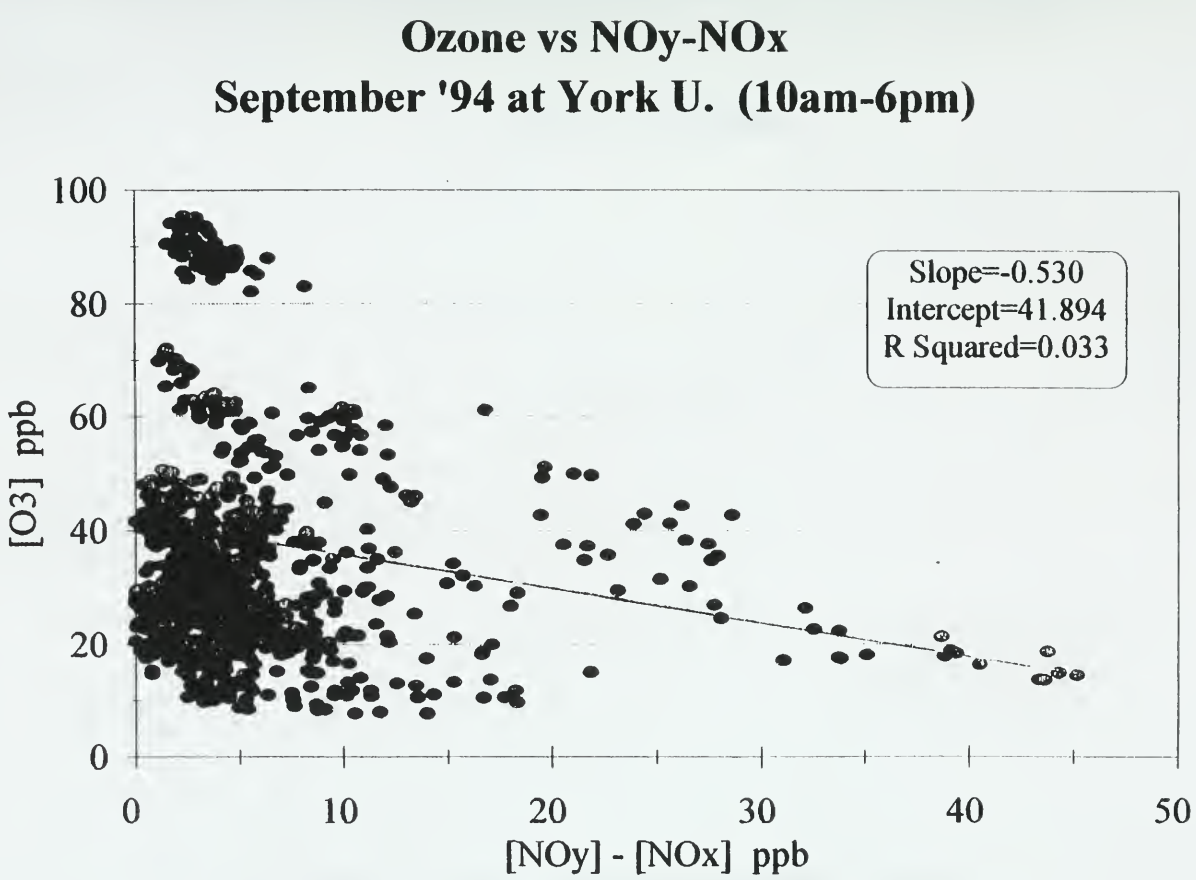

Figure 24c. Daytime plot of O_3 against NO_z at York University in September.

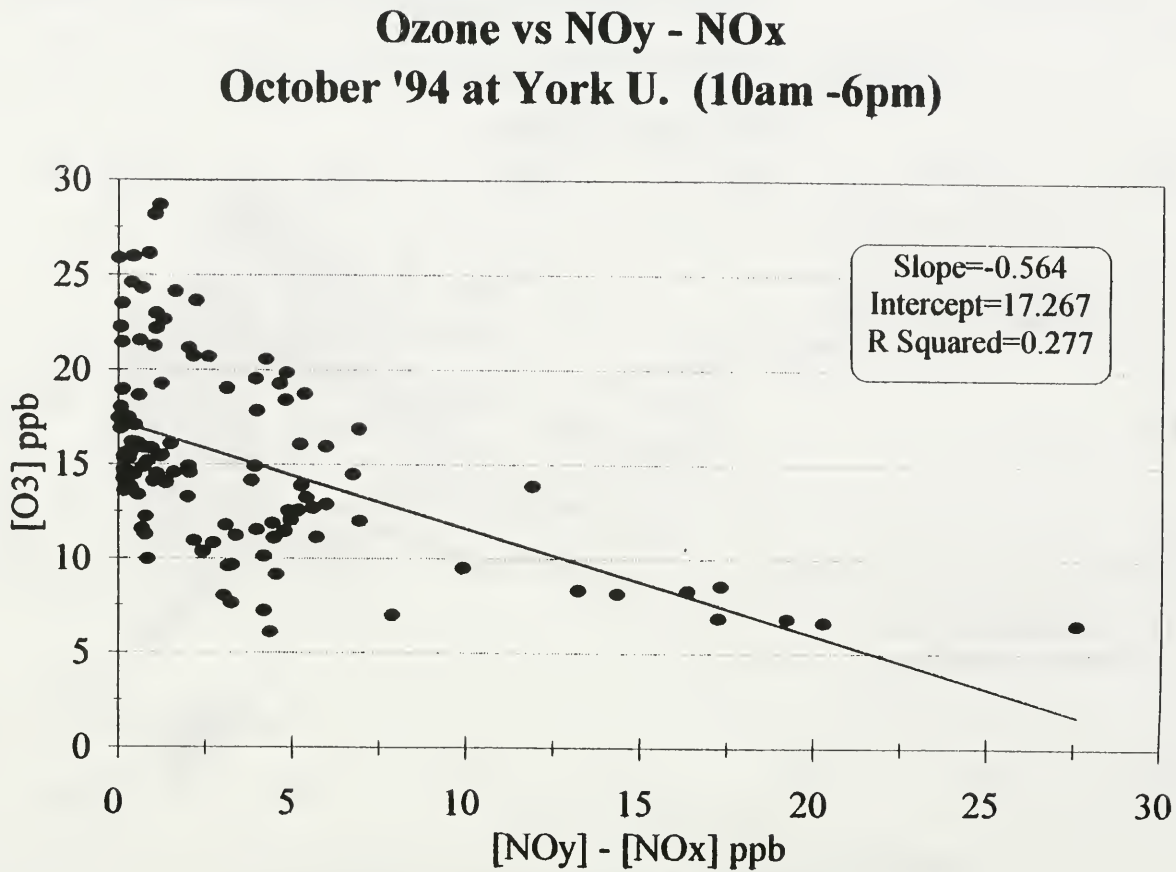

Figure 24d. Daytime plot of O_3 against NO_z at York University in October.